



UNIL | Université de Lausanne

Unicentre
CH-1015 Lausanne
<http://serval.unil.ch>

2013

A genetic and chemical investigation of malondialdehyde production and turnover in *Arabidopsis*

Emanuel Schmid-Siegert

Emanuel Schmid-Siegert, 2013, A genetic and chemical investigation of malondialdehyde and turnover in *Arabidopsis*

Originally published at : Thesis, University of Lausanne

Posted at the University of Lausanne Open Archive.
<http://serval.unil.ch>

Droits d'auteur

L'Université de Lausanne attire expressément l'attention des utilisateurs sur le fait que tous les documents publiés dans l'Archive SERVAL sont protégés par le droit d'auteur, conformément à la loi fédérale sur le droit d'auteur et les droits voisins (LDA). A ce titre, il est indispensable d'obtenir le consentement préalable de l'auteur et/ou de l'éditeur avant toute utilisation d'une oeuvre ou d'une partie d'une oeuvre ne relevant pas d'une utilisation à des fins personnelles au sens de la LDA (art. 19, al. 1 lettre a). A défaut, tout contrevenant s'expose aux sanctions prévues par cette loi. Nous déclinons toute responsabilité en la matière.

Copyright

The University of Lausanne expressly draws the attention of users to the fact that all documents published in the SERVAL Archive are protected by copyright in accordance with federal law on copyright and similar rights (LDA). Accordingly it is indispensable to obtain prior consent from the author and/or publisher before any use of a work or part of a work for purposes other than personal use within the meaning of LDA (art. 19, para. 1 letter a). Failure to do so will expose offenders to the sanctions laid down by this law. We accept no liability in this respect.



Faculté de biologie et de médecine
Department of Plant Molecular Biology (DBMV)

**A genetic and biochemical investigation of
malondialdehyde production and turnover in *Arabidopsis***

Thèse de doctorat ès sciences de la vie (PhD)

présentée à la
Faculté de biologie et de médecine
de l' Université de Lausanne
par

Emanuel Schmid-Siegert

Biologist diplômé de l'Université de Erlangen-Nürnberg, Allemagne

Jury

Prof. Jérôme Goudet, président
Prof. Edward E. Farmer, directeur de la thèse
Prof. Teresa B. Fitzpatrick, expert externe
Prof. Dr. rer. nat. Med. Martin J. Müller, expert externe

Lausanne 2013

Imprimatur

Vu le rapport présenté par le jury d'examen, composé de

<i>Président</i>	Monsieur Prof. Jan Roelof Van der Meer
<i>Directeur de thèse</i>	Monsieur Prof. Edward E. Farmer
<i>Experts</i>	Madame Prof. Teresa Fitzpatrick
	Monsieur Prof. Martin J. Mueller

le Conseil de Faculté autorise l'impression de la thèse de

Monsieur Emanuel Schmid-Siegert

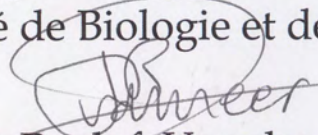
Biologiste diplômé de l'Université d'Erlangen-Nürnberg, Allemagne

intitulée

**A genetic and biochemical investigation of malondialdehyde
production and turnover in *Arabidopsis***

Lausanne, le 5 avril 2013

pour Le Doyen
de la Faculté de Biologie et de Médecine


Prof. Jan Roelof Van der Meer

Acknowledgements

I want to thank my "Doktorvater" Edward Farmer for the opportunity to work on this project, but more importantly for the guidance and support throughout the PhD thesis. You strongly encouraged self-dependence working but were always curious about new results and left your work unattended to discuss new developments.

Merci to all recent and former lab-members who provided a great atmosphere and support, especially in rough times. Whether it was by professional advice and help or a shared beer to relax. Victor a good friend, who taught me the principles of the PhD and helped a lot to hunt the ghost of MDA. Jorge the other member in the tiny MDA-group in our lab who was a great team player and without whom the realization of the paper would have been impossible. A big merci goes to Aurore for correction of the French abstract.

I want to thank my parents who supported me from the first childish idea to become a biologist till the successful end, through moral and financial support and who always encouraged me to follow up what I am most interested in. A special thanks goes to to my loving wife Stefanie who was always a big supporter of my work and without whom I may have never successfully succeeded that far!

Abstract

Malondialdehyde (MDA) is a small reactive molecule which occurs ubiquitous among eukaryotes. Interest in this molecule stems from the fact that it can be highly reactive. In green tissues of plants it is apparently formed predominantly by reactive oxygen species (ROS)-mediated non-enzymatic oxidation (nLPO) of triunsaturated fatty acids (TFAs). MDA which is formed by nLPO is widely used as a disease marker and is regarded to be a cellular toxin. Surprisingly, sites of ROS production like mitochondria and chloroplasts possess membranes which are enriched in nLPO-prone polyunsaturated fatty acids (PUFAs). In this work we showed that chloroplasts are the major site of MDA production in leaves of adult *Arabidopsis thaliana* plants, whereas analyses in seedlings revealed accumulation in meristematic tissues like the root tip, lateral roots and the apical meristem region. Characterizing the MDA pools in more detail, we could show that MDA in plants was predominantly present in a free, non-reactive enolate form. This might explain why it is tolerated in sites where its protonated form could potentially damage the genome and proteome. Analyzing the biological fate of MDA in leaves using labeled MDA-isotopes, we were able to show that MDA is metabolized and used to assemble lipids. The major end-point metabolite was identified as 18:3-16:3-monogalactosyldiacylglycerol (MGDG), which is the most abundant lipid in chloroplasts. We hypothesize that PUFAs in sites of ROS production, like at PS II in chloroplasts, might act as buffers preventing damage of proteins, thereby generating molecules such as MDA. The MDA produced in this way appears predominantly in a non-reactive enolate form in the cell until it fulfills a biological function or until it is metabolized in order to assemble polyunsaturated MGDGs. Additionally, nLPO has been reported to increase in pathogenesis and we challenged seedlings and adult plants with necrotrophic fungi. Monitoring MDA during the infections, we found MDA pools in seedlings were highly inducible although they were tightly controlled in the leaves of adult plants.

Résumé

Malondialdehyde (MDA) est une petite molécule réactive présente de manière ubiquitaire dans les eucaryotes. L'intérêt de cette molécule vient du fait que celle-ci pourrait être très réactive. Dans les tissus verts des plantes, la majorité du MDA est apparemment formée par l'oxydation non-enzymatique (nLPO) des acides gras polyinsaturés (PUFAs) transmis par des espèces actives d'oxygène (ROS). Le MDA formé par nLPO est souvent utilisé comme marqueur de maladies et il est considéré comme une toxine cellulaire.

Étonnamment, les sites de production comme les mitochondries et les chloroplastes sont riches en PUFAs qui sont sensibles à la nLPO. Dans cette thèse nous montrons que les chloroplastes représentent le site de production de MDA dans les feuilles adultes d'*Arabidopsis thaliana*. Les analyses de MDA dans les plantules ont révélé que le MDA s'accumule dans les tissus meristematiques comme celles de la pointe de la racine, des racines latérales et du meristème apical. Par la caractérisation du MDA présent nous avons pu montrer que la majorité du MDA était présent sous la forme d'un énolate non-réactif. Ceci pourrait expliquer pourquoi le MDA est toléré dans les sites où il pourrait casser le génome ou le protéome s'il est présent sous sa forme protonée. Les analyses du devenir du MDA dans les feuilles par des isotopes du MDA ont montré que celui-ci est métabolisé et utilisé pour assembler des lipides. Le lipide majoritairement métabolisé a été identifié comme étant le 18:3-16:3-monogalactosyldiacylglycerole (MGDG); le lipide le plus abondant dans les chloroplastes. Nous supposons que la présence des PUFAs dans les sites de production du ROS, tout comme le PS II dans les chloroplastes, pourrait jouer un rôle de tampon pour prévenir les protéines de différentes dégradations et ainsi générer des molécules telle que le MDA. La majorité du MDA produit par cette réaction est présente dans la cellule sous la forme d'énolate non-réactif, jusqu'au moment de son utilisation ou lorsqu'il sera métabolisé pour produire des MGDGs polyinsaturés. De plus, il a été décrit que nLPO pourrait augmenter dans la pathogenèse, et nous

avons testé des plantes adultes et des plantules en présence de champignons nécrotrophiques. L'observation du MDA pendant les infections a montré que les concentrations en MDA sont fortement induites dans les plantules mais contrôlées dans les plantes adultes.

Contents

List of Figures	ix
List of Tables	xi
Abbreviations	xiii
1 Introduction: Malondialdehyde in eukaryotes	1
1.1 The oxidation of lipids	1
1.2 Features of malondialdehyde	2
1.2.1 Chemistry of malondialdehyhde	2
1.2.2 Chemical generation and purification of MDA	3
1.3 Determination of malondialdehyde	4
1.3.1 TBARS, an assay to assess MDA levels ?	4
1.3.2 Quantitative methods for MDA determination	5
1.4 Sources and occurrence of MDA in higher eukaryotes	5
1.4.1 MDA in the angiosperm <i>Arabidopsis thaliana</i>	6
1.4.2 MDA in animals	7
1.5 The role of malondialdehyde in eukaryotes	8
1.5.1 The toxicity of malondialdehyde	8
1.5.2 Possible beneficial roles of malondialdehyde	9
1.6 The metabolism of malondialdehyde	10
2 Goals of the thesis	13
3 Characterization of resting MDA pools in plants	15
3.1 Introduction	15
3.2 Material and Methods	16
3.3 Results	18
3.3.1 Adult leaves	18

CONTENTS

3.3.2	Whole seedlings	20
3.3.3	Seedling roots	20
3.3.4	Sub-cellular localization of MDA in leaves	20
3.3.5	Isolation of chloroplasts	21
3.3.6	Characterization of chloroplastic MDA	22
3.3.7	Localization of MDA in roots	24
3.3.8	MDA in cell proliferation zones	24
3.3.9	Alternative sources for MDA generation in plants	27
3.4	Discussion	31
3.4.1	MDA Localization in the leaf	32
3.4.2	Seedling- and Root-associated MDA Pools	33
3.4.3	New potential sources of MDA formation	34
4	Induction of malondialdehyde pools	39
4.1	Introduction	39
4.2	Material and Methods	40
4.3	Results	41
4.3.1	Light-induced changes of MDA levels	41
4.3.2	MDA dynamics during infection with necrotrophic fungi	41
4.4	Discussion	47
4.4.1	Light-induced changes of MDA levels	47
4.4.2	MDA inducibility upon infection with necrotrophic fungi	48
5	Generation of isotope-labeled malondialdehyde	51
5.1	Introduction	51
5.2	Material and Methods	54
5.3	Results	56
5.3.1	Enzymatic generation of MDA with alcohol dehydrogenase	56
5.3.2	Purification of MDA by anion exchange chromatography	56
5.3.3	GC/MS-Characterization of purified MDA	58
5.4	Discussion	63
6	Metabolism of malondialdehyde in the leaves of <i>A. thaliana</i>	65
6.1	Introduction	65
6.2	Material and Methods	67
6.3	Results	71

6.3.1	Successful uptake and turnover of exogenous MDA	71
6.3.2	¹⁴ C-MDA derived radioactivity can be found in plant lipids	71
6.3.3	Successful identification of an MDA end-point metabolite	74
6.3.4	MDA is incorporated into the FA-moiety of glycerolipids	78
6.3.5	Comparison of ¹⁴ C-acetate and ¹⁴ C-MDA incorporation into lipids	83
6.3.6	Testing the role of acetate as a potential MDA metabolite using the <i>acs</i> mutant	85
6.3.7	Evaluation of MDA-microarray analysis	86
6.3.8	Screening mutant which are potentially involved in MDA metabolism	87
6.3.9	Extraction and analysis of organic acids as possible MDA turnover intermediates	89
6.4	Discussion	94
6.4.1	18:3-16:3-MGDG is a major MDA end-point metabolite	94
6.4.2	18:2-16:2-MGDG is the major MDA metabolite in the TFA-mutant <i>fad3-2,fad7-2,fad8</i>	96
6.4.3	Phospholipids represent a minor sink of MDA metabolism	96
6.4.4	Fatty acid assembly: the major route of MDA metabolism into lipids	96
6.4.5	Acetate is not an MDA metabolism intermediate	97
6.4.6	The metabolism of MDA: a model	98
6.4.7	Evaluation of MDA microarray data	101
6.4.8	Testing potential mutants of MDA metabolism with a ¹⁴ C-MDA incorporation assay	102
6.4.9	Small carboxylic acids might represent MDA metabolism interme- diates	103
7 Final conclusions and outlook		105
References		111
8 Supplementary material		119
8.0.9.1	List of upregulated genes from MDA microarray, orga- nized in GO-terms by GOrilla	141

CONTENTS

List of Figures

1.1	Structure of malondialdehyde as a function of pH	3
1.2	Derivatization of MDA with TBA	4
1.3	Michael adduct formation of α, β -unsaturated carbonyls	8
3.1	Scale and origin of MDA pools	19
3.2	<i>In situ</i> MDA staining in leaves	21
3.3	Peroxisomes in chloroplast extracts	22
3.4	Isolated chloroplasts contain MDA	23
3.5	Distribution of putative MDA pools in the lower root	25
3.6	Characterization of MDA-TBA adducts in the root tip.	26
3.7	MDA in zones of cell proliferation	28
3.8	Characterization of <i>fad2-2, fad6</i> plants	29
3.9	GC/MS measurements of MDA in WT and <i>fad2-2, fad6</i> rosettes	30
4.1	$^1\text{O}_2$ produced in the light alters MDA levels	42
4.2	MDA pools in seedlings respond to pathogenesis and to plant-derived stress mediators	43
4.3	Inducible TBA staining in seedlings.	45
4.4	MDA dynamics during infection with the pathogen <i>P. cucumerina</i>	46
5.1	Scheme for enzymatic MDA generation catalyzed by equine alcohol dehydrogenase	52
5.2	Derivatization of small aldehydes prior to GC/MS analysis	53
5.3	MDA purification and concentration by anion exchange chromatography	57
5.4	GC/MS characterization of MDA purified by anion-exchange chromatography	59
5.5	Analysis of 1,3-propanediol in anion exchange fractions by GC/MS	62

LIST OF FIGURES

6.1	Potential routes of MDA metabolism	66
6.2	Uptake of volatile ^{13}C -MDA in <i>Arabidopsis</i> leaves	72
6.3	Turnover of exogenous MDA in <i>Arabidopsis</i> leaves	73
6.4	TLC-analysis of ^{14}C -MDA incorporation into plant lipids	73
6.5	TLC-analysis of ^{14}C -MDA incorporation into polar plant lipids	75
6.6	HPLC separation of polar lipids and ^{14}C -incorporation analysis	76
6.7	Identification of an MDA end-point metabolite by UPLC-TOF-MS	77
6.8	Incorporation of ^{14}C -MDA into lipids from <i>fad3-2,fad7-2,fad8</i> plants	78
6.9	Identification of an MDA-derived metabolite in the <i>fad3-2,fad7-2,fad8</i>	79
6.10	GC/MS analysis of FAs from hydrolyzed 18:3-16:3-MGDG	80
6.11	GC/MS analysis of FAs from hydrolyzed 18:2-16:2-MGDG	81
6.12	GC/MS analysis of FAs from an hydrolyzed HPLC void peak-	82
6.13	^{14}C -acetate incorporation into polar plant lipids	83
6.14	Comparison of ^{14}C -MDA and ^{14}C -acetate incorporation in lipids 3 h after application	84
6.15	TLC analysis of total plant lipids after exposure to volatile ^{14}C -MDA for 6 h	85
6.16	^{14}C -MDA incorporation analysis in leaves of <i>acs</i> plants	86
6.17	Enrichment of gene ontologies in MDA upregulated genes	88
6.18	Screening potential MDA turnover mutants for altered ^{14}C incorporation into lipids	90
6.19	GC/MS analysis of extracted and purified organic acids from <i>Arabidopsis</i>	92
6.20	Incorporation of ^{14}C -MDA in small organic acids	93
6.21	Model of MDA metabolism in plastids of <i>Arabidopsis</i>	99
8.1	MDA fluorescence in <i>Arabidopsis</i> flowers	119
8.2	MDA staining in <i>C. elegans</i>	120

List of Tables

3.1	Summary of fatty acid (FA) composition in leaves and roots of FA-desaturases mutants	35
3.2	Expression analysis of <i>FAD2</i> and <i>FAD6</i> in different tissues and developmental stages of <i>Arabidopsis</i> plants	36
6.1	Gene ontology "Biological Processes" from MDA-microarray	89
6.2	Mutants tested for altered ^{14}C -MDA incorporation	91
8.1	Microarray of MDA-treated <i>Arabidopsis</i> plants	121

LIST OF TABLES

Abbreviations

$^1\text{O}_2$	Singlet oxygen	eLPO	Enzymatic lipid oxidation
^{13}C -MDA	[U - ^{13}C]-malondialdehyde	FAs	Fatty acids
^{14}C -acetate	[1, 2- ^{14}C]-acetate	FFAs	Free fatty acids
^{14}C -MDA	[2- ^{14}C]-malondialdehyde	GC/MS	Gas chromatography coupled with mass spectrometry
16:0	Hexadecanoic acid	GO	Gene ontology
16:2	Hexadecadienoic acid	H₂O₂	Hydrogen peroxide
16:3	Hexadecatrienoic acid	HO·	Hydroxyl radical
18:0	Stearic acid	HPLC	high-performance liquid chromatography
18:2	Linoleic acid	IS	Internal standard
18:3	Linolenic acid	LOD	Limit of detection
3-HPA	3-hydroxypropanal	LOQ	Limit of quantification
<i>A. thaliana</i>	<i>Arabidopsis thaliana</i>	LP	Left primer
<i>E. coli</i>	<i>Escherichia coli</i>	LPO	Lipid oxidation
<i>fad3-2, 7-2, 8</i>	<i>fad3-2, fad7-2, fad8</i>	lyso-PC	Lyso-phosphatidylcholine
<i>fad7</i>	<i>fad3-2, fad7-2, fad8</i>	MDA	Malondialdehyde
ACP	Acyl carrier protein	MGDG	Monogalactosyl-diacylglycerol
ADH	alcohol dehydrogenase	MSA	Malonic semialdehyde
BHT	2,6-tert-butyl-4-methylphenol	nLPO	Non-enzymatic lipid oxidation
BSTFA	N,O-Bis(trimethylsilyl) trifluoroacetamide	NMR	nuclear magnetic resonance
Ci	Curie	O₂⁻	Superoxide radical
DAPI	4',6-diamidino-2-phenylindole	PA	Piperonylic acid
DNA	Deoxyribonucleic acid	PC	Phosphatidylcholine
DNPH	2,4-dinitrophenylhydrazine	PCI	Positive chemical ionization mode
dpm	Disintegration per minute	PE	Phosphatidylethanoamine
		PFBHA	O-(2,3,4,5,6-pentafluorobenzyl)-hydroxylamine hydrochloride
		PFPH	Pentafluorophenylhydrazine
		PI	Phosphatidylinositol
		PNPA	β -(p-nitrophenoxy)acrolein
		PSI	Photosystem I
		PSII	Photosystem II
		PUFAs	Poly unsaturated fatty acids

Abbreviations

RES	Reactive electrophile species	TEP	1,1,3,3-tetraethoxypropane
RNAi	RNA interference	TFAs	Triunsaturated fatty acids
ROS	Reactive oxygen species	TLC	Thin layer chromatography
RP	Right primer	TMPBA	4-(trifluoromethyl)phenylboronic acid
RT	Room temperature	Trolox	6-hydroxy- 2,5,7,8-tetramethylchroman-2-carboxylic acid
SA	Specific activity	UV	Ultraviolet light
SIM	Selected ion monitoring	WT	<i>Arabidopsis thaliana</i> WT Col-0
TBA	Thiobarbituric acid		
TBARS	TBA-reactive substances		
TCA	Trichloroacetic acid		

Introduction:

The origin, role and metabolism of malondialdehyde in eukaryotes

Polyunsaturated fatty acids (PUFAs) are important structural components of membranes that partition cell compartments and directly affect or control many physiological and biochemical processes in plants and animals. They also provide substrates for a cascade of regulatory molecules which have multiple functions in eukaryotes. The biosynthesis of PUFAs differs greatly between plants and mammals (reviewed in Wallis and Browse, 2002). Plants are capable of assembling all PUFAs themselves whereas mammals lack this possibility and can only elongate and desaturate precursors which they have to take up by their diet. The direct functions of PUFAs in plants include increase of membrane fluidity linked with thermotolerance (Miquel et al., 1993) and photosynthetic competence (McConn and Browse, 1998). In mammals, PUFAs were shown to modify the activity of many ion channels (Bruno et al., 2007) and alter the activity of membrane-bound enzymes and receptors (Yehuda et al., 2002). PUFAs in mammals have also been shown to increase membrane fluidity and modulate expression of membrane-bound proteins (Shaikh and Edidin, 2006).

1.1 The oxidation of lipids

Importantly, PUFAs provide substrates for many biologically active molecules which are formed either through enzymatic or non-enzymatic oxidation of lipids (nLPO). These molecules are called oxylipins. Prominent examples of enzymatic lipid oxidation (eLPO) products are prostaglandins, leukotrienes (Funk, 2001) and thromboxanes (Smith, 1992) in mammals or jasmonic acid and precursors (Acosta and Farmer, 2010; Browse, 2009)

1. INTRODUCTION: MALONDIALDEHYDE IN EUKARYOTES

in plants. eLPO has been reviewed extensively and the present work will focus on nLPO, more precisely on one representative product of such reactions; the small aldehyde malondialdehyde (MDA). The impact of non-enzymatic lipid oxidation (nLPO) is often difficult to evaluate since it is not genetically regulated - at least it is not under the direct control of enzymes. nLPO is a widespread reaction in unsaturated membranes of all eukaryotes and was shown to increase significantly within stress, as for example in disease in mammals (Reed, 2011) or plants (Weber et al., 2004; Zoeller et al., 2012). nLPO can generate myriads of breakdown products, many of them falling in the class of reactive electrophile species (RES). RES can covalently modify macromolecules and the underlying mechanism is discussed later in this report in more detail. Early on, the oxidation of unsaturated FAs was described to result in the formation of peroxides (reviewed in Oppenheimer and Stern, 1939). nLPO by reactive oxygen species (ROS) can be categorized into two different reaction types according to the resulting pattern of oxidized PUFAs (Montillet et al., 2004). Type I oxidation is initiated by free radicals, and type II by singlet oxygen ($^1\text{O}_2$). O_2^- and H_2O_2 can themselves not oxidize PUFAs but can be converted non-enzymatically to hydroxyl radicals ($\text{HO}\cdot$) which belong to the type I reaction family. Both, type I and type II reactions lead after rearrangement to PUFA hydroperoxides which can be further fragmented non-enzymatically, resulting in the generation of small breakdown products, one of them being MDA. The underlying chemical mechanisms are described in more detail in Farmer and Mueller (2013).

The nLPO product MDA is the focus of extensive studies since the beginning of the 20th century. Its formation is associated with diseases (Del Rio et al., 2005) and nowadays widely used as a nLPO marker. Despite the impressive amount of literature (close to 30'000 citations concerning MDA in PubMed in January 2012), little is known about the role and fate of MDA *in vivo*. MDA is considered to be an important marker for nLPO (Esterbauer et al., 1991). All this makes it important to investigate MDA production and dynamics in depth. Here, we studied the source, dynamics and the metabolism of MDA in the model organism *Arabidopsis thaliana*. Investigating the fundamentals of MDA in *Arabidopsis* might not only help to understand better the link between nLPO and MDA in plants, but might provide new important information about MDA in eukaryotes in general.

1.2 Features of malondialdehyde

1.2.1 Chemistry of malondialdehyde

MDA is a 3-carbon volatile molecule with two aldehyde groups at the 1 and 3-positions and a molecular mass of 72.07. The interest in MDA results from its unique chemical

1. INTRODUCTION: MALONDIALDEHYDE IN EUKARYOTES

1979) or volatilization and trapping in ethanol (Vollenweider et al., 2000). Aqueous solutions of MDA can be stored at 4 °C for several days if sufficiently diluted, favorable at a pH higher than its pK. In millimolar concentrations on the other hand, MDA tends to form dimers and trimers (Golding et al., 1989).

1.3 Determination of malondialdehyde

1.3.1 TBARS, an assay to assess MDA levels ?

Some of the first observations linking nLPO and potential MDA generation were based on the detection of a color-complex after incubation of oxidized egg lecithin and oxidized FAs with thiobarbituric acid (TBA; Bernheim et al., 1948). It was speculated that double bonds of unsaturated FAs such as linolenic acid are probable sites of oxidation, based on the absence of the color-complex in oxidized saturated lyso-lecithin samples. Analysis of the oxidation product revealed 3 carbons and oxygen. The absorption spectrum of the adduct peaked at ~ 530 nm, similar to MDA(TBA)₂ complexes, and even though Bernheim et al. (1948) did not identify the oxidation product as MDA it is very likely that the latter was observed. Today, the thiobarbituric acid-reactive substances (TBARS) assay is still the most commonly used method to estimate MDA. The name derives from the derivatization of MDA with TBA and is based on the electrophilic character of MDA, binding readily at low pH and elevated temperature to the nucleophilic site of TBA. The adduct formed, MDA(TBA)₂ (Figure 1.2), is both pigmented and fluorescent and can easily be measured by spectrophotometry (Sinnhuber et al., 1958). MDA(TBA)₂

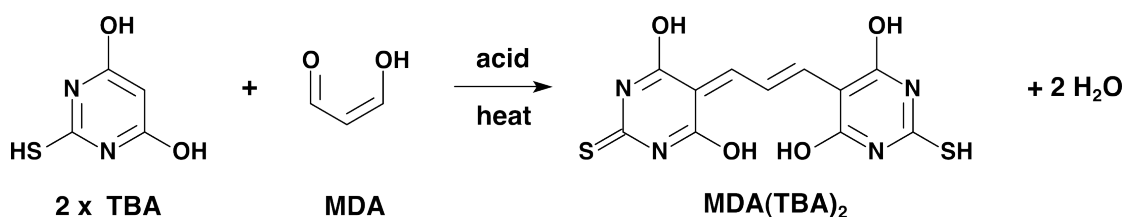


Figure 1.2: Derivatization of MDA with TBA - Formation of the adduct between thiobarbituric acid (TBA) and malondialdehyde (MDA). The resulting MDA(TBA)₂ adduct is red and also displays green fluorescence.

absorbance was originally thought to be specific for MDA, and even nowadays MDA levels are often evaluated with this assay. It was demonstrated that the reaction of MDA with TBA is not specific and this is reflected in reported MDA levels; e.g. human plasma reports ranged from MDA-concentrations of 0.32 to 47.2 nmol/ml (Esterbauer et al., 1991). One problem which arises from the commonly used TBA-assay conditions is the ability of many carbonyl groups to be susceptible to the nucleophilic attack by TBA

1.4 Sources and occurrence of MDA in higher eukaryotes

within these conditions. Molecules other than MDA were shown to bind to TBA and this resulted in absorption spectra which overlapped with that of the MDA(TBA)₂ adduct, or even generated highly similar spectra (e.g. Kosugi and Kikugawa, 1986, 1989). The specificity of MDA detection can be enhanced by separating the MDA(TBA)₂ adduct by high pressure liquid chromatography (HPLC) coupled with UV detection, but specificity problems might still occur. The incubation of e.g. pyrimidine, 2-aminopyrimidine or sulfadiazine (Knight et al., 1988), as well as LPO products such as 2-alkenals, hexanal and 2,4-hexadienal (Kosugi et al., 1987; Sun et al., 2001) with TBA led to adducts which were indistinguishable by HPLC absorption spectrometry from MDA(TBA)₂. In summary, the TBARS method is not quantitative but it can sometimes help to obtain a basic idea of MDA levels in a given system. Recently, a method to visualize MDA *in situ* in seedlings of *Arabidopsis* based on TBA-derivatization and detection was presented (Mène-Saffrané et al., 2007). These experiments have to be well controlled (genetic and chemical controls) and must be validated by rigorous quantitative methods.

1.3.2 Quantitative methods for MDA determination

One way to overcome the pitfalls in MDA detection can be through the use of mass spectrometry to unambiguously identify peaks generated by gas chromatography (GC) or HPLC. For derivatization, 2,4-dinitrophenylhydrazine (DNPH; Shara and Dickson (1992)), O-(2,3,4,5,6-pentafluorobenzyl) hydroxylamine (PFBHA; Long et al. (2008)) or pentafluorophenyl hydrazine (PFPH; Yeo et al., 1994) are often employed. Yeo et al. (1994) described a method for the successful extraction of MDA from biological samples and the quantification of MDA based on an isotope-labeled (²H₂)-MDA internal standard. Comparison of this method with the commonly used TBARS assay proved the TBARS method to be inadequate as a quantification method, especially for *ex vivo* measurements (Liu et al., 1997). The TBARS assay was found to overestimate MDA levels between 2 to 10-fold (Fan, 2002; Liu et al., 1997; Yeo et al., 1994). Another way to detect MDA is with the help of antibodies which recognize epitopes of MDA cross-linked with proteins (Choi et al., 2003). This method is limited to the detection of bound MDA, but allows the detection of MDA cross-linked with proteins by immunohistochemistry or by Western-blotting (Choi et al., 2010; Taylor et al., 2011).

1.4 Sources and occurrence of MDA in higher eukaryotes

It is commonly believed that the bulk of MDA derives from the oxidation of lipids, and it is therefore used as an indicator for nLPO. Polyunsaturated fatty acids (PUFAs) with more than two methylene-interrupted double bounds are thought to provide the predominant substrate for MDA generation by nLPO (Esterbauer et al., 1991). The

1. INTRODUCTION: MALONDIALDEHYDE IN EUKARYOTES

susceptibility of PUFAs towards nLPO increases with increases in their length and more unsaturation, as demonstrated by *in vitro* oxidation of fatty acids (FAs; Liu et al., 1997). The order of susceptibility was 22 carbon-FAs > 20 > 18 with 22:6 > 22:4 > 22:3, and 18:3 > 18:2 > 18:1. Whether short diunsaturated FAs such as linoleic acid (18:2) provide a good substrate remains controversial. Esterbauer and Cheeseman (1990) reported that the efficiency of auto-oxidized 18:2 as a substrate for MDA generation was > 10-times lower than for γ -linolenic acid (18:3), 20:4 or 22:6. Quantitative comparison by GC/MS of *in vitro* oxidation of multiple FAs drew a different picture: the oxidation of 22:6 resulted in ~ 150 μmol MDA per mmol of FA and the oxidation of 18:3 and 18:2 resulted in $\sim 50\%$ and 30% of this, respectively (Liu et al., 1997). This underscores the necessity of performing studies where different PUFA levels are altered genetically.

1.4.1 MDA in the angiosperm *Arabidopsis thaliana*

The levels of ROS which drive nLPO and therefore MDA formation, are controlled by a very tight scavenging network in plants (Mittler et al., 2004). This reflects their reactive damaging character as well as their function as mediators in response to stress (Mittler et al., 2004). Despite their beneficial function as signals ROS are best known for their destructive potential, damaging DNA and proteins and lipids if not sufficiently scavenged (reviewed in Sharma et al., 2012). For plants the underlying mechanism of lipid peroxidation by ROS was shown to depend on the tissue; whether it is aerial or underground (Triantaphylidès et al., 2008). In photosynthetically active tissue, singlet oxygen ($^1\text{O}_2$) dominates as an oxidant whereas in root tissue radical-catalyzed lipid peroxidation drives the majority of nLPO. $^1\text{O}_2$ is formed in side reactions of photosynthesis in which triplet excited chlorophyll can act as a photosensitizer and pass its energy to molecular oxygen generating $^1\text{O}_2$ (Krieger-Liszkay, 2005). $^1\text{O}_2$ was shown to drive 85% of nLPO in leaves (Triantaphylidès et al., 2008) and might be responsible for the majority of peroxides which are substrates for MDA generation. Since ROS pose a potential threat to cells by damaging DNA and proteins, plants possess an entire arsenal of scavenging mechanisms (Mittler et al., 2004). These include enzymes such as superoxide dismutase, ascorbate peroxidase, catalase, glutathione peroxidase and peroxiredoxin and antioxidants like ascorbic acid and glutathione. They are complemented by the lipidic scavengers carotenoids and α -tocopherol. Recently, it was proposed that PUFAs might not simply be a target of harmful ROS but might provide supramolecular ROS sinks to prevent damage to other molecules such as proteins (Farmer and Mueller, 2013; Mène-Saffrané et al., 2009). This hypothesis is supported by the fact that membranes of ROS producing organelles such as chloroplasts are highly enriched in PUFAs (Li-Beisson et al., 2010). Furthermore, photosystem II (PS II), the major site of $^1\text{O}_2$ generation in plant cells, is surrounded and stabilized by these lipids (Loll

1.4 Sources and occurrence of MDA in higher eukaryotes

et al., 2005). This raises the question of whether the generation of MDA by nLPO is indeed a byproduct of a harmful non-intended reaction or might be beneficial for the cell.

To our knowledge, studies with the plant *Arabidopsis thaliana* have so far been the only ones showing that PUFAs can act as substrates for MDA generation *in vivo* (Mène-Saffrané et al., 2007; Weber et al., 2004; Yamauchi et al., 2008). Quantitative comparison between plants from a triunsaturated fatty acid (TFA)-lacking mutant (*fad3-2,fad7-2,fad8*; McConn and Browse, 1996) with WT plants revealed significantly reduced MDA levels (Weber et al., 2004). This triple mutant lacks all fatty acid desaturases which are responsible for the third desaturation of FAs. Quantitative measurements of MDA in this mutant demonstrated that $\sim 75\%$ of MDA in leaves of plants is derived from TFAs. Alternative sources which provide the remaining pools of MDA are not known so far. Interestingly, these results were not conferrable onto seedlings of *Arabidopsis*. Non-quantitative visualization of MDA pools in 4-d old seedlings of *Arabidopsis* plants showed no major difference in MDA-fluorescence between WT and *fad3-2,fad7-2,fad8* plants (Mène-Saffrané et al., 2007). This data suggested either different sources of MDA in roots of seedlings or a different underlying mechanism of formation. Analysis with a mutant lacking tocopherols and their intermediates (*vte2-1*) displayed increased MDA levels during the first days post germination (Sattler et al., 2006). These results suggested that tocopherols provide essential antioxidants during this short period protecting lipids from nLPO. Crosses of plants from the *fad3-2,fad7-2,fad8* mutant with *vte2-1* restored a *fad3-2,fad7-2,fad8* phenotype, demonstrating that TFAs were the major target producing MDA in *vte2-1* plants (Mène-Saffrané et al., 2007).

1.4.2 MDA in animals

Since MDA has been used extensively as an nLPO marker in disease, great attention was drawn to blood, plasma and serum levels of MDA in mice and man. As previously mentioned, huge variations of MDA levels were reported in different reports which can be explained by the use of the TBARS assay. The TBARS assay can at best be only considered as semi-quantitative for MDA. Strictly quantitative measurements reported low or undetectable levels of MDA in plasma (Liu et al., 1997). Comparison of MDA levels extracted from different tissues of rats (brain, liver, kidney and heart) revealed ranges between ~ 30 and 110 pmol mg^{-1} of protein (Liu et al., 1997). The highest concentrations were found in kidney and heart tissues. This correlates roughly with the ratio of PUFAs found in these tissues; 25% - 30% of PUFAs were reported for liver tissue and brain tissue of rodents (Igarashi et al., 2009; Kelley et al., 2006), whereas heart and kidney tissue contained 45-50% of PUFAs (Kelley et al., 2006; Kumasaka et al., 2007).

1. INTRODUCTION: MALONDIALDEHYDE IN EUKARYOTES

This correlation suggests that tissues which are enriched in PUFAs contain more MDA since it is formed from the latter. The underlying mechanism of MDA formation by nLPO in animal organs is likely driven by type I radical reactions. An exception might be light exposed tissue such as the skin and cornea. The type II nLPO inducing ROS $^1\text{O}_2$ was detected in the skin of rats (Yamazaki et al., 1999) and in the cornea (Wu et al., 2006), and might be responsible in these tissues for MDA generation. To our knowledge, no comprehensive study compared PUFA composition and MDA concentrations in mammals. A mouse model for the fatty acid desaturase 2 (FADS2) knock-out became available recently, diminishing radically the PUFAs content (Stoffel et al., 2008; Stroud et al., 2009). The MDA content of such mice has not yet been compared with WT rats and the genetic proof that MDA derives *in vivo* from PUFAs in mammals still remains elusive.

Deoxyribonucleosides in the presence of oxidizing conditions were shown to give rise to MDA and might provide an alternative source *in vivo* (Miyake and Shibamoto, 1999) in both, mammals and plants. Similarly, ionizing radiation caused the MDA formation from fructose, sucrose and glucose (Fan, 2003). The formation was hypothesized to derive from the reaction of sugars with free radicals. Furthermore, there is evidence that MDA is formed as a byproduct of the conversion of prostaglandins to thromboxane by the thromboxane synthase (Hecker et al., 1987), an enzyme which is absent in plants.

1.5 The role of malondialdehyde in eukaryotes

1.5.1 The toxicity of malondialdehyde

MDA is often regarded as a very toxic end-product of harmful nLPO, damaging the proteome and genome of cells (reviewed in Del Rio et al., 2005). This image is based on the reactive character of MDA readily binding at low pHs to nucleophilic sites such as thiols or amines forming Michael-type adducts (Figure 1.3). The reaction of MDA with

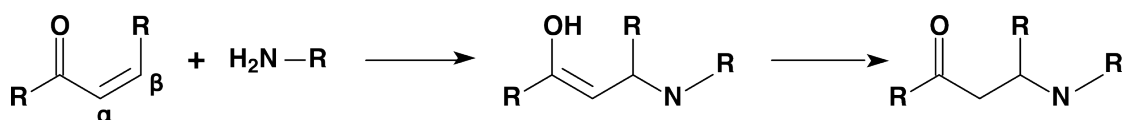


Figure 1.3: Michael adduct formation of α,β -unsaturated carbonyls - Mechanism of Michael-adduct formation between the electrophilic β -carbon of α,β -unsaturated carbonyls and the nucleophilic thiol or amine-groups. In this case reaction with an amine group is shown.

nucleic acid bases can form different adducts like pyrimido-[1,2- α]purin-10(3H)-one deoxyribose (M1dG, M1GdR or M1G) or cross-links between DNA strands (Niedernhofer

1.5 The role of malondialdehyde in eukaryotes

et al., 2003). These cross-links were also reported between MDA, DNA and proteins (Voitkun and Zhitkovich, 1999). A role of MDA was suggested in several cancer-related diseases as being a "biomarker of lipid oxidation and a potential concurrent cause of cancer initiation" (Del Rio et al., 2005). MDA concentrations necessary for these DNA modifications were often in the millimolar range and the experiments used MDA generated from 1,1,3,3-tetraethoxypropane (TEP) without further purification. Marnett and Tuttle (1980) demonstrated that MDA was only very weakly mutagenic and that mutagenesis was mainly due to TEP byproducts. The side products β -methoxy-acrolein 3,3-dimethoxypropionaldehyde, were shown to be > 35 -fold more toxic to *Salmonella typhimurium* than MDA (Marnett and Tuttle, 1980).

Whereas the genotoxic effect of MDA *in vivo* remains controversial, cross-linking with proteins is better understood. Studies with antibodies showed that MDA can cross-link to proteins (Choi et al., 2003) and screening of tissues of old and young rats revealed increased MDA cross-linking in kidneys of aged individuals (Choi et al., 2010). Aldehyde dehydrogenase 2 (ALDH2) was identified in this study as the main target of MDA. Linkage to MDA inhibited the nuclear translocation of ADH2 and it was suggested that MDA might be involved in the deleterious effects of aging processes. Similarly, MDA was shown to decrease mitochondrial respiration and the activity of respiratory enzymes (mitochondrial complexes IV, α -ketoglutarate dehydrogenase and pyruvate dehydrogenase) in isolated rat brain mitochondria (Long et al., 2009). It was hypothesized that this contributes to brain aging and neurodegenerative diseases. Similar, there is evidence in plants that MDA might have damaging effects such as inactivation of photosynthesis (Mano et al., 2009) and protein modification (Yamauchi et al., 2008; Yamauchi and Sugimoto, 2010). Using monoclonal antibodies recognizing MDA bound to protein, Yamauchi et al. (2008) found a temperature-dependent binding of MDA to proteins *in vitro* and *in vivo*. This reaction increased with higher MDA concentrations and with elevated temperatures. In another study, these results were extended and MDA was found to bind to the oxygen-evolving complex 33 kDa protein (OEC33), which decreased its binding capabilities towards photosystem II (Yamauchi and Sugimoto, 2010).

1.5.2 Possible beneficial roles of malondialdehyde

nLPO was reported to increase during stress such as pathogenesis leading to the generation of many oxylipin reactive electrophile species (RES) (Alm eras et al., 2003). RES oxylipins were shown to be biologically active and to stimulate the expression of pathogenesis-related genes independent of jasmonate signaling. A comparison of gene expression profiles of plants treated with RES or with avirulent bacteria revealed sim-

1. INTRODUCTION: MALONDIALDEHYDE IN EUKARYOTES

ilar results, suggesting a role of RES oxylipins in defense signal transduction (Alméras et al., 2003). This idea was extended for MDA, which was also found to induce a specific set of abiotic stress related genes, many of them being associated with pathogenesis (Weber et al., 2004). RES are found ubiquitously in eukaryotes and are present in the healthy resting state (Mueller, 2004; Weber et al., 2004). Pre-treatment with the RES B₁-phytoprostane has been shown to help plants to cope with nLPO, providing further evidence that RES might act as mediators communicating stress to cells (Loeffler et al., 2005). Infection experiments with the pathogens *Botrytis cinerea* (Muckenschabel, 2002) and *Alternaria brassiciola* (Weber et al., 2004) revealed that MDA levels were tightly controlled during pathogenesis, supporting the idea that MDA levels might be regulated in plants. It was hypothesized that basal MDA pools might become activated within stress responses and provide mediator function until an excessive level is reached which the cell is not capable to control anymore and in which situation MDA can become toxic (Farmer and Davoine, 2007). Farmer and Davoine (2007) suggested that basal levels of MDA are present in the non-reactive charged form (the enolate) and can quickly be turned into a more reactive form by a pH change. Generation of ROS during the hypersensitive reaction, or simple rupture of cells is likely to change the surrounding pH and make MDA a reactive molecule. The term "latent RES" was therefore proposed for MDA, a molecule which through a simple change in protonation could be rapidly mobilized in case of stress to activate cell survival signaling. This would explain why MDA levels first might decrease at the onset of stress, since they are used up in action (Farmer and Davoine, 2007).

1.6 The metabolism of malondialdehyde

In vitro experiments with purified mitochondria revealed turnover of exogenous MDA that was suggested to be driven by its oxidation via aldehyde dehydrogenases (Ghoshal and Recknagel, 1965; Haining et al., 1970). Placer et al. (1965) reported decreasing levels of TBA-reactive substances after the administration of MDA to rats, concluding that MDA might be metabolized. The potential metabolism of MDA was initially studied in detail by Siu and Draper (1982) *in vivo* and *in vitro*. Radiolabeled MDA was administered as a oral dose and the rats were then transferred into metabolic cages for analysis of exhaled CO₂, blood, urine and feces for radioactivity. The recovered radioactivity was predominant (> 60%) in the exhaled CO₂ after 12 h. *In vitro* experiments with mitochondria from liver extracts showed a decline of TBA-reactive substances over time after application of ¹⁴C-MDA together with ¹⁴CO₂ release. The reaction speed and the CO₂ release from MDA turnover was not altered by malonate addition prior to MDA application and, based on these observations, malonate might not represent

1.6 The metabolism of malondialdehyde

an intermediate in a potential MDA metabolism. Siu and Draper (1982) proposed an oxidation of MDA to malonic semialdehyde (MSA) and decarboxylation to acetaldehyde which would cause the CO₂ release. This was in accordance with the accumulation of acetate in the *in vitro* samples. These findings were extended shortly afterwards by Marnett et al. (1985). More detailed distribution analysis of orally administered ¹⁴C-MDA showed that MDA was quickly distributed within all organs and turned over within a few hours. This was accompanied with the release of ¹⁴CO₂. As potential intermediates, different labeled isotopes of ¹⁴C-acetate, ¹⁴C-malonate and ¹⁴C-β-alanine (as MSA precursor) were administered to rats and the results of their metabolism were compared with the results from MDA. All of the molecules tested, except 2-¹⁴C-malonate and 2-¹⁴C-β-alanine, led to a recovery greater than 70% which suggested similarities in the turnover with MDA (Marnett et al., 1985). Importantly, the administration of labeled acetate led as well to a recovery of >70% in CO₂ similar to 1,3-¹⁴C-MDA. Since acetate is not decarboxylated prior to FA-assembly, it suggested a TCA-cycle-dependent or FA-β-oxidation-dependent turnover and release of ¹⁴CO₂. To further test acetate and malonic semialdehyde as intermediates, these compounds were administered shortly prior to MDA application. Low doses of acetate and high doses of β-alanine showed inhibitory effects on MDA metabolism, which supported the hypothesis that they might be intermediates. MDA metabolism was inhibited by the aldehyde dehydrogenase inhibitors ethanol (5 mmol/mouse) and Disulfiram (134 μm/mouse), by 40% and 70% respectively, which suggested involvement of these enzymes. Separation and analysis of lipids revealed 20% of the administered radioactivity in lipids, mostly in cholesterol. The overall conclusion was that ¹⁴C-MDA-derived ¹⁴CO₂ came from either a.) earlier metabolic steps including decarboxylation, b.) β-oxidation of FAs or c.) that the intermediate acetyl-CoA might enter the TCA cycle and release ¹⁴CO₂ (Marnett et al., 1985).

To our knowledge there are no reports concerning MDA metabolism in plants. Application of exogenous MDA was reported to be turned over and underlying detoxification mechanisms were suggested (Weber et al., 2004). Recently, Mène-Saffrané et al. (2009) suggested that PUFAs might provide a sink for ROS similar to an antioxidant which is used up in action. This idea is supported by the independent study of Zoeller et al. (2012). This suggested that nLPO itself might represent a process that has adaptive value for cells and this complements the idea that MDA is turned over efficiently. The presence of chloroplasts with the possibility to assemble fatty acids from acetate and malonate, helps us to make predictions for MDA metabolism based on results from rats (Marnett et al., 1985; Siu and Draper, 1982). It is furthermore likely that CO₂ release from a potential decarboxylating mechanism will not be easily measurable, since the plant might use it directly for CO₂ fixation.

1. INTRODUCTION: MALONDIALDEHYDE IN EUKARYOTES

2

Goals of the thesis

In this thesis, I attempt to characterize first the sites of MDA localization and sources of its production throughout the plant body and at different developmental stages. It is necessary to assess whether the sites of MDA formation differ in their spatial and temporal appearance, as well as their inducibility. A non-quantitative technique to visualize MDA pools will be used, complemented by quantitative GC/MS measurements. The GC/MS analyses allow us to go beyond MDA quantification and to distinguish the nature of MDA pools: whether MDA is mainly present as a free enolate or, as the result of potentially harmful reactions, bound to macromolecules. The mutant *fad3-2,fad7-2,fad8* which lacks triunsaturated fatty acids will serve as a genetic tool to evaluate the source of MDA formation from the different sites. The quantitation and localization of MDA is necessary prior to understanding the biological functions of MDA.

In a next step I want to extend the hypothesis that nLPO of PUFAs in plants might be a part of a ROS-protection mechanism, preventing damage of macromolecules such as PS II in the chloroplasts. It is intriguing that PS II, a site of ROS production, is surrounded by PUFAs which are prone to oxidation by the latter. We hypothesize that nLPO might be a beneficial mechanism and that the subsequent MDA generation and its fate might be controlled by the plant. Therefore, we want to follow the fate of MDA using isotope-labeled MDA and test the hypothesis that MDA might be recovered upon formation to recycle its carbon and detoxify a potential harmful molecule. In order to do this it is necessary to develop new tools for the efficient production and purification of isotope-labeled MDA.

2. GOALS OF THE THESIS

3

Characterization of resting MDA pools in plants ¹

3.1 Introduction

During a study of *Arabidopsis* seedlings undergoing severe oxidative stress (Mène-Saffrané et al., 2007) we developed a method for localizing pools of MDA *in situ* using the reagent 2-thiobarbituric acid (TBA). The method serves as a complement to specific quantitative assays based on a cognate MDA internal standard: 2H_2 -MDA (Liu et al., 1997; Yeo et al., 1994). TBA is a non-specific chemical reagent for MDA detection, but its specificity is enhanced by using fluorescence detection of MDA-TBA adducts (Janero, 1990; Tatum et al., 1990). In the present work we first conducted a quantitative analysis of MDA pools throughout the vegetative body of *Arabidopsis*. We then used *in situ* MDA detection and genetic analyses to localize major pools of MDA at the cellular and sub-cellular levels in leaves, in seedlings, and in the roots of seedlings. This revealed several cell types associated with high MDA levels but the largest pools of the aldehyde in the plant body were found in mesophyll cell chloroplasts (where a high proportion of MDA originates from TFAs). We show that the root proliferation zones (meristems) contain intracellular MDA most of which is not derived from TFAs. MDA was also detected in the pericycle, a cell type that retains its capacity to proliferate. In a next step, we provide evidence for a potential new source of MDA, beyond the present known lipid oxidation of TFAs.

¹This chapter was taken from Schmid-Siegert et al. (2012) with minor modifications. Emanuel Schmid-Siegert and Jorge Loscos contributed equally, as well as to the experimental part of the characterization of *fad2-2,fad6* mutants. Sequencing of the *fad2-1* mutation was obtained with help of O. Stepushenko.

3. CHARACTERIZATION OF RESTING MDA POOLS IN PLANTS

3.2 Material and Methods

Plant growth conditions, genotypes and chemicals - Wild-type (WT) *Arabidopsis* (Col-0), *fad3-2,fad7-2,fad8* (McConn and Browse, 1996), *jar1* (Staswick et al., 1992), *npr1* (Cao et al., 1994) and peroxisome targeting sequence1:green fluorescent protein: (PTS1:GFP) expressing plants (Mano et al., 2002) were grown on soil at 22°C for 5 weeks (light: 100 $\mu\text{E m}^{-2} \text{s}^{-1}$, 9 h light/15 h dark), or on 0.7% agar (w/v, in water) for 4 d (15 h light/9 h dark). Chemicals used were purchased from Sigma (St. Louis, Missouri, USA) unless indicated. (2D₂)-1,1,3,3-tetraethoxypropane was purchased from Dr. Ehrenstorfer GmbH, Augsburg, Germany.

Organelle purification and characterization - Chloroplasts were purified as described (Rodríguez et al., 2010) and chlorophyll was determined by spectrophotometry (Porra, 2002). Mitochondria were enriched by differential centrifugation (Jauh et al., 1999). The mitochondrial pellet was resuspended in buffer (20 mM Tricine/KOH pH 7.6, 2.5 mM EDTA, 5 mM MgCl₂, 300 mM sorbitol). Proteins were precipitated at 2°C using trichloroacetic acid (TCA, 8% w/v), quantified with a bicinchoninic acid (BCA) protein assay Kit (Thermo Scientific, Waltham, Massachusetts, USA), and separated by electrophoresis on SDS-PAGE gels (12% w/v acrylamide). Blotting was conducted using a semi-dry blotter (Bio-Rad Hercules, California, U.S.) and protein loading was evaluated by staining with Ponceau red (1% v/v). For the detection of proteins with antibodies, the membrane (Trans-Blot, Bio-Rad Hercules, California) was incubated with Amersham ECL Plus™ Western Blotting Detection Reagents for 2 min followed by phosphor-imaging with an ImageQuant (GE Healthcare, Little Chalfont, United Kingdom). Antibodies used were against gamma tonoplast intrinsic protein (γ -TIP; Jauh et al., 1999), catalase (Mano et al., 2002), lipoxygenase 2 (AtLOX2; Glauser et al., 2009) and voltage-dependent anion channel1 (VDAC1; Clausen et al., 2004). Nuclei and damaged chloroplasts stain with DAPI (4',6-diamidino-2-phenylindole, 0.1 $\mu\text{g ml}^{-1}$ for 0.5 h on ice) and their number per non-stained chloroplasts was assessed by fluorescence microscopy as was the number of peroxisomes in chloroplast preparations from PTS1:GFP-expressing plants. Fluorescence and transmitted light photos (100x magnification) of chloroplast samples were taken with a stereo-microscope (Leica ZM16FA, Solms, Germany).

2-Thiobarbituric acid (TBA) staining - Leaves (still attached to the plant) were soaked in 35 mM TBA solution and vacuum infiltrated (3 times 10 seconds). Next, samples were incubated for 60 min at 35°C and fluorescence monitored by confocal microscopy (Leica SP2 confocal microscope). Extracted chloroplasts were incubated in 35

3.2 Material and Methods

mM TBA (or 35 mM TCA as control) for 1 h at 35°C in the dark and the fluorescence was monitored. Seedlings were grown at 22°C for 4 d on 0.7% agar (w/v, in water) and transferred into 35 mM TBA or TCA solutions and incubated at 25°C for 90 min prior to microscopy. MDA-TBA adduct emission: 555 ± 15 nm, excitation 515 nm; auto-fluorescence of chloroplasts: emission 664-696 nm, excitation: 488 nm.

Gas Chromatography / Mass Spectrometry (GC/MS) - Quantification based on a specific pentafluorophenylhydrazine (PFPH)-MDA adduct was used with (D₂)-MDA as an internal standard (IS) based on Yeo et al. (1994). (D₂)-MDA was obtained by hydrolysis from (D₂)-1,1,3,3-tetraethoxypropane (TEP). Plant material (about 150 mg) was harvested, frozen in liquid nitrogen and ground to a fine powder. The frozen powder was added to PBS containing 1 mM deferoxamine mesylate, 50 μ M 6-hydroxy-2,5,7,8-tetramethylchroman-2-carboxylic acid (Trolox), 50 pmol IS and 6.6 N H₂SO₄ (10 μ l) and incubated for 10 min on ice, in the dark. Sodium tungstate (0.3 M, 75 μ l) was then added and the samples centrifuged to precipitate protein (Yeo et al., 1994). The supernatant was combined with buffer (0.21 M citric acid, 0.58 M Na₂HPO₄; pH 4) and 50 μ l of PFPH reagent (5 mg ml⁻¹ in water) and incubated for 3 h at 22°C. 9 μ l of 9 N H₂SO₄ was added, and the MDA-PFPH product was extracted with 125 μ l of iso-octane. The organic phase was recovered, and 1 μ l of a 1:5 dilution was analyzed by GC/MS in electron ionization (EI) mode with split-injection (1:50), except for MDA analysis in the extracted chloroplasts samples (splitless mode, no dilution, chemical ionization using methane). The temperature gradient was 50°C for 1 min, 50 - 150°C at 10°C min⁻¹ and 150 - 280°C at 20°C min⁻¹. Quantification was carried out using selective ion monitoring measuring (*m/z* 234 for MDA and 236 for the internal standard).

Root sectioning - Seedlings were grown at 22°C for 4 d on 0.7% agar (w/v in water) plates and transferred into 35 mM TBA or TCA solutions, incubated at 25°C for 90 min, washed with 50 mM potassium phosphate buffer (pH 6) and incubated with Calcofluor White (0.1% w/v) and Evan's Blue (0.05% w/v) for 5 min. Plants were then washed as before and vacuum-infiltrated (3 x 15 min each) with 4% (w/v) paraformaldehyde in buffer (50 mM PIPES/KOH pH 6.5, 5 mM EGTA, 5 mM MgSO₄). Seedlings were then embedded in agarose (10% w/v) and sectioned (50 μ m) with a Vibrotome (Leica VT1000S). Samples were visualized using a DM5000 Leica epifluorescence microscope with a YFP (yellow fluorescent protein) filter for MDA(TBA)₂ or a blue filter for cell wall fluorescence (Leica filter cube A4 : excitation 320-400 nm, emission 430-510 nm). Confocal microscopy and comparison of emission spectra for TBA-MDA adducts and root tips treated with TBA used a Leica SP2 microscope. Piperonylic acid (PA) was dissolved in ethanol (10 mM stock solution in ethanol) and diluted 1:1000 in water prior

3. CHARACTERIZATION OF RESTING MDA POOLS IN PLANTS

incubation (16 h at 22°C) of seedlings.

Generation and identification of fad2,fad6 double mutants - F2 seeds from crosses of *fad2-2* and *fad6* plants were germinated on Gamborg salt (3.1 g l⁻¹, Gibco) media pH 5.6, 0.6% agar (w/v) and 1% (w/v) sucrose. For growth in flasks, they were transferred in 250 ml Erlenmeyers with 50 ml media (Gamborg salt 3.1 g l⁻¹ and 1% sucrose) and continuously shaken at 120 rpm in short-day growth conditions. Fatty acid analysis by GC/MS was done after derivatization with 2.5% (v/v) H₂SO₄ in MeOH (Miquel and Browse, 1992). Leaf tissue was submerged in 1 ml acidic MeOH and heated for 90 min at 80°C. 1.5 ml of 0.9 % NaCl solution and 1 ml of hexane were added and vortexed to extract the FAs in the organic phase. The organic phase was concentrated with N₂ prior GC/MS-analysis (initial T = 150°C for 3 min, followed by an increase of 15°C min⁻¹ to 210°C). Sequencing of *fad6* was done with the following primers: *fad6*-f1: gaggtgagggctcttcacag, *fad6*-f2: gtggttggttggttgatg, *fad6*-f3: gctctctccactgtcctctt, *fad6*-f4: gagcgaggtgaatagggtga, *fad6*-R1: agaagctcatcgcttgaaa.

3.3 Results

The quantitative GC/MS method developed by Yeo et al. (1994) was used to measure malondialdehyde (MDA). A potential complication during MDA extraction is the formation of reactive oxygen species to cause lipid oxidation, a potential source of MDA (Esterbauer et al., 1991; Janero, 1990). We sought to minimize this and found that replacing the 2,6-tert-butyl-4-methylphenol from (Yeo et al., 1994) with Trolox (6-hydroxy-2,5,7,8-tetramethylchroman-2-carboxylic acid) reduced MDA production *in vitro*, a known phenomenon with plant tissues (Weber et al., 2004). Also, the procedure was conducted under low light and on ice. Total and free MDA in the leaves of adult plants and in whole 4 d old seedlings was measured, as were MDA levels in the dissected roots of seedlings. The use of the *fad3-2 fad7-2 fad8* mutant (McConn and Browse, 1996) enabled us to quantify the proportion of MDA that originates from TFAs in each of these tissues. The TBA staining method (Mène-Saffrané et al., 2009) was used to identify cell types containing MDA and to look for inducibility in MDA pools.

3.3.1 Adult leaves

Levels of MDA in expanded Arabidopsis leaves were 33.01 ± 1.63 nmol g⁻¹ dry weight (D.W.) for the WT and 13.74 ± 0.70 nmol g⁻¹ D.W. for the *fad3-2,fad7-2,fad8* mutant (Figure 3.1 A). These values indicated that approximately 58% of total MDA in resting leaves derives from the oxidation of TFAs. Omitting incubation with 6.6 N H₂SO₄ during the MDA extraction protocol allowed us to discriminate between the free and

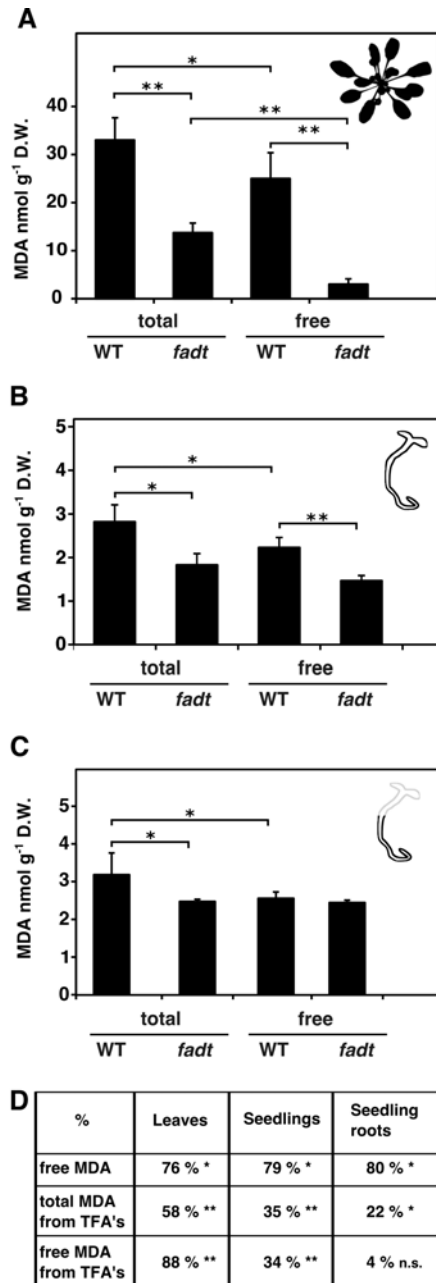


Figure 3.1: Scale and origin of MDA pools - Bound and free MDA pools in adult leaves and 4 d seedlings of WT and *fad3-2,fad7-2,fad8* (*fadt*) were quantified by GC/MS. Acid hydrolysis prior to derivatization was used to measure total MDA and omitted for measurement of unbound MDA. **A.** Rosette leaves; 8 biological replicates, **B.** Whole seedlings; 8 replicates, **C.** Seedling roots; 5-8 replicates. **D.** Overview of results. * $P < 0.05$; ** $P < 0.001$; n.s. = not significant.

3. CHARACTERIZATION OF RESTING MDA POOLS IN PLANTS

bound pools of MDA (Yeo et al., 1994). An estimated 25.02 ± 2.03 nmol g⁻¹ D.W. of the MDA in WT and 3.02 ± 0.39 nmol g⁻¹ D.W. in *fad3-2,fad7-2,fad8* leaves was found to occur in its free form. This represents 76% of total MDA in WT leaves and 22% of total MDA in the *fad3-2,fad7-2,fad8* mutant. Quantities of bound MDA were estimated to be similar in both genotypes.

3.3.2 Whole seedlings

Levels of bound and free MDA pools in 4 d old seedlings were established (Figure 3.1 B). Non-TFA derived MDA represents the majority in whole seedlings, being responsible for 65% of the total MDA. In WT seedlings, the percentage of free to total MDA was 79%, similar to the results obtained in WT leaves. The ratio for *fad3-2,fad7-2,fad8* seedlings on the other hand was 80% of free MDA, compared to 22% of free MDA in the leaves.

3.3.3 Seedling roots

Putative pools of MDA in the roots of both the WT and *fad3-2,fad7-2,fad8* seedlings were reported (Mène-Saffrané et al., 2007). Here we used quantitative MDA measurements to validate these initial observations. Roots were dissected off 4 d old seedlings just below the hypocotyl (Figure 3.1 C). Approximately 50 mg D.W. of roots (equal between 1500-2000 roots) were used for each data point and this was replicated five times to provide an average value. The total root MDA levels were 3.18 ± 0.20 nmol g⁻¹ D.W. and 2.47 ± 0.03 nmol g⁻¹ D.W. for the WT and *fad3-2,fad7-2,fad8*, respectively. In contrast to total MDA levels in leaves and whole seedlings, levels in isolated roots were very similar between WT and *fad3-2,fad7-2,fad8* and only 22% ($P=0.01$) of the MDA in the root was found to be derived from TFAs. The ratio of the free MDA pool with respect to the total MDA in WT roots was approximately the same as in leaves or whole seedlings (~80%).

3.3.4 Sub-cellular localization of MDA in leaves

There is little information on the localization of MDA in plants although there are reports that it is found in chloroplasts in heat-stressed plants (e.g. Yamauchi et al., 2008). To localize MDA, expanded leaves were infiltrated with 35 mM TBA (or with 35 mM trichloroacetic acid [TCA] as negative control) and fluorescence was observed using confocal microscopy (Figure 3.2). As expected, both the TCA control and the TBA-treated samples showed chloroplast auto-fluorescence. However, only in the TBA-incubated sample was green fluorescence clearly visible. The auto-fluorescence and the green TBA-associated fluorescence of the chloroplasts co-localized well, although we noted stronger fluorescence in the chloroplast regions proximal to the tonoplast (arrowhead in Figure

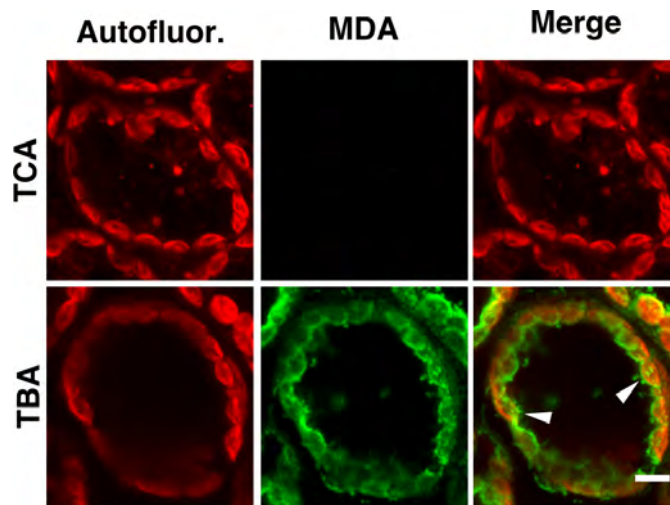


Figure 3.2: *In situ* MDA staining in leaves - TBA (35 mM) or TCA (35 mM, as a control) solutions were vacuum infiltrated into leaves of intact 5 week old plants 1 h prior to microscopy. Red auto-fluorescence of chloroplasts is shown in the first column. Green fluorescence is only visible in the leaves infiltrated with TBA. Arrowheads indicate polarization of MDA staining. Pictures taken with the same settings, scale bar = 5 μ m.

3.2). During these experiments we noted that TBA-generated fluorescence was weak in the epidermis except in stomata (not shown).

3.3.5 Isolation of chloroplasts

Intact chloroplasts were purified from leaves and DAPI staining allowed us to estimate a maximum contamination with $0.50\% \pm 0.36\%$ S.D. of nuclei and broken chloroplasts. Chloroplast isolates from plants expressing a fluorescent peroxisome marker (Mano et al., 2002) were next analyzed by microscopy to estimate the contamination by peroxisomes (Figure 3.3) and a maximum of 1.5% of contaminating organelles were peroxisomes. Next, a series of organelle-specific antigens was chosen for immunoblot analysis of chloroplast fractions (Figure 3.4 A). LOX2 protein bands were visible in both intact chloroplasts and, as expected, in the crude extract which was rich in chlorophyll and broken chloroplasts. Anti- γ -TIP antibody (Jauh et al., 1999) was used to evaluate contamination by tonoplasts and the lack of this band in the chloroplast sample indicates a lack of tonoplast contamination. An anti-catalase antibody (Mano et al., 2002) was used as a second test for peroxisome contamination; the results were negative. Finally, immunodetection of the mitochondrion-specific marker protein VDAC1 (Clausen et al., 2004) revealed a weak band in the positive control and no band in the chloroplast fraction. We extended this investigation by using an enrichment for mitochondria to provide

3. CHARACTERIZATION OF RESTING MDA POOLS IN PLANTS

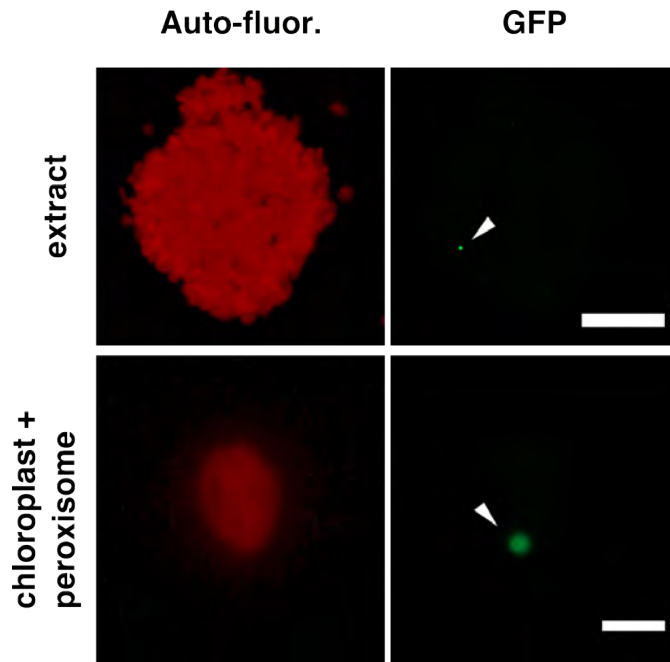


Figure 3.3: Peroxisomes in chloroplast extracts - Evaluation of peroxisomes in chloroplast extract to estimate the purity of the extracts. Chloroplasts were extracted from GFP:catalase expressing plants. Chloroplast-auto-fluorescence in the first column, GFP fluorescence in the second column. Extract = chloroplast clusters from extracted chloroplast samples, scale bar = 50 μm ; second row higher magnification of a single peroxisome attached to a chloroplast, scale bar = 5 μm .

a second positive control to verify the proper functioning of the antibody. Only the mitochondrion-enriched sample showed a clear band for the VDAC1 protein.

3.3.6 Characterization of chloroplastic MDA

Isolated chloroplasts were stained with TBA to visualize MDA (Figure 3.4 B). Again, faint auto-fluorescence was observed in the TCA control reflecting the observation made during *in situ* MDA staining (Figure 3.2). However, the WT TBA-treated sample showed a strong green fluorescence although the asymmetry of the TBA staining seen *in situ* (Figure 3.2) was lost in isolated chloroplasts. The fluorescence in TBA-treated *fad3-2,fad7-2,fad8* chloroplast isolates appeared much reduced compared to the WT isolates indicating the presence of residual MDA pools in *fad3-2,fad7-2,fad8* chloroplasts. WT chloroplasts were found to contain 3.50 ± 1.10 nmol MDA mol⁻¹ of chlorophyll and *fad3-2,fad7-2,fad8* 1.50 ± 0.85 nmol MDA mol⁻¹ of chlorophyll (Figure 3.4C) and this difference was significant ($p = 4.6 * 10^{-6}$). MDA levels in the *fad3-2,fad7-2,fad8* chloroplasts represent 42% of MDA levels in the WT.

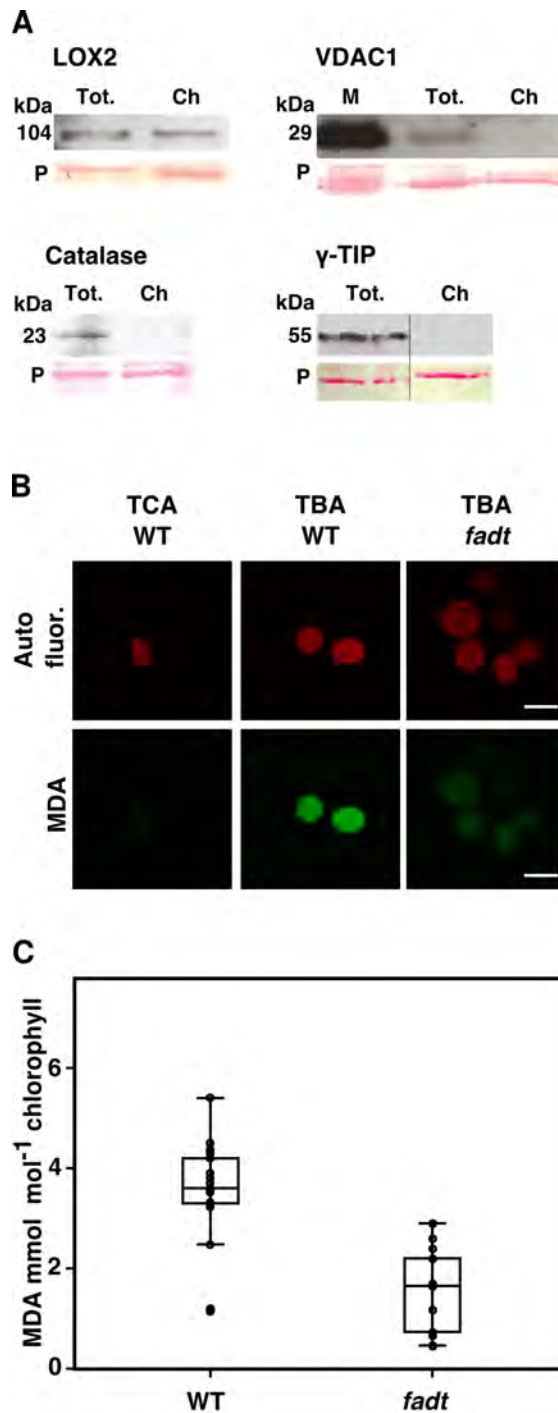


Figure 3.4: Isolated chloroplasts contain MDA - A. Immunological characterization of chloroplasts. Markers: LOX2 (chloroplasts), γ -TIP (tonoplast), catalase (peroxisomes), VDAC1 (mitochondria). Tot. = total crude extract, Ch = purified chloroplasts, M = mitochondrion-enriched sample. P = Ponceau Red staining for the RuBisCO large subunit and served as a protein loading control. **B.** Incubation of chloroplasts with TBA (or TCA as a control). In the first row red chloroplast auto-fluorescence is shown. The second row shows the fluorescence of WT and TFA-lacking chloroplasts after TBA-staining. All pictures were taken with the same settings, scale bar = 5 μ m. **C.** MDA levels normalized to chlorophyll levels in isolated chloroplasts. The circles represent single samples and the horizontal bar represent medians. Three biologically independent extractions, 16 replicates.

3. CHARACTERIZATION OF RESTING MDA POOLS IN PLANTS

3.3.7 Localization of MDA in roots

Roots have very different optical properties to those of leaves, so TBA staining of roots was optimized by testing various incubation times (30 min to 5 h) and temperatures (20 to 37°C). The incubation of seedlings with 35 mM TBA at 25°C for 90 min resulted in good visualization of the putative MDA pools in roots. Consistent with Mène-Saffrané et al. (2007) we found strong TBA-dependent fluorescence near the root tips and there was little or no difference in the intensity of the fluorescence between the two genotypes. WT roots were treated with TBA (or TCA as a control) and then sectioned (Figure 3.5). No strong auto-fluorescence signal was observed in roots incubated with TCA (data not shown). TBA-dependent fluorescence in the proliferation region localized inside the undifferentiated meristematic cells. In contrast, TBA-dependent fluorescence in the sections of the elongation zone had a complex pattern with staining falling into two categories. Firstly, diffuse staining was seen in the stele and in particular in the pericycle and extending into other smaller cells in the stele (Figure 3.5 C). However, with the exception of casparian strips, the endodermis was not stained. A second type of staining pattern in the elongation zone was less diffuse. This was always associated with cell surfaces and included the protoxylem walls, casparian strips, and the outer face of epidermal cells. With the exception of the casparian strips, this staining co-localized with the Calcofluor cell wall stain. Both xylem and casparian strips contain phenolic material so we used the lignin synthesis inhibitor piperonylic acid (PA; Schalk et al., 1998) to investigate a possible association of TBA staining and lignification. Treatment of 4 d old WT seedlings for 18 h with PA (10 μ M) did not affect the overall TBA staining pattern seen in the plants (not shown). Comparison of the emission spectrum of synthetic MDA-TBA adducts with that of TBA-stained roots cells under closely similar conditions in a confocal microscope yielded similar but not identical spectra (Figure 3.6 A). Specifically, the tissue stacks displayed both an emission maximum near 550 nm (also seen with synthetic TBA-MDA adducts) as well as a prominent shoulder near 560 nm. We further examined the tips of WT roots with confocal microscopy. Using DAPI staining we were able to localize nuclei in outer cells near the root tip. In contrast, fluorescence due to TBA treatment of tissues was diffuse. This green fluorescence was observed in the nuclei in some cells near the cortex but was far weaker in cells in the outermost cell layers (Figure 3.6).

3.3.8 MDA in cell proliferation zones

In seedling roots the majority of MDA fluorescence was located in the root tip (Figure 3.6), a zone of high cell proliferation. We examined leaf and root primordia in seedlings to validate whether MDA accumulation and cell proliferation might correlate. MDA

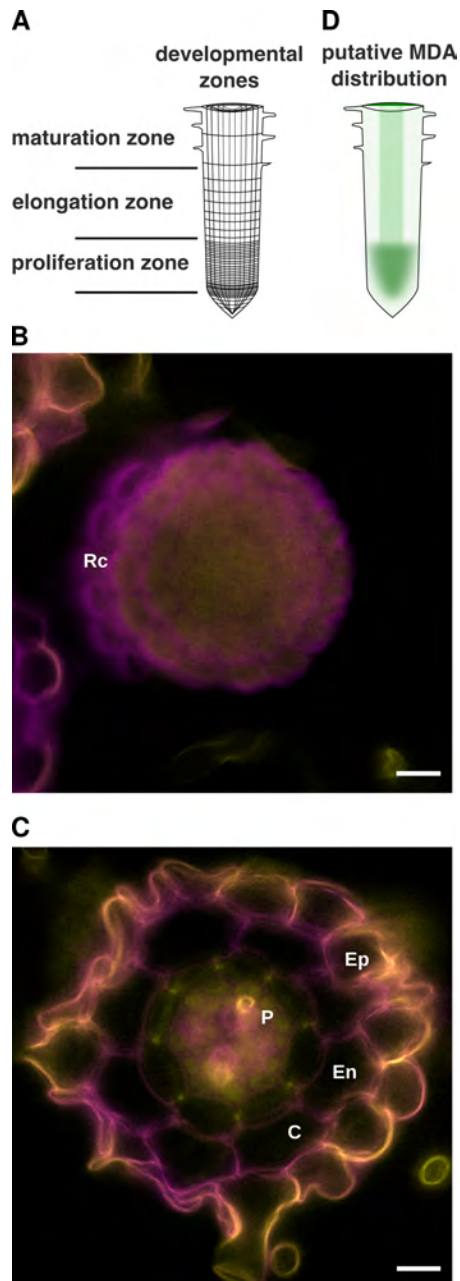


Figure 3.5: Distribution of putative MDA pools in the lower root - **A.** Developmental regions in the root. **B.** and **C.** Merged confocal images of fluorescence generated by staining with Calcofluor White/Evans Blue (magenta signal) and TBA (yellow signal). **B.** Transverse section of the root tip cell proliferation zone. Rc = root cap cells. **C.** Transverse section of the elongation zone. P = pericycle, En = endodermis, C = cortex, Ep = epidermis. Scale bars = 10 μ m. **D.** Scheme summarizing the localization of putative MDA pools relative to developmental zones.

3. CHARACTERIZATION OF RESTING MDA POOLS IN PLANTS

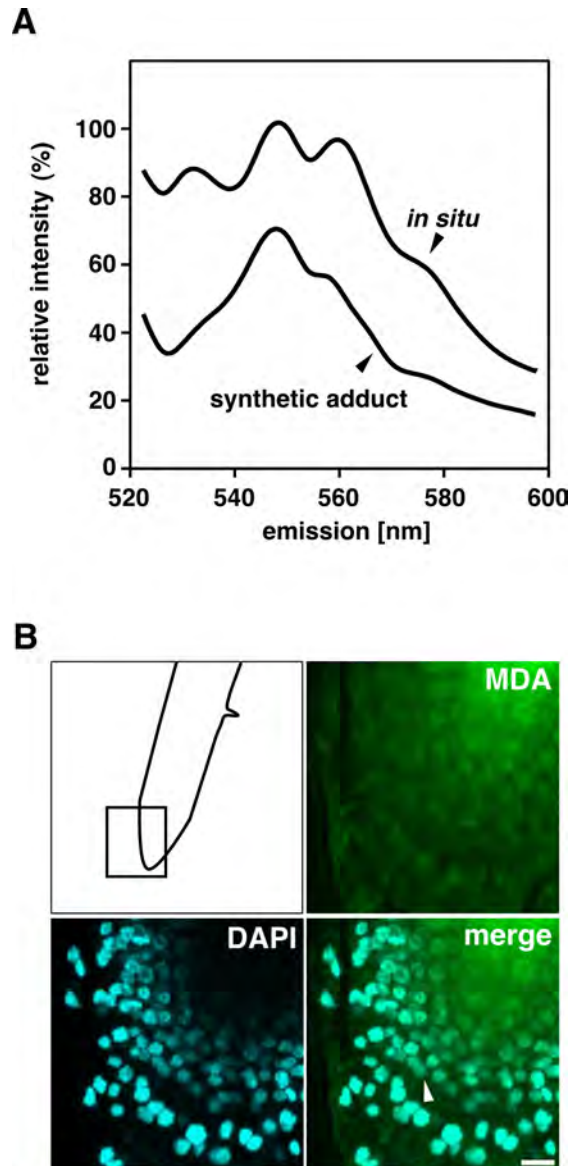


Figure 3.6: Characterization of MDA-TBA adducts in the root tip. - **A.** Emission spectra of soluble TBA-MDA adducts produced in solution (synthetic adduct) and *in situ* stained root tips. Data sets were gathered under identical conditions using confocal fluorescence microscopy. **B.** Confocal images of the root tip stained with DAPI to detect nuclei (cyan) and with TBA to detect MDA (green). The arrowhead shows a nucleus that showed TBA-related fluorescence.

was visualized by TBA staining in the region of the apical meristem and within sites of lateral root formation (Figure 3.7). To promote lateral root initiation we grew seedlings on naphthyl acetic acid prior MDA staining. This facilitated visualization of MDA during different stages of lateral root formation. MDA-fluorescence was increased in cells upon the initiation of lateral root formation and during the entire process of lateral root emergence (Figure 3.7 A). The accumulation of MDA in emerging roots was not derived from cell damage initiated during the epidermis rupturing process, as judged by strong MDA presence prior to this emergence. The apical meristematic zone of seedlings was analyzed next and showed strong MDA fluorescence in zones of cell division (Figure 3.7 B, white arrow). The increased MDA concentration in proliferating tissue seemed to be valid as well in reproductive tissue of flowering plants, e.g. in the stigma and style (Supplementary Figure 8.1).

3.3.9 Alternative sources for MDA generation in plants

The fact that the leaves of the *fad3-2,fad7-2,fad8* mutant still contain MDA suggested alternative sources of MDA formation beyond TFAs. This became more evident for seedling roots, in which only 22% of MDA was derived from TFAs (Figure 3.1 C,D). One possibility, based on a similar mechanism as MDA formation from TFAs, remained the non-enzymatic oxidation of diunsaturated FAs, like hexadecadienoic acid (16:2) and linoleic acid (18:2). To test this hypothesis we analyzed a mutant lacking di- and triunsaturated FAs, the *fad2-2,fad6* mutant (McConn and Browse, 1998). Homozygous plants were not readily available and we crossed plants of *fad2-2* with *fad6*. McConn and Browse (1998) reported, that homozygous double mutants failed to grow autotrophically and needed to be supported with sucrose. F2-plants were therefore grown on Gamborg salt media and supplemented with 1% sucrose. First, homozygous double mutants were identified by their dwarfish and chlorotic phenotype and their FA-composition compared with wild-type plants (Figure 3.8 A). The FAs 18:3, 16:3, 16:0 and 18:2 were detected in the WT leaves. Among them 18:3 and 16:3 were most abundant which correlated with published data (summarized in Table 3.1). In plants which were identified by their dwarf phenotype to be homozygous *fad2-2,fad6*, only 18:1 and 16:0 FAs but no PUFAs were detected. The 18:1 represented $\sim 80\%$ and 16:0 $\sim 20\%$ of the total FAs content, which was in accordance with published data (85% of 18:1 and 15% of 16:1; McConn and Browse, 1998). Next, homozygous *fad2-2,fad6* plants were transferred into liquid media and grown for 7 weeks. *fad2-2,fad6* plants grew very slowly compared to mixed genotype- and WT-plants and showed chlorotic leaves (Figure 3.8 B). We measured MDA levels in rosettes of potential homozygous *fad2-2,fad6* plants and compared them with rosettes of wild-type and mixed genotype plants (from F2, but not homozygous according to their morphological WT-phenotype). The same amount of tissue (~ 18

3. CHARACTERIZATION OF RESTING MDA POOLS IN PLANTS

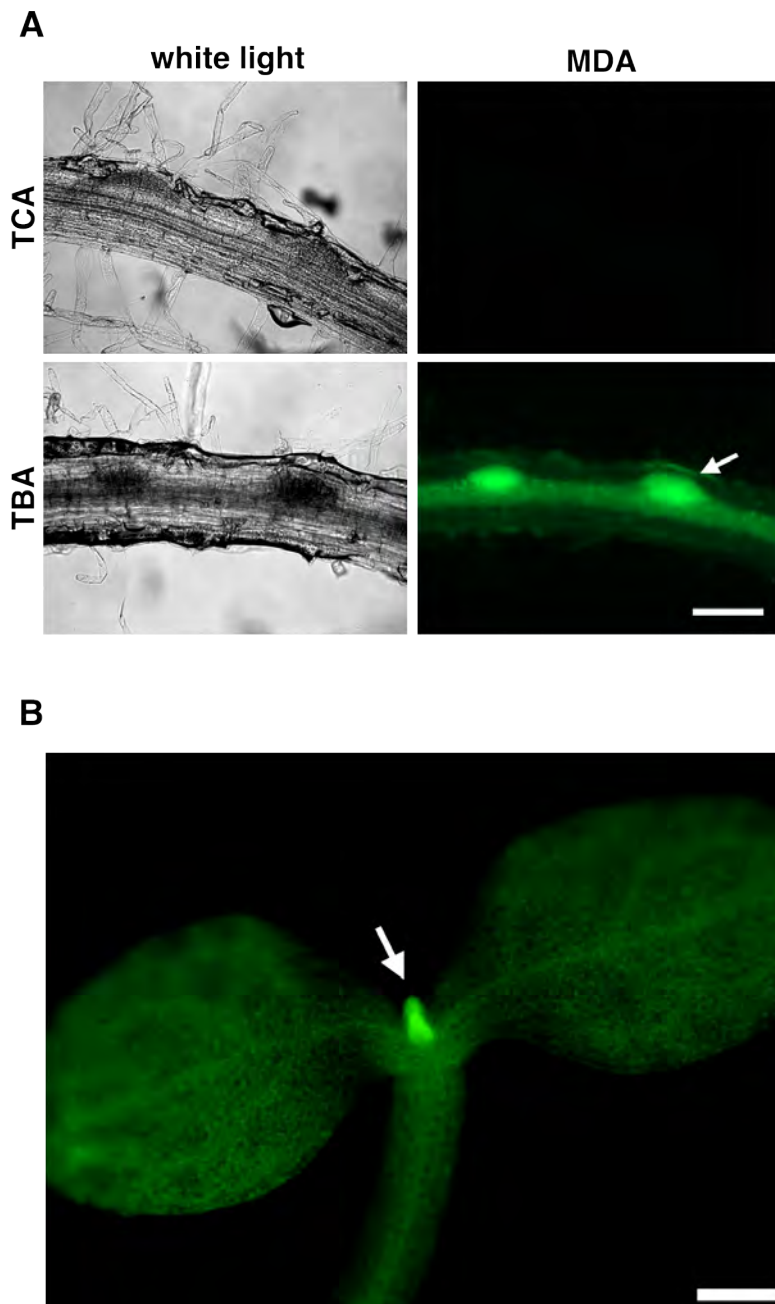


Figure 3.7: MDA in zones of cell proliferation - **A.** Accumulation of MDA in newly formed lateral roots of *Arabidopsis* seedlings (5 d old). Green MDA- fluorescence correlated with lateral root primordia (white arrowheads). Seedlings were grown on agar + 10^{-7} M naphthyl acetic acid to stimulate lateral root formation (scale bar = 100 μ m). **B.** Pools of MDA in the aerial parts of seedlings. Strong MDA fluorescence in the leaf primordia zone highlighted with the white arrow (scale bar = 255 μ m).

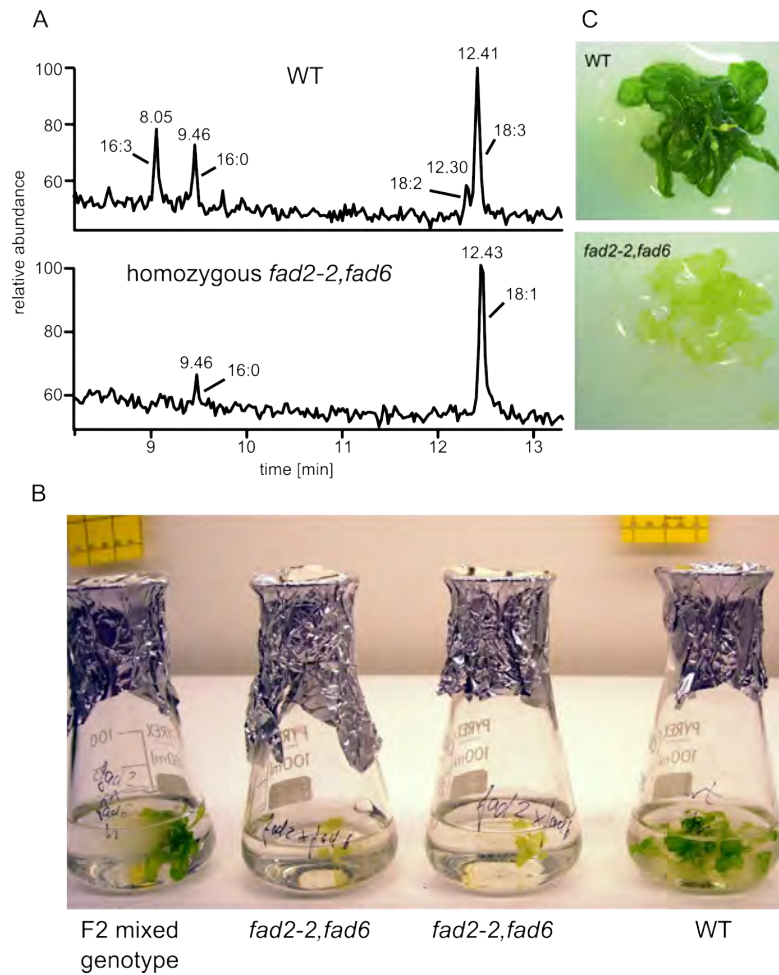


Figure 3.8: Characterization of *fad2-2, fad6* plants - **A** GC/MS analysis of methylated fatty acids extracted from *Arabidopsis* rosettes. The WT FA profile consisted mainly of 18:3 and 16:3 FAs, whereas in homozygous *fad2-2, fad6* plants 16:0 and 18:1 FAs dominated. No PUFAs were detectable in *fad2-2, fad6* plants. **B** and **C** Growth of homozygous mutants in liquid media after 7 weeks. Homozygous double mutants have less chlorophyll than the WT, chlorotic leaves and retarded growth.

3. CHARACTERIZATION OF RESTING MDA POOLS IN PLANTS

mg D.W.) was collected for all genotypes to provide accurate GC/MS measurements. We were able to detect MDA in rosettes of WT plants, grown in liquid sucrose supplemented media (example in Figure 3.9). The MDA peak in F2-plants with unknown

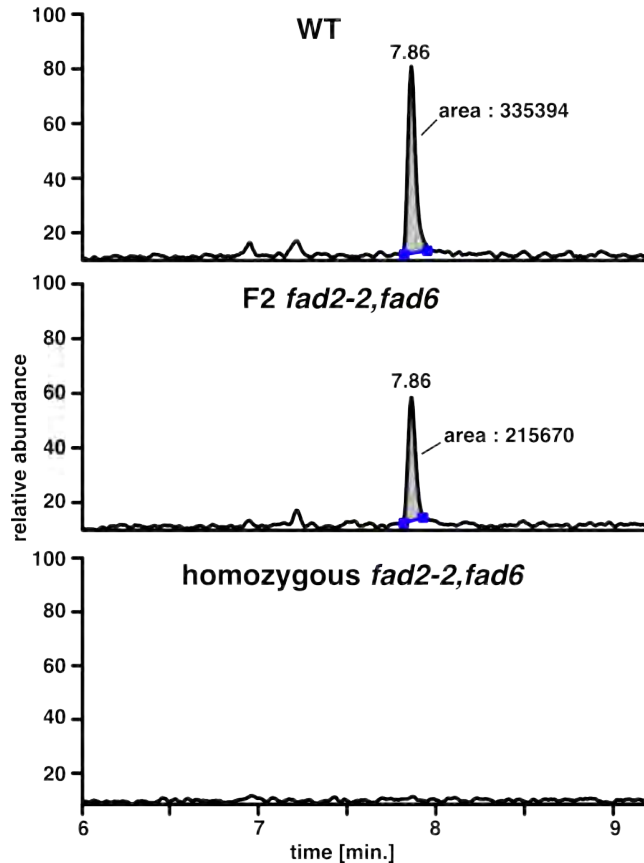


Figure 3.9: GC/MS measurements of MDA in WT and *fad2-2,fad6* rosettes - Examples of MDA measurement in rosettes from different *Arabidopsis* genotypes by GC/MS. MDA was not detectable anymore in 2 out of 3 rosettes from potential homozygous *fad2-2,fad6* plants. Randomly selected plants from the F2 generation, which had no morphological phenotype, did not show altered MDA levels. ~ 18 mg D.W. of tissue were taken per measurement and MDA analyzed by SIM for MDA-PFPH.

phenotype was lower compared to WT plants but resulted in a similar MDA concentration when corrected with the internal standard and the rosette weight. Strikingly, we were not able to detect MDA in 2 out of 3 *fad2-2,fad6* rosettes and the only potential homozygous *fad2-2,fad6* rosette in which we detected MDA, contained < 10 % of WT MDA levels. Next, single *fad2-2* and *fad6* mutants as well as crosses were sequenced to identify their exact mutation. The mutation in the *FAD6* gene was found to be a

point mutation in the 4th exon of the gene at the absolute position 15058780 on the chromosome 4, resulting in a nucleic acid change from G to A (absolute position determined with TIGR4.0). It resulted in an amino-acid change from glycine (G160R) to arginine (Zhang et al., 2009). Sequencing the *FAD2* gene, we did not find a clear result in potential homozygous *fad2-2* plants or for potential homozygous *fad2-2,fad6* crosses. We next sequenced *fad2-1* plants obtained from the Arabidopsis Biological Resource Center collection (CS8041) and found the mutation recently as described (Zhang et al., 2012). The *fad2-1* mutation was in the second exon, 310 bp downstream of the ATG, which leads to a nonsynonymous amino acid change (A104T). We confirmed that the *fad2-2* allele did not contain this mutation.

3.4 Discussion

TBA staining is a non-quantitative and potentially non-specific method that must be supported with analytic data based on the use of an appropriate internal standard and, if possible, with reference mutants or else using conditions that affect MDA levels. Previous mass spectral analysis has detected the presence of MDA-TBA₂ adducts in TBA-treated seedlings (Mène-Saffrané et al., 2007). The findings herein suggest that it is unbound MDA that reacts with TBA to produce this fluorescence since free pools of MDA in WT root tissue are much larger than those of bound MDA. Furthermore, the concentrations of TBA (35 mM) we used, combined with mild incubation conditions (25 °C for 90 min for roots) are unlikely to release bound MDA efficiently (Esterbauer et al., 1991; Yeo et al., 1994). As we show herein, overall TBA staining correlates with quantitative MDA measurements. Nevertheless, the fluorescence emission spectrum of TBA-stained root tip cells was more complex than that of synthetic MDA-TBA adducts, which were similar to previously published spectra (e.g. Janero, 1990) but with a slight shoulder near 560 nm. This shoulder was more dominant in TBA-stained root tips. We conclude that the spectrum of fluorescent TBA adducts made *in situ* is likely to contain multiple species including (TBA)₂-MDA. This underscores the importance of quantitative assays to confirm MDA presence and abundance in biological samples. In terms of total MDA per unit of dry mass, there is roughly an order of magnitude more of this aldehyde in leaves than in seedlings or seedling roots. Levels of unbound MDA ranged from 2 nmol g⁻¹ D.W. in seedlings and isolated roots to 25 nmol g⁻¹ D.W. in leaves of adult plants, as measured by performing quantitative analyses in the absence of strong acid hydrolysis. In contrast, pools of bound recoverable MDA throughout the vegetative body of *Arabidopsis* are, in general, low. We regard our estimates for the size of these bound pools as approximate; they are derived by subtracting free from total MDA pools. The bound pools ranged from 0.59 nmol g⁻¹ in seedlings to 8.00 nmol g⁻¹

3. CHARACTERIZATION OF RESTING MDA POOLS IN PLANTS

D.W. in the leaves of adult plants. Here, again there is a correlation between higher bound MDA pools and the presence of expanded leaves. Another generality to emerge from our data is that the *fad3-2,fad7-2,fad8* mutation had a high impact on total MDA levels in leaves and a low impact on total MDA pools in roots. Overall estimates for total, bound and unbound MDA in leaves support data published previously. However the present estimate for how much MDA in leaves is derived from TFAs (58%) is lower than a previous estimate of 76% (Mène-Saffrané et al., 2009). This difference may be due to better sample protection in the present analysis. Unexpectedly, the *fad3-2,fad7-2,fad8* mutant has differential effects on free and bound pools depending on the plant stage. The most extreme example of this is in roots where almost all free MDA is derived from unknown sources, that is, not from TFAs.

3.4.1 MDA Localization in the leaf

TBA staining and confocal microscopy was used to localize MDA pools at the subcellular level. Shown in Figure 3.4 are mesophyll cells, and we noted that chloroplasts in these cells appeared to be the main sites of MDA accumulation in the leaf. We did not observe TBA staining in vacuoles suggesting at least some specificity in the subcellular localization of unbound MDA. TBA-infiltrated leaves occasionally show some staining associated with structures estimated to be less than 1 μm in diameter, so plastids may not be the only organelles to harbor the aldehyde. During these experiments we did not detect strong fluorescence in epidermal pavement cells, but we noted that stomatal guard cells fluoresced after TBA (but not TCA) treatment. Pavement cells do not contain chloroplasts, whereas stomata do. Based on this, and on the observation of putative pools of MDA in mesophyll cell chloroplasts (Figure 3.4), these organelles were purified from whole leaves, characterized rigorously, and found to contain MDA. Consistent with chloroplasts being an important source of MDA, the analysis of isolated chloroplasts revealed that they contained the same ratio of TFA-derived MDA (58%) as whole leaves. Previous publications have suggested that MDA is present in plastids (e.g. Yamauchi et al., 2008) but until now this has not been shown with rigorously purified organelles or with quantitative assays based on cognate internal standards. It is of interest that the site of MDA localization, the chloroplast stroma, contains DNA, RNA, and ribosomes. If MDA has genotoxic or proteotoxic effects in leaves these effects might be manifested on the chloroplast genome and proteome. Alternatively, and as suggested previously, MDA might act to regulate stress-related gene expression in expanded leaves (Weber et al., 2004).

3.4.2 Seedling- and Root-associated MDA Pools

Most fluorescence in the root proliferation (meristematic) zone appeared to be intracellular in undifferentiated cells. This was diffuse staining as would be expected for a low molecule mass adduct formed between TBA and MDA (Esterbauer et al., 1991; Janero, 1990), adducts that we have detected previously by mass spectrometry in TBA-treated seedlings (Mène-Saffrané et al., 2007). We could not identify TBA labeled subcellular compartments in root cells, although while we noted that nuclei in the root cap region did not stain strongly for MDA some nuclei in the outer layers of the proliferation zone did. It is possible that this was due to TBA-MDA adduct diffusion either into nuclei or, in outer cell layers, loss of adducts into the bathing solution. Diffuse TBA staining was also seen in the pericycle, a cell type that continues to proliferate after leaving the meristem and that gives rise to lateral roots (Dubrovsky, 2000). Consistent with this we have observed strong TBA-dependent fluorescence in lateral root primordia (see Figure 3.7). We note that the stele contains other vascular system progenitor cells (cambium) between the paired xylem and phloem poles. This region was also stained with TBA but it was not possible to resolve the identity of any of the stained cell types. A commonality between the pericycle and the root tip meristematic region is that they both contain stem cells. Complicating the analysis of the root was the punctuate TBA-dependent staining seen most strongly in the paired protoxylem poles, casparian strips, and the outer epidermal cell walls, and more weakly elsewhere in or near cell walls throughout the plant. We interpret this non-diffuse staining as being possibly artifactual. For example, it is conceivable that single molecules of TBA react with endogenous molecules at these sites to create tethered fluorescent molecules. The fact that a lignin synthesis inhibitor (PA) did not affect the overall staining pattern of the seedlings suggests that most of the MDA is not lignin-derived. The root tip cell proliferation zone can be calculated to be about 0.004 mm^3 in volume making it difficult to analyze biochemically and it is noteworthy that, without TBA staining, MDA in this zone would not have been discovered. Even for MDA quantification in detached whole roots it was necessary to analyze between 7500 and 10,000 individual roots per replicated measurement. In general MDA pools were found to correlate with zones of cell proliferation. MDA was found to be concentrated in seedling primordia: the root tip meristematic zone, in lateral root formation and in the apical meristem. In regard to the commonly believed role of MDA as a genotoxin and proteotoxin this was surprising. It provided evidence that MDA might exist in cells in a non-reactive form and might be even beneficial in zones of cell proliferation. The presence of MDA in meristematic zones could provide a defense mechanism to protect zones of growth in juvenile tissue, until complex defense mechanism as the jasmonate pathway are fully established. Our results suggest that TBA staining could be used to search for putative MDA pools and also to search for remodeling of MDA pools even

3. CHARACTERIZATION OF RESTING MDA POOLS IN PLANTS

in the absence of overall concentration changes within whole organisms. The use of the TBA staining technique is not necessarily restricted to plants but may be applicable to other organism as well. Experiments with *Caenorhabditis elegans* showed that MDA staining with the TBA-assay is possible in principle (see supplementary data, Figure 8.2). So far, the majority of the observed MDA fluorescence seemed to be restricted to the gastrointestinal tract. This might be due to penetration problems of the TBA and would need further investigation.

3.4.3 New potential sources of MDA formation

Seeking for alternative sources of MDA in plants we found evidence for MDA generation from diunsaturated FAs. Hydroperoxide and endoperoxides from lipid oxidation are not only produced on TFAs but also on diunsaturated FAs. These also provide potential substrates for MDA formation. Leaves of *fad3-2,fad7-2,fad8* plants were shown to lack all TFAs but accumulate instead a high proportion of diunsaturated FA compared to WT (Table 3.1). Diunsaturated FAs have been shown to be less susceptible to oxidation than TFAs, but can provide a substrate for MDA generation *in vitro* under oxidation (Liu et al., 1997) and therefore might present a source *in vivo*. We wanted to test this hypothesis using mutants in desaturation, lacking as well diunsaturated FAs. Both, *FAD2* (Miquel and Browse, 1992) and *FAD6* (Falcone et al., 1994) were reported to be desaturases, responsible for the unsaturation of monounsaturated FAs. The *FAD2* protein was predicted to be located in the endoplasmatic reticulum (Okuley et al., 1994), whereas the *FAD6* protein was shown to be located in plastids (Ferro et al., 2010). According to their residence *FAD2* is responsible for the unsaturation in the eukaryotic pathway and the *FAD6* in the prokaryotic pathway (reviewed in Ohlrogge et al., 1995). Expression comparison with the program Genevestigator was done to compare their expression throughout different tissues and developmental stages (Table 3.2). Interestingly were *FAD2* and *FAD6* often expressed in complementary ways throughout the tissue and growth stage. For example, *FAD6* was found to expressed at low levels in root tissues, where the expression of *FAD2* was high. *FAD6* on the other hand was highly expressed in shoot tissue as leaves, axillary buds and cotyledons in which the *FAD2* expression was reduced. This difference in expression is reflected as well in the FA-composition in the respective tissues of these mutants (summarized in Table 3.1). The FA-composition of *fad6* in the roots is similar to wild-type plants with ~ 60 % of PUFAs. The *fad2-1* mutant on the other hand contains only 19% of PUFAs in roots. The FA composition in leaves of the *fad2-1* and *fad6* mutant shows reduced PUFAs content but individual differences are minor than in roots, indicating that both desaturases are redundant in leaves. The double knock-out of *fad2-2,fad6* was reported to contain no PUFAs in leaves (McConn and Browse, 1998). To test the hypothesis

Fatty acids	roots			
	WT	<i>fad2-1</i>	<i>fad6</i>	<i>fad2-2,fad6</i>
16:0	24.7	14	-	-
16:1	1.2	2.3	-	-
16:3	-	-	-	-
18:0	3.2	1.7	total sat.: 31	total sat.: 15
18:1	6.8	55.9	total mono.: 10	total mono.: 80
18:2	29.8	6.4	total PUFAs: 59	total PUFAs: 5
18:3	29.1	12.8	-	-

Fatty acids	leaves				
	WT	<i>fad2-1</i>	<i>fad6</i>	<i>fad2-2,fad6</i>	<i>fad3-2,fad7-2,fad8</i>
16:0	13.7	13.9	18.1	20	11.54
16:1	2.4	2.2	14.6	-	3.04
16:3	16.0	18.5	-	-	-
18:0	0.4	0.5	3.1	-	0.64
18:1	2.3	20.9	15.5	80	4.02
18:2	14.5	3.8	10.5	-	54.5
18:3	50.8	39.6	32.7	-	0.26

Table 3.1: Summary of fatty acid (FA) composition in leaves and roots of FA-desaturases mutants- FA-composition expressed in mol % for fatty acid desaturase mutants. Data for WT and *fad2-1* composition in leaves and roots measured by Okuley et al. (1994). FA-composition of *fad2-2,fad6* was extrapolated from (McConn and Browse, 1998) and *fad6* from (Falcone et al., 1994). FAs in *fad3-2,fad7-2,fad8* leaves were extrapolated from (McConn and Browse, 1996). The data for *fad2-2,fad6* composition in leaves was experimentally obtained (see Figure 3.8). Sat. = saturated FAs, mono. = monounsaturated FAs, PUFAs = polyunsaturated FAs. Growth conditions varied between different analysis.

whether diunsaturated FAs might be a source of MDA formation *in vivo*, we attempted to measure MDA in this double mutant. *Fad2-2* and *fad6* plants were crossed and the progeny of the cross scanned for homozygous plants. The morphological phenotype of *fad2-2,fad6* was described to be dwarf and chlorotic. We selected potential homozygous *fad2-2 -/-, fad6 -/-* plants on 1 % sucrose supplemented media based on this phenotype. GC/MS-analysis of FA-compositions was done to confirm the genotype. No PUFAs were detectable in the suspected double homozygous plants, but only 18:1 and 16:0. The levels of MDA in leaves from *fad2-2,6* plants were below the limit of detection (LOD) in 2 out of 3 samples. The 3rd sample contained only $\sim 10\%$ of WT MDA. Further analysis should include *fad3-2,fad7-2,fad8* plants to dissect the impact of di- and triunsaturated FAs on these diminished MDA levels. The previous collected data regarding the con-

3. CHARACTERIZATION OF RESTING MDA POOLS IN PLANTS

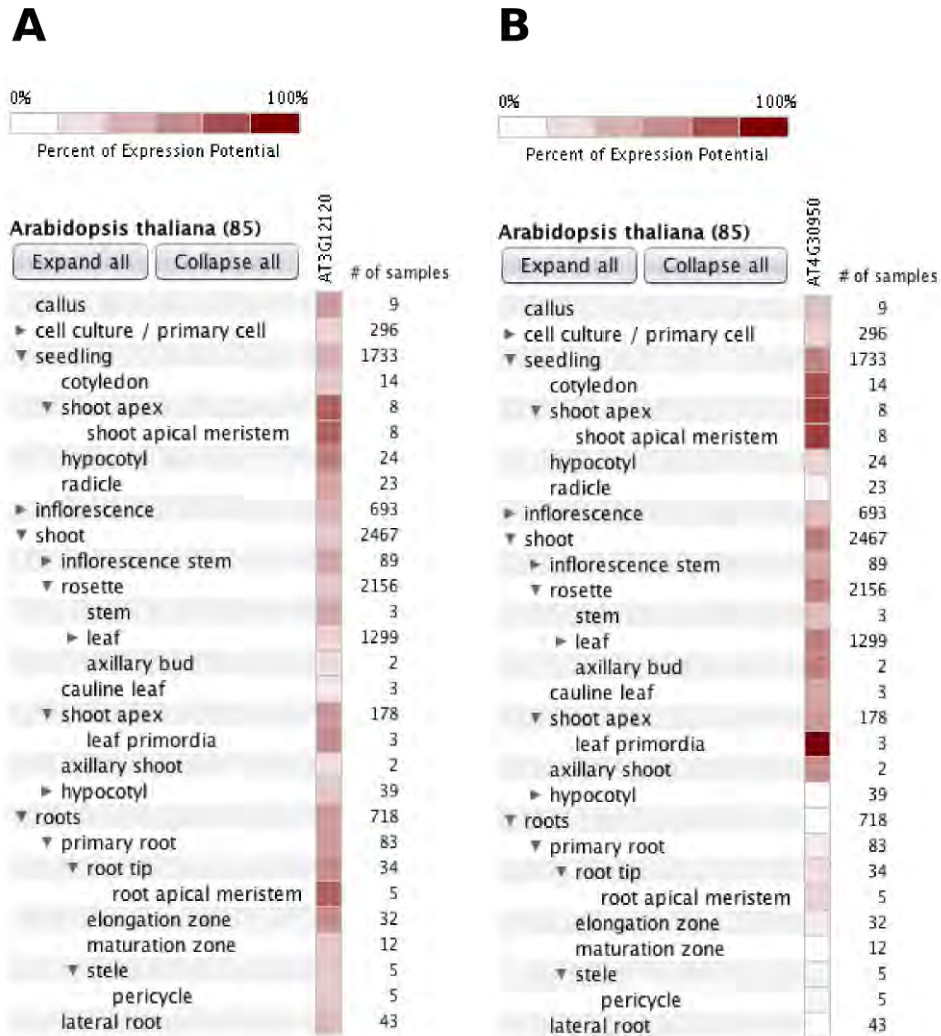


Table 3.2: Expression analysis of FAD2 and FAD6 in different tissues and developmental stages of *Arabidopsis* plants - Analysis of the expression of the **A** FAD2 (At3g12120) and **B** FAD6 (At4g30950) gene, visualized as heat maps in Genevestigator. Intensity of red color equals the percent of expression potential. Analysis was based on ATH1: 22k array (<https://www.genevestigator.com/gv/plant.jsp>; Hruz et al., 2008).

tribution of TFAs on MDA levels in leaves (58% less in *fad3-2,fad7-2,fad8*) might not apply within these special growth conditions. More biological replicates were necessary for a full scale MDA quantification, but homozygous *fad2-2,fad6* never flowered and propagation failed. *Fad2-2,fad6* homozygous seedlings from the F2 generation had to be manually selected for each experiment and the segregation rate in the F2 generation of the *fad2-2,fad6* cross for both genes being in a homozygous state was $\frac{1}{16}$ according to Mendelian inheritance. This segregation ratio was observed selecting mutants by morphological phenotype and represented additional evidence that homozygous plants could be identified that way. We sought to generate *fad2-2 -/-, fad6 +/-, or fad2-2 +/-, fad6 -/-* genotypes to obtain a $\frac{50}{50}$ segregation rate. Since both mutants derived from an EMS-mutagenesis, we sequenced the *fad2-2* and *fad6* genes to identify their mutations. We were able to confirm the mutation in the *fad6* mutant (Zhang et al., 2009), but the site(s) of mutation in *fad2-2* plants remained unsolved so far. We recently confirmed the reported point mutation in another FAD2 allele (Zhang et al., 2012), *fad2-1*, which offers in parallel to *fad2-2* the possibility to tie in with the present evidence that diunsaturated as well as triunsaturated FAs can be substrates for MDA generation *in vivo*. In conclusion, by depleting di- and tri-unsaturated FAs in the *fad2-2,fad6* double mutants, MDA in 7 week old plants was almost undetectable. Further work is needed to determine how much each allele contributes to MDA production as well in different developmental stages and tissues.

3. CHARACTERIZATION OF RESTING MDA POOLS IN PLANTS

4

Induction of malondialdehyde pools¹

4.1 Introduction

MDA levels in plants are tightly regulated (Farmer and Davoine, 2007; Schmid-Siegert et al., 2012; Weber et al., 2004). In order to study MDA dynamics we sought ways to alter it in *Arabidopsis*. Chloroplastic triunsaturated fatty acids (TFAs) were found to be the major source of MDA generation by nLPO in adult leaves (Chapter 3). Since singlet oxygen ($^1\text{O}_2$) has been demonstrated to drive 85% of nLPO in *Arabidopsis* leaves (Triantaphyllidès et al., 2008) it is therefore likely responsible for the initiation of MDA formation. The very reactive $^1\text{O}_2$ is generated from molecular oxygen upon energy transfer by triplet energy state chlorophylls, which can act as photosensitizers (Krieger-Liszkay, 2005). Plants developed scavengers like tocopherols and quenchers like carotenoids to reduce the threat of this reactive molecule. Lately TFAs have been proposed to represent a buffer for $^1\text{O}_2$ and nLPO acting as a mechanism to prevent damage to other important cell structures such as proteins (Mène-Saffrané et al., 2009). We used leaves from adult plants and extracted chloroplasts to study whether light capture and related nLPO might alter MDA levels at their source. Additionally we used an $^1\text{O}_2$ generating herbicide to analyze whether $^1\text{O}_2$ formation might be directly coupled with MDA formation.

In a next step we turned towards the dynamics of MDA in the resting plant and looked at its behavior in pathogenesis. Weber et al. (2004) showed that exogenous MDA was able to induce a set of abiotic and biotic stress-related genes, some associated with pathogenesis. Measurements of MDA levels upon infection indicated that MDA levels

¹Chapter partially taken from (Schmid-Siegert et al., 2012), E. Schmid-Siegert and J. Loscos contributed equally to Figure 4.2 and Figure 4.3

4. INDUCTION OF MALONDIALDEHYDE POOLS

might be well regulated since only minor changes were observed (Muckenschnabel, 2002; Weber et al., 2004). In order to investigate MDA dynamics in pathogenesis we infected juvenile and mature plants with the pathogens *Botrytis cinerea* and *Plectosphaerella cucumerina*. We then visualized MDA by TBA staining and quantified changes in MDA levels by GC/MS.

4.2 Material and Methods

Plant genotypes and growth conditions - Wild-type (WT) *Arabidopsis* (Col-0), *fad3-2,fad7-2,fad8* (McConn and Browse, 1996), *jar1* (Staswick et al., 1992) and *npr1* (Cao et al., 1994) were grown on soil at 22°C for 5 weeks (light: 100 $\mu\text{E m}^{-2} \text{s}^{-1}$, 9 h light/15 h dark), or on 0.7% agar (w/v, in water) for 4 d (15 h light/9 h dark). For high light experiments, plants grown in the conditions described previously were shifted into the following conditions: 12°C, light (500 $\mu\text{E m}^{-2} \text{s}^{-1}$) and 9°C during dark periods.

Gas Chromatography / Mass Spectrometry (GC/MS) - Chemicals used were purchased from Sigma (St. Louis, Missouri, USA) unless indicated. Quantitative MDA measurements were conducted as previously described in Chapter 3.2.

Treatment with the herbicide Bromoxynil - Plants grown in short day conditions, were shifted into Plexiglas boxes (15 l volumes, 15 plants) and sprayed with 10 ml of 100 μM Bromoxynil. Tissue was collected 4 d after treatment and MDA analyzed by GC/MS.

Infection with Botrytis cinerea and mediator treatment - Conidia from *B. cinerea* grown on 0.5x potato dextrose agar (Mène-Saffrané et al., 2009) were filtered and diluted to 10^6 spores ml^{-1} in 0.5x potato dextrose broth (PDB) and stored at -80°C prior application (Gindro and Pezet, 2001). Seedlings were grown in water in continuous light for 2 d post-germination. The water was replaced by 5 μl of fungal spore suspension or with 0.5x PDB for the controls. To look at the root tip cell proliferation region in more detail we treated 4 d-old WT and *fad3-2,fad7-2,fad8* seedlings with JA (50 μM) or with salicylic acid (250 μM) for 15-18 h prior to treatment with 2-thiobarbituric acid (TBA).

Infection with Plectosphaerella cucumerina- *P.cucumerina* spores were a gift from B. Mauch-Mani, Neuchatel in Switzerland. A culture of the fungus was maintained on potato dextrose agar plates and collected spores were diluted to 10^7 spores ml^{-1} in 0.5 x PDB and stored at -80°C prior to application. For the infection, plants were shifted into Plexiglas boxes (15 l volume, 15 plants/box; 6 weeks old) and sprayed with 10 ml of 2.5×10^6 conidia in 10 mM MgSO_4 (diluted 10x from frozen stock) and infection allowed

to proceed.

4.3 Results

4.3.1 Light-induced changes of MDA levels

Since the majority of MDA derived from the oxidation of TFAs in chloroplasts was likely to be initiated by singlet oxygen, we first looked at MDA dynamics in relation to light (Figure 4.1). Chloroplasts were extracted, shifted to $100 \mu\text{E m}^{-2} \text{ s}^{-1}$ at 22°C , and the MDA levels were monitored over time (Figure 4.1 A). Chloroplasts from the same extraction kept in the dark served as a control. After 1 h the MDA levels increased $\sim 60\%$ in light-exposed chloroplasts compared to their dark control, doubled after 2 hours and tripled after 4 hours. This suggested that events associated with light capture led to the accumulation of MDA in the extracted chloroplasts. It is noteworthy that MDA levels increased in the dark kept controls over the monitored time span, underlining the necessity to keep chloroplast samples on ice and process them as fast as possible in absence of light for MDA quantification. Next, accumulation of MDA in relation to light was analyzed in expanded leaves. A set of plants was exposed for 1 week to high light ($500 \mu\text{E m}^{-2} \text{ s}^{-1}$) and low temperature (12°C) and the MDA levels visualized by TBA-staining and confocal microscopy (Figure 4.1 B). The MDA fluorescence in mesophyll cells of control plants was mainly co-localized with chloroplasts (first row) which was in accordance with previous results (see Chapter 3.3). In high light treated plants, the localization of MDA was not limited to the chloroplasts anymore but spread throughout the entire cell. Some of this fluorescence seemed to be concentrated in single concrete spots (see magnified picture). In order to investigate whether the previously observed MDA increases might be singlet oxygen-induced, we sprayed plants with the singlet oxygen-generating herbicide Bromoxynil (Krieger-Liszky and Rutherford, 1998). Plants that were sprayed with $100 \mu\text{m}$ Bromoxynil showed bleaching and cell death. The MDA levels were quantified by GC/MS after 4 days of treatment and compared to mock treated plants (Figure 4.4 C). The MDA levels were higher upon Bromoxynil treatment and increased from $27 \pm 7.6 \text{ nmol g}^{-1} \text{ D.W.}$ in mock-treated plants to $55 \pm 24.2 \text{ nmol g}^{-1} \text{ D.W.}$ in Bromoxynil-treated plants. The mock-treated plant levels were very similar to our previous data (see Chapter 3.3: WT $33.01 \pm 1.63 \text{ nmol g}^{-1} \text{ D.W.}$) and mock treatment did not seem to affect the MDA levels.

4.3.2 MDA dynamics during infection with necrotrophic fungi

Even though MDA has been implicated as a signal in pathogenesis, MDA levels were found to be well controlled (Weber et al., 2004). We wanted to tie in with these first

4. INDUCTION OF MALONDIALDEHYDE POOLS

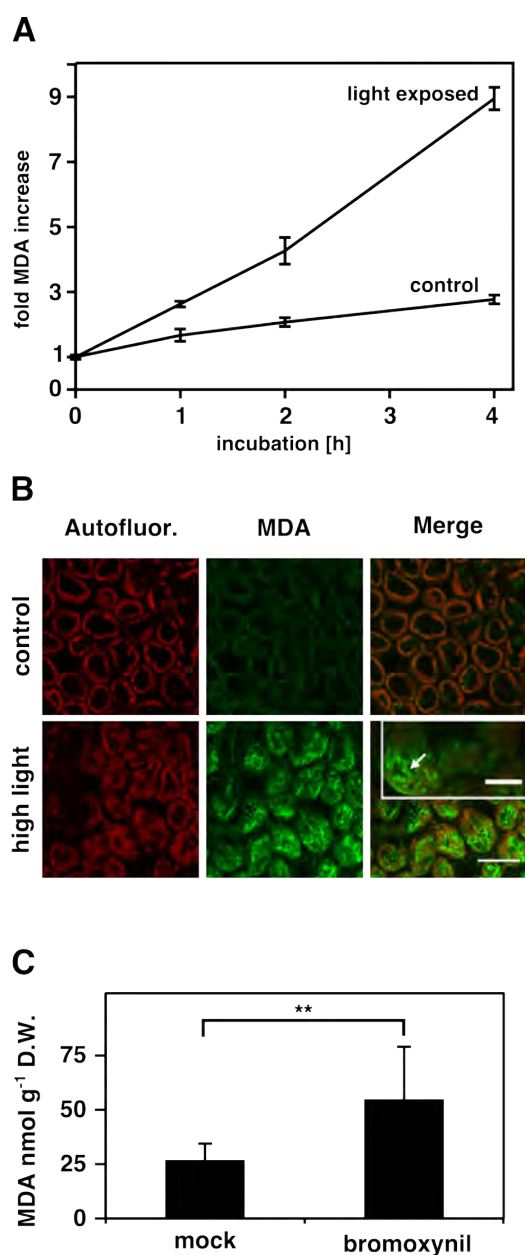


Figure 4.1: $^1\text{O}_2$ produced in the light alters MDA levels - **A.** MDA levels of light-exposed chloroplasts measured by GC/MS and expressed in their fold increase ($n=3$) **B.** Microscopic analysis of MDA levels after exposure to high light. MDA was visualized after TBA staining. Plants (6 weeks old) were exposed for 7 d to high light ($500 \mu\text{E m}^{-2} \text{s}^{-1}$) and low temperature (12°C) (stacks with scale = $50 \mu\text{m}$, inset scale bar = $10 \mu\text{m}$). **C.** GC/MS analysis of plants sprayed with Bromoxynil ($100 \mu\text{M}$) and collected after 4 d ($P = 0.0008$, 5 biological and 3 technical replicates).

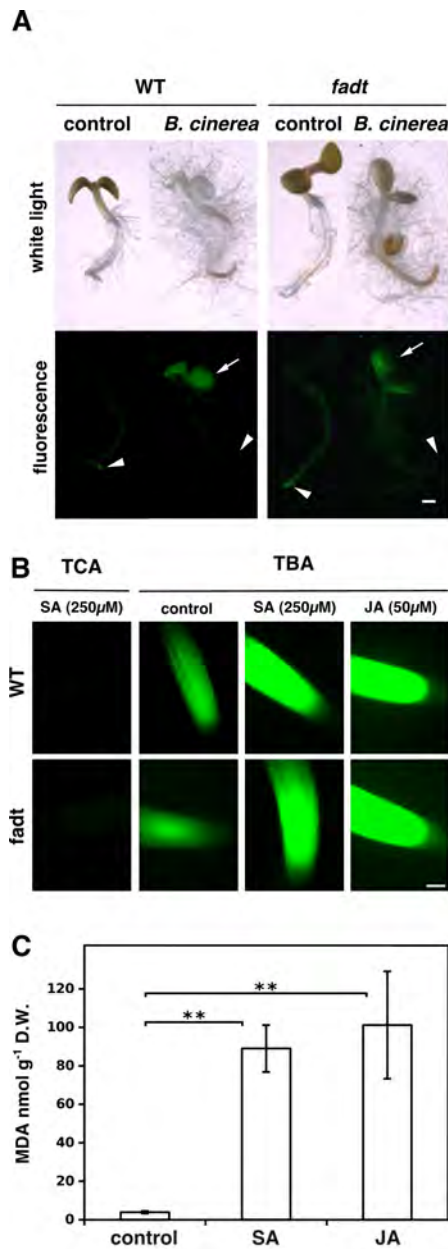


Figure 4.2: MDA pools in seedlings respond to pathogenesis and to plant-derived stress mediators - A. MDA staining in WT and *fad3-2,fad7-2,fad8 (fadt)* *Arabidopsis* seedlings after infection. Upper panel, white light. Lower panel, TBA staining after infection with *B. cinerea* (40 h post-infection with 5 µl containing 106 spores ml⁻¹). Arrowheads: root tip pools of MDA. Arrows: MDA accumulation after infection in the shoot apex, hypocotyl and cotyledons. Scale bar = 500 µm. **B.** TBA staining of MDA pools in root tips of WT and *fadt* seedlings treated with jasmonic acid (JA) or salicylic acid (SA). Note lack of staining in the extremity of the root, the root cap region. Scale bar = 50 µm. **C.** Quantitative analysis of MDA levels in WT seedlings after treatment with JA (50 µM) or SA (250 µM) for 18 h at 22°C prior to harvest.

results and compare MDA levels upon pathogenesis in seedlings and adult plants. We first analyzed MDA levels upon infection of young seedlings with the necrotrophic fungus *Botrytis cinerea*, visualizing changes with the TBA-assay and quantifying MDA by GC/MS. As the fungus grew we observed changes in TBA-dependent fluorescence in the seedlings (Figure 4.2 A). An apparent increase of MDA in the cotyledons, hypocotyl region and apical meristem (leaf primordia) could be observed for both WT and *fad3-2,fad7-2,fad8* seedlings. On the other hand, MDA labeling disappeared in necrotic tissue, as observed in the root tips of the WT. At 40 h post infection both genotypes were heavily infected, showing necroses and chloroplast bleaching although there was a

4. INDUCTION OF MALONDIALDEHYDE POOLS

strong increase in MDA fluorescence in the cotyledons. Both jasmonic acid (JA) and salicylic acid (SA) are known to accumulate in this pathosystem (Pan et al., 2008). We first treated 4 d-old seedlings for 18 h with JA (50 μ M). This led to changes in TBA-dependent fluorescence throughout the seedling with the strongest effect on the cotyledons and also on the apical meristem and root tip (Figure 4.3 A). TBA-associated fluorescence was strongly induced by treatment with SA or JA in both the WT and the *fad3-2,fad7-2,fad8* root tips (Figure 4.2 B). Control seedlings were found to contain 3.92 ± 0.64 nmol g⁻¹ D.W. MDA. Upon treatment of the WT seedlings the amount of MDA increased to 89.02 ± 12.17 nmol g⁻¹ D.W. and 101.20 ± 27.91 nmol g⁻¹ D.W. upon SA and JA treatment, respectively (Figure 4.2 C). We tested whether mutants known to block elements of salicylate and jasmonate signaling interfered with MDA induction in root tips and found that *jar1* blocked MDA induction by JA but that *npr1* did not block MDA induction by SA (Figure 4.3 B).

In the case of young *A. thaliana* seedlings, we were able to visualize alterations of MDA levels during infection. To investigate whether these dynamics also applied to later growth stages we next challenged adult plants with the fungus *Plectosphaerella cucumerina*. This fungus was chosen for adult-phase plants, since MDA levels during infection with *B. cinerea* were already shown to be tightly controlled (Weber et al., 2004). We focused on the potential involvement of the jasmonic acid pathway and underlying changes of MDA levels. Therefore the *aos* and *fad3-2,fad7-2,fad8* mutants were selected as genetic controls to distinguish jasmonic acid and TFAs. Allene oxide synthase (AOS) is essential for jasmonic acid (JA) synthesis from TFAs, whereas the *fad3-2,fad7-2,fad8* mutant lacks both TFAs and all their oxidation products (including JA). Infection of 6 week-old WT plants with the fungus *P. cucumerina* led to phenotypical symptoms including lesions and local cell death, but plants were able to resist the pathogen (Figure 4.4 A). Upon infection of the *aos* and the *fad3-2,fad7-2,fad8* mutants major differences were observed. After 5 days of infection, the *aos* mutant was more affected than the WT as judged by tissue necrosis. More importantly, the *fad3-2,fad7-2,fad8* mutant failed to resist the pathogen and was almost completely necrotic. MDA as a TFA-derived representative molecule was next quantified during pathogenesis. Its dynamics during infection with *P. cucumerina* were quantified by GC/MS against mock-infected plants as controls (Figure 4.4). Resting MDA levels of mock treated plants showed differences within different genotypes and were in general lower than in previous experiments. The *aos* mutant plants had significantly less MDA compared to the WT ($P = 0.0022$) in its resting state and *fad3-2,fad7-2,fad8* plants showed strongly impaired MDA levels as previously reported. After 1 day post infection (dpi), wild-type plants did not show any significant increase in MDA compared to their mock controls. The levels increased on

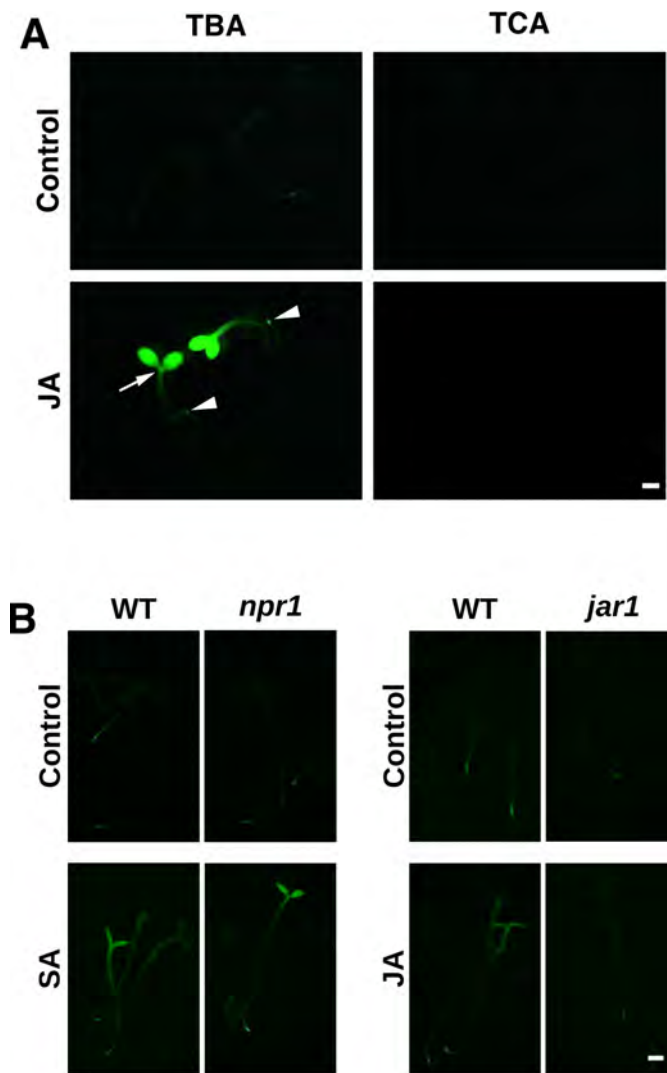


Figure 4.3: Inducible TBA staining in seedlings. - **A.** Increased TBA staining of WT seedlings after incubation for 15 h with jasmonic acid (JA) (50 μ M). Arrow: apical meristem region. Arrowheads: root meristems. **B.** The *jar1* mutation greatly reduces JA (50 μ M)-induced TBA staining in seedlings, whereas the *npr1* mutation does not strongly affect SA (250 μ M)-induced TBA staining.

4. INDUCTION OF MALONDIALDEHYDE POOLS

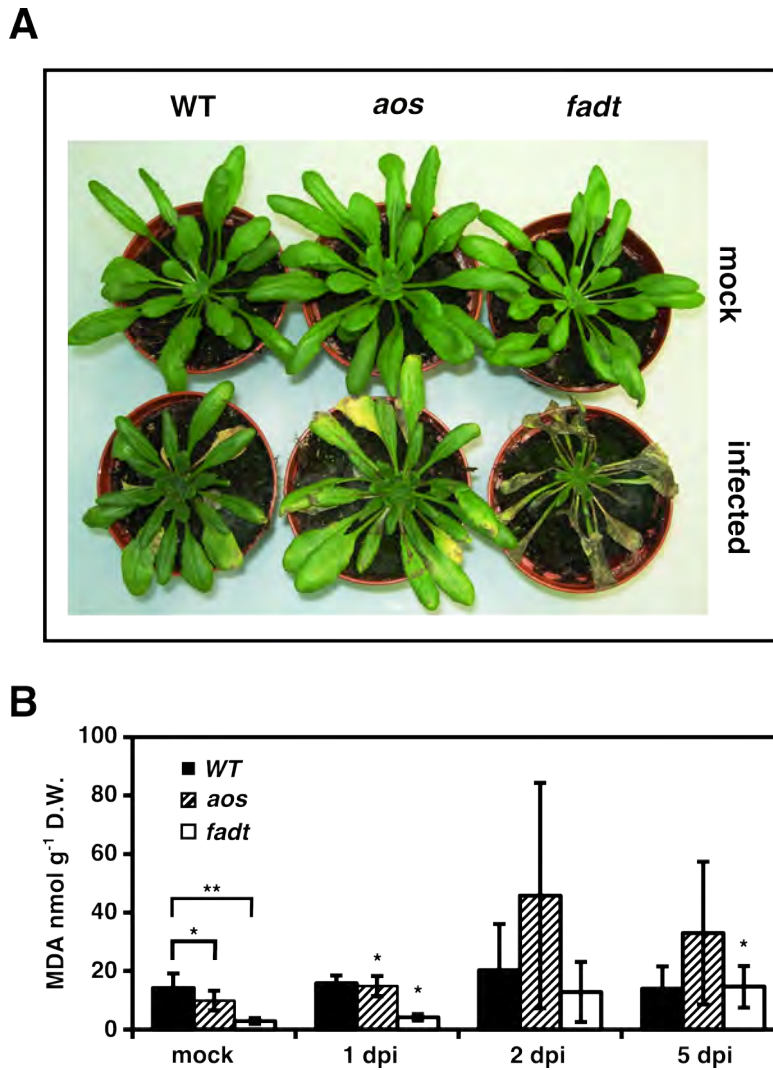


Figure 4.4: MDA dynamics during infection with the pathogen *P. cucumerina* - Adult *Arabidopsis* rosettes were sprayed with 10 ml 2.5×10^6 conidia in MgSO_4 (10 mM) **A.** Phenotypical comparison of the infection after 5 days of infection (*fadt* = *fad3-2, fad7-2, fad8*). **B.** Quantitative MDA measurements at different time points during the infection. Significance of altered MDA levels after 1,2 and 5 dpi were tested against the corresponding mock control (biological replicates $n \geq 5$; * $p < 0.05$; ** $p < 0.001$).

the other hand by 50% in *aos* ($P = 0.045$) and 43 % in *fad3-2,fad7-2,fad8* plants ($P = 0.0132$) compared to their mock control. At 2 dpi the WT MDA levels were similar between infected and non-infected plants, whereas they increased 4-fold in infected *aos* and *fad3-2,fad7-2,fad8* plants compared to their controls. This trend was not statistically significant, due to high deviations, which might have resulted from heterogeneous spread of the fungus among tissue of different ages. Mature expanded leaves were more susceptible to the fungus than younger ones towards the center of the rosette. 5 dpi the MDA levels in the WT plants still remained equal in respect to their control plants and did therefore not show any dynamics throughout the monitored time of infection with *P. cucumerina*. The MDA concentrations in *fad3-2,fad7-2,fad8* remained on the same level as after 2 dpi but the increase was now significant in respect to its mock control ($P = 0.021$). The MDA levels in the infected *aos* still remained higher than its mock controls, but the change was again not statistically significant. Interestingly, MDA level in the jasmonic acid deficient mutants appeared to be inducible whereas levels in WT plants seemed to be tightly controlled.

4.4 Discussion

4.4.1 Light-induced changes of MDA levels

It was shown that most MDA in expanded leaves derives from TFAs (Weber et al., 2004), which are highly enriched in chloroplast lipids. The underlying mechanism is likely initiated by the action of reactive $^1\text{O}_2$ generating LOOH and subsequently in a second step MDA. Since $^1\text{O}_2$ is a reactive by-product of photosynthesis we investigated the potential link of light capturing and MDA generation. Chloroplasts were extracted from mature leaves, exposed to light and MDA measured by GC/MS. Interestingly the MDA levels increased in chloroplast extracts exposed to light, compared with dark kept control chloroplasts and the difference increased over time. This indicated that mechanism involved with light capturing generated MDA and one can speculate that MDA levels were lower in dark kept controls due to lower $^1\text{O}_2$ generation. We tried to confirm the link of light generation and MDA inducibility in chloroplasts by looking into intact leaves. Therefore, MDA-fluorescence was analyzed in adult plants treated temporarily with high light and low temperature. In control plants, MDA-fluorescence was mainly limited to chloroplasts as already observed earlier. Fluorescence in high-light treated plants was stronger and no longer limited to the chloroplasts but present in other compartments as well. One of these potential compartments might have been for example peroxisomes according to their size. This needs to be confirmed with specific marker lines for peroxisomes (e.g. PTS1:GFP; Mano et al., 2002; see Chapter 3). Photosynthetic efficiency was reported to decrease within high light conditions, leading to an accumulation of ROS

4. INDUCTION OF MALONDIALDEHYDE POOLS

like $^1\text{O}_2$ (Krieger-Liszkay, 2005). The low temperature increases TFA levels in *Arabidopsis* (Somerville and Browse, 1991) and therefore provides more substrate for LPO. Together, these conditions promote nLPO and might be responsible for the increased MDA-fluorescence. In an attempt to better understand the link between light capture and increases in MDA levels, we treated plants with the herbicide Bromoxynil. This herbicide is known to cause $^1\text{O}_2$ accumulation in plants (Krieger-Liszkay and Rutherford, 1998) and we measured MDA levels of plants after treatment. Quantitative MDA measurements revealed that the Bromoxynil treated plants possessed more MDA than the control plants. This provided additional evidence that light capturing-linked MDA accumulation might derive from $^1\text{O}_2$ induced nLPO. It remained unclear though whether the increase in MDA was a direct effect of singlet oxygen derived nLPO. More detailed experiments with mutants affected in singlet oxygen generation such as the *flu* mutant (Meskauskiene et al., 2001) might help to resolve this question.

4.4.2 MDA inducibility upon infection with necrotrophic fungi

There are reports that MDA levels increase modestly (i.e not more than 2-fold) in expanded leaves exposed to heat stress or hypoxia (Weber et al., 2004) and other work suggests that MDA levels in expanded leaves sometimes decrease in pathogenesis (Farmer and Davoine, 2007; Muckenschnabel, 2002; Weber et al., 2004). In contrast, when we infected seedlings with *B. cinerea*, MDA was found to be highly inducible in cotyledons, apical meristems and root meristems. These tissues are all preformed in the embryo. However, we could not distinguish whether the plant or the fungus produced this MDA. In an attempt to resolve this we grew plants in the absence of the fungus and treated them with two mediators known to accumulate in this pathosystem (SA and JA; Pan et al., 2008). Treatment with the mediators resulted in 20-fold increases in MDA levels in the seedlings, allowing us to correlate increases in MDA with increases in TBA-dependent staining. The correlation between staining pattern and MDA levels validated the staining method for the root, an organ for which we have yet to find a mutant that strongly impacts resting MDA levels. Moreover, the results now show that certain MDA pools associated with proliferating and embryonic cells are highly responsive to biological mediators involved in stress responses. That is, there is an association between MDA inducibility and growth potential. The JAR1-dependent and NPR1-independent induction of MDA by JA and SA, respectively is interesting since elevated levels of both mediators are known to inhibit plant growth (Mauch et al., 2001; Staswick et al., 1992). Additionally, it is possible that MDA functions as an inducible defense chemical in young tissues.

In contrast to the results from seedlings, MDA levels seemed to be tightly controlled

in mature tissue as observed upon infection of adult-phase plants. Even though wild-type plants showed infection symptoms if challenged with *P. cucumerina*, no changes in MDA concentrations were detected. This was not entirely surprising since previous attempts with other pathogens reported similar findings for adult plants (Muckenschnabel, 2002; Weber et al., 2004). JA might be involved in this tight regulation as suggested by altered MDA levels in resting plants of the jasmonate synthesis mutant *aos*. More importantly, we found MDA levels in both JA-lacking mutants to be inducible upon pathogenesis. A possible explanation might be that the lack of JA increases susceptibility against *P.cucumerina* and both mutants struggle with severe cell damage and subsequent MDA formation. It is known on the other hand that other sources of MDA must exist and might even be driven enzymatically. One could imagine the JA derivate jasmonyl isoleucine, as a major player in pathogenesis, controlling the generation of defense related compounds one of them being MDA. After infection with *P. cucumerina*, the mutant *fad3-2,fad7-2,fad8* lacking JA and TFAs was more susceptible than the *aos* mutant lacking only JA. This confirmed findings previously reported for infection with *B. cinerea*. Mène-Saffrané et al. (2009) found that *fad3-2,fad7-2,fad8* plants lacking both, TFAs and JA, were much more susceptible than the JA mutant *aos*. Both were more susceptible to the pathogen compared to the WT and they concluded that TFAs or TFA-derived signals were more important for defense against this pathogen. This was supported by our results with another pathogen.

Together the results suggest that TFA-derived molecules other than JA derivatives are important in defense against pathogens in adult leaves. MDA seemed not to play an active role, as judged by stable levels in WT leaves upon infection. Since MDA was shown to activate genes associated with pathogenesis, its role might lie in signaling rather than as an antimicrobial compound in expanded leaves. In conclusion, MDA pools in young, dividing tissues appeared to be more inducible than their counterparts in expanded leaves.

4. INDUCTION OF MALONDIALDEHYDE POOLS

5

Generation of isotope-labeled malondialdehyde

5.1 Introduction

Isotope labeling facilitates the study of the metabolic fate of small molecules. Isotope-tagged malondialdehyde (MDA) is not readily available and therefore must be generated enzymatically or non-enzymatically from precursors. One goal of this study was to establish a new cheap, simple and reliable method to obtain purified isotope-labeled MDA. Enzymatic generation of MDA by an equine alcohol dehydrogenase (ADH) from 1,3-propanediol was described earlier (Summerfield and Tappel, 1978) and reported not to generate any reactive side products as is the case for the generation of MDA by acidification of 1,1,3,3-tetraethoxypropane (TEP; Marnett and Tuttle, 1980). ADH in this reaction first oxidizes the substrate 1,3-propanediol to the intermediate 3-hydroxypropanal (3-HPA) and subsequently in a second oxidation step to MDA, using NAD^+ as a co-factor (Figure 5.1). NADH , H^+ generated in the reaction is recycled to NAD^+ by a second enzymatic reaction in which lactate dehydrogenase reduces pyruvate to lactate. Except for the intermediate 3-HPA, no other aldehydes are produced and lactate and pyruvate are not isotope-labeled when isotope-tagged 1,3-propanediol is used. The maximum conversion efficiency in this reaction was reported to be up to 60%, resulting in residual 1,3-propanediol and 3-HPA. These have to be removed prior to using MDA in experiments and particularly if the MDA is used in a biological system. Previous attempts to purify MDA have used HPLC (Bull and Marnett, 1985; Kakuda et al., 1981; Lacombe et al., 1990) which is not ideal for small sample sizes, furthermore 1,3-propanediol, 3-HPA and MDA have similar chemical properties. Finally, MDA is unstable, cannot be stored easily in its pure form and has to be produced fresh for each experiment (Marnett and Tuttle, 1980). The generation of the sodium salt of MDA and its long term storage

5. GENERATION OF ISOTOPE-LABELED MALONDIALDEHYDE

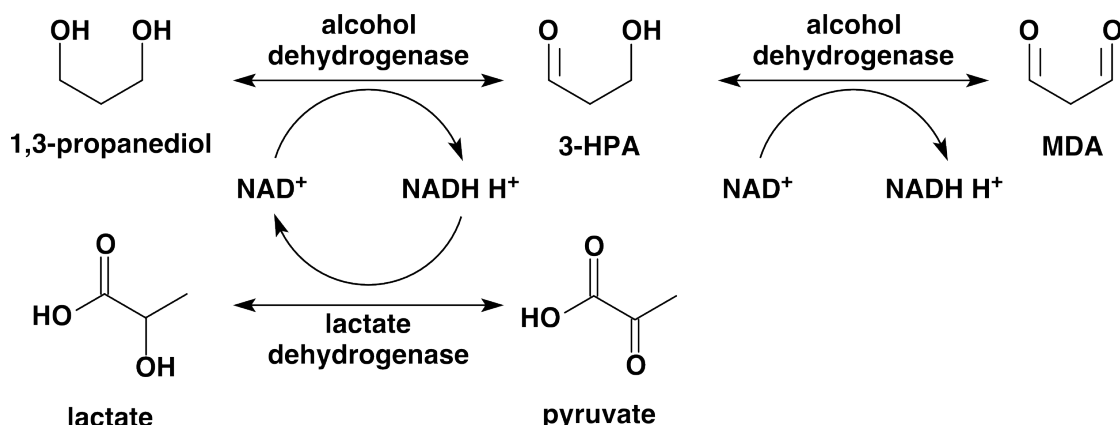


Figure 5.1: Scheme for enzymatic MDA generation catalyzed by equine alcohol dehydrogenase - The initial substrate for the enzymatic conversion, 1,3-propanediol, is oxidized to 3-HPA by the equine alcohol dehydrogenase using NAD⁺ as cofactor. A second enzymatic recycling system for NADH, H⁺ was introduced to avoid the backward reaction and to provide constant NAD⁺ supply. The 3-HPA intermediate is oxidized to MDA. MDA is drawn as the uncharged dialdehyde but will be present as an enolate ion at the pH of the reaction buffer (pH 9).

on the other hand is possible, but was reported to result in a loss of more than 40% after lyophilization (Lacombe et al., 1990). In theory, the purification of the enolate form of MDA by anion exchange chromatography should provide a convenient tool due to its simplicity and the possibility of purifying small amounts of MDA. Furthermore, if working with radio-isotopes, anion exchange offers the advantage that all components are cheap and easily replaceable. MDA in its charged form above its pK_a of 4.46 should bind to an anion exchange column whereas uncharged 1,3-propanediol and 3-HPA would elute without binding. In order to investigate this, we examined the ability of anion exchange resins to bind MDA.

Eluted MDA fractions were analyzed with spectrophotometry and GC/MS to evaluate their purity. For the GC/MS analysis, the PFPH derivatization used previously for MDA quantification was replaced by a derivatization with PFBHA. In contrast to PFPH, PFBHA forms only linear imines with aldehydes due to the presence of one amine (Figure 5.2 A). This results in at least two peaks for each aldehyde according to their *syn*- and *anti*-conformation. PFBHA can aid to identify molecules in the mass spectrum, since the mass fragments are less complex than with PFPH. In the case of MDA, two molecules of PFBHA bind one molecule of MDA and generate a new product of *m/z* 463. In addition, a second derivatization with BSTFA was done to protect free hydroxy-groups (Figure 5.2 B). This was necessary to monitor the reaction intermediate 3-HPA. 3-HPA contains one aldehyde group that can react with PFPH and an alcohol

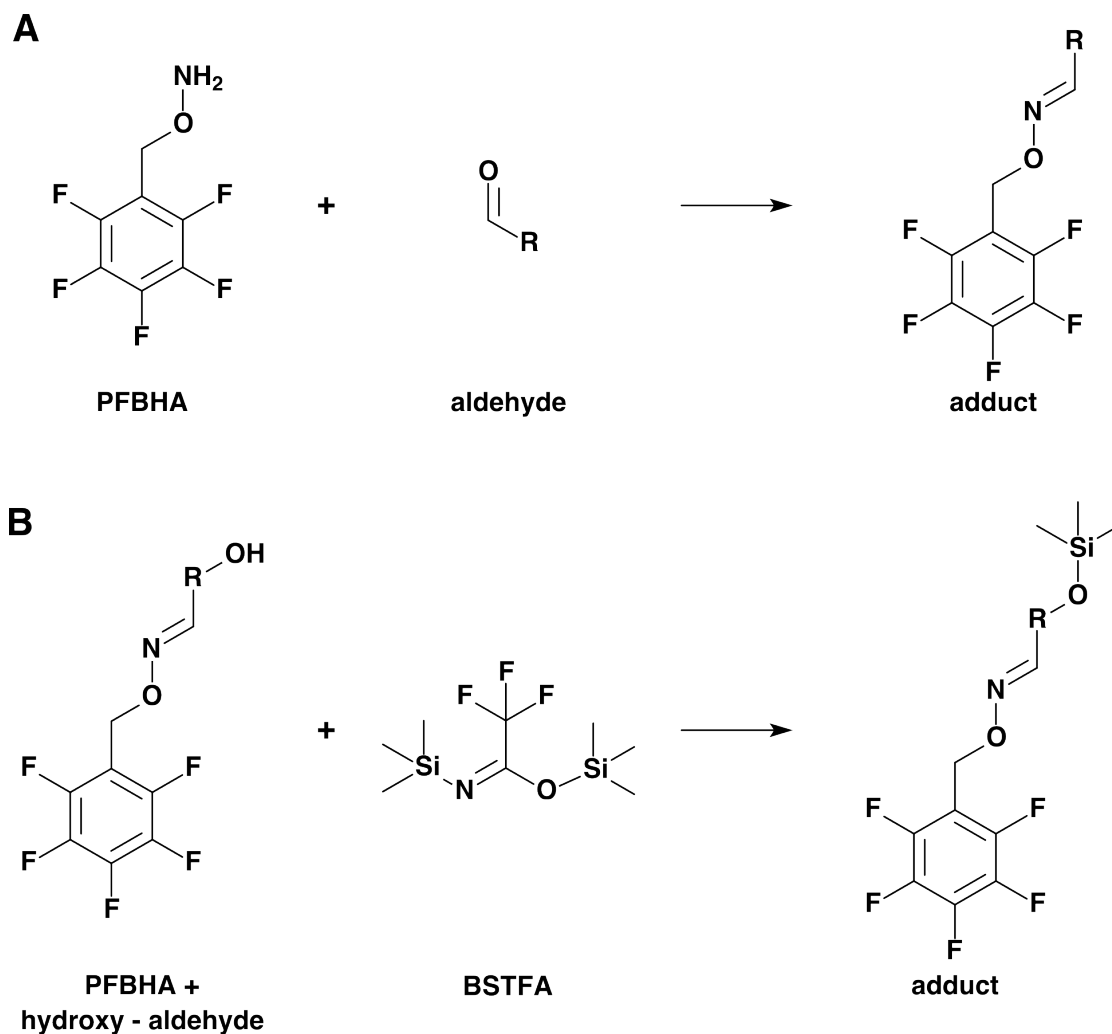


Figure 5.2: Derivatization of small aldehydes prior to GC/MS analysis - A Derivatization of aldehydes using O-(2,3,4,5,6-pentafluorobenzyl) hydroxylamine hydrochloride (PFBHA) in order to separate them from polar molecules and increase the mass for mass spectrometry analysis. **B** Second derivatization for hydroxy aldehydes with N,O-Bis(trimethylsilyl)trifluoroacetamide (BSTFA) to protect hydroxy- and carboxy-groups, which interfere in GC/MS analysis.

5. GENERATION OF ISOTOPE-LABELED MALONDIALDEHYDE

group that is derivatized with BSTFA. The methods we developed for MDA purification and analysis also provided us with a tool to study 3-HPA. Little is known about 3-HPA in living organisms and research derives mainly from probiotic bacteria (Talarico and Dobrogosz, 1989; Voisenet, 1910; Vollenweider et al., 2003) where it was originally described under the name *reuterin* as a cell growth inhibitor for gram-negative bacteria, yeast, fungi and protozoa. So far it has not been described or even been detected in plants but might potentially exist.

Concerning 1,3-propanediol a specific derivatization method for GC/MS had to be applied since it poses no aldehyde group for PFBHA derivatization. Direct injection and analysis by GC/MS is possible but lacks the possibility to first separate it from contaminants. We therefore decided to derivatize the 1,3-propanediol with boronate, which forms cyclic structures with 1,3- and 1,2-diols (Brooks and Maclean, 1971). The boronate derivative chosen for our analysis was 4-(trifluoromethyl) phenylboronic acid (TMPBA) due to large adduct masses, which facilitates GC/MS analysis. GC/MS combined with UV-spectrophotometry permitted us to monitor the enzymatic reaction and more importantly, the purity of the MDA after anion exchange.

5.2 Material and Methods

Generation of isotope-labeled malondialdehyde - 1,3-propanediol isotopes were purchased from the following companies: [^{12}C]-1,3-propanediol, Sigma-Aldrich in Buchs, Switzerland; [$U-^{13}\text{C}$]-1,3-propanediol, 99% ^{13}C from Campro Scientific GmbH in Berlin, Germany; [$2-^{14}\text{C}$]-1,3-propanediol (55 mCi mmol $^{-1}$) from Hartmann Analytics in Braunschweig, Germany. The 1,3-propanediol was enzymatically converted by equine alcohol dehydrogenase (Sigma-Aldrich, recombinantly expressed in *E. coli* with 0.5 U mg $^{-1}$) to MDA as described previously (Summerfield and Tappel, 1978). Briefly, 10 ml reactions in 50 mM sodium pyrophosphate buffer pH 9 (reaction buffer, RB) were prepared containing 2 mM 1,3-propanediol, 2 mM NAD $^{+}$, 2.4 U lactate dehydrogenase, 20 mM sodium pyruvate and 15 U of recombinant alcohol dehydrogenase. The reaction was evaluated by spectrophotometry at 266 nm against an equal enzymatic mix containing 20 mM pyrazole as inhibitor. Evaluation of the single recycling reaction was done using 1 ml reactions containing 1.7 U of lactate dehydrogenase, 4 mM pyruvate and 0.1 mM of NADH in 50 mM sodium pyrophosphate buffer pH 9, monitoring NADH oxidation at 340 nm by spectrophotometry.

Purification of MDA by anion exchange chromatography- The purification of MDA was based on a weak anion exchange resins (Dowex Marathon WBA free base form,

Sigma-Aldrich) or strong anion exchange resins (Dowex 1x8 or 1x2, Cl⁻ form, Sigma-Aldrich). Strong anion exchange resin was first activated as described by the manufacturer. Weak anion resin (Dowex Marathon) was used without activation by a strong acid and only soaked with the reaction buffer. The column consisted of a poly-prep chromatography column (0.8 x 4 cm, Biorad in Reinach, Switzerland) filled with the resin (2 ml) and a syringe needle (Becton Dickinson AG (BD) Alschwil, Switzerland Microlance 3 25-G^{5/8}, 0.5 x 16 mm gauge) plugged at the end to reduce and control the flow. On top of this system, an empty 10 ml syringe was fixed as buffer reservoir (BD Discardit syringe 10 ml). The reservoir flow was controlled by another syringe needle (BD Sterican 23-G-2^{3/8}, 0.6 x 600 mm). The column was first conditioned with 5 volumes (10 ml) of RB-buffer before the reaction mix was applied. After the reaction mix passed through the column and MDA was bound, the column was washed with 5 volumes (10 ml) of RB-buffer. To elute bound MDA, 0.5 N NaCl in RB was added (5 volumes = 10 ml). Eluting fractions containing MDA were collected in 24-well plates (Falcon Multiwell, BD France). MDA in these fractions was measured by spectrophotometry (Genesys 10S UV-Vis, Thermo Wohlen, Switzerland) at 267 nm in Na₃PO₄ buffer pH 11 (10 mM) and the MDA concentration calculated based on molar absorption coefficient $\epsilon = 31500 \text{ M}^{-1} \text{ cm}^{-1}$ (Esterbauer et al., 1991). Absorbance wave scans of the combined MDA fractions were made by scanning from 200 to 350 nm measured against a control run lacking 1,3-propanediol and MDA.

Gas Chromatography / Mass Spectrometry (GC/MS) analysis of aldehydes - The detection of aldehydes was based on combined PFBHA- and BSTFA-derivatization. Sodium tungstate (0.3 M, 100 μl) was added to 400 μl of crude or purified fractions and the samples centrifuged for 5 min at 1000 g to precipitate protein. The supernatant was combined with 450 μl of buffer (0.21 M citric acid, 0.58 M Na₂HPO₄; pH 4). The pH was verified to be 4 and if necessary adjusted with 9 N H₂SO₄. For derivatization, 100 μl of PFBHA reagent (5 mg ml⁻¹ in water) was added and incubated for 1 h at 22°C. The PFBHA adducts were extracted by adding 0.5 ml MeOH and 2 ml hexane, and the organic phase acidified with 10 μl 9 N H₂SO₄. The organic phase was recovered after centrifugation for 5 min at 1000 g and brought to dryness with N₂. BSTFA (pure, 50 μl) was added and silylation conducted for 30 min at 60°C. Samples were injected directly into the GC/MS and analyzed in the positive chemical ionization mode (PCI) with selected ion monitoring (SIM) for the mass of MDA(PFBHA)₂ = m/z 463 and 3-HPA(PFBHA)(Si(CH₃)₃) = m/z 342. Splitless injection at 250°C and carrier flow of 1.5 ml min⁻¹. Initial oven temperature 60°C for 2 min, followed by a ramp of 8°C min⁻¹ till 320°C.

5. GENERATION OF ISOTOPE-LABELED MALONDIALDEHYDE

GC/MS analysis of alcohols -The detection of 1,3-propanediol was based on boronate derivatization. 10 μl of the fractions of interest were taken and mixed with 50 μl of 100 mM 4-(trifluoromethyl) phenylboronic acid (TMPBA) in MeOH. Derivatization was allowed to proceed for 10 min at 25 °C. The adduct was extracted by adding 100 μl isooctane, mixing and centrifugation at 1000 g for 5 min at room temperature to separate the phases. The organic phase was then analyzed by GC/MS: splitless injection (240°C) with methane for PCI, initial oven temperature 50°C for 1 min, ramp with 40°C min^{-1} till 280°C, gas flow of 1.5 l min^{-1} .

5.3 Results

5.3.1 Enzymatic generation of MDA with alcohol dehydrogenase

1,3-propanediol represents a poor substrate for alcohol dehydrogenase (ADH) purified from horse and was reported previously to have a K_m of about 1.7 mM. Additionally, the enzyme operates with a lag phase of 20 min (Summerfield and Tappel, 1978). As the enzyme preparation as used in the original report by (Summerfield and Tappel, 1978) was unavailable commercially, we used recombinant equine ADH produced in *E. coli*. To first evaluate whether the coupling reaction providing fresh NAD^+ worked correctly we monitored NADH oxidation at 340 nm. The initial reaction speed was found to be $v = 140 \pm 45 \mu\text{M min}^{-1}$ for 1.7 U of lactate dehydrogenase, 4 mM pyruvate and 0.1 mM of NADH. For the complete reaction the maximum efficiency of 1,3-propanediol conversion to MDA was originally found to be approximately 65% with 0.0015 U of enzyme per 1 mM of 1,3-propanediol after 24 hours (Summerfield and Tappel, 1978). This resulted in a reaction speed of approximately 50 nmol hour^{-1} . The highest efficiency observed in our setup was between 40 - 50% conversion with 7.5 U mM^{-1} of 1,3-propanediol and a speed of about 400 pmol hour^{-1} in the first 24 hours. The maximum conversion was obtained after 2-3 days for 10 ml preparations containing 2 mM 1,3-propanediol. The concentration was monitored spectrophotometrically for specific absorbance of MDA at 267 nm in 10 mM Na_3PO_4 buffer, pH 11. An identical enzymatic mix but with 20 mM pyrazole, a specific ADH inhibitor (Theorell and Yonetani, 1963) was used as a control. Additional MDA quantification by GC/MS was used to confirm the spectrophotometrical analysis. In our hands, the recombinant enzyme worked less efficiently than reported for the extracted horse ADH.

5.3.2 Purification of MDA by anion exchange chromatography

MDA is known to be negatively charged at a pH above its pK of 4.46 (Esterbauer et al., 1991) and in the enzymatic mix at pH 9 it is therefore present as the enolate.

1,3-propanediol on the other hand is uncharged. Using an anion-exchange column thus allowed us to bind MDA and elute unbound 1,3-propanediol (Figure 5.3 A). Both weak and strong anion exchange resins were tested for their ability to bind MDA.

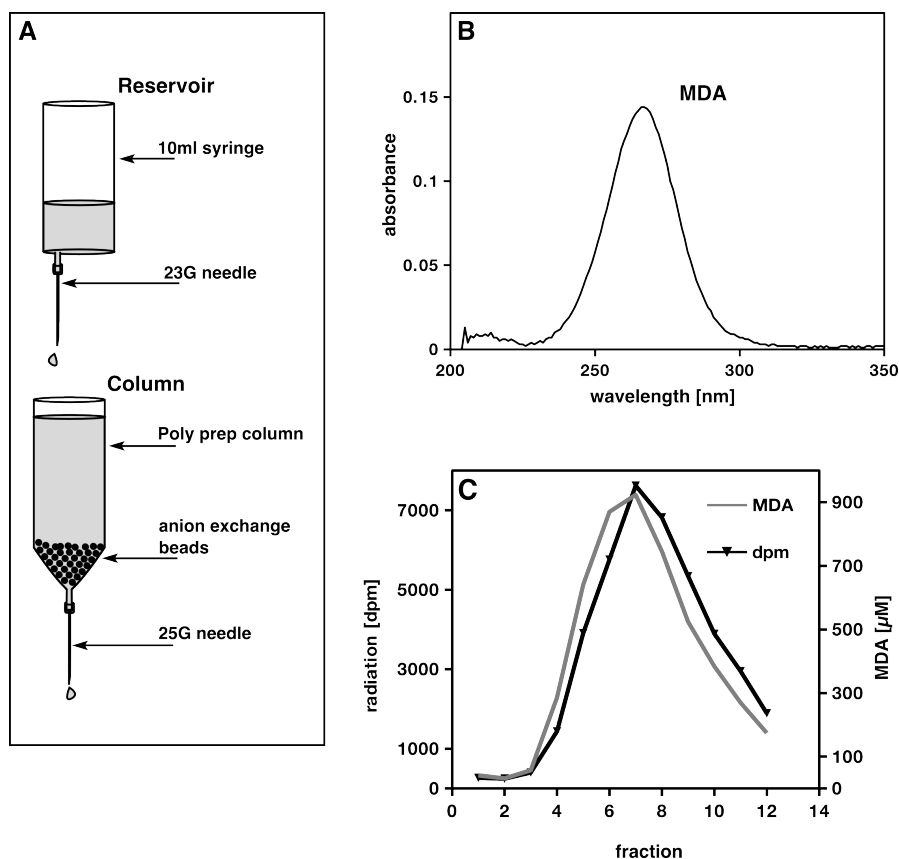


Figure 5.3: MDA purification and concentration by anion exchange chromatography - **A**. Poly-prep column loaded with conditioned basic anion exchange beads was used to bind MDA and elute 1,3-propanediol in the flow-through. After washing, MDA was eluted with 0.5 N NaCl and fractions were collected in micro-titre plates. **B**. Absorbance spectrum of combined eluted MDA fractions, diluted 1:100 in 10 mM Na_3PO_4 pH 11 measured against a control lacking 1,3-propanediol. Maximum absorbance at 266 nm **C**. Characterization of anion exchange eluted ^{14}C -MDA fractions. Right y-axis: MDA concentration measured by spectrophotometry at 266 nm; left y-axis: radiation measured by liquid scintillation

The resins were prepared as described by the manufacturer. Soaked resins (2 ml) were poured into the column and then washed with pyrophosphate buffer pH 9 before the enzymatic mix was applied. The enzymatic mix was loaded and unbound material was washed off with buffer. The amount of MDA in the flow-through was low. We used 0.5 N NaCl to elute bound MDA. Lower NaCl concentrations resulted in an increased elution volume and therefore the MDA was too diluted for applications, whereas higher concentrations caused crystal precipitates if kept at 4°C. An absorbance wave scan of

5. GENERATION OF ISOTOPE-LABELED MALONDIALDEHYDE

combined eluted MDA fractions was compared by spectrophotometry to a control purification run lacking 1,3-propanediol (Figure 5.3 B). The absorbance spectrum correlated with the reported MDA absorbance (Esterbauer et al., 1991) showing a maximum at 267 nm. This was also the case for MDA fractions diluted in 10 mM Na₃PO₄, pH 11, buffer and measured against NaCl in buffer as control. Further evaluation of eluted MDA fractions diluted in Na₃PO₄ buffer was performed using a molar absorption coefficient of $\epsilon = 31500 \text{ M}^{-1} \text{ cm}^{-1}$ (Esterbauer et al., 1991). Spectrophotometry was found to serve as a fast and easy tool to check the eluted MDA concentration. Absorbance wave scans of 1,3-propanediol in Na₃PO₄ buffer did not show any absorbance in the MDA range. About 2 ml of resin was capable of binding 5 μmol of MDA with $94 \pm 6 \%$ of the loaded MDA being recovered. The efficiency for the strong anion exchange resins was slightly lower. This agreed with earlier findings that little MDA was detected in the flow-through from the weaker ion exchange resin. For further experiments, the weak anion resin was used and only fractions with an MDA concentration higher than 300 μM were pooled. Fractions eluting earlier and containing less MDA were discarded. This guaranteed a high final concentration of MDA and minimized potential impurities. Replacing some of the 1,3-propanediol with labeled [2-¹⁴C]-1,3-propanediol, we were able to generate labeled [2-¹⁴C]-malondialdehyde (¹⁴C-MDA). When we compared the anion exchange fractions of purified ¹⁴C-MDA for their absorbance and the emitted radiation, we found a strong correlation between the maximum concentration of MDA and radiation (Figure 5.3 C).

To summarize, we were able with our present setup to obtain from starting 20 μmol of 1,3-propanediol between 6 and 9 μmol of purified MDA, usually in a concentration between 1 and 2 mM. The generated MDA was used immediately for further experiments but can be stored for several hours at room temperature or up to several days at 4°C. Long term storage should be avoided since the final concentration is in the millimolar range and MDA tends to dimerize (Golding et al., 1989). In addition, precipitates occurred if purified MDA was stored at 4°C for several hours, which are likely to be the MDA sodium salt formed with the Na⁺ from the 0.5 N NaCl elution solution. In accordance with Lacombe et al. (1990), we were able to lyophilize the MDA and obtain MDA sodium salt, but found much lower concentrations when resuspended afterwards. This might be due to the volatile character of MDA and was therefore not favorable for our experimental setup.

5.3.3 GC/MS-Characterization of purified MDA

GC/MS analysis with selected ion monitoring (SIM) for MDA and 3-HPA was used to examine the purity (Figure 5.4). The MDA standard from tetrabutylammonium MDA

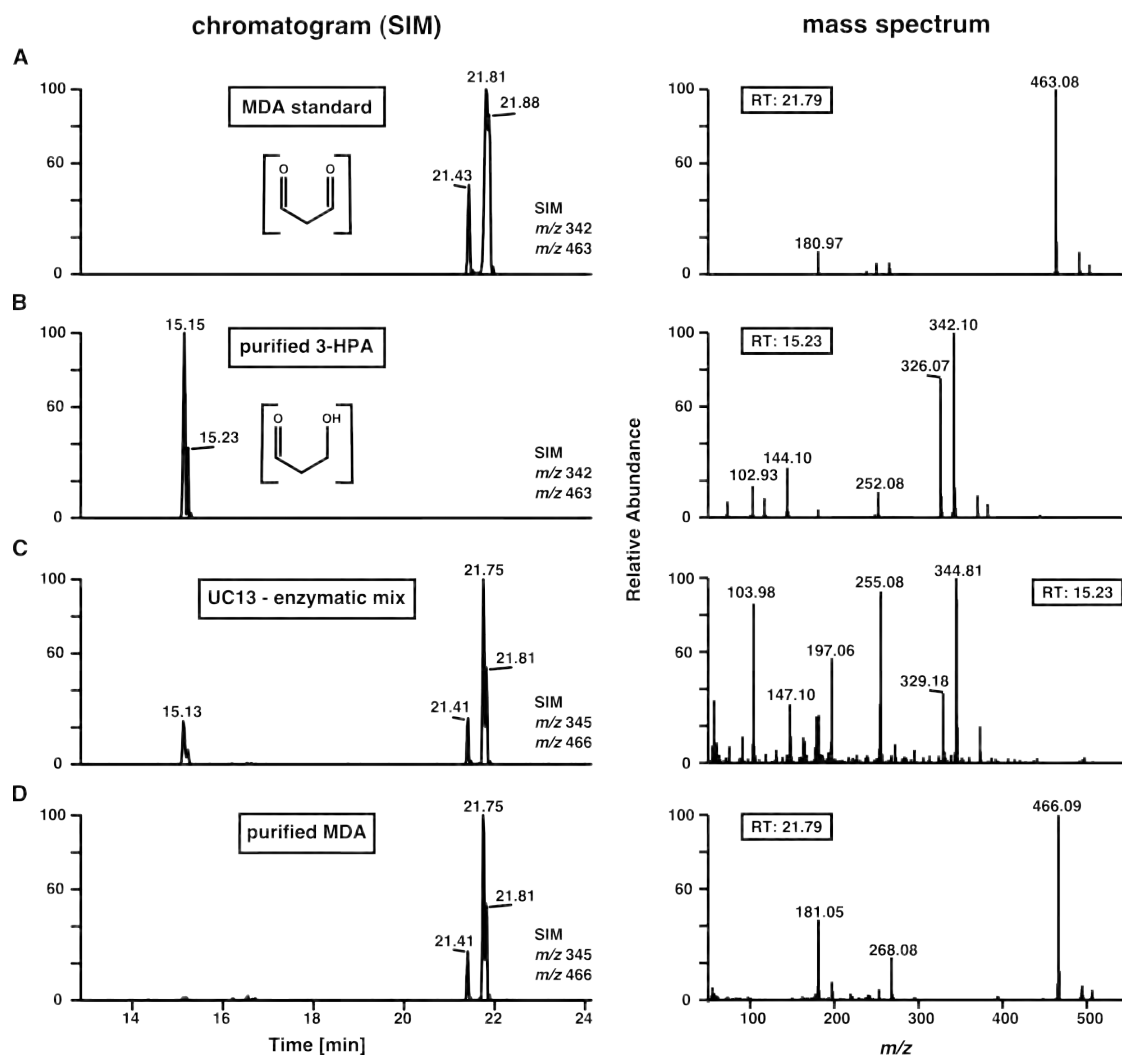


Figure 5.4: GC/MS characterization of MDA purified by anion-exchange chromatography - The left column shows the chromatogram and the right side the corresponding mass spectrum obtained in PCI mode. **A.** MDA generated from tetrabutylammonium malondialdehyde salt. **B.** Purified 3-HPA. **C.** [$U-^{13}C$]-labeled enzymatic mix to generate ^{13}C -MDA after 3 days of incubation. Both, MDA and 3-HPA were observed showing the expected +3 m/z mass shift. **D.** MDA purified by anion-exchange chromatography with the +3 m/z mass shift. Samples were derivatized using PFHBA.

5. GENERATION OF ISOTOPE-LABELED MALONDIALDEHYDE

showed two major peaks after derivatization with PFBHA in the gas chromatogram (Figure 5.4 A). These peaks showed the expected mass of m/z 463 in PCI, which derives from the bonding of one PFBHA molecule per aldehyde group of MDA (Figure 5.4 A, right panel). Running a 3-HPA standard we found a double peak that eluted earlier with the expected calculated mass of m/z 342 (Figure 5.4 B). 3-HPA binds to one molecule of PFBHA and the free hydroxy-group is further derivatized by the BSTFA adding an additional $(\text{Si}(\text{CH}_3)_3)$ -group (Figure 4.3 B). No MDA was detected in the 3-HPA standard. For the evaluation of MDA purity after column purification we replaced the 1,3-propanediol by an $[U-^{13}\text{C}]$ -labeled isotope and converted it enzymatically as described (Figure 5.4 C). Therefore, the mass for the GC/MS SIM analysis was shifted for MDA and 3-HPA by $+3$ m/z to m/z 466 and m/z 345, respectively. The gas-chromatogram showed the same retention times as those observed previously for MDA and 3-HPA. Analyzing the mass spectrum of the first double peak eluting at 15.13 and 15.23 min (Figure 5.4 C, right panel) showed a similar mass spectrum to the 3-HPA standard (Figure 5.4 B) with an mass shift $m/z + 3$ for the parent ion, but as well for some fragments. The background noise in the mass spectrum from the enzymatic mix was higher since another peak eluted at a very similar retention time to the peak of 3-HPA. The major peak eluting later between 21.41 and 21.81 min was found to be MDA. It showed a similar retention time as the MDA standard and furthermore, a similar mass spectrum with the expected mass shift (mass spectrum not shown, similar to figure 5.4 D, right panel). The peak area for MDA was higher than 3-HPA, underlining again the fact that 3-HPA is an intermediate in the reaction. The GC/MS analysis confirmed that both, $[U-^{13}\text{C}]$ -labeled 3-HPA and MDA are generated by this enzymatic reaction. The enzymatic mix was further purified with the weak anion exchange system to obtain purified MDA, which was again analyzed by GC/MS after derivatization (Figure 5.4 D). MDA was dominant in the purified elute and 3-HPA was not detected anymore in the SIM chromatogram. A small peak was present at the previously observed 3-HPA retention time, but the abundance of the parent ion (m/z 345) was barely detectable anymore against the noise in the mass spectrum. The mass spectrum of the purified MDA showed a shift of $m/z + 3$ to m/z 466 in the mass spectrum (Figure 5.4 D, right panel). The absence of 3-HPA in the final MDA elute proves, that the weak anion exchange column provides a reliable and fast method to generate purified ^{13}C -labeled MDA.

Theoretically, 1,3-propanediol cannot bind to the anion exchange column due to its uncharged state. To test whether 1,3-propanediol binds to the weak anion exchange resin, we charged 1 mM 1,3-propanediol in reaction buffer (10 ml) onto a weak anion exchange column and proceeded similarly to the MDA purification procedure: The flow-through was collected, non-bound material was washed off with buffer, and bound

compounds were eluted with 0.5 N NaCl. Fractions at all steps were collected and analyzed by GC/MS after derivatization with TMPBA (Figure 5.5). The chemical structure of the 1,3-propanediol:TMPBA adduct is shown in (Figure 5.5 A) together with its specific mass spectrum obtained in PCI-mode. The sample with 1,3-propanediol in buffer, similar to the enzymatic conversion mix, showed a dominant peak eluting at 4.88 min, which was identified by its mass spectrum to be 1,3-propanediol (Figure 5.5 B). This peak was also present with almost the same intensity in the collected flow-through, indicating that no interaction between 1,3-propanediol and the resins took place. The collected wash fractions still contained some 1,3-propanediol as shown by the presence of its specific peak. The final eluate with 0.5 N NaCl contained only MDA and no 3-HPA or 1,3-propanediol.

5. GENERATION OF ISOTOPE-LABELED MALONDIALDEHYDE

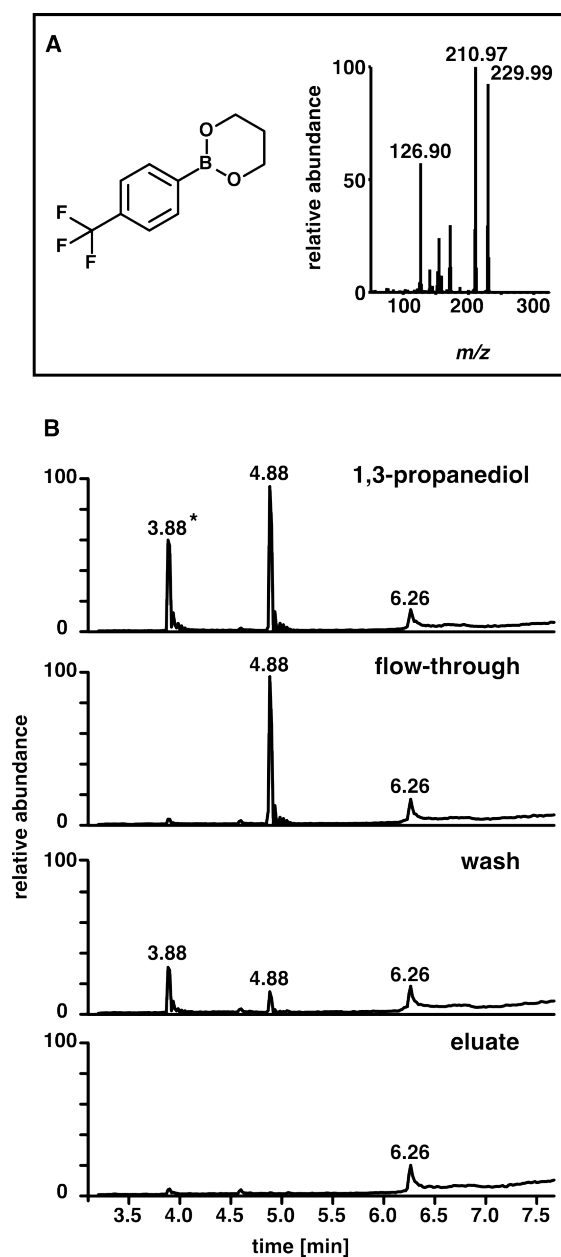


Figure 5.5: Analysis of 1,3-propanediol in anion exchange fractions by GC/MS - A. Chemical structure of the 1,3-propanediol:TMPBA adduct and its mass spectrum analysis by PCI **B.** Evaluation of 1,3-propanediol presence in different anion exchange fractions (GC-TIC). 1,3-propanediol (1 mM) in 50 mM pyrophosphate buffer pH 9 eluting at 4.88 min retention time. Flow-through = flow-through after the mix was loaded on a weak basic anion exchange column, wash = wash of the column with pH 9 pyrophosphate buffer, eluate = combined fractions eluted with 0.5 N NaCl. * = contaminant.

5.4 Discussion

The MDA employed in laboratories is commonly obtained from the tetrabutylammonium MDA salt or from the acid hydrolysis of 1,1,3,3-tetraethoxypropane (TEP). Neither of these methods was useful for the generation of isotope-labeled MDA. Concerning ^{14}C the salt suffers from potential decay due to intramolecular damage often caused by beta decay and was not available upon request from any manufacturer. The generation of MDA from TEP on the other hand was shown to result not only in MDA release but also in the generation of other side products such as β -ethoxy-acrolein and β -methoxy-acrolein which are known to be equally or even more reactive than MDA (Marnett and Tuttle, 1980). Since the standard MDA generation methods were unable to serve our needs another way to generate and purify MDA had to be developed. The enzymatic conversion of 1,3-propanediol to MDA promised to be a very robust reaction and isotope-labeled 1,3-propanediol was readily available from different suppliers. The reaction worked less efficiently with the *E. coli* derived recombinant enzyme compared to enzyme extracted from horse. Nevertheless, sufficient amounts of MDA could be prepared. Special attention is necessary when purchasing isotope-labeled 1,3-propanediol. Often alcohols like EtOH (for example 0.1% (v/v) in water) are used as solvents and show a higher affinity towards the enzyme than 1,3-propanediol. This can interfere with the reaction leading to a lower yield of MDA than expected. One way to overcome this - used for one batch of $[2-^{14}\text{C}]$ -1,3-propanediol - was by carefully evaporating the more volatile EtOH and evaluating the purity of the remaining 1,3-propanediol by injecting it directly into the GC/MS. However, this was accompanied with a loss of 1,3-propanediol and should therefore be avoided if possible.

In the original publication (Summerfield and Tappel, 1978) MDA was purified by shifting the pH to pH 3 and therefore making MDA more volatile. The MDA was then evaporated by heating to 50 °C and condensing the steam at -78 °C. This method was found to be suboptimal for MDA purification suffering from poor and variable recovery as well as the danger of generating analytic artifacts (Janero, 1990). One threat in the particular case might come from contamination with 1,3-propanediol or 3-HPA both of which are volatile and might not be removed from the sample. Possible contamination by these intermediates was not further investigated by Summerfield and Tappel (1978), since the only method for MDA evaluation used was the TBARS method, which lacks specificity for MDA and does not allow any evaluation of non-reactive side-products. Therefore, final purified MDA might still contain one or both of the precursors and since they represent more than 40% of the reaction mix they cannot be ignored.

5. GENERATION OF ISOTOPE-LABELED MALONDIALDEHYDE

In the present study we used the fact that MDA is charged at a pH higher than 4.5, making it unique among the molecules in this reaction. It was possible to trap generated MDA on anion exchange columns, while the unbound alcohols were eluted. The three anion exchange resins tested showed different efficiencies for trapping the MDA and, surprisingly, the free base form of the weak anion exchange anions was found to be most efficient, even though it was used in the free base form without activation by any strong acid. For the elution of MDA from the column a high salt concentration was chosen over a pH change by acidification in order to prevent MDA being present in a volatile form and losing it before it might be applied.

The technique we developed permitted MDA to be isolated in millimolar concentrations, but, more importantly, 3-HPA and 1,3-propanediol were shown to be absent from the purified MDA. Since 3-HPA was not present in the final purified MDA we conclude that it was either retained unspecifically and washed off in the washing step or, more probably it was eluted very early with the NaCl eluting step due to its weak attraction towards the resins. As described earlier these first eluting fractions were discarded due to their low MDA concentration. GC/MS was an indispensable tool at all stages of the synthesis and purification, helping to verify whether recorded spectrophotometrical absorbance changes corresponded to MDA formation. The purification technique is simple and versatile and should prove useful in further studies employing MDA.

6

Metabolism of malondialdehyde in leaves of *Arabidopsis thaliana*¹

6.1 Introduction

Lipid oxidation by reactive oxygen species (ROS) and the resulting breakdown products are in general considered to be harmful in humans (e.g. Marnett, 2002; Refsgaard et al., 2000) and plants (Mano, 2012; Yamauchi et al., 2008). Lipid bilayers in organelles like mitochondria and chloroplasts have to cope with the omnipresent threat of ROS since both are active sites of ROS production (Blokhina and Fagerstedt, 2010; Krieger-Liszkay, 2005). It is therefore surprising that these membranes were found to contain a high percentage of polyunsaturated fatty acids (PUFAs), like α -linolenic acid (Li-Beisson et al., 2010), which were shown to be very susceptible to non-enzymatic oxidation (nLPO) by ROS (Liu et al., 1997). One reason is the necessity of enhanced fluidity which increases with the proportion of PUFAs. Fluidity was shown to facilitate enhanced chilling tolerance (Falcone et al., 2004; Miquel et al., 1993) and accelerating the re-organization of the photosystem II (PS II) macrostructure (Goral et al., 2012). Recently PUFAs have been proposed to represent a potential buffer system for ROS-induced cell damage (Farmer and Mueller, 2013; Mène-Saffrané et al., 2009). The idea is that FAs act as ROS sinks and in particular for singlet oxygen ($^1\text{O}_2$), thereby protecting other molecules such as proteins. This mechanism might explain how plants handle the threat posed by $^1\text{O}_2$ that is constantly generated in chloroplasts (Zoeller et al., 2012). This hypothesis is supported by the fact that PS II, the major site of $^1\text{O}_2$ generation, is surrounded by PUFAs. About two thirds of the thylakoid FAs are TFAs, which are prone to nLPO (Vijayan, 2002). nLPO might therefore represent a beneficial rather than cell threat-

¹Identification of unknown lipid species was done in collaboration with Dr. G. Glaussen from the Chemical Analytical Service (CAS), University of Neuchâtel in Switzerland; MDA microarray analyses were conducted by S. Stolz

6. METABOLISM OF MALONDIALDEHYDE IN THE LEAVES OF *A. THALIANA*

ening process *in vivo*. Furthermore, lipid breakdown products represent an important source of reduced carbon and might, in theory, be recycled as building blocks for FA- and lipid-synthesis. We raised the question whether small molecules produced by nLPO such as MDA might be recycled to synthesize lipids.

Early experiments in rats suggested that MDA was metabolized through the TCA cycle (Siu and Draper, 1982) or might be used in fatty acid (FA) assembly (Marnett et al., 1985). Potential first steps and routes of MDA metabolism were summarized by Janero (1990) (Figure 6.1). Against the general opinion of MDA being consumed

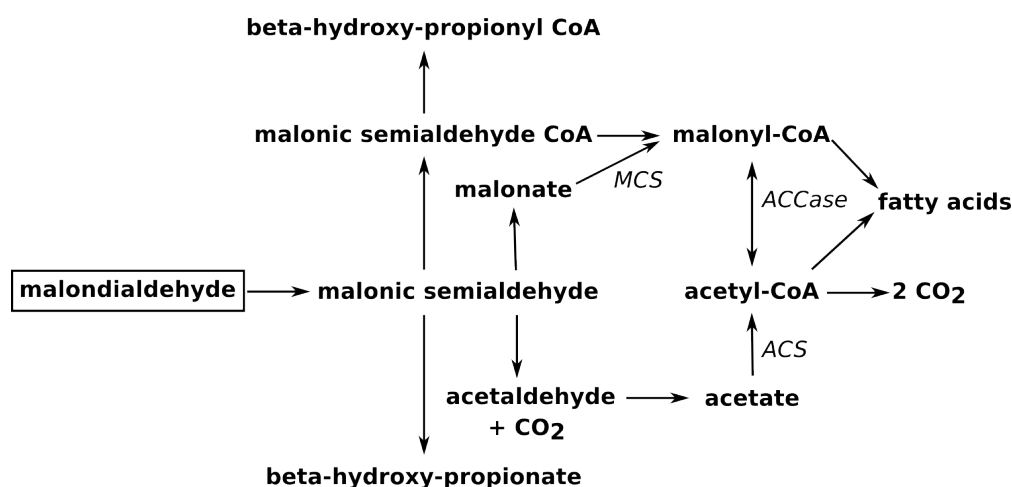


Figure 6.1: Potential routes of MDA metabolism - Simplified hypothetical pathway of MDA metabolism as suggested by Janero (1990). The oxidation of aldehydes to carboxylic acids can be catalyzed by aldehyde dehydrogenases. Enzymes catalyzing the conversion from the carboxylic acid to its acyl-CoA thioester were recently identified in plants as acetyl-CoA synthetase (*ACS*; Behal et al., 2002) and malonyl-CoA synthetase (*MCS*; Chen et al., 2011). Acetyl-CoA carboxylase (*ACCse*) in plants catalyzes the final assembly of the FAs.

by harmful interaction with proteins and DNA, we now suggest that MDA might be metabolized by cells in order to recycle reduced carbon. This hypothesis is consistent with our finding that > 75% of MDA in leaves was present in the free (unbound) form and therefore not bound to macromolecules (see Chapter 3). In the present work we investigated MDA metabolism in plants with the aid of stable isotope-labeled MDA. With our *in vitro* MDA synthesis system (see Chapter 5) we were able to generate and purify ^{13}C - and ^{14}C - isotopes of MDA. Following delivery of these MDA isotopes to the plant we quantified ^{14}C -derived radiation after thin layer chromatography (TLC) and by scintillation counting, and we also analyzed ^{13}C -MDA isotopes by GC/MS. MDA-derived radiolabeled carbons were found in extracted lipids and the particular lipid species were purified and identified by UPLC-TOF-MS. We next studied the dynamics and routes

of this metabolism using mutants for enzymes involved in the sort of reactions that metabolize MDA.

6.2 Material and Methods

Plant growth conditions, genotypes and chemicals - Wild-type (WT) *Arabidopsis* (Col-0) and T-DNA insertion lines from the European Arabidopsis Stock Center were grown on soil at 22°C for 5 weeks (light: 100 $\mu\text{E m}^{-2} \text{s}^{-1}$, 9 h light/15 h dark). *opr1,2* RNA interference (RNAi) lines (O1 and C3) were provided by N. Bruce (Beynon et al., 2009). Chemicals and analytic standards used were purchased from Sigma-Aldrich (St. Louis, Missouri, USA) unless indicated. [1, 2- ^{14}C]- acetic acid sodium salt (^{14}C -acetate) 100-120 mCi mmol $^{-1}$ was purchased from Hartmann Analytics, Braunschweig, Germany. [U- ^{13}C]-1,3-propanediol, 99% ^{13}C was obtained from Campro Scientific GmbH, Berlin, Germany, [2- ^{14}C]-1,3-propanediol 55 mCi mmol $^{-1}$ from Hartmann Analytics. Phospholipid standards from wheat and soybean were purchased from Supelco Analytical via Sigma-Aldrich.

Application of volatile malondialdehyde and quantification by GC/MS - Purified MDA ([^{12}C], [U- ^{13}C] or [2- ^{14}C]) was acidified with 4.5 N HCl to volatilize it. The acidified MDA (200 nmols / plant l $^{-1}$) was pipetted onto cotton sticks and plunged into the plant pot (3 cotton sticks per pot). The plants were kept during the application in transparent, sealed Plexiglas boxes (15 l volume, 15 plants per box) or glass jars (1 l volume, 1 plant), depending on the overall size of the experiment. MDA was quantified by GC/MS as described (see Chapter 3.2).

Lipid extraction from Arabidopsis leaves - Lipids were extracted based on a recommended protocol¹ from the Kansas Lipidomics Research Center with minor changes. Leaves were quickly submerged in 3 ml 75°C pre-heated isopropanol (+0.01 % BHT) and heated for 15 min at 75°C to deactivate phospholipase D. The samples were vortexed for 1 h after addition of 1.5 ml CHCl₃ and 0.6 ml H₂O. The extracts were transferred in new tubes and the leaves were extracted again with 4 ml CHCl₃/MeOH (2:1 + 0.01 % BHT). The combined extractions were cleaned by the addition of 1 M KCl (1 ml) and subsequent vortexing and centrifugation. The organic phase was kept and the aqueous one discarded. The organic phase was then washed again with 2 ml H₂O. Samples were stored at -20 °C prior to experiments or subsequently evaporated to dryness with nitrogen for analysis.

¹<http://www.k-state.edu/lipid/lipidomics/leaf-extraction.html>

6. METABOLISM OF MALONDIALDEHYDE IN THE LEAVES OF *A. THALIANA*

TLC analysis of extracted lipids - For long duration (24 h) MDA incorporation experiments, lipids from 4 plants were combined and extracted as described. After evaporation of the solvent with N₂ the lipids were resuspended in 100% diethylether and loaded onto diethylether-conditioned silica columns (5 ml volume). Unretained lipids were discarded and the column was washed with 1 vol of diethylether. Next, polar lipids were eluted with 5 vol of MeOH (100%) and concentrated with a N₂ stream. The polar lipids were then spotted onto silica TLC plates (silica gel on Al foils or glass, Sigma) and run for 1 h with acetone:toluene:H₂O (90:3:7%) as the mobile phase. Staining for unsaturated bonds was performed with volatile iodine in TLC chambers. Radiation was detected after exposure to a storage phosphor screen (Typhoon FLA 7000 phosphor-imager, GE Healthcare, UK). For short (6 h) ¹⁴C-MDA incorporation experiments lipids were extracted as above. In these experiments, after N₂ evaporation of the solvent, lipids from 3 plants were resuspended in 20 µl of CHCl₃/MeOH (2:1 + 0.01% BHT) and directly spotted onto TLC plates. Very apolar lipids and FFAs were first separated with a mobile phase of diethylether/hexane (50:50%) until the front reached the top of the plate. A second run with acetone:toluene:H₂O (70:23:7) was conducted to separate neutral lipids. Very polar lipids were further separated by a third run with butanol:formate:H₂O (40:10:40%; aqueous phase after funnel partitioning).

HPLC analysis of polar lipids- Lipids were extracted as described and after evaporation of the solvent, resuspended in MeOH (1 ml) in order to recover polar lipids. Lipids which did not dissolve in the MeOH were discarded. The polar lipids were then analyzed on a reverse phase C18 column (XTerra Prep MSC18, 5µm , 10x150mm; Waters GmbH, Eschborn, Germany) with the following gradient: 1-100 min from 93% MeOH and H₂O to 100% MeOH with a flow rate of 2 ml min⁻¹. This was followed by a wash for 30 min with 100% MeOH and a flow rate of 5 ml min⁻¹. The column size exceeded the oven size and was therefore put into a homemade cooling device, keeping the temperature at ~16°C. The fractions obtained were transferred into 15 ml of Flo-Scint scintillation cocktail (PerkinElmer, Schwerzenbach, Switzerland) and counted with Tri-Carb 2800TR (PerkinElmer) after letting the samples rest overnight in the dark. The fractions containing the peak of interest (18:3-16:3-MGDG for WT and 18:2-16:2-MGDG for *fad3-2,fad7-2,fad8*) were combined prior to scintillation counting (3 fractions) and only an aliquot used for the scintillation: the majority was used for further analysis.

Hydrolysis of lipids - Total lipids or purified lipids were evaporated to dryness and resuspended in 5 ml of methanolic KOH (1 M). The saponification reaction was allowed to proceed overnight at room temperature. 10 ml NaCl 0.9 % (w/v) was added and non-saponified lipids were removed by extracting 3 times with diethylether (5 ml). The

aqueous phase was acidified with 600 μl HCl (4.5 M) and the FFAs extracted with 3 x 5 ml hexane. The combined hexane fractions were washed again with H_2O . The aqueous phase was mixed with 15 ml scintillation cocktail (Ultima Gold, PerkinElmer) and counted. FFAs were treated with 0.5 ml of NaClO 13% (w/v, commercial bleach) for 1 h to deplete chlorophyll prior to scintillation counting in Insta-Fluor cocktail (PerkinElmer). To correct for counting efficiency, samples were counted again and a known amount of radiation (^{14}C -18:3 for apolar samples, ^{14}C -1,3-propanediol for polar samples) was added to the samples.

GC/MS analysis - The GC/MS analysis of FAs was conducted as described (see Chapter 3.2). For the analysis of organic acids, dried extracts were derivatized after purification using BSTFA (N,O-Bis(trimethylsilyl)trifluoroacetamide). They were dissolved in 50 μl pure BSTFA and derivatization was conducted at 60°C for 30 min. After concentration under N_2 the samples were directly injected (splitless mode) into the GC/MS and analyzed by positive chemical ionization (PCI). Temperature-gradient: initial T = 60°C, followed by a ramp of 10°C min^{-1} up to 300°C.

UPLC-TOF-MS analysis - Polar lipids were first separated from apolar ones by resuspension of total dried lipid extracts in 1 ml MeOH. The soluble lipids were then separated by HPLC, monitored by UV absorbance and the eluted peaks of interest were concentrated. A fraction (1 μl) of the concentrated HPLC fraction was separated and identified with an Acquity UPLC coupled to a quadrupole time-of-flight mass spectrometer (Waters, Milford, MA, USA) using negative electrospray ionization. Column: Acquity BEH C18, 50x1.0 mm i.d., 1.7 μm particle size. Solvents: A, water; B, methanol. Solvent gradient was 0-2 min from 85 to 100% MeOH, followed by 1 min of 100% MeOH and 1 min of 85% MeOH with a flow rate of 200 $\mu\text{l min}^{-1}$. The high resolution mass spectrometer was operated in MSE mode with alternating scans at low and high collision energies.

Organic acid extractions- Organic acids were extracted according to Stumpf and Burris (1979) with minor changes. Plant rosettes were ground to fine powder using liquid N_2 and transferred into 8 ml 95% EtOH (1 adult plant/vial). The vials were heated at 100°C for 15 min and then centrifuged for 5 min at 1000 g to precipitate the debris. The supernatant was transferred to a new vial and evaporated to dryness under a stream of N_2 at 50 °C. The precipitate was resuspended in H_2O (1 ml) with 5 min sonication. Then, 0.5 ml of CHCl_3 was added and the mixture was centrifuged for 5 min at 20000 g to remove any apolar contaminants in the aqueous phase. The aqueous phase was then loaded onto a Poly-Prep column (0.8 x 4 cm, Biorad, Cressier Switzerland) filled with

6. METABOLISM OF MALONDIALDEHYDE IN THE LEAVES OF *A. THALIANA*

0.5 ml of strong acid cation exchange resins in the H⁺ form (Dowex 50 Wx8 H⁺ 200-400 mesh, Sigma-Aldrich). This column was placed over another column containing 1 ml of strong anion exchange resins (Dowex 1x8, 200-400 mesh Cl⁻, Sigma-Aldrich) in the formate form. Molecules bound non-specifically were eluted from the anion exchange column using 3 ml of H₂O and then organic acids were eluted with 10 ml 2 N formate. The eluate was lyophilized, resuspended in 1 ml H₂O and again lyophilized to dryness for further use.

The strong anion exchange resins were converted from the original Cl⁻-form into the formate-form after soaking the resins (10 ml) first in 1 N NaOH (40 ml) for 1 h. The NaOH was decanted and replaced with of 1 N formic acid (40 ml), stirred and let to settle again for 1 h. The formic acid was decanted and the resin was washed 4 times with H₂O (40 ml).

MDA microarray experiments- Microarray analyses of differentially regulated genes from MDA treated plants were performed by S. Stolz based on published extraction and hybridization protocols (Hilson et al., 2004; Reymond et al., 2004). Adult *Arabidopsis* plants were exposed for 2 h to 10 µm / plant l⁻¹ MDA or pyruvaldehyde (PVA) as a control in Plexiglas boxes (6 replicates, 50 µg RNA total). Differential gene expression was evaluated against mock control plants (5 replicates, $P = 0.05$). Two fold induction/repression was used as a cut-off for final presentation of altered genes. Gene ontology (GO) was analyzed with the tool Bingo¹ (Maere et al., 2005), evaluating up-regulated genes against the CATMA catalog as reference set (18121 genes, threshold $P = 0.05$). Overrepresentation was analyzed using hypergeometrical statistical tests and false discovery rate (FDR) correction. GO slim (V1.2) for plants was used with annotations based on the Tair² database (updated:10/23/2012). Ontology networks were visualized using Cytoscape³ (Smoot et al., 2011).

Primers for genotyping - Acetyl-CoA synthetase, *acs*: left primer (LP) ggcaagt-gcaataagetgac, right primer (RP) tgccggatattatttcagtgg; At3g44190: LP aatgggtctgaat-gtttgaac, RP ttacggatcaatgagggtgag; *aldh7b4*: LP aggtaaaccatcatttgc, RP caatcca-
caacaaccaacc.

¹<http://www.psb.ugent.be/cbd/papers/BiNGO/Home.html>

²<http://www.arabidopsis.org/>

³<http://www.cytoscape.org/>

6.3 Results

In order to study the fate of MDA *in planta* we used stable- and radioisotope metabolite tracers. This required the development of a synthetic purification system for MDA (see Chapter 5). The final MDA eluates from our anion exchange system contained non-physiologically high NaCl concentrations which might have influenced the experimental outcome if infiltrated directly into leaves. Therefore, MDA-infiltration by syringe (Weber et al., 2004) was not suitable and we chose instead to introduce MDA into plants in its gaseous form by acidifying it (Mène-Saffrané et al., 2007).

6.3.1 Successful uptake and turnover of exogenous MDA

To validate the successful uptake of MDA its levels in leaves were quantified by GC/MS after application. [U- ^{13}C]-malondialdehyde (^{13}C -MDA) was used to distinguish by mass spectrometry exogenous from endogenous MDA (Figure 6.2). The application of 25 nmol ^{13}C -MDA /plant l^{-1} doubled the resting level of MDA in leaves and, more importantly, a new parent ion with a mass shift appeared in the mass spectrum of MDA (Figure 6.2 B). MDA-PFPH adducts displayed a mass of m/z 234 whereas the new parent ion was shifted by m/z 3 to m/z 237, indicating three ^{13}C -labeled carbons. The ratio of the m/z 234 to m/z 237 parent ion reflected the increased level of MDA in leaves - approximately 90% more was present compared to the resting state levels. To investigate next whether exogenous MDA was turned over *in vivo*, plants were exposed to volatile MDA and MDA levels monitored by GC/MS over time (Figure 6.3). Upon application of 200 nmol of MDA /plant l^{-1} for 30 min, the levels increased ~ 15 -fold (Figure 6.3, time-point 0). The plants were then allowed to turn over the applied MDA and the concentration dropped rapidly to 4-fold resting state level within 60 min. After 2 h of turnover the concentration was 2-fold resting level and 1.5-fold after 4 h. MDA was being turned over at the fastest observed speed with $\sim 18 \text{ nmol min}^{-1}$ and g^{-1} dry weight (D.W.).

6.3.2 ^{14}C -MDA derived radioactivity can be found in plant lipids

We tested the hypothesis that lipid-derived MDA might be recovered for *de novo* FA synthesis by analyzing extracted lipids from ^{14}C -MDA treated plants. Therefore, fresh ^{14}C -MDA [0.45 nCi nmol^{-1}] was enzymatically generated from ^{14}C -1,3-propanediol and purified by anion exchange chromatography. Plants were incubated with the acidified volatile ^{14}C -MDA for 24 h and lipids subsequently extracted. First, the separation of the entire lipid spectrum by thin layer chromatography (TLC) was done with apolar solvents as mobile phase and radiation was detected after phosphor-imaging (Figure 6.4). The radiation was limited to the start point, suggesting more polar molecules to be potential metabolites. Due to the absence of radiation in apolar lipids, we concentrated

6. METABOLISM OF MALONDIALDEHYDE IN THE LEAVES OF *A. THALIANA*

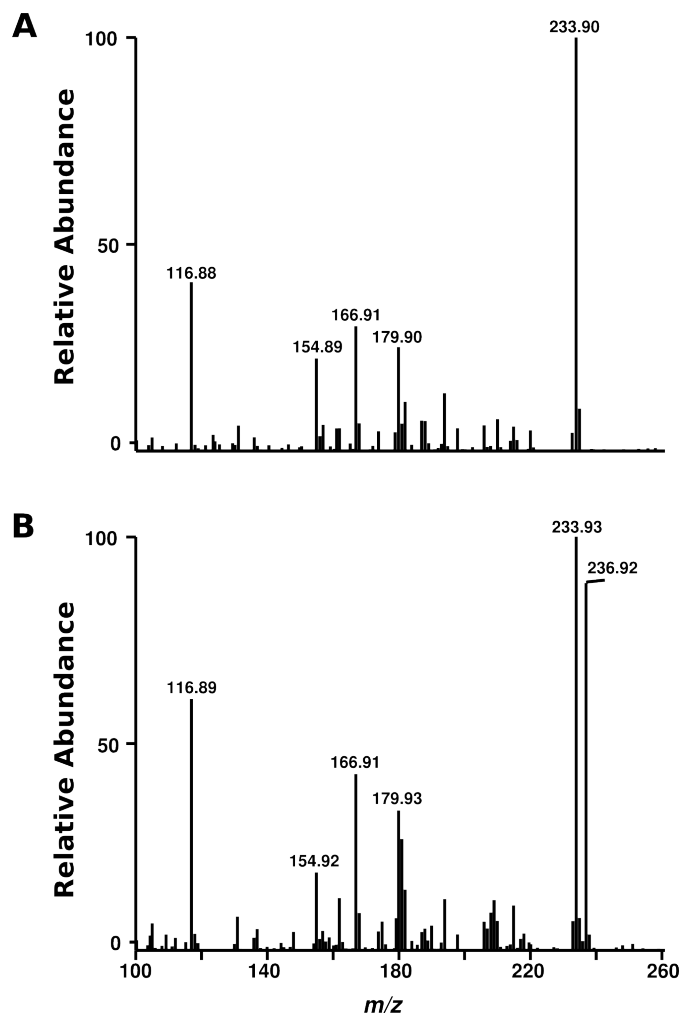


Figure 6.2: Uptake of volatile ^{13}C -MDA in *Arabidopsis* leaves - The successful uptake of MDA was tested by application of $25 \text{ nmol /plant l}^{-1}$ volatile ^{13}C -MDA for 60 min. **A.** Mass spectrum of MDA in leaves of control plants **B.** MDA mass spectrum of ^{13}C -MDA-treated plants. The mass of m/z 234 results from the derivatization with PFPH and the mass shift from m/z 234 to m/z 237 from ^{13}C -MDA.

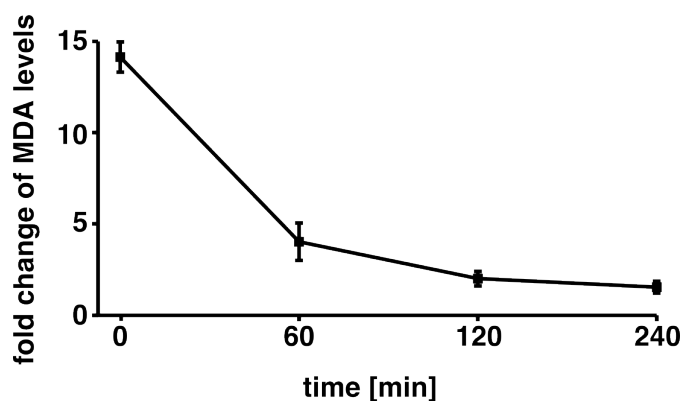


Figure 6.3: Turnover of exogenous MDA in *Arabidopsis* leaves - MDA turnover was investigated after application of $200 \text{ nmol /plant l}^{-1}$ of volatile MDA. The plants were incubated for 30 min with gaseous MDA ($t = 0$) and MDA levels in leaves measured after 60, 120 and 240 min of turnover. MDA levels were expressed in nmol g^{-1} dry weight and normalized to non-exposed control plants. Each data point was from 3 biological replicates.

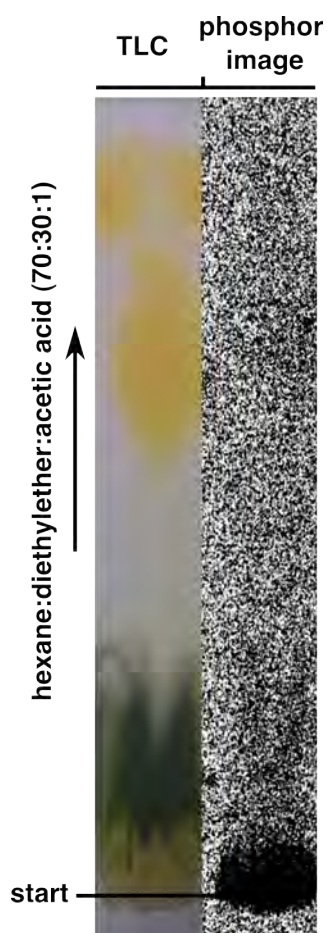


Figure 6.4: TLC-analysis of ^{14}C -MDA incorporation into plant lipids - Separation by TLC of entire lipid extracts from 4 rosettes after ^{14}C -MDA treatment and phosphor-imaging to visualize radiation (24 h, $200000 \text{ dpm /plant l}^{-1}$; specific activity (SA): $0.45 \text{ nCi nmol}^{-1}$). The TLC was run for 1 h with hexane:diethylether:acetic acid (70:30:1) as mobile phase.

6. METABOLISM OF MALONDIALDEHYDE IN THE LEAVES OF *A. THALIANA*

on the polar lipid species and removed apolar lipids and FFAs prior to further analyses. This was achieved by loading the extracted lipid mix dissolved in 100% diethylether onto small columns filled with silica (2 ml) and conditioned with diethylether. After binding to the column, polar and neutral lipids were eluted with 100% MeOH and spotted onto TLC plates. This technique removed most chlorophyll and apolar lipids which remained bound to the column and allowed successful separation of the more polar lipids (Figure 6.5 A). Upon phosphor-imaging of the separated polar lipids, 4 bands appeared and the fastest migrating band contained most of the radiation (Figure 6.5 B). This band migrated just below the chlorophyll band and was colored by the iodine staining indicating unsaturation. Another band containing less radioactivity co-migrated with a phospholipid mix from wheat (containing phosphatidylethanoamine = PE, phosphatidylcholine = PC, phosphatidylinositol = PI and lyso-phosphatidylcholine = lyso-PC), suggesting that ^{14}C -MDA might be incorporated into phospholipids. Not all apolar lipids were successfully removed, as judged by bands running further than the chlorophyll and being stained by the iodine.

6.3.3 Successful identification of an MDA end-point metabolite

In order to identify and purify molecules with ^{14}C -MDA incorporation we analyzed next polar lipids by high pressure liquid chromatography (HPLC). Total lipid extracts were dried with a stream of N_2 and resuspended in MeOH; insoluble triacylglycerols and sterol esters were discarded. Reverse phase HPLC was conducted and monitored at UV-wavelength 200-500 nm (Figure 6.6 A). Since the double bonds of lipids absorb at 206 nm, this wavelength was chosen as a lipid indicator (Holte et al., 1990). The eluted fractions were subsequently mixed with scintillation cocktail and analyzed by liquid scintillation for their radiation (Figure 6.6 B). Many different compounds were found to elute with the chosen gradient indicated by overall UV absorbance (Figure 6.6 A). Quantitative scintillation of the fractions revealed that most ^{14}C -MDA-derived radiation seemed to accumulate in one molecule at a retention time of about 32 min (Figure 6.6 B). This correlated with the observation from the TLC on which we found most radiation concentrated in one band. Nevertheless, radiation was also observed on other regions of the HPLC and the TLC. The major radiolabeled molecule seemed to be rather pure as judged by its absorbance at 206 nm (Figure 6.6 A, black box). To reveal its identity the fraction was isolated from an identical HPLC separation (^{12}C -MDA) and analyzed by UPLC-TOF-MS (Figure 6.7). In the UPLC-TOF-MS analysis one major peak was observed together with some early eluting putative breakdown products (Figure 6.7 A). Analyzing the mass of the major peak eluting at 2.25 min, we concluded that the molecule was 18:3-16:3-monogalactosyldiacylglycerol (18:3-16:3-MGDG, Figure 6.7 B) with a parent ion of m/z 745 and a formate adduct of m/z 791. The pseudo

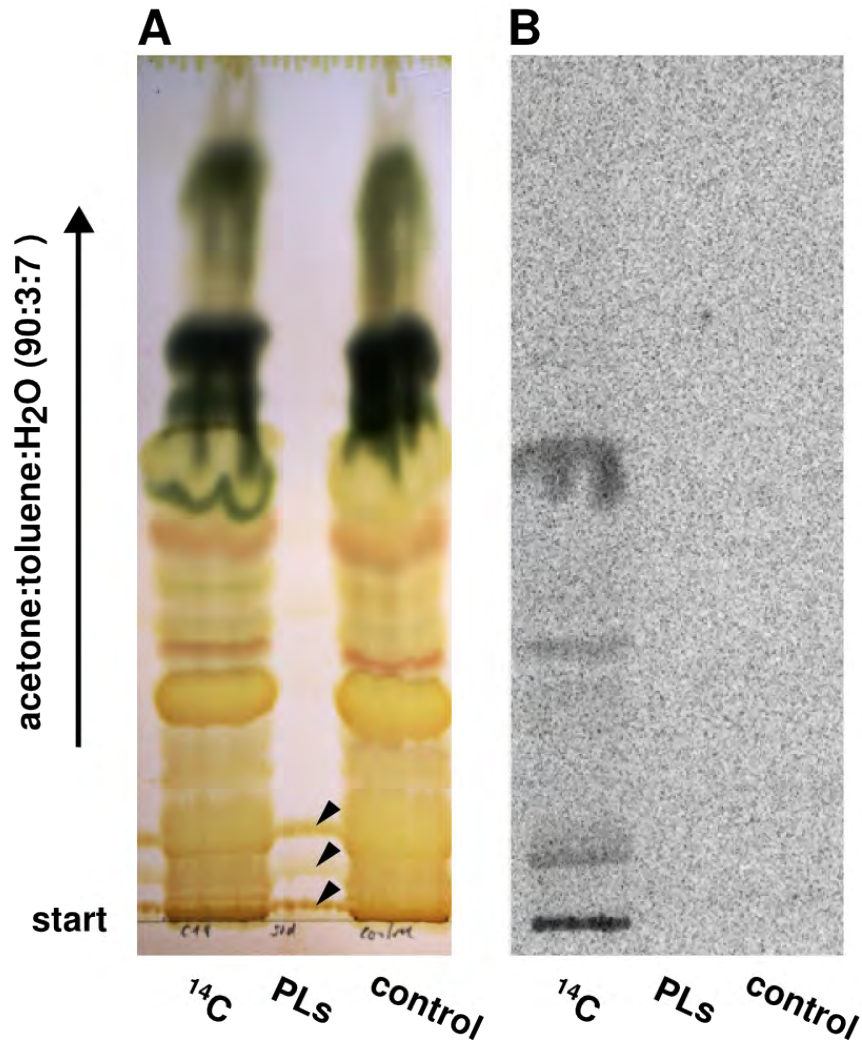


Figure 6.5: TLC-analysis of ^{14}C -MDA incorporation into polar plant lipids - A TLC-separation of plant lipids from 4 control plants and 4 ^{14}C -MDA exposed plants ($200000 \text{ dpm}/\text{plant l}^{-1}$; SA: $0.45 \text{ nCi nmol}^{-1}$). Plants were incubated for 24 h in the presence of MDA, total lipids were then extracted and apolar lipids removed with a silica column. The mobile phase was acetone:toluene: H_2O (90:3:7). TLC plates were stained with iodine vapor for unsaturation (yellow color). Arrowhead point to phospholipid species. PLs = phospholipid mix from wheat containing phosphatidylethanoamine, phosphatidylcholine, phosphatidylinositol and lyso-phosphatidylcholine. **B** Phosphor-imaging of the separated lipids.

6. METABOLISM OF MALONDIALDEHYDE IN THE LEAVES OF *A. THALIANA*

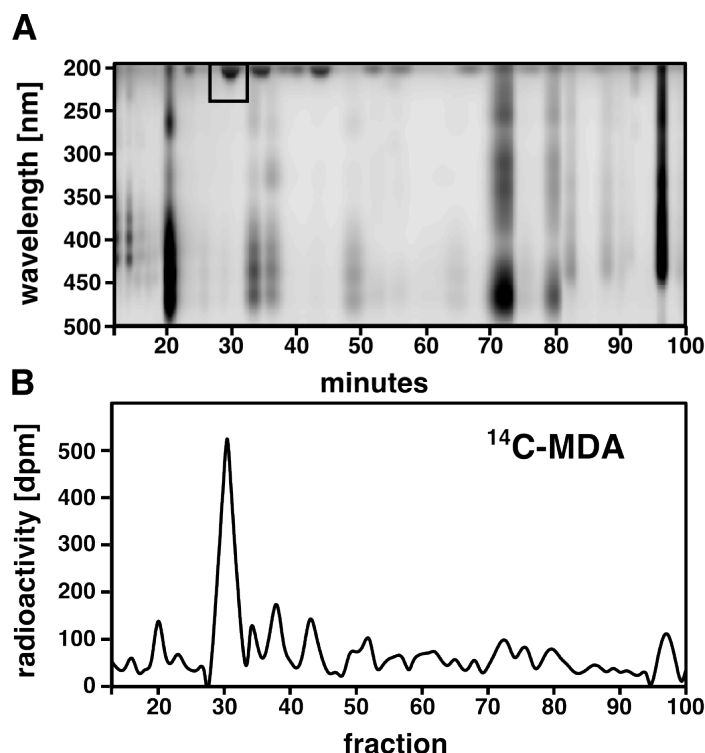


Figure 6.6: HPLC separation of polar lipids and ^{14}C -incorporation analysis - A. Polar leaf lipids from ^{14}C -MDA treated plants, separated by HPLC and monitored by UV (200-500 nm). **B.** Radiation distribution in HPLC-fractions measured by liquid scintillation. (Pool of leaves from 4 plants, 300000 dpm /plant l^{-1} ; SA: 0.67 nCi nmol^{-1}).

MS-MS mass peaks of m/z 249 and m/z 277 represented the linolenic acid (18:3) and hexadecatrienoic acid (16:3) moiety, respectively. The hypothesis that 18:3-16:3-MGDG might contain ^{14}C from ^{14}C -MDA was tested using the *fad3-2,fad7-2,fad8* mutant which lacks TFAs. *fad3-2,fad7-2,fad8* plants were exposed for 24 h to ^{14}C -MDA and polar lipids analyzed by HPLC and scintillation (Figure 6.8). The polar lipid composition of these plants (Figure 6.8 A) was strikingly different compared to that one of the WT (Figure 6.6 A) as judged by the UV-absorbance profile. Most importantly, the *fad3-2,fad7-2,fad8* mutant lacked the 18:3-16:3-MGDG lipid, previously observed at 32 min in the WT. Radioactivity analysis (Figure 6.8 B) mirrored this result, lacking the major radiation peak at 32 min but showing instead a new one at 45 min (Figure 6.8, black box). UPLC-TOF-MS confirmed that the ^{14}C -MDA incorporation peak in *fad3-2,fad7-2,fad8* lipids was not 18:3-16:3-MGDG, since its retention time and pseudo-MS-MS spectrum differed (Figure 6.9). The pseudo MS-MS revealed a parent ion with m/z 750 and moieties of m/z 251 and m/z 279, indicating hexadecadienoic acid (16:2) and linoleic acid (18:2), respectively. Based on the FA-moiety and the parent ion, the molecule was identified

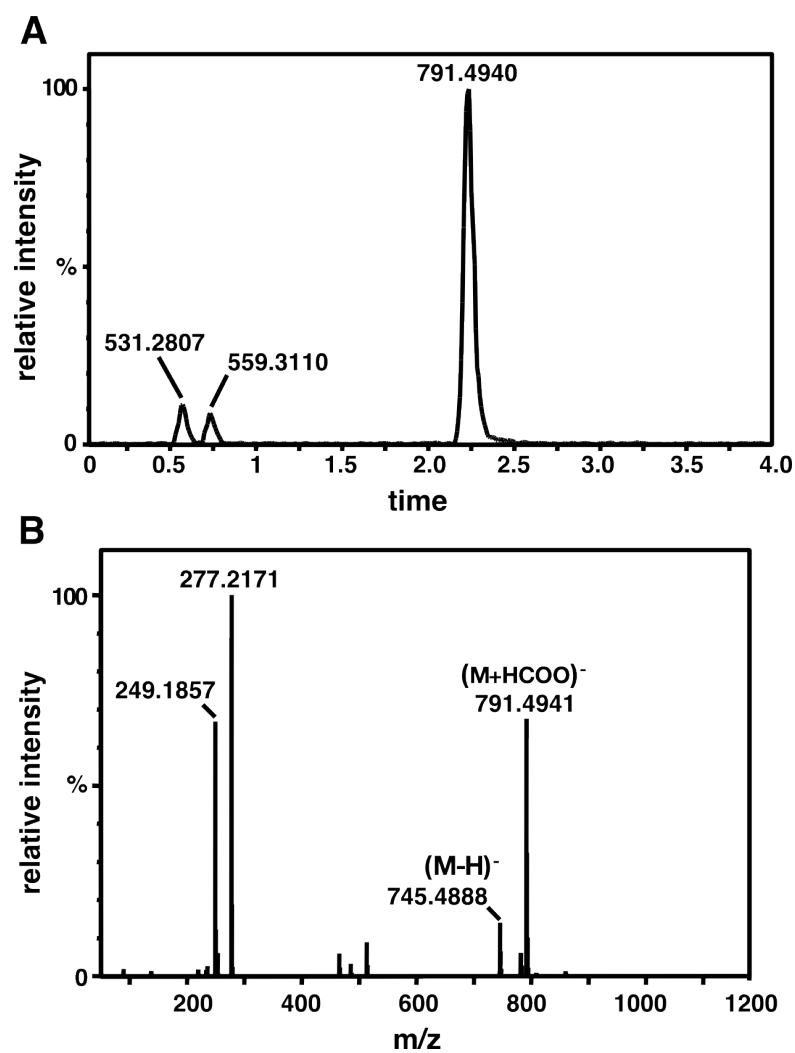


Figure 6.7: Identification of an MDA end-point metabolite by UPLC-TOF-MS -
A. UPLC-TOF-MS analysis of the major molecule of ^{14}C -MDA incorporation (Figure 6.6 B) extracted from ^{12}C -MDA treated plants (4 plants combined) and pre-separated by HPLC . **B.** Mass spectrum of the peak at 2.25 min RT.

6. METABOLISM OF MALONDIALDEHYDE IN THE LEAVES OF *A. THALIANA*

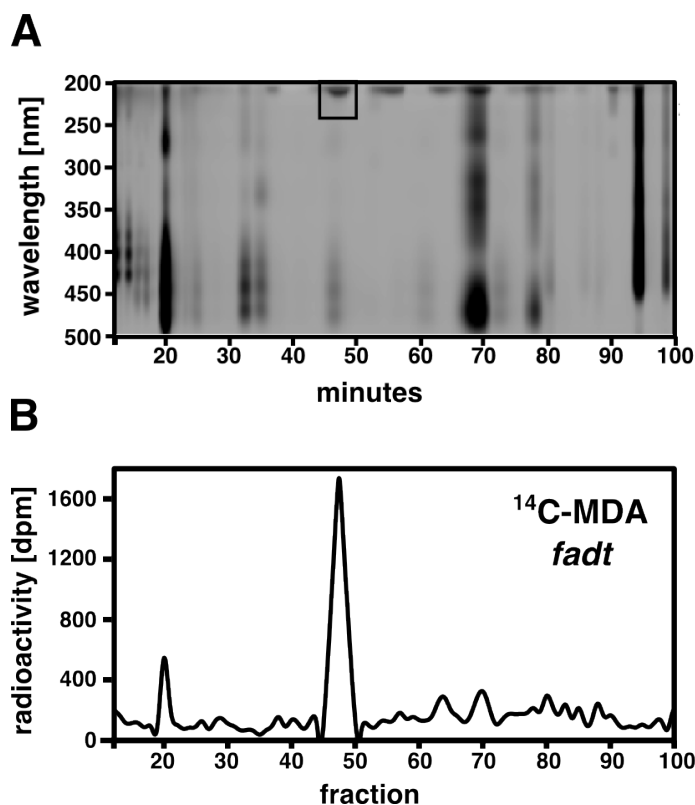


Figure 6.8: Incorporation of ^{14}C -MDA into lipids from *fad3-2, fad7-2, fad8* plants - **A.** Polar plant lipids from *fad3-2, fad7-2, fad8* plants separated by HPLC and monitored by UV (200-500 nm). **B.** Radiation distribution within the fractions measured by liquid scintillation (Pool of leaves from 5 plants, 400000 dpm /plant l^{-1} ; SA: 0.9 nCi nmol^{-1}).

as 18:2-16:2-MGDG. This result supported the previous finding that the major MDA metabolite was 18:3-16:3-MGDG in wild-type *Arabidopsis* plants.

6.3.4 MDA is incorporated into the FA-moiety of glycerolipids

Next, the radioactively labeled lipids that had been extracted from ^{14}C -MDA-labeled leaves were non-enzymatically cleaved by saponification to gather more information as to which part of ^{14}C -MDA was incorporated; in the polar head- or the apolar tail-group. Lipids were hydrolyzed and the polar head-groups separated from the FA-tails by solvent fractionation (Behal et al., 2002). Quantitative scintillation analysis revealed that 84 ± 3.3 % of the ^{14}C -counts in lipids was present in the FA-moiety.

GC/MS analysis of FAs from hydrolyzed 18:3-16:3-MGDG was conducted to validate its identity obtained by UPLC and verify successful hydrolysis (Figure 6.10). Two peaks were obtained and the first (9.14 min retention time (RT)) was identified as the methyl ester of 16:3, the 16:3-moiety of the 18:3-16:3-MGDG (Figure 6.10 B). The second peak

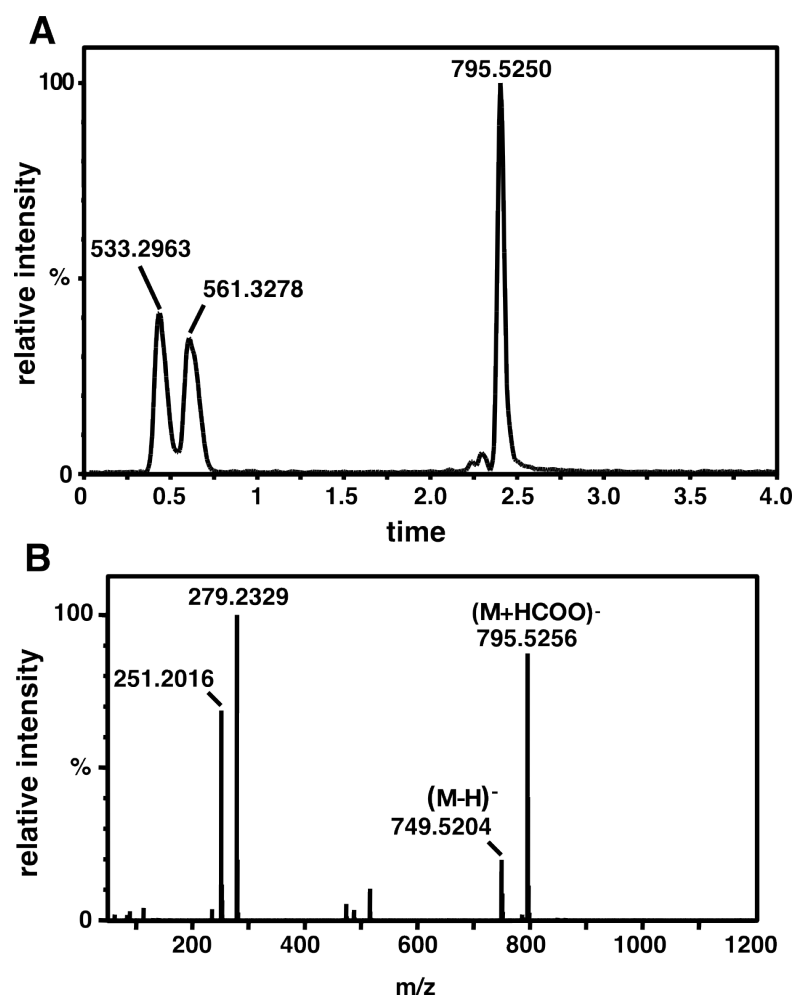


Figure 6.9: Identification of an MDA-derived metabolite in the *fad3-2, fad7-2, fad8* - **A** UPLC-TOF-MS analysis of the major molecule of ¹⁴C-MDA incorporation (Figure 6.8 B) in *fad3-2, fad7-2, fad8* plants. Lipids were extracted from ¹²C-MDA treated plants (Pool of leaves from 4 plants) and pre-separated by HPLC. **B**. Mass spectrum of the peak at 2.4 min RT.

6. METABOLISM OF MALONDIALDEHYDE IN THE LEAVES OF *A. THALIANA*

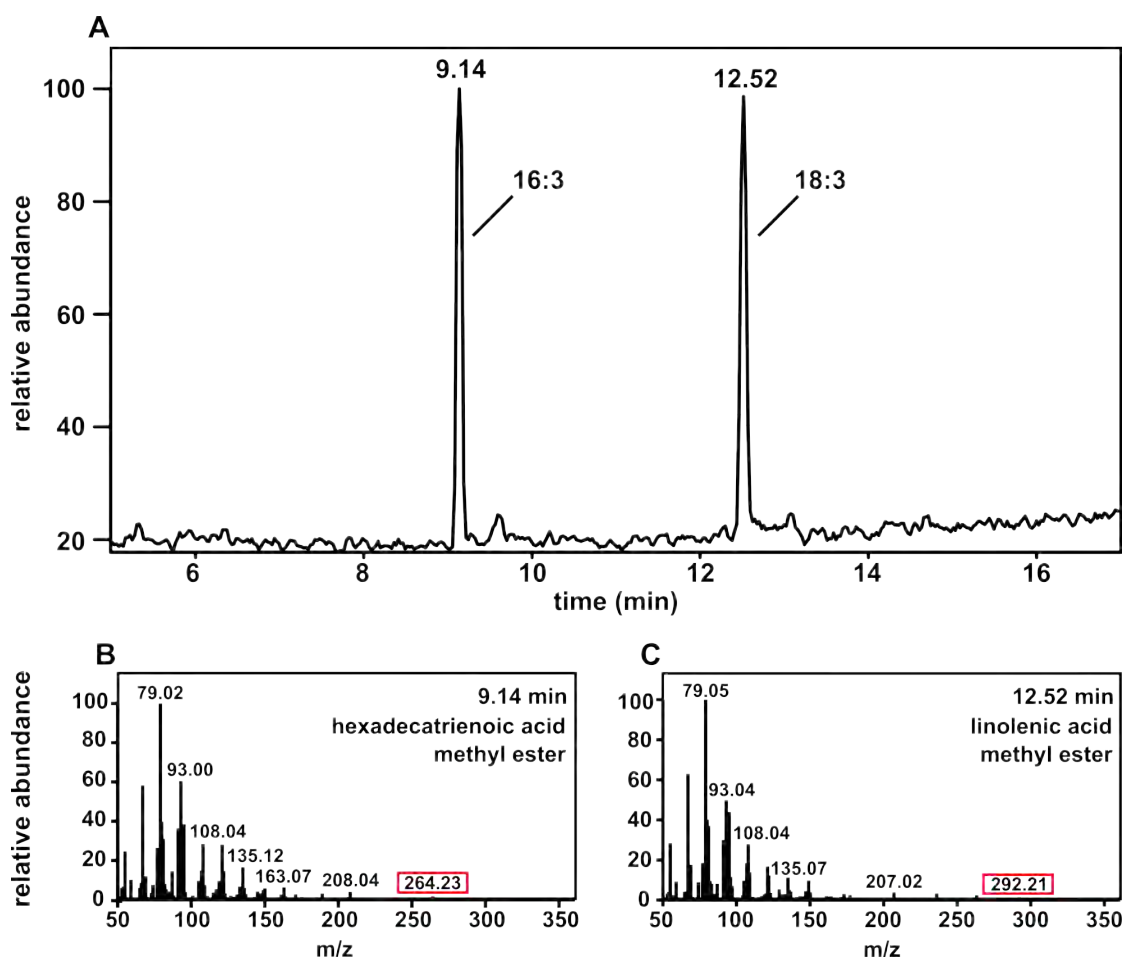


Figure 6.10: GC/MS analysis of FAs from hydrolyzed 18:3-16:3-MGDG - Analysis by GC/MS of FA-methyl esters from 18:3-16:3-MGDG. **A.** Gas chromatogram **B.** Mass spectrum of the peak at 9.14 min retention time. The peak was identified as methyl ester of hexadecatrienoic acid (16:3). Parent ion of m/z 264 is emphasized in the red box **C.** Mass spectrum of the 12.52 min retention time peak. The peak was identified as linolenic acid methyl ester (18:3). Parent ion m/z 292 is emphasized in the red box.

(12.52 min RT) was identified as the 18:3 methyl ester (Figure 6.10 C). In a next step, hydrolysis and GC/MS analysis was conducted with previously identified 18:2-16:2-MGDG from *fad3-2, fad7-2, fad8* (Figure 6.11). Again, two FA-derived peaks were observed (Fig-

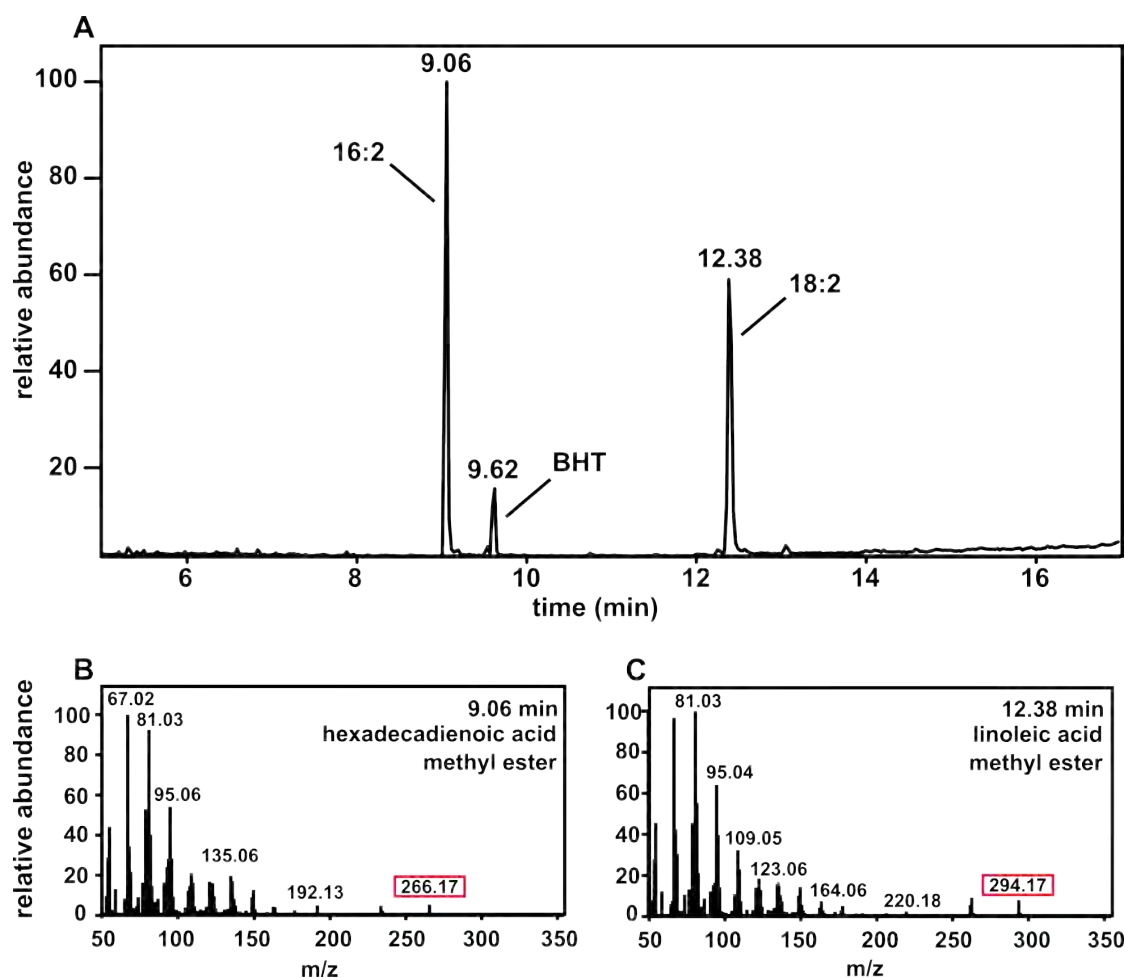


Figure 6.11: GC/MS analysis of FAs from hydrolyzed 18:2-16:2-MGDG - Analysis by GC/MS of FA-methyl esters from *fad3-2, fad7-2, fad8* isolated 18:2-16:2-MGDG. **A.** Gas chromatogram; the peak at 9.62 min was 2,6-tert-butyl-4-methylphenol (BHT). **B.** Mass spectrum of the peak at 9.06 min retention time. The peak was identified as the methyl ester of hexadecadienoic acid (16:2). Parent ion of m/z 266 is emphasized in the red box **C.** Mass spectrum of the 12.38 min retention time peak. The peak was identified as linoleic acid (18:2) methyl ester. Parent ion m/z 294 emphasized in the red box.

ure 6.11 A), accompanied this time with an extra peak at 9.62 min. This extra peak derived from 2,6-tert-butyl-4-methylphenol (BHT), an antioxidant used during the lipid extraction process. The peak eluting at 9.06 min was identified as the methyl ester of 16:2, the other at 12.38 min as 18:2-methyl ester. The FA-analyses confirmed the results from the UPLC-TOF-MS and present additional controls supporting the obtained lipid

6. METABOLISM OF MALONDIALDEHYDE IN THE LEAVES OF *A. THALIANA*

identities.

Next, we used this method to obtain more information about non-retained HPLC molecules. The previous HPLC- and scintillation analyses of polar lipids showed ^{14}C -labeled molecules in the void peak (data not shown). To validate whether the void might contain polar lipids, we hydrolyzed it and analyzed its FAs by GC/MS (Figure 6.12). Again, 3 major peaks were present in the chromatogram as previously observed (9.54

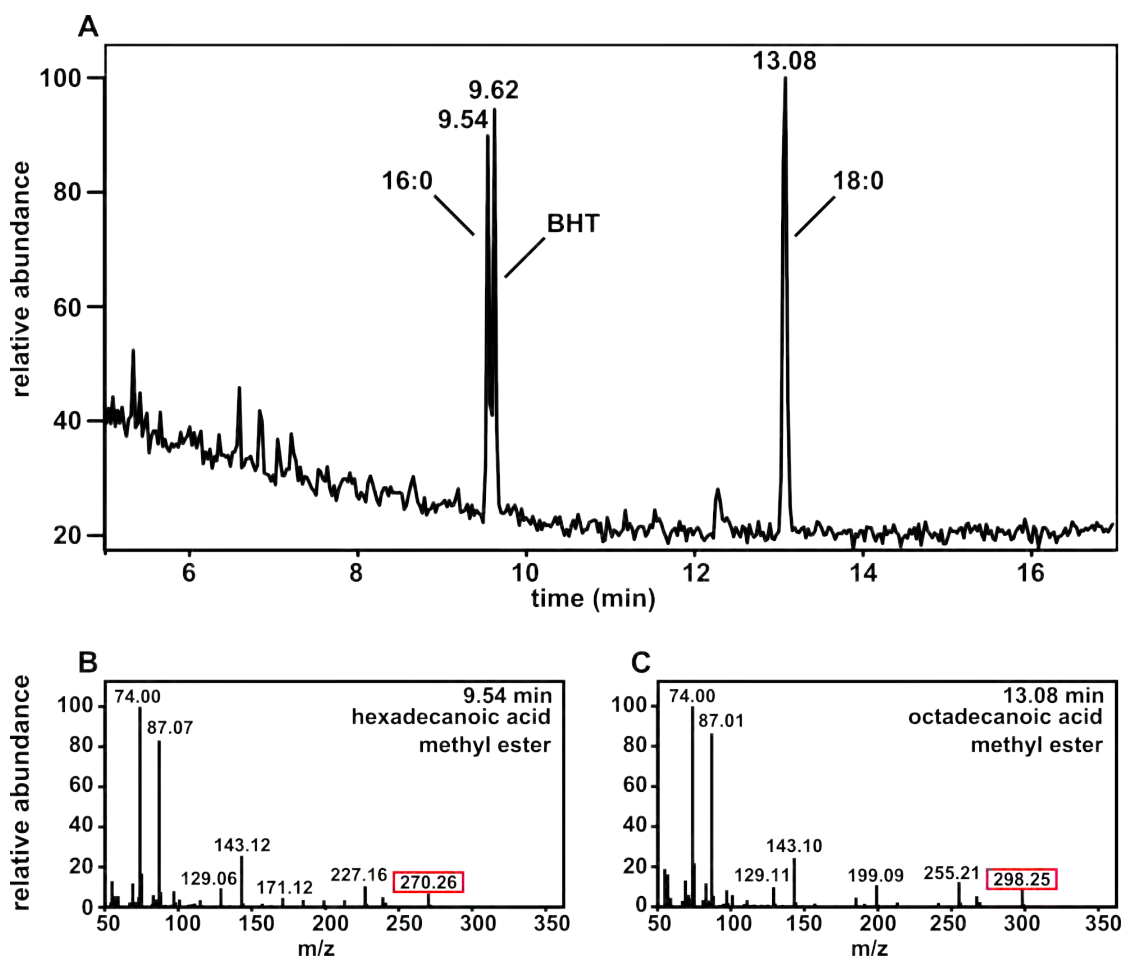


Figure 6.12: GC/MS analysis of FAs from an hydrolyzed HPLC void peak- Fatty acid-GC/MS analysis of the hydrolyzed HPLC void peak from analysis of ^{14}C -MDA treated plants. **A.** Gas chromatogram; peak at 9.62 min was BHT. **B.** Mass spectrum of the peak at 9.54 min retention time. The peak was identified as the methyl ester of hexadecanoic acid (16:0). Parent ion of m/z 270 is emphasized in the red box **C.** Mass spectrum of the 13.08 min retention time peak. The peak was identified as stearic acid (18:0) methyl ester. Parent ion m/z 298 is emphasized in the red box.

min and 12.08 min; 9.62 min identified as BHT). MS-analyses of the GC-peaks (Figure 6.12 B) identified them as hexadecanoic acid (16:0) methyl ester and octadecanoic acid

(18:0) methyl ester, suggesting that another metabolite might be a 18:0-16:0-lipid.

6.3.5 Comparison of ^{14}C -acetate and ^{14}C -MDA incorporation into lipids

[1,2- ^{14}C]-acetate was used to investigate whether MDA might travel through acetate for *de novo* FA-synthesis. The pattern of ^{14}C -acetate incorporation into polar lipids was compared after 24 h exposure with the one of ^{14}C -MDA incorporation (Figure 6.13). The HPLC-UV profile of the lipids was similar (Figure 6.13 A), but more importantly,

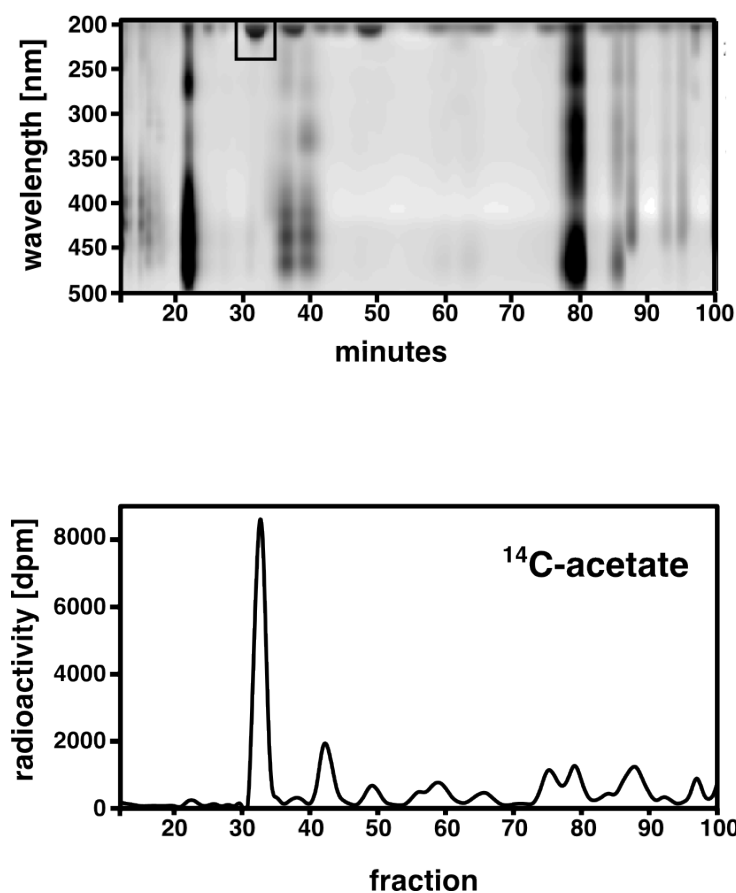


Figure 6.13: ^{14}C -acetate incorporation into polar plant lipids - Analysis of ^{14}C incorporation into polar plant lipids extracted from 5 plants after 24 h of ^{14}C -acetate application (500000 dpm /plant l^{-1} ; SA: 1.126 nCi nmol^{-1}). **A.** HPLC-separation visualized by UV absorbance (200-500 nm). **B.** Distribution of radioactivity in HPLC fractions, measured by liquid scintillation.

so was the pattern of ^{14}C distribution in the eluted fractions (Figure 6.13 B). Overall, the volatility, uptake or turnover of ^{14}C -acetate was better than for ^{14}C -MDA and more counts were found in these fractions. We compared next the incorporation of ^{14}C -acetate

6. METABOLISM OF MALONDIALDEHYDE IN THE LEAVES OF *A. THALIANA*

and ^{14}C -MDA after 3 h of application (Figure 6.14). The peaks after scintillation count-

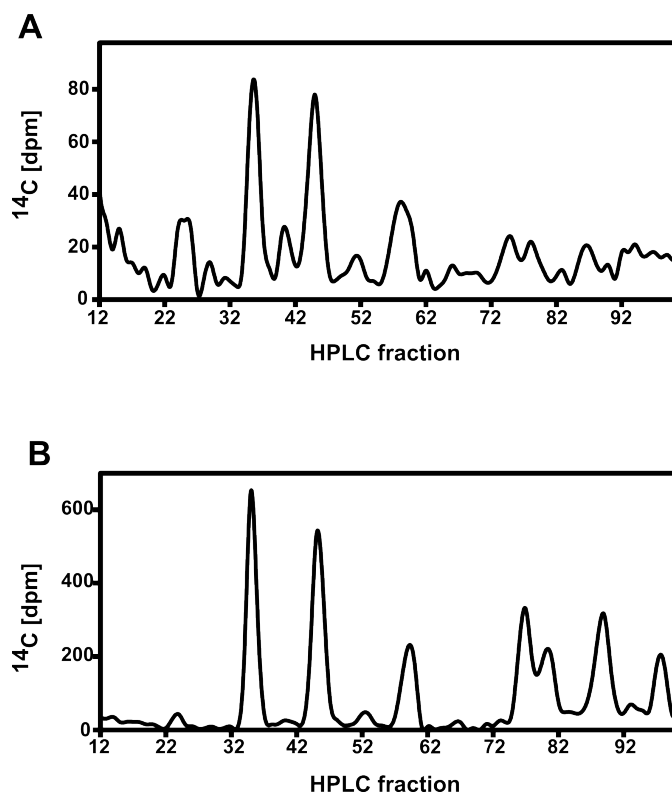


Figure 6.14: Comparison of ^{14}C -MDA and ^{14}C -acetate incorporation in lipids 3 h after application - Polar lipids were extracted 3 h after exposure of plants to ^{14}C -MDA or ^{14}C -acetate and analyzed by HPLC. **A.** ^{14}C -MDA incorporation into lipids. **B.** ^{14}C -acetate derived radioactivity in lipids. In both cases radiation was measured by liquid scintillation. (^{14}C -acetate: 600000 dpm /plant l^{-1} ; SA: 1.35 nCi nmol^{-1} , ^{14}C -MDA: 350000 dpm /plant l^{-1} ; SA: 0.79 nCi nmol^{-1})

ing were similar between ^{14}C -acetate and ^{14}C -MDA treated plants. The distribution of ^{14}C was for both not concentrated in one peak anymore, but spread among multiple peaks. These peaks were present after 24 h, but their intensity was weaker. 18:3-16:3-MGDG which, in previous experiments, contained most radioactivity was observed (35 min RT) but was no longer dominant over the other peaks. The application of ^{14}C -MDA for 3 h resulted only in low incorporation of radioactivity and made it difficult to work with, whereas 24 h presented a rather long application period. Investigating shorter application times we found that 6 h of application mirrored the radiation distribution after 24 h; with 18:3-16:3-MGDG being the major site of incorporation. Further investigations were done with this shorter application frame. Using phospholipid standards from soybean, we obtained more information about potential ^{14}C -MDA metabolites by TLC (Figure 6.15). A standard for phosphatidylcholine (PC) co-migrated with a ra-

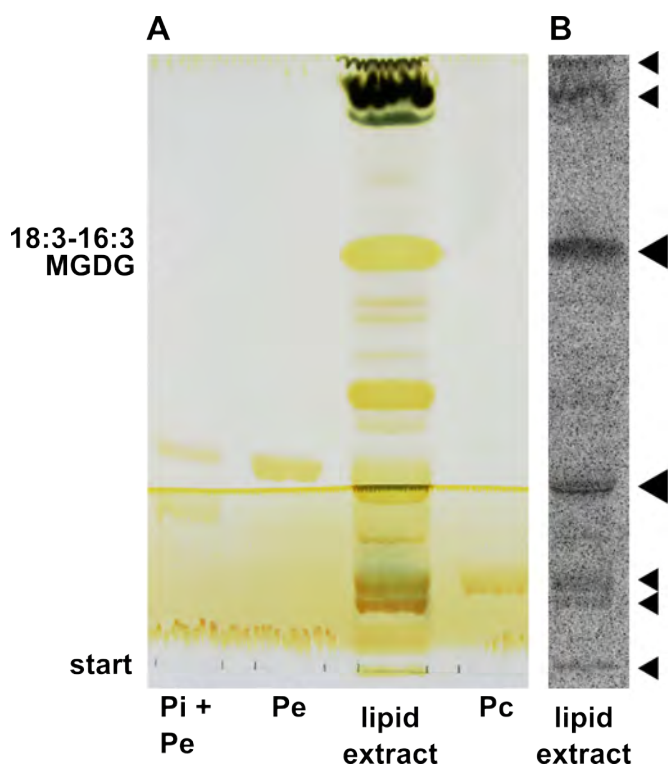


Figure 6.15: TLC analysis of total plant lipids after exposure to volatile ^{14}C -MDA for 6 h - A. Triple TLC run of extracted total lipids after ^{14}C -MDA application (300000 dpm /plant l^{-1} ; SA: 0.67 nCi nmol^{-1}). 1st mobile phase: diethylether:hexane, 2nd: acetone:toluene: H_2O , 3rd: butanol:formate: H_2O . Lipids were stained with iodine vapor for double bonds. Phospholipid standard from soybean: Pi = phosphatidylinositol, Pe = phosphatidylethanolamine, Pc = phosphatidylcholine **B.** Phosphor-imaging of the plant lipid run for ^{14}C incorporation. Arrowheads show position of ^{14}C -containing molecules.

dioactive band as well as a phosphatidylinositol (PI) standard. These species were more polar than 18:3-16:3-MGDG and might be non-retained lipids in the void peak of the HPLC-analyses.

6.3.6 Testing the role of acetate as a potential MDA metabolite using the *acs* mutant

To verify whether MDA might travel through acetate as a metabolic intermediate, we tested a mutant for this pathway - the acetyl-CoA synthetase mutant *acs* (Behal et al., 2002). This enzyme (*ACS*) uses acetate, ATP and CoA in chloroplasts to generate acetyl-CoA which can be used for FA synthesis. Originally, a 90% decrease of ^{14}C -acetate incorporation into FAs relative to the WT was reported for *acs* plants (Lin and Oliver, 2008). We compared the ^{14}C -MDA incorporation into FAs between mutant and WT plants (Figure 6.16). First, ^{14}C -acetate incorporation was quantified and the

6. METABOLISM OF MALONDIALDEHYDE IN THE LEAVES OF *A. THALIANA*

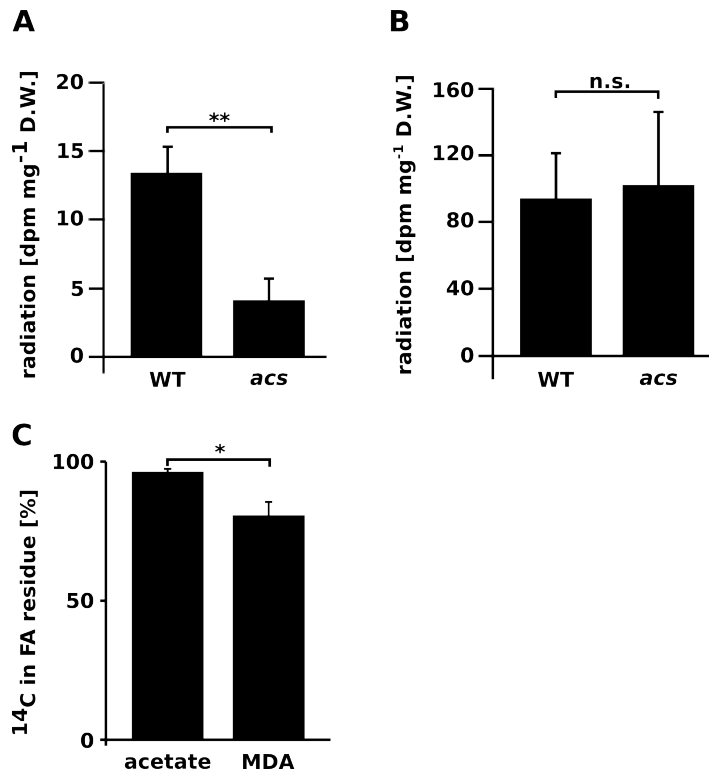


Figure 6.16: ¹⁴C-MDA incorporation analysis in leaves of *acs* plants - **A.** Comparison of ¹⁴C-acetate incorporation into lipids of WT and *acs* plants. **B.** ¹⁴C-MDA incorporation into lipids of WT and *acs* plants. Total extracted lipids of both genotypes were saponified after 6 h of application and the FA-containing phase counted for radiation using scintillation. 5 biological replicates per genotype and treatment were used (¹⁴C-acetate: 100000 dpm /plant l⁻¹; SA: 0.225 nCi nmol⁻¹, ¹⁴C-MDA: 400000 dpm /plant l⁻¹; SA: 0.9 nCi nmol⁻¹). **C.** Proportion of ¹⁴C in the FA residue of lipids compared to the polar head-group after application of ¹⁴C- acetate or -MDA. * $P < 0.05$; ** $P < 0.001$; n.s. = not significant.

incorporation of ¹⁴C-acetate into FAs was found to be reduced by 70% in *acs* plants compared to the WT (Figure 6.16 A). ¹⁴C-MDA incorporation on the other hand was not affected (Figure 6.16 B) and scintillation counts in FAs were similar between the *acs* mutant and the WT ($P = 0.74$). Next, the distribution of ¹⁴C incorporation between the head- and tail- group was analyzed by hydrolysis of the lipids. We found $80.7 \% \pm 4.9 \%$ of the counts from ¹⁴C-MDA in the FA chain, closely similar to previous results ($84 \pm 3.3 \%$ after 24 h). The ¹⁴C-distribution from ¹⁴C-acetate was $96.4 \% \pm 1 \%$ in the FA tail and this difference was significant compared to ¹⁴C-MDA ($P=0.0015$).

6.3.7 Evaluation of MDA-microarray analysis

To complement the biochemical analysis of the MDA incorporation and obtain novel information on the genetic level, MDA-microarray experiments were conducted (full list see

supplementary data, Table 8.1). The differential regulation of genes was assessed comparing MDA treated plants with pyruvaldehyde treated ones as controls. Both molecules were acidified and $10 \mu\text{mol /plant l}^{-1}$ applied for 2 h in sealed Plexiglas glass boxes. A two fold-change was set as cut off for the evaluation and transcripts with $P > 0.05$ were excluded. We found 334 genes to be significantly up-regulated and 119 down-regulated after MDA treatment. To obtain more information about the biological processes which were altered, the list of genes was analyzed for gene ontology. Therefore, upregulated genes were analyzed against the CATMA catalog (12755 genes; Hilson et al., 2004) for significant enrichment of GO-terms and a threshold of $P = 0.05$ was chosen. Their enrichment was analyzed using Bingo (see Table 6.1) and their relationship and organization within each other was visualized using Cytoscape (Figure 6.17). In the category of enriched biological processes "response to stress" was most significantly enriched and represented 161 of total 334 MDA-upregulated genes. The next most significant category "response to abiotic stimulus" contained 105 of the 161 "response to stress" genes. From all enriched genes in this category, 90% were found in "response to stress" as well. Present were drought stress related genes (e.g. *DREB2C*, and *DREB2A*), high light (*NAC2*, *RHL41* and *DDB2*), ROS (*GSTU19*, *GAPC1*, *NAC053*, *GPX6*, *GSTU19*, *AOX1A* and *GSTF8*) and heat shock proteins (e.g. *HSP70-2*, *HSP60*, *HSP70*, *HSP81-2* and *HSP90.1*). Another highly enriched category was the "response to biotic stimulus" including 61 of MDA-upregulated genes. Out of this category 86% of the genes were found in the category "response to stress" and this category was biased towards biotic stress. Members were wound-inducible genes like *JAZ1*, *ACX1*, *OPR3* and *LOX3* and pathogenesis-associated genes like *BIK1* and *SOT12*. 33 of the genes were shared between abiotic and biotic stimuli. In the sub-node of cellular processes, communication and signal transduction were overrepresented. The enrichment in metabolic process could further be categorized into an enrichment in secondary metabolic processes, catabolic processes and catalytic activity - more precisely transferase activity. Analyzing the sub-cellular compartments which are enriched in MDA-upregulated genes, the plasma membrane, vacuole and mostly the cytosol were enriched.

6.3.8 Screening mutant which are potentially involved in MDA metabolism

We tested potentially promising T-DNA insertion lines for genes which might affect MDA metabolism (Table 6.2). One set of mutants was chosen based on published results from other species, which suggested that equivalent enzymes in *Arabidopsis* might use MDA as a substrate, or might act on predicted intermediates. The other set of mutants was chosen based on genes which were upregulated in the MDA-microarray experiments. To screen these mutants, ^{14}C -MDA was applied to plants for 6 h and the total lipids

6. METABOLISM OF MALONDIALDEHYDE IN THE LEAVES OF *A. THALIANA*

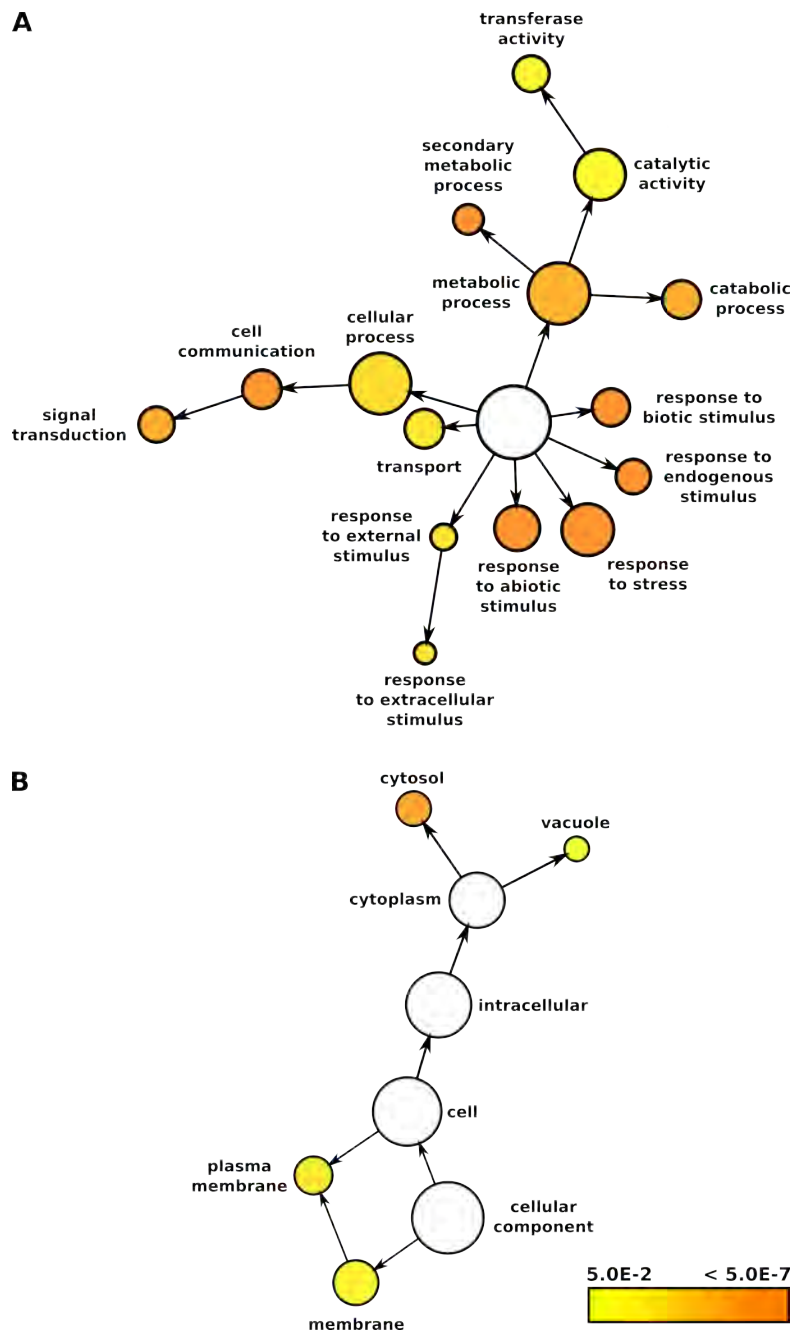


Figure 6.17: Enrichment of gene ontologies in MDA upregulated genes - Upregulated genes upon MDA treatment were tested for enrichment of gene ontologies against all genes from the CATMA chip as reference set. **A.** Processes enriched outgoing from "biological processes" (white circle) **B.** Subcellular enrichment of MDA upregulated genes. Color intensity from white (= 0) to orange represents corrected *P*-values for enrichment in this node.

Description	corr <i>P</i> -value	x	n
response to stress	9.9341E-40	161	3393
response to abiotic stimulus	1.7008E-26	116	2433
response to biotic stimulus	2.3593E-19	71	1245
metabolic process	3.1097E-12	236	10455
response to endogenous stimulus	1.8293E-11	60	1357
cell communication	3.8795E-09	72	2058
cellular process	6.6836E-09	231	10803
signal transduction	2.016E-08	62	1721
catabolic process	4.3722E-08	72	2199
protein binding	0.00086471	58	2176
response to external stimulus	0.001422	25	697
protein metabolic process	0.016793	80	3669
transport	0.016793	68	3023
catalytic activity	0.018	141	7174
response to extracellular stimulus	0.021945	12	307
transferase activity	0.030885	57	2548

Table 6.1: Gene ontology "Biological Processes" from MDA-microarray - Enrichment of biological processes in upregulated genes of MDA treated plants. Plants were treated for 2 h with 10 $\mu\text{mol MDA /plant l}^{-1}$ or pyruvaldehyde as control. Upregulated genes were analyzed for their gene ontology using Bingo. x = number of MDA upregulated genes present in this GO-category; n = all genes from the CATMA reference set present in this GO-category. List of genes included in each GO-term, see supplementary data page 141

from leaves were extracted and separated on TLC (example, Figure 6.18). We focused above all on differential ^{14}C -MDA-incorporation into 18:3-16:3-MGDG, but compared the general ^{14}C -MDA-incorporation pattern as well. ^{14}C -MDA incorporation into the *acs* and the RNAi *OPR1,2* line (Beynon et al., 2009) were additionally quantitatively determined by scintillation counting. In general, ≥ 4 plants per genotype were treated and compared with WT plants, but none of the chosen mutants revealed differences in the pattern of radiation visualization after TLC separation of their lipids.

6.3.9 Extraction and analysis of organic acids as possible MDA turnover intermediates

Organic acids are likely to represent a step in a putative reductive MDA metabolism. We therefore analyzed them next, based on a published micro-extraction and purification method of Stumpf and Burris (1979). To validate the method, organic acids were extracted from *Arabidopsis* leaves, purified and derivatized with N,O-Bis(trimethylsilyl) trifluoroacetamide (BSTFA) prior to GC/MS analysis. Synthetic standards were used to identify common organic acids by their retention time and MS in plant extracts (Fig-

6. METABOLISM OF MALONDIALDEHYDE IN THE LEAVES OF *A. THALIANA*

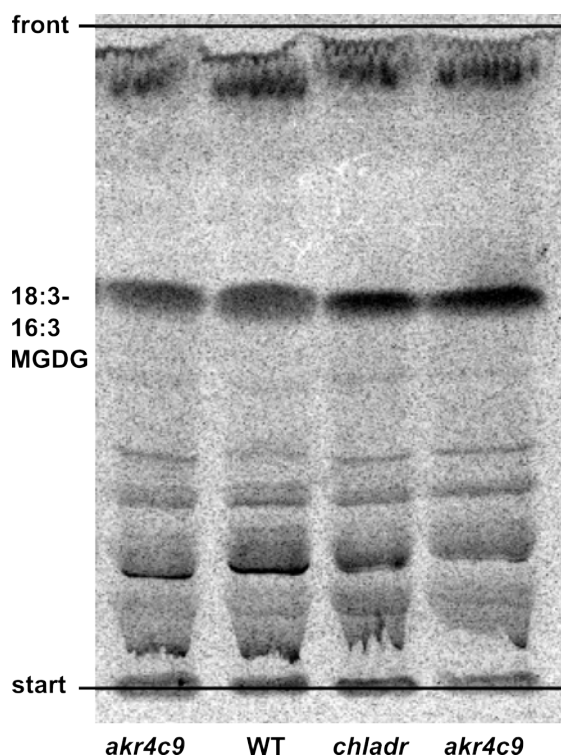


Figure 6.18: Screening potential MDA turnover mutants for altered ^{14}C incorporation into lipids - Representative examples, showing the incorporation of ^{14}C -MDA into lipids of WT and different mutant plants. *AKR4C9* encodes an aldo-keto reductase, which was shown to use MDA as substrate *in vitro*. *ChlADR* encodes an aldehyde dehydrogenase, which was upregulated in the MDA microarray data. (^{14}C -MDA: 550000 dpm /plant l^{-1} ; SA: 1.24 nCi nmol^{-1} , 6 h application). Lipids were separated with diethylether:hexane: H_2O (50:50:1) for 45 min and a second run with acetone:toluene: H_2O (70:23:7) for 1 h.

ure 6.19). Using standards, we were able to identify malonic acid, α -ketoglutaric acid, fumaric acid and citric acid, but many more peaks were observed. Plants were next treated for 1 h with $\sim 1,2 \times 10^6$ dpm of ^{14}C -MDA /plant l^{-1} (SA: 2.7 nCi nmol^{-1}) and the organic acids were extracted as described. The final concentrated organic acid extract was then separated by 2-D TLC and radiation visualized by auto-radiography (Figure 6.20). As a first dimension, we used a polar alkaline mobile phase, and in the second dimension an apolar acidic phase (Robinson, 1963). Two radioactive spots were detected, one at the start point which did not migrate and another one which was well migrating with the acidic, apolar phase. We tried to reveal more information about the second spot by derivatization with BSTFA, methanolic acid or diazomethane followed by GC/MS analysis. However, no potentially interesting candidates were identified. The retention of our molecule of interest on the 2D-TLC was on the other hand modified after derivatization with diazomethane or methanolic acid (data not shown). To obtain

AGI Code	Gene	Function	MDA-induced expression (log ₂)
At1g44170	ALDH3H1	protein similar to the aldehyde dehydrogenase	/
At1g54100	ALDH7B4	aldehyde dehydrogenase	+ 1.2
At1g76680	OPR1	oxophytodienoate reductases 1	/
At1g76690	OPR2	oxophytodienoate reductases 2	/
At2g24270	ALDH11A3	glyceraldehyde-3-phosphate dehydrogenase	/
At2g37770	AKR4C9	aldo-keto reductase	/
At3g04000	ChIADR	aldehyde reductase	+ 1.6
At3g14620	CYP72A8	putative cytochrome P450	+ 1.8
At3g24503	ALDH1A	aldehyde dehydrogenase	/
At3g44190	-	FAD/NAD(P)-binding oxidoreductase	+ 3.1
At4g01950	GPAT3	glycerol-3-phosphate acyltransferase activity	+ 1.7
At4g13180	-	oxidoreductase activity	+ 2.8
At4g27710	CYP709B3	monooxygenase activity	- 1.1
At4g34240	ALDH3I1	aldehyde dehydrogenase	/
At5g06300	LOG7	putative lysine decarboxylase family protein	/
At5g16970	AER	2-alkenal reductase	/
At5g36880	ACS	acetyl-CoA synthetase	/
At5g43940	ADH2	class III type alcohol dehydrogenase	/

Table 6.2: Mutants tested for altered ¹⁴C-MDA incorporation- Selected *Arabidopsis* mutants, which were tested for altered ¹⁴C-MDA incorporation. Their differential expression upon MDA-treatment from microarray studies is indicated (log₂). Blank fields represent genes which were not tested with the chip used (see Annex 8.1).

more information about the nature of the molecule, we tested small intermediates such as acetyl-CoA, malonyl-CoA, glycerate-3-phosphate and 3-phosphoglycerol to compare their migration with the one of our unknown molecule. They all migrated for a short distance with the polar, alkaline phase but not with the other phase, not overlapping with our molecule. Malonic acid and MDA were tested for their migration but migrated with the first dimension far further than our molecule of interest. We have not been able so far to reveal the identity of this molecule but suspect it to be a small polar anion, likely having a carboxyl group.

6. METABOLISM OF MALONDIALDEHYDE IN THE LEAVES OF *A. THALIANA*

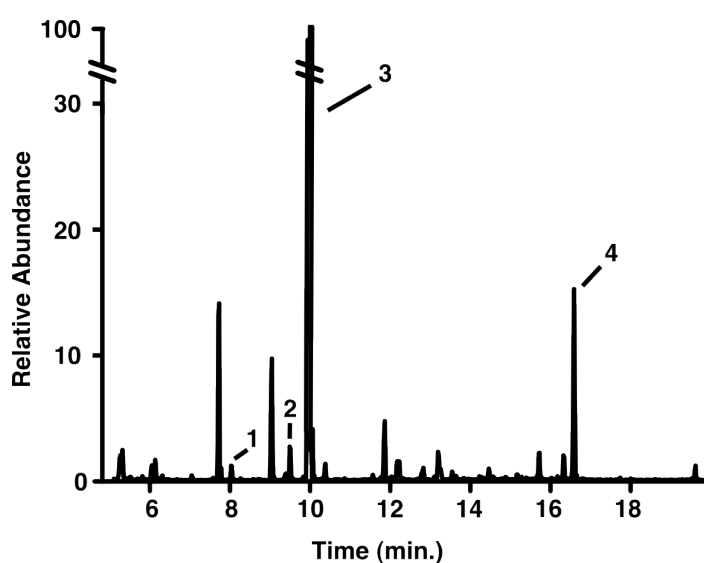


Figure 6.19: GC/MS analysis of extracted and purified organic acids from *Arabidopsis* - Organic acids from *Arabidopsis* leaves (fusion from 4 plants), extracted and purified as previously described (Stumpf and Burris, 1979). Final eluates were derivatized with BSTFA. The following organic acids were identified using standards: 1 at 8.03 min = malonic acid; 2 at 9.50 min = α -ketoglutaric acid; 3 at 10.01 min = fumaric acid; 4 at 16.58 min = citric acid.

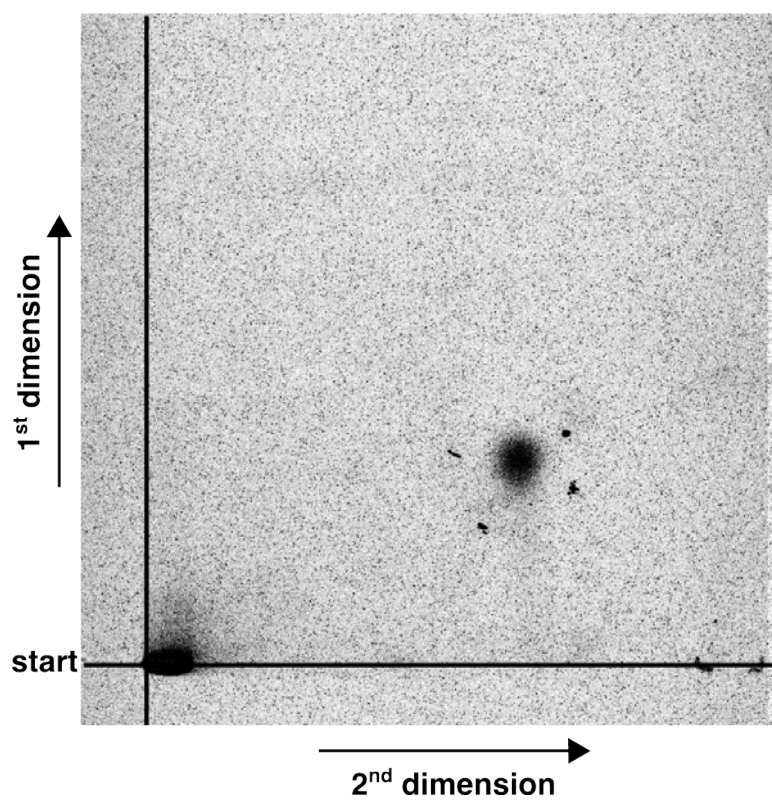


Figure 6.20: Incorporation of ¹⁴C-MDA in small organic acids - Phosphor-imaging of organic acid extracts after 2D-TLC separation. Plants were exposed for 1 h to ¹⁴C-MDA ($1,2 \times 10^6$ dpm /plant l⁻¹; SA: 2.7 nCi nmol⁻¹). 1st dimension: 95% EtOH:NH₄⁺ (95:5) for 1.5h, 2nd dimension: diethylether:formate (7:1) equilibrated with H₂O for 2 h.

6.4 Discussion

MDA is generally considered to be a toxic molecule presenting a threat to the genome and proteome of all cells that produce it. Research in plants now suggests that this might have to be partially reconsidered. Mapping MDA pools in different tissues and growth stages of *Arabidopsis*, we were able to extend the idea that MDA is not predominantly toxic, showing that > 75% of MDA in plants was present in a free unbound form that is most likely to be an enolate (see Chapter 3). This result challenges the dogma that most nascent MDA binds rapidly to proteins or DNA (Marnett, 1999; Yamauchi et al., 2008). Furthermore, TFAs which represent the major source of MDA in leaves, were recently proposed to represent a buffer system for ROS in plants (Farmer and Mueller, 2013; Mène-Saffrané et al., 2009). This implies that non-enzymatic lipid oxidation (nLPO) might be a useful mechanism to prevent damage of proteins, and it challenges the idea that MDA is formed as the result of non-intended harmful reactions. Weber et al. (2004) were able to show that exogenous MDA was rapidly turned over by plants and the question arose as to how MDA levels are controlled in cells and what would be the metabolic fate of the MDA. Part of the answer might come from research in rats which showed that exogenous fed MDA was incorporated into FAs, suggesting a form of metabolism or a detoxification mechanism (Draper et al., 1986; Marnett et al., 1985; Siu and Draper, 1982). We wanted to test the hypothesis that MDA might be metabolized for *de novo* synthesis of lipids; in other words might it be recycled ? To address this question, exogenous isotope-labeled MDA was applied to plants and its dynamics and potential metabolism were investigated.

6.4.1 18:3-16:3-MGDG is a major MDA end-point metabolite

Using stable ^{13}C -MDA isotopes we were able to distinguish endogenous from exogenous MDA, and showed that exogenous applied MDA was successfully taken up by the plant. Next, the turnover of exogenous MDA was investigated and the results compared with previous findings (Weber et al., 2004). Absolute numbers were difficult to compare due to differences in experimental designs, but the overall result was similar, showing that exogenous MDA was rapidly turned over in *Arabidopsis* leaves. Since bound and free MDA were quantified together, one can exclude the possibility that the measured decrease in MDA concentration was due to the binding of MDA to proteins and DNA (although we cannot guarantee the full recovery of bound MDA). These results supported the idea that MDA was converted into another molecule. In order to follow MDA metabolism throughout the plant we used ^{14}C -labeled MDA. According to our hypothesis that MDA might be recovered and used for *de novo* assembly of lipids, we investigated whether radioactive ^{14}C was detectable in lipids after exposure of plants for 24 h to ^{14}C -MDA.

Separation of extracted lipids by TLC revealed radioactivity in polar lipids and we purified them by HPLC coupled to UV detection. The eluted radioactivity was quantified by scintillation and most was found concentrated in one HPLC-peak which we identified by UPLC-TOF-MS as 18:3-16:3-MGDG. This is the most dominant lipid species in plants (> 40 % of total leaf lipids; Li-Beisson et al., 2010). We judge our method to be non-quantitative, but rough estimation after 24 h of ^{14}C -MDA incorporation revealed that only 5-10% of the total applied ^{14}C was detectable in the leaf tissue. This might be either due to a reduced volatility of MDA if the air in the glass jar becomes saturated or, more likely, to an active closure of the plant stomata. From the total recovered counts which were extracted from leaf tissue, 50 - 70% were found in the water soluble fraction or remained bound in the tissue, whereas 30 - 50% of the ^{14}C was recovered in apolar lipid-containing extracts. These findings recapitulated similar observations from ^{14}C -MDA feeding experiments in rats (Marnett et al., 1985). After feeding of rats with ^{14}C -MDA, 20% of the radioactivity was found 4 h later in mouse lipids.

In accordance with the endosymbiotic theory the composition of chloroplast membranes is very similar between different photosynthetic organisms, such as higher plants and cyanobacteria (Doermann, 2007). The thylakoid membranes of chloroplasts from *Arabidopsis* hosting the photosystems consist of two thirds of the PUFAS 16:3 and 18:3 and are mainly present as MGDGs ($\sim 90\%$, Vijayan, 2002). MGDGs provide an important structural and functional role, stabilizing photosystem II (Loll et al., 2005). It was shown that a belt of 11 lipids surrounds the reaction center, most of them being MGDGs. They separate PS II from the antenna and subunits and provide a flexible environment facilitating turnover of the D1 sub-unit (Loll et al., 2005). Accordingly, TFAs were found to be necessary for recovery from photoinhibition, a mechanism which is based on the degradation and novel synthesis of the D1 sub-unit (Vijayan, 2002). PS II is the site of the non-intended side reaction forming the ROS $^1\text{O}_2$. The presence of a belt of lipids surrounding PS II, reinforces the hypothesis that lipids might provide a buffer to protect its proteins from damage. Since we assume that MDA in chloroplasts derives mainly from nLPO by $^1\text{O}_2$, it is intriguing that the major end-point metabolite of MDA metabolism represents the substrate for the latter. PUFAS, which are enriched in chloroplasts, have been shown to be essential for photosynthesis and mutants lacking these (*fad2*, *fad6*) contained only $\sim 10\%$ of WT photosynthetic complexes (McConn and Browse, 1998). These observations are in accord with experiments specifically blocking the formation of MGDG. The knock-out of MGDG synthase 1 (*mgd1-2*) in *Arabidopsis* causes a dwarf-albino phenotype and is incapable of developing a photosynthetic apparatus, more precisely the formation of the subunit-proteins for PS II (Kobayashi

6. METABOLISM OF MALONDIALDEHYDE IN THE LEAVES OF *A. THALIANA*

et al., 2007, 2012). Treatment with the inhibitor galvestine-1 led to a reduced MGDG content which was accompanied by an impaired chloroplasts development and fewer thylakoids (Botté et al., 2011). Together these results strongly underline the necessity of polyunsaturated MGDGs for the proper function of the photosynthetic machinery.

6.4.2 18:2-16:2-MGDG is the major MDA metabolite in the TFA-mutant *fad3-2,fad7-2,fad8*

To further investigate MDA metabolism in *Arabidopsis*, we then analyzed lipids from ^{14}C -MDA treated *fad3-2,fad7-2,fad8* plants. This fatty acid desaturase triple mutant lacks all TFAs including lipids such as 18:3-16:3-MGDG. Instead, the mutant contains a high proportion of diunsaturated FAs and lipids (McConn and Browse, 1996). The HPLC-UV spectrum of extracted polar lipids from *fad3-2,fad7-2,fad8* plants was strikingly different compared to the WT and 18:3-16:3-MGDG was not detectable anymore. This was confirmed by the absence of the previously observed radiation peak for 18:3-16:3-MGDG from the WT and the occurrence of a new major radioactive peak. Using UPLC-TOF-MS we identified the new peak as 18:2-16:2-MGDG, which represents the most abundant lipid in leaves of this mutant (McConn and Browse, 1996). These results clearly showed that MDA was incorporated into lipids from leaves and the comparison with plants from *fad3-2,fad7-2,fad8* plants suggested that MDA was distributed in lipids according to their absolute abundance in leaves.

6.4.3 Phospholipids represent a minor sink of MDA metabolism

Investigating the dynamics of MDA incorporation into polar lipids, we found that 6 h of exposure mimicked the long term (24 h) results. Using standards for phospholipids from soybean, we identified other MDA metabolites with lower ^{14}C -incorporation as to be likely phosphatidylcholine (PC) and phosphatidylinositol (PI). The exposure of plants to ^{14}C -MDA for shorter periods (3 h) resulted, on the other hand, in a more diverse ^{14}C -distribution pattern among the polar lipids. Recently small aldehydes like MDA were shown to bind to phosphatidylethanolamine by interacting with its amine group (Guo et al., 2012). The minor end-point metabolites identified in our study (PC and PI) did not contain such a nucleophile group.

6.4.4 Fatty acid assembly: the major route of MDA metabolism into lipids

In order to dissect how ^{14}C -MDA was incorporated into plant lipids, we non-enzymatically separated the lipid FA-tail from the head-group by saponification. Hydrolysis of the lipids revealed that most (> 80%) MDA was incorporated in the FA moiety of the

lipids. This suggested that MDA might be used for *de novo* assembly of fatty acids (FAs). To test this hypothesis we investigated the incorporation of radioactivity from ^{14}C -labeled acetate. Acetate is known to be converted to acetyl-CoA and is used in FA-assembly (Lin and Oliver, 2008). First, ^{14}C -acetate incorporation into polar plant lipids of WT plants after 24 h was compared to the previously obtained pattern of incorporation from ^{14}C -MDA incubated plants. Interestingly, the obtained pattern was very similar between ^{14}C -acetate and -MDA, the only major difference was the efficiency of ^{14}C incorporation. Even though the scintillation analyses of HPLC fractions were non-quantitative, we found more counts in polar lipids upon ^{14}C -acetate exposure than after ^{14}C -MDA exposure. This might be due to a better volatility or uptake of the acetate as well as possible closure of stomata as a response to volatile MDA. At the cellular level, ^{14}C -acetate is likely directly metabolized to acetyl-CoA and FAs, whereas ^{14}C -MDA might have to travel through multiple intermediates as proposed by Janero (1990). In order to investigate whether the dynamics of incorporation of the two molecules might differ, we exposed plants for a shorter time (3 h) to radiolabeled acetate or MDA. The pattern of ^{14}C -distribution among polar lipids was again similar between ^{14}C -acetate and ^{14}C -MDA. The distribution within the polar lipids was altered for both compared to 24 h time points and radioactivity was not dominant in 18:3-16:3-MGDG anymore but spread among all lipids. Previous studies of ^{14}C -acetate incorporation into plant lipids revealed similar results (Browse et al., 1986); during the first 3 h ^{14}C -acetate derived radioactivity was more diversely spread among lipids but dominant in MGDG and in PC, whereas later, at (> 10 h) ^{14}C was predominantly found in MGDG. This was explained by a transfer of radiation from phosphatidylcholine to galactolipids by the action of the eukaryotic FA-biosynthesis pathway using PC as a precursor for galactolipid synthesis. Overall, our results suggested that MDA is metabolized for the assembly of FAs similar to the dynamics which are known for acetate.

6.4.5 Acetate is not an MDA metabolism intermediate

Potential routes for the incorporation of MDA into FAs were suggested earlier (Figure 6.1, Janero (1990)) based in part on the presence of $^{14}\text{CO}_2$ in the breath of ^{14}C -MDA fed rats (Marnett et al., 1985). MDA was hypothesized to travel through aldehyde- and organic acid-intermediates to result either in acetyl-CoA or malonyl-CoA formation. These were proposed to be substrates for FA synthesis. In plants, the enzyme *ACS* converts acetate to acetyl-CoA (Lin and Oliver, 2008) and malonyl-CoA synthase *MCS* converts malonic acid to malonyl-CoA (Chen et al., 2011) in plastids. We tested the potential pathway through acetate, comparing incorporation of ^{14}C -acetate and ^{14}C -MDA in WT and *acs* plants. The *acs* mutant lacks the enzyme used to form acetyl-CoA from the precursor acetate and was previously shown to have a 90% reduction of

6. METABOLISM OF MALONDIALDEHYDE IN THE LEAVES OF *A. THALIANA*

^{14}C -acetate incorporation into lipids compared to the WT (Lin and Oliver, 2008). We first tried to repeat the published result and found 70% less ^{14}C -acetate incorporation into lipids. The incorporation of ^{14}C -MDA on the other hand was not altered in *acs* compared to the WT. The distribution of ^{14}C between the FA- and the head-group of the lipids differed between ^{14}C -acetate and -MDA incorporated plants and the proportion of ^{14}C in the head group was higher in ^{14}C -MDA treated plants. This indicated that MDA is not exclusively metabolized into FAs but might in addition be incorporated into glycerol. The results suggested that MDA is not metabolized through acetate. Lin and Oliver (2008) speculated that the main function of *ACS* might be the reduction of potentially toxic ethanol and acetaldehyde pools. FA-biosynthesis might be fed from different pathways to cope with potentially reactive aldehydes and alcohols in plastids as well as to recover the carbon.

6.4.6 The metabolism of MDA: a model

Based on the results we obtained and literature from other organisms, we propose two different pathways of MDA metabolism; a reductive or an oxidative one (Figure 6.21). The scheme for the oxidative route is largely based on the model proposed by Janero (1990), updated for the potential route through acetate. Aldehyde dehydrogenases were proposed to catalyze the very first step of MDA oxidation to malonic semialdehyde (Marnett et al., 1985). These enzymes might be responsible as well for the second following oxidation from malonic semialdehyde to malonate. One has to bear in mind nevertheless, that all steps of the oxidative pathway remain speculative. Most importantly, this applies to the very first step since malonic semialdehyde (MSA) has not, to our knowledge, been reported in *Arabidopsis*. We were able to produce MSA based on conversion from ethyl 3,3-diethoxypropanoate (Robinson and Coon, 1963) and we used it as an analytical standard for GC/MS analysis. However, we were unable to detect MSA in leaves (data not shown). In our hands MSA was very unstable and decomposed almost completely within 24 h, except if derivatized (e.g. with PFPH). GC/MS analysis of decomposed MSA samples revealed high levels of acetaldehyde and we therefore hypothesize that MSA might, if formed *in vivo*, be rapidly non-enzymatically converted to acetaldehyde and CO_2 . A bypass in the potential oxidative pathway of MDA metabolism was described in the alga *Prototheca zopfii* and man; the direct oxidation of malonic semialdehyde to acetyl-CoA by a malonic semialdehyde oxidative decarboxylase (Lloyd, 1965; Scholem and Brown, 1983). A Blast-search¹ of the amino acid sequence from this decarboxylase resulted in less than 30% homology to the closest enzyme in *Arabidopsis* and the occurrence of this enzyme in plants remains unclear.

¹ <http://blast.ncbi.nlm.nih.gov/>

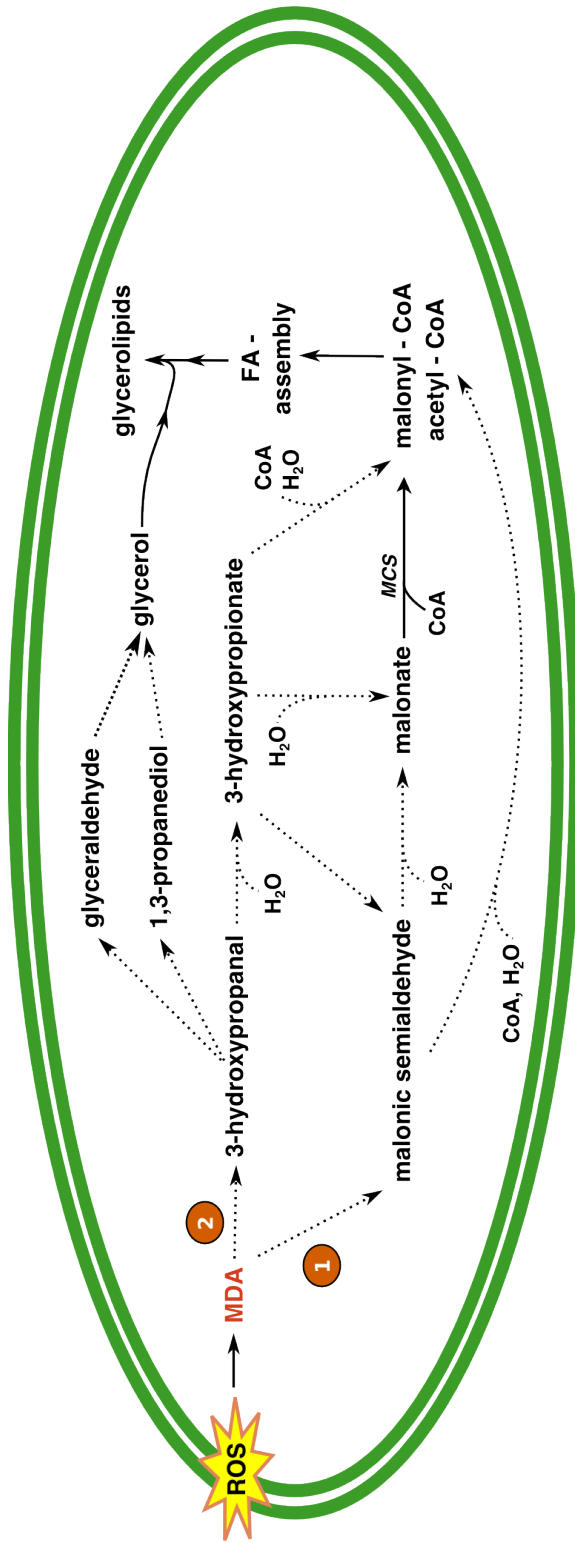


Figure 6.21: Model of MDA metabolism in plastids of *Arabidopsis* - Hypothetical pathway of MDA metabolism after its formation from lipids through the action of reactive oxygen species (ROS). The first step of MDA metabolism can be either oxidative (1) or reductive (2). The oxidation of aldehydes to carboxylic acids can be catalyzed by aldehyde dehydrogenases and the reduction of aldehydes to the corresponding alcohol by alkenal oxidoreductases or aldo-keto reductase. The enzyme catalyzing the conversion from malonate to its acyl-CoA thioester was recently identified in plants as malonyl-CoA synthetase (*MCS*). Dashed lines represent reactions that are not characterized in plants.

6. METABOLISM OF MALONDIALDEHYDE IN THE LEAVES OF *A. THALIANA*

The potential route of the oxidative MDA pathway via acetate (Figure 6.1) was originally hypothesized to present the predominant route in eukaryotes (Janero, 1990). Our experiments with the acetyl-CoA synthetase mutant (*acs*), showed no differences in MDA metabolism compared to the WT. The enzyme responsible for the formation of malonyl-CoA from malonate (*MCS*) was recently characterized (Chen et al., 2011) and remains an interesting candidate for MDA metabolism studies. Potential issues might have to be overcome regarding the severely altered growth and development of *mcs* mutant plants which will complicate direct comparison of MDA incorporation between mutant and WT.

In theory, MDA might not be oxidized but instead reduced. It would then follow a completely different route into FAs - reductive MDA metabolism in (Figure 6.21). Enzymes with alkenal oxidoreductase- or aldo-keto reductase-activity might catalyze the reduction of MDA. Recently Yamauchi et al. (2011) characterized *in vitro* several plant enzymes capable of "detoxifying" reactive carbonyls, which might represent candidates for this reaction. The aldo-keto reductase (At2g37770), two aldehyde reductases (At1g54870, At3g04000) and an 2-alkenal reductase (At5g16970) were shown to reduce aldehyde groups e.g. from acrolein or crotonaldehyde. A potential product of MDA reduction might be 3-hydroxypropanal (3-HPA), in which one MDA-aldehyde group is replaced by an alcohol group. 3-HPA was so far not described in plants, but preliminary GC/MS results from our experiments suggested its presence in *Arabidopsis* (data not shown). 3-HPA might be further reduced to 1,3-propanediol or, alternatively, oxidized to 3-hydroxypropionate. The generation and metabolism of 3-hydroxypropionate is not well studied in plants but has been more extensively investigated in some bacteria, which possess a 3-hydroxypropionate cycle (Eisenreich et al., 1993) as an additional mechanism for autotrophic CO₂ fixation. In this cycle, CO₂ is fixed converting acetyl-CoA via malonyl-CoA and malonic semialdehyde to 3-hydroxypropionate. Some of these steps are likely to be bidirectional as e.g. the oxidation of malonic semialdehyde to 3-hydroxypropionate (Den et al., 1959). Some of the enzymes involved as well as the occurrence of 3-hydroxypropionate have been reported in plants (Lucas et al., 2007) and were predicted to be in mitochondria and peroxisomes. The hydrolysis analysis of labeled lipids revealed ~ 20% incorporation of ¹⁴C-MDA into the polar head-group of lipids. This might derive from labeled glycerol-3-phosphate, which is used by glycerol phosphate acyltransferase (*GPATs*) together with 18:0-acyl carrier protein to build glycerolipids. Glycerol-3-phosphate in plants can derive either from the reduction of dihydroxyacetonephosphate (Gee et al., 1988) or from glycerol (Eastmond, 2004).

6.4.7 Evaluation of MDA microarray data

Genes potentially involved in our hypothetical MDA pathways were unknown and we sought alternative ways to find candidates. Therefore, plants were treated with gaseous MDA and differentially expressed genes analyzed on microarrays. In a previously published MDA-microarray analysis 26 genes were found to be upregulated from a catalog of 150 stress- and defense-related genes against EtOH as carrier control (Weber et al., 2004). In the present MDA-microarray experiment, we increased the set of tested genes and the MDA concentration and chose pyruvaldehyde as a control compound. Pyruvaldehyde has the same overall atomic composition as MDA but is not an electrophilic molecule. From 12755 tested genes, 334 were significantly upregulated and 119 were downregulated. Comparing the results from Weber et al. (2004) with our data revealed 10 co-upregulated genes. The gene *ROF1*, an MDA reporter gene (Weber et al., 2004), was upregulated in our array as well. The majority of the novel upregulated genes clustered to GO-terms like "response to stress" and "response to biotic or abiotic stimulus". Both categories, response to abiotic and biotic stimulus, displayed mostly genes from the "stress response category" and were therefore biased towards stress. The abiotic stimuli contained more of the MDA-upregulated genes and was significantly more enriched than for biotic stimuli ($P = 1.7008E-26$ vs. $2.3593E-19$). The category of response to abiotic stimuli contained drought stress-related genes as *DREB2C* and *DREB2A* (Nakashima et al., 2000), which were also found in the previous MDA microarray. Genes which were classified to be expressed upon response to high light (*NAC2*, *RHL41* and *DDB2*), supported the previous observed link between high light and increased levels of MDA in cells (see Chapter 4). Genes which are linked with ROS (*GSTU19*, *GAPC1*, *NAC053*, *GPX6*, *AOX1A* and *GSTF8*) and heat shock proteins (e.g. *HSP70-2*, *HSP60*, *HSP70*, *HSP81-2* and *HSP90.1*) were MDA-upregulated. These genes are often described as being responsive to many stresses. *HSP70* for example, is expressed in response to bacterial pathogens, high light, hydrogen peroxide and temperature stimulus (TAIR annotation¹) and cannot strictly be assigned to one stress. The diverse pattern of MDA-responsive genes related to different stresses was reflected comparing them with ROS inducible genes. Gadjev et al. (2006) presented an integrative comparison of oxidative stress-related genome-wide expression studies and presented specific marker transcripts for ROS-induced gene expression. From a set of 168 H₂O₂-specific genes only 6 were upregulated after MDA treatment (KO-*Apx1* and *CAT2HP1* specific). For the ROS-species O₂⁻ and ¹O₂ only few specific genes were upregulated with MDA (4 out of 146 genes from KD-*SOD* plants and 9 out of 289 *flu*-mutant specific, respectively) and MDA treatment did not mimic one particular ROS-signaling response. The biotic stress section included genes from the jasmonate pathway like *JAZ1*, *OPR3*, *LOX3* and *ACX1* (reviewed in Acosta and Farmer,

¹<http://arabidopsis.org/>

6. METABOLISM OF MALONDIALDEHYDE IN THE LEAVES OF *A. THALIANA*

2010), as well as pathogenesis induced genes like *BIK1* (resistance to necrotrophic fungi, (Veronese et al., 2006)) and *SOT12* (resistance to bacteria, (Baek et al., 2010)). This was in contrast to the results from Weber et al. (2004) who did not find significant upregulation of biotic stress related genes. This discrepancy might result from the small chosen set of genes examined in the Weber et al., 2004 study. The upregulation of many heat shock genes was reported to be a generality from lipid derived RES (Mueller et al., 2008; Weber et al., 2004), the underlying physiological purpose remains unclear so far though. We found genes which were upregulated after MDA treatment and annotated to have aldehyde dehydrogenase- (At1g54100, At3g04120), reductase- or oxidoreductase function (e.g. At4g13180, At4g02940, At2g06050, At2g06050, At3g04000, and At5g54206). These genes offer promising candidates to be involved in MDA metabolism and will have to be tested with the ^{14}C -MDA incorporation assay.

6.4.8 Testing potential mutants of MDA metabolism with a ^{14}C -MDA incorporation assay

To easily test candidates in MDA metabolism, the extraction of lipids coupled with HPLC separation and scintillation was too complex and time consuming. We therefore established a quicker assay to evaluate altered ^{14}C -MDA metabolism: ^{14}C -MDA was freshly generated by enzymatic conversion from ^{14}C -1,3-propanediol and purified by the anion-exchange microcolumn system. Mutant and WT plants are then exposed for 6 h to 200 nmol ^{14}C -MDA (SA: 1.24 nCi nmol $^{-1}$), followed by the extraction of all lipids. Lipids from single plants were spotted onto TLC-plates and separated first by a strong apolar mobile phases, followed by a more polar mobile phase. This technique allowed a good separation of the polar lipids like MGDGs.

We next selected a set of genes potentially involved in MDA metabolism and compared ^{14}C -MDA metabolism in mutants for the genes with WT plants. Genes which were upregulated in the microarray and might catalyze reactions in MDA metabolism were selected together with genes which were not present on the CATMA chip but which were annotated as encoding aldehyde dehydrogenases or oxidoreductases. One aldehyde reductase (At3g04000, 3-fold upregulated in the microarray) was chosen together with a 2-alkenal reductase (At5g16970) since both were recently shown to reduce aldehyde groups (Yamauchi et al., 2011). Overexpression of aldehyde dehydrogenase 3 (*ALDH3*) members led to decreased MDA levels in lipids of plants undergoing cadmium-induced lipid peroxidation (Sunkar et al., 2003) and a mutant for *ALDH3* was tested. The mammalian homolog of *ALDH3l1*, *ALDH3A1*, showed affinity towards MDA as a substrate *in vitro* and the protein is localized in the cornea (Lassen et al., 2007). Furthermore, mouse mutants in *ALDH3A1* showed increased levels of MDA and we tested this mu-

tant. *ALDH11A3* was chosen based on homology with mammalian *ALDH1A3*, which showed high affinity to LPO derived aldehydes (Marchitti et al., 2008). The mammalian enzymes *ALDH1A1,A2* and *A3* are highly conserved isoenzymes, which act in the cytosol and experiments with the *A1* form showed affinity to MDA as a substrate (Yoval-Sánchez and Rodríguez-Zavala, 2012). Interestingly, *ALDH1A1* and *ALDH3A1* are highly expressed in the mammalian cornea, suggesting involvement in $^1\text{O}_2$ -linked LPO. The plant gene *AKR4C9* encodes an aldo-keto reductase, which was shown *in vitro* to use MDA as a substrate (Simpson et al., 2009). The testing of all these mutants did not reveal any differences in MDA metabolism and we hypothesize that there might exist redundancy, especially among the ALDHs.

6.4.9 Small carboxylic acids might represent MDA metabolism intermediates

Since screening of several mutants did not reveal any novel information, we attempted to directly identify MDA intermediates. Oxidation of MDA leading to a carboxylic-acid was predicted as an intermediate in the route to FA synthesis. We extracted organic acids from ^{14}C -MDA-treated plants to investigate possible organic acid intermediates. The time of ^{14}C -MDA application time was reduced to 1 h to be able to detect these earlier intermediates. Extracting organic acids first from non-treated plants and subsequent GC/MS analysis, we were able to confirm successful extraction of these molecules. The extraction of organic acids from ^{14}C -MDA treated plants and separation on a 2D-TLC resulted in two radioactive bands, one of which migrated well with the chosen mobile phases. Direct extraction and derivatization of this molecule followed by GC/MS was not successful, even though we were able to change its retention on the 2D-TLC by acidic methylation or diazomethane-derivatization. This indicated that the molecule contained a carboxylic group or another group with an active hydrogen. The problem of detecting the compound by GC/MS might derive from incomplete derivatization.

6. METABOLISM OF MALONDIALDEHYDE IN THE LEAVES OF *A. THALIANA*

7

Final conclusions and outlook

The majority of studies consider MDA as a toxic molecule that represents a threat to the genome and proteome of cells and is widely used as a marker for nLPO in disease (reviewed in Del Rio et al., 2005). nLPO in plants was recently described to have potential benefits for plants, preventing damage of membrane bound proteins by ROS (Farmer and Mueller, 2013; Mène-Saffrané et al., 2009). This hypothesis might explain the enrichment of oxidation-prone PUFAs at sites of high ROS production such as the chloroplasts. Photosystem II (PS II) is a prominent example where the ROS production site is surrounded by a belt of lipids and embedded in membranes which are rich in PUFAs (Loll et al., 2005; Vijayan, 2002). One can imagine therefore, that nLPO could be a beneficial mechanism and that it, if so, would be well controlled by cells. In this thesis we studied MDA, a product of such nLPO reactions. We wanted to map MDA throughout the plant body to identify the sites of its generation and to understand its dynamics in different conditions. In a next step we then wanted to test the hypothesis whether the fate of nLPO-derived MDA might be controlled by the cells and whether it might be recycled to assemble lipids.

Characterization of MDA pools in *Arabidopsis thaliana* - Most MDA in leaves is derived from TFAs (Weber et al., 2004) and, using TBA-staining and confocal microscopy, I found MDA to be highly enriched in chloroplasts. Optimizing the original MDA quantification protocol for chloroplasts and establishing a more sensitive GC/MS-PCI method, I was able to quantify MDA at the subcellular level. Extracting and comparing chloroplasts from WT and *fad3-2,fad7-2,fad8* plants, I detected the exact same proportion of TFA-derived MDA as for entire leaves. These data show for the first time rigorously that chloroplasts present the major site of MDA generation in leaves of *Arabidopsis*.

In seedlings the sources and sites of MDA generation were strikingly different to

7. FINAL CONCLUSIONS AND OUTLOOK

those in leaves of adult plants - the only similarity being the low recoverable proportion of MDA bound to macromolecules. Strikingly, MDA was present and possibly enriched in zones of cell proliferation like the root tip, lateral roots and the apical meristematic region. It is curious that MDA a genotoxin, is enriched in stem cell-rich zones. Analyzing transverse sections of roots, we were able to detect MDA in the root elongation zone in pericycle cells, whereas MDA in the root proliferation zone was distributed among the entire root body and apparently not limited to a certain cell type. Quantitative measurements revealed that free MDA in roots was not predominantly derived from TFAs but originated from an as yet unknown source.

We were able to show by quantitative measurements that most MDA in plants is not bound to macromolecules in the resting state which, I believe, might be a generality that applies to other cells and organisms and will have an important impact for further studies on MDA. This data suggests that most MDA *in vivo* is not likely to be toxic for the cells, since the enolate would not bind to macromolecules. Our findings also question the relevance of studies, which demonstrated MDA toxicity at non-physiological (high millimolar) MDA concentrations (e.g. Niedernhofer et al., 2003).

The characterization of MDA pools in *Arabidopsis* revealed the presence and importance of sources other than TFAs. But analysis in leaves of a mutant for diunsaturated FAs (*fad2,fad6*) proved to be difficult due to the dwarfish heterotrophic phenotype. I suggest for further investigations to assess this question using seedling roots since we found only a low proportion of MDA to derive from TFAs in the roots of seedlings. The availability of a mutant with low levels of MDA in the roots might help to understand better the role of MDA in meristematic zones which, are rich in MDA.

Dynamics of MDA during light stress - nLPO in healthy leaves was recently described to be almost exclusively due to photosynthesis-derived $^1\text{O}_2$ (Triantaphylidès et al., 2008) and one can therefore hypothesize that light-associated processes represent the major driving force of MDA generation in leaves. Exposure of extracted chloroplasts to light or entire leaves to excessive light, resulted in increased levels of MDA and supported the idea of MDA generation through light capturing processes. The close spatial relation between the PS II and lipids in PS II place PUFAs in a site where they are prone to oxidation by PS II driven ROS generation. It remains unclear whether $^1\text{O}_2$ -induced nLPO directly drove MDA generation and further analysis remains necessary. The constitutive *flu* mutant (Meskauskiene et al., 2001) which accumulates $^1\text{O}_2$ upon a dark/light shift might provide a useful model. One could use an approach similar to investigations of nLPO mechanism in the spontaneous lesion mutant *acd2-*

2. Mène-Saffrané et al. (2009) was able to show through crosses of *acd2-2* with the *fad3-2,fad7-2,fad8* mutant, that MDA generation in this mutant derived from nLPO of TFAs. Similarly, crosses between *fad3-2,fad7-2,fad8* and *flu* might reveal whether $^1\text{O}_2$ accumulation increases directly MDA production.

MDA in pathogenesis - With the help of the TBA-assay, I was able to visualize for the first time redistribution of MDA pools during infection of seedlings with *B. cinerea*. We used the mediators jasmonic acid (JA) and salicylic acid (SA), which are known to play active roles in defense against this pathogen (Pan et al., 2008) to quantify changes in MDA. Treatment with both mediators increased MDA levels in resting seedlings and a mutant for JA signaling, *jar1*, blocked the effect on MDA levels by JA-treatment (Schmid-Siegert et al., 2012). This result supports the idea that MDA might be involved in pathogenesis and may aid the plant to cope with the attacker. The underlying molecular mechanisms are unknown so far and open the door for more profound analysis in the future. In contrast, studies with the necrotrophic fungus, *P. cucumerina* in adult plants did not result in significant changes of MDA and levels seemed to be tightly controlled. Comparing infections of mutants for jasmonic acid (*aos*) and for TFAs (*fad3-2,fad7-2,fad8*) I was able to demonstrate the importance of TFAs in defense against this pathogen. These results complemented previous findings with the fungus *B. cinerea* (Mène-Saffrané et al., 2009) and suggest a general role of TFAs in defense against necrotrophic fungi. In conclusion, we found MDA pools in seedlings to be more inducible than in adult leaves and we speculate that MDA might provide a basic mechanism in defense during the juvenile state of plants until more advanced defense mechanisms are fully developed. This might either be due to a role of MDA in signaling (Weber et al., 2004) or as a direct antimicrobial defense compound.

Glycerolipids are MDA end-point metabolites - Little was known about the fate of MDA in resting plants. Earlier results suggested that MDA might be turned over and we wanted to tie in these results following MDA in plants with labeled-MDA isotopes. Due to the lack of readily available MDA-isotopes, I enzymatically converted isotope-labeled 1,3-propanediol to MDA. Through developing a novel anion-exchange micro-purification method, I was able to purify the labeled MDA away from 1,3-propanediol and the reaction intermediate 3-hydroxypropanal. This technique guarantees that MDA is the only labeled molecule prior to application, which was more difficult to achieve with any formerly available method.

Using ^{13}C -MDA, I could show that exogenous MDA was taken up and turned over in leaves and I was able to recover radioactivity from lipids of ^{14}C -MDA treated plants. We

7. FINAL CONCLUSIONS AND OUTLOOK

were able to identify 18:3-16:3-MGDG as the major MDA end-point metabolite. Using mutants and ^{14}C -labeled acetate I was further able to show that MDA was metabolized for the assembly of FAs and then distributed non-specifically among lipids. Thereby, I confirmed our initial hypothesis that nLPO-formed MDA might be recovered to recycle the reduced carbon. These results allow us to draw the following picture of MDA in chloroplasts: PS II is embedded in a bilayer rich in polyunsaturated MGDGs which are prone to nLPO. The ROS $^1\text{O}_2$ is constantly produced in PS II and accumulates in light stress. PUFAs can help to buffer $^1\text{O}_2$, preventing damage of other macromolecules such as PS II, and, through nLPO a cascade of new molecules is generated - one of them is MDA. The hypothesis that PUFAs can act as a ROS buffer is supported by experiments comparing recovery of photoinhibition in the TFA mutant *fad3-2,fad7-2,fad8* (Vijayan, 2002). This mutant was found to recover more slowly from photoinhibition than WT plants, which might point to increased damage to the PS II D1 sub-unit in these plants due to the lack of the TFA buffering effect. Most MDA from nLPO is present in its free enolate form and is likely turned over to be incorporated into 18:3-16:3-MGDG. This particular lipid is the most abundant species in chloroplast thylakoids (Vijayan, 2002) and thereby closes the circle of MDA metabolism. One can imagine that this represents a general mechanism for cells to recover carbon from nLPO and might apply similarly to other nLPO generated molecules.

First steps of MDA metabolism - In order to identify the missing steps of MDA metabolism to glycerolipid synthesis, I proposed two routes of MDA metabolism: a reductive and an oxidative route. Most of the suggested reactions and intermediates have not been described in plants so far and we conducted microarray experiments to identify potentially involved genes and test them for altered MDA metabolism. As in a previous study (Weber et al., 2004), MDA induced mainly abiotic stress related genes in the microarray analysis. We additionally found many biotic stress related genes, and, more importantly for potential MDA metabolism, genes which were associated with catalytic activity and transferase activity. I studied potential candidates for altered MDA metabolism but was not able to identify any yet. The assay for ^{14}C -MDA incorporation which I developed offers a powerful tool for further studies to screen for mutants in MDA metabolism. To limit the range of proteins which might be involved in MDA metabolism, *in vivo* studies with specific enzyme inhibitors coupled with the incorporation assay might be promising. A wide spectrum of inhibitors of aldehyde dehydrogenases is known (reviewed in Koppaka et al., 2012) and disulfiram, for example, might present a good candidate for testing. Other tools would be assays to test the abilities of extracted proteins from plants to convert MDA. This might first be tested with entire protein extracts and might be further specified with the help of different

co-factors limited to particular enzyme-families or specific inhibitors.

In this study, I succeeded to show for the first time that MDA is metabolized in plants, I characterized the underlying inducibility and thereby extended in more detail previous studies about MDA turnover in mammals (Marnett et al., 1985; Siu and Draper, 1982). I further suggested that MDA metabolism might be part of a recycling pathway to regenerate PUFAs, which can act as buffer for ROS (Mène-Saffrané et al., 2009). One can assume that cells possess mechanisms to regulate the formation, levels and metabolism of MDA and this offers many perspectives to follow up. These findings raise questions about the generally accepted fact that MDA is simply toxic to cells and the ideas might begin to change our understanding of MDA not only in plants, but in other organisms too.

7. FINAL CONCLUSIONS AND OUTLOOK

References

- Acosta IF and Farmer EE** (2010) Jasmonates. In: The Arabidopsis book, vol. 8, The American Society of Plant Biologists.
- Almérás E, Stolz S, Vollenweider S, Reymond P, Mène-Saffrané L and Farmer EE** (2003) Reactive electrophile species activate defense gene expression in Arabidopsis. *The Plant Journal* **34**: 205–16.
- Baek D, Pathange P, Chung JS, Jiang J, Gao L, Oikawa A et al.** (2010) A stress-inducible sulphotransferase sulphonates salicylic acid and confers pathogen resistance in Arabidopsis. *Plant, Cell & Environment* **33**: 1383–92.
- Behal RH, Lin M, Back S and Oliver DJ** (2002) Role of acetyl-coenzyme A synthetase in leaves of Arabidopsis thaliana. *Archives of Biochemistry and Biophysics* **402**: 259–67.
- Bernheim F, Bernheim M and Wilbur K** (1948) The reaction between thiobarbituric acid and the oxidation products of certain lipides. *The Journal of Biological Chemistry* **174**: 257–264.
- Beynon ER, Symons ZC, Jackson RG, Lorenz A, Rylott EL and Bruce NC** (2009) The role of oxophytodienoate reductases in the detoxification of the explosive 2,4,6-trinitrotoluene by Arabidopsis. *Plant Physiology* **151**: 253–61.
- Blokhina O and Fagerstedt KV** (2010) Reactive oxygen species and nitric oxide in plant mitochondria: origin and redundant regulatory systems. *Physiologia Plantarum* **138**: 447–62.
- Botté CY, Deligny M, Roccia A, Bonneau AL, Saïdani N, Hardré H et al.** (2011) Chemical inhibitors of monogalactosyldiacylglycerol synthases in Arabidopsis thaliana. *Nature Chemical Biology* **7**: 834–42.
- Brooks C and Maclean I** (1971) Cyclic n-butylboronates as derivatives of polar bifunctional groups for gas chromatography and mass spectrometry. *Journal of Chromatography* **9**: 193–204.
- Browse J** (2009) Jasmonate passes muster: a receptor and targets for the defense hormone. *Annual Review of Plant Biology* **60**: 183–205.
- Browse J, Warwick N, Somerville CR and Slack CR** (1986) Fluxes through the prokaryotic and eukaryotic pathways of lipid synthesis in the '16:3' plant Arabidopsis thaliana. *Biochemical Journal* **235**: 25–31.
- Bruno MJ, Koeppel RE and Andersen OS** (2007) Docosahexaenoic acid alters bilayer elastic properties. *Proceedings of the National Academy of Sciences of the United States of America* **104**: 9638–43.
- Bull AW and Marnett LJ** (1985) Determination of malondialdehyde by ion-pairing high-performance liquid chromatography. *Analytical Biochemistry* **149**: 284–290.
- Cao H, Bowling SA, Gordon AS and Dong X** (1994) Characterization of an Arabidopsis mutant that is nonresponsive to inducers of systemic acquired resistance. *The Plant Cell* **6**: 1583–1592.
- Chen H, Kim HU, Weng H and Browse J** (2011) Malonyl-CoA synthetase, encoded by ACYL ACTIVATING ENZYME13, is essential for growth and development of Arabidopsis. *The Plant Cell* **23**: 2247–2262.
- Choi JW, Kim DJ, Rhim JH, Chung JH and Chung HK** (2003) Generation and Characterization of IgG Monoclonal Antibodies Specific for Malondialdehyde. *Hybridoma and Hybridomics* **22**: 3–6.
- Choi JWW, Kim JHH, Cho SCC, Ha MKK, Song KYY, Youn HDD et al.** (2010) Malondialdehyde inhibits an AMPK-mediated nuclear translocation and repression activity of ALDH2 in transcription. *Biochemical and Biophysical Research Communications* **404**: 400–6.
- Clausen C, Ilkavets I, Thomson R, Philippar K, Vojta A, Möhlmann T et al.** (2004) Intracellular localization of VDAC proteins in plants. *Planta* **220**: 30–37.
- Del Rio D, Stewart AJ and Pellegrini N** (2005) A review of recent studies on malondialdehyde as toxic molecule and biological marker of oxidative stress. *Nutrition, Metabolism, and Cardiovascular Diseases* **15**: 316–28.

REFERENCES

- Den H, Robinson W and Coon M** (1959) Enzymatic conversion of beta-hydroxypropionate to malonic semialdehyde. *The Journal of Biological Chemistry* **234**: 1666–1671.
- Doermann P** (2007) Lipid Synthesis, Metabolism and Transport. In: *The Structure and Function of Plastids*, pp. 335–353, Springer.
- Draper HH, McGirr LG, Hadley M, Toxicity C, Mda OF and Animals IN** (1986) The metabolism of malondialdehyde. *Lipids* **21**: 305–307.
- Dubrovsky JG** (2000) Pericycle Cell Proliferation and Lateral Root Initiation in Arabidopsis. *Plant Physiology* **124**: 1648–1657.
- Eastmond PJ** (2004) Glycerol-insensitive Arabidopsis mutants: gli1 seedlings lack glycerol kinase, accumulate glycerol and are more resistant to abiotic stress. *The Plant Journal* **37**: 617–625.
- Eisenreich W, Strauss G, Werz U, Fuchs G and Bacher A** (1993) Retrobiosynthetic analysis of carbon fixation in the phototrophic eubacterium *Chloroflexus aurantiacus*. *European Journal of Biochemistry* **215**: 619–32.
- Esterbauer H and Cheeseman KH** (1990) Determination of aldehydic lipid peroxidation products: malonaldehyde and 4-hydroxynonenal. *Methods in Enzymology* **186**: 407–21.
- Esterbauer H, Schaur RJ and Zollner H** (1991) Chemistry and bio-chemistry of 4-hydroxynonenal, malonaldehyde and related aldehydes. *Free Radical Biology & Medicine* **11**: 81–128.
- Falcone DL, Gibson S, Lemieux B and Somerville C** (1994) Identification of a gene that complements an Arabidopsis mutant deficient in chloroplast omega 6 desaturase activity. *Plant Physiology* **106**: 1453–1459.
- Falcone DL, Ogas JP and Somerville CR** (2004) Regulation of membrane fatty acid composition by temperature in mutants of Arabidopsis with alterations in membrane lipid composition. *BMC Plant Biology* **4**: 1–15.
- Fan X** (2002) Measurement of malonaldehyde in apple juice using GCMS and a comparison to the thiobarbituric acid assay. *Food Chemistry* **77**: 353–359.
- Fan X** (2003) Ionizing radiation induces formation of malondialdehyde, formaldehyde, and acetaldehyde from carbohydrates and organic acid. *Journal of Agricultural and Food Chemistry* **51**: 5946–9.
- Farmer EE** (2001) Surface-to-air signals. *Nature* **411**: 854–856.
- Farmer EE and Davoine C** (2007) Reactive electrophile species. *Current Opinion in Plant Biology* **10**: 380–386.
- Farmer EE and Mueller MJ** (2013) ROS-Mediated Lipid Peroxidation and RES-Activated Signaling. *Annual review of plant biology* **accepted**.
- Ferro M, Brugière S, Salvi D, Seigneurin-Berny D, Court M, Moyet L et al.** (2010) AT_CHLORO, a comprehensive chloroplast proteome database with subplastidial localization and curated information on envelope proteins. *Molecular & Cellular Proteomics* **9**: 1063–1084.
- Funk CD** (2001) Prostaglandins and leukotrienes: advances in eicosanoid biology. *Science* **294**: 1871–1875.
- Gadjev I, Vanderauwera S, Gechev TS, Laloi C, Minkov IN, Mittler R et al.** (2006) Transcriptional footprints disclose specificity of reactive oxygen species signaling in Arabidopsis. *Plant Physiology* **141**: 436–445.
- Gee RW, Byerrum RU, Gerber DW and Tolbert NE** (1988) Dihydroxyacetone phosphate reductase in plants. *Plant Physiology* **86**: 98–103.
- Ghoshal A and Recknagel R** (1965) Positive evidence of acceleration of lipoperoxidation in rat liver by carbon tetrachloride : in vitro experiments. *Life Sciences* **4**: 1521–1530.
- Gindro K and Pezet R** (2001) Effects of long-term storage at different temperatures on conidia of *Botrytis cinerea*. *FEMS Microbiology Letters* **204**: 101–104.
- Glauser G, Dubugnon L, Mousavi SaR, Rudaz S, Wolfender JL and Farmer EE** (2009) Velocity estimates for signal propagation leading to systemic jasmonic acid accumulation in wounded Arabidopsis. *The Journal of Biological Chemistry* **284**: 34506–34513.
- Golding BT, Patel N and Watson WP** (1989) Dimer and trimer of malonaldehyde. *Journal of the Chemical Society* **1**: 668–669.

- Goral TK, Johnson MP, Duffy CDP, Brain APR, Ruban AV and Mullineaux CW** (2012) Light-harvesting antenna composition controls the macrostructure and dynamics of thylakoid membranes in *Arabidopsis*. *The Plant Journal* **69**: 289–301.
- Guo L, Chen Z, Amarnath V and Davies SS** (2012) Identification of novel bioactive aldehyde-modified phosphatidylethanolamines formed by lipid peroxidation. *Free Radical Biology & Medicine* **53**: 1226–1238.
- Haining J, Legan J and Lovell W** (1970) Synthesis and degradation of rat liver xanthine oxidase as a function of age and protein deprivation. *Journal of Gerontology* **25**: 205–209.
- Hecker M, Haurand M and Ullrich V** (1987) Products, kinetics, and substrate specificity of homogeneous thromboxane synthase from human platelets: Development of a novel enzyme assay. *Archives of Biochemistry and Biophysics* **254**: 124–135.
- Hilson P, Allemeersch J, Altmann T, Aubourg S, Avon A, Beynon J et al.** (2004) Versatile gene-specific sequence tags for *Arabidopsis* functional genomics: transcript profiling and reverse genetics applications. *Genome Research* **14**: 2176–2189.
- Holte LL, van Kuijk FJ, Dratz Ea and Kuijk JGMV** (1990) Preparative high-performance liquid chromatography purification of polyunsaturated phospholipids and characterization using ultraviolet derivative spectroscopy. *Analytical Biochemistry* **188**: 136–141.
- Hruz T, Laule O, Szabo G, Wessendorp F, Bleuler S, Oertle L et al.** (2008) Genevestigator v3: a reference expression database for the meta-analysis of transcriptomes. *Advances in Bioinformatics* **2008**: 1–5.
- Igarashi M, Gao F, Kim HW, Kaizong Ma JMB and Rapoport SI** (2009) Dietary n-6 PUFA deprivation for 15 weeks reduces arachidonic acid concentrations while increasing n-3 PUFA concentrations in organs of post-weaning male rats. *Biochimica et Biophysica Acta* **1791**: 132–139.
- Janero DR** (1990) Malondialdehyde and thiobarbituric acid-reactivity as diagnostic indices of lipid peroxidation and peroxidative tissue injury. *Free Radical Biology & Medicine* **9**: 515–540.
- Jauh G, Phillips T and Rogers J** (1999) Tonoplast intrinsic protein isoforms as markers for vacuolar functions. *The Plant Cell* **11**: 1867–1882.
- Kakuda Y, Stanley DW and Voort FR** (1981) Determination of TBA number by high performance liquid chromatography. *Journal of the American Oil Chemists Society* **58**: A773–A775.
- Kelley DS, Bartolini GL, Newman JW, Vemuri M and Mackey BE** (2006) Fatty acid composition of liver, adipose tissue, spleen, and heart of mice fed diets containing t10, c12-, and c9, t11-conjugated linoleic acid. *Prostaglandins, Leukotrienes, and Essential Fatty Acids* **74**: 331–338.
- Knight J, Pieper R and McClellan L** (1988) Specificity of the thiobarbituric acid reaction: its use in studies of lipid peroxidation. *Clinical Chemistry* **34**: 2433–2438.
- Kobayashi K, Kondo M, Fukuda H, Nishimura M and Ohta H** (2007) Galactolipid synthesis in chloroplast inner envelope is essential for proper thylakoid biogenesis, photosynthesis, and embryogenesis. *Proceedings of the National Academy of Sciences of the United States of America* **104**: 17216–17221.
- Kobayashi K, Narise T, Sonoike K, Hashimoto H, Sato N, Kondo M et al.** (2012) Role of galactolipid biosynthesis in coordinated development of photosynthetic complexes and thylakoid membranes during chloroplast biogenesis in *Arabidopsis*. *The Plant Journal* **73**: 250–261.
- Koppaka V, Thompson DDC, Chen Y, Ellermann M, Nicolaou KC, Juvonen RO et al.** (2012) Aldehyde dehydrogenase inhibitors: a comprehensive review of the pharmacology, mechanism of action, substrate specificity, and clinical application. *Pharmacological reviews* **64**: 520–539.
- Kosugi H, Kato T and Kikugawa K** (1987) Formation of yellow, orange, and red pigments in the reaction of alk-2-enals with 2-thiobarbituric acid. *Analytical Biochemistry* **165**: 456–464.
- Kosugi H and Kikugawa K** (1986) Reaction of thiobarbituric acid with saturated aldehydes. *Lipids* **21**: 537–542.
- Kosugi H and Kikugawa K** (1989) Potential thiobarbituric acid-reactive substances in peroxidized lipids. *Free Radical Biology and Medicine* **7**: 205–207.

REFERENCES

- Krieger-Liszkay A** (2005) Singlet oxygen production in photosynthesis. *Journal of Experimental Botany* **56**: 337–346.
- Krieger-Liszkay A and Rutherford AW** (1998) Influence of herbicide binding on the redox potential of the quinone acceptor in photosystem II: relevance to photodamage and phytotoxicity. *Biochemistry* **37**: 17339–17344.
- Kumasaka R, Nakamura N, Yamabe H, Osawa H, Shirato KI, Shimada M et al.** (2007) Fatty acid composition of plasma and kidney in rats with anti-Thy1.1 nephritis. *In Vivo* **21**: 77–79.
- Lacombe A, Kermasha S, Voort FRVD, Millst BL, Van de Voort FR and Mills BL** (1990) Preparation and purification of malonaldehyde sodium salt. *Journal of Agricultural and Food Chemistry* **38**: 418–423.
- Lassen N, Bateman JB, Estey T, Kuszak JR, Nees DW, Piatigorsky J et al.** (2007) Multiple and additive functions of ALDH3A1 and ALDH1A1: cataract phenotype and ocular oxidative damage in Aldh3a1(-/-)/Aldh1a1(-/-) knockout mice. *The Journal of Biological Chemistry* **282**: 25668–25676.
- Li-Beisson Y, Shorosh B, Beisson F, Andersson MX, Arondel V, Bates PD et al.** (2010) Acyl-lipid metabolism. *The Arabidopsis Book* **8**: e0133.
- Lin M and Oliver DJ** (2008) The role of acetyl-coenzyme a synthetase in Arabidopsis. *Plant Physiology* **147**: 1822–1829.
- Liu J, Yeo HC, Doniger SJ and Ames BN** (1997) Assay of aldehydes from lipid peroxidation: gas chromatography-mass spectrometry compared to thiobarbituric acid. *Analytical Biochemistry* **245**: 161–166.
- Lloyd D** (1965) The purification and properties of malonic semialdehyde oxidative decarboxylase from *Prototheca zopfii*. *The Biochemical journal* **96**: 766–770.
- Loeffler C, Berger S, Guy A, Durand T, Bringmann G, Mueller MJ et al.** (2005) B 1 - Phytoprostanes Trigger Plant Defense and Detoxification Responses. *Plant Physiology* **137**: 328–340.
- Loll B, Kern J, Saenger W, Zouni A and Biesiadka J** (2005) Towards complete cofactor arrangement in the 3.0 Å resolution structure of photosystem II. *Nature* **438**: 1040–1044.
- Long EK, Smoliakova I, Honzatko A and Picklo MJ** (2008) Structural characterization of alpha,beta-unsaturated aldehydes by GC/MS is dependent upon ionization method. *Lipids* **43**: 765–774.
- Long J, Liu C, Sun L, Gao H and Liu J** (2009) Neuronal mitochondrial toxicity of malondialdehyde: inhibitory effects on respiratory function and enzyme activities in rat brain mitochondria. *Neurochemical Research* **34**: 786–794.
- Lucas KA, Filley JR, Erb JM, Graybill ER and Hawes JW** (2007) Peroxisomal metabolism of propionic acid and isobutyric acid in plants. *The Journal of Biological Chemistry* **282**: 24980–24989.
- Maere S, Heymans K and Kuiper M** (2005) BiNGO: a Cytoscape plugin to assess overrepresentation of gene ontology categories in biological networks. *Bioinformatics* **21**: 3448–3449.
- Mano J** (2012) Reactive carbonyl species: Their production from lipid peroxides, action in environmental stress, and the detoxification mechanism. *Plant Physiology and Biochemistry* **59**: 90–97.
- Mano J, Miyatake F, Hiraoka E and Tamoi M** (2009) Evaluation of the toxicity of stress-related aldehydes to photosynthesis in chloroplasts. *Planta* **230**: 639–648.
- Mano S, Nakamori C, Hayashi M, Kato A, Kondo M and Nishimura M** (2002) Distribution and Characterization of Peroxisomes in Arabidopsis by Visualization with GFP : Dynamic Morphology and Actin-Dependent Movement. *The Plant Cell* **43**: 331–341.
- Marchitti Sa, Brocker C, Stagos D and Vasiliou V** (2008) Non-P450 aldehyde oxidizing enzymes: the aldehyde dehydrogenase superfamily. *Expert Opinion on Drug Metabolism & Toxicology* **4**: 697–720.
- Marnett LJ** (1999) Lipid peroxidation-DNA damage by malondialdehyde. *Mutation Research* **424**: 83–95.
- Marnett LJ** (2002) Oxy radicals, lipid peroxidation and DNA damage. *Toxicology* **181-182**: 219–222.
- Marnett LJ, Buck J, Tuttle MMA, Basu AKA and Bull AW** (1985) Distribution and oxidation of malondialdehyde in mice. *Prostaglandins* **30**: 241–254.

- Marnett LJ and Tuttle Ma** (1980) Comparison of the mutagenicities of malondialdehyde and the side products formed during its chemical synthesis. *Cancer Research* **40**: 276–282.
- Marnett LLJ, Bienkowski MJ, Raban M and Tuttle MA** (1979) Studies of the hydrolysis of 14 C-labeled tetraethoxypropane to malondialdehyde. *Analytical Biochemistry* **99**: 458–463.
- Mauch F, Mauch-Mani B, Gaille C, Kull B, Haas D and Reimann C** (2001) Manipulation of salicylate content in *Arabidopsis thaliana* by the expression of an engineered bacterial salicylate synthase. *The Plant Journal* **25**: 67–77.
- McConn M and Browse J** (1996) The critical requirement for linolenic acid is pollen development, not photosynthesis, in an *Arabidopsis* mutant. *The Plant Cell* **8**: 403–416.
- McConn M and Browse J** (1998) Polyunsaturated membranes are required for photosynthetic competence in a mutant of *Arabidopsis*. *The Plant Journal* **15**: 521–530.
- Mène-Safrané L, Davoine C, Stolz S, Majcherczyk P, Farmer EE, Of WbM et al.** (2007) Genetic removal of tri-unsaturated fatty acids suppresses developmental and molecular phenotypes of an *Arabidopsis* tocopherol-deficient mutant. Whole-body mapping of malondialdehyde pools in a complex eukaryote. *The Journal of Biological Chemistry* **282**: 35749–35756.
- Mène-Safrané L, Dubugnon L, Chételat A, Stolz S, Gouhier-Darimont C and Farmer EE** (2009) Nonenzymatic oxidation of trienoic fatty acids contributes to reactive oxygen species management in *Arabidopsis*. *The Journal of Biological Chemistry* **284**: 1702–1708.
- Meskauskiene R, Nater M, Goslings D, Kessler F, op den Camp R and Apel K** (2001) FLU: a negative regulator of chlorophyll biosynthesis in *Arabidopsis thaliana*. *Proceedings of the National Academy of Sciences of the United States of America* **98**: 12826–12831.
- Miquel M and Browse J** (1992) *Arabidopsis* Mutants Deficient in Polyunsaturated Fatty Acid Synthesis. *The Journal of Biological Chemistry* **267**: 1502–1509.
- Miquel M, James D, Dooner H and Browse J** (1993) *Arabidopsis* requires polyunsaturated lipids for low-temperature survival. *Proceedings of the National Academy of Sciences of the United States of America* **90**: 6208–6212.
- Mittler R, Vanderauwera S, Gollery M and Van Breusegem F** (2004) Reactive oxygen gene network of plants. *Trends in Plant Science* **9**: 490–498.
- Miyake T and Shibamoto T** (1999) Formation of malonaldehyde and acetaldehyde from the oxidation of 2'-deoxyribonucleosides. *Journal of Agricultural and Food Chemistry* **47**: 2782–2785.
- Montillet JLL, Cacas JLL, Garnier L, Montané MHH, Douki T, Bessoule JJ et al.** (2004) The upstream oxylipin profile of *Arabidopsis thaliana*: a tool to scan for oxidative stresses. *The Plant Journal* **40**: 439–451.
- Muckenschnabel I** (2002) Infection of leaves of *Arabidopsis thaliana* by *Botrytis cinerea*: changes in ascorbic acid, free radicals and lipid peroxidation products. *Journal of Experimental Botany* **53**: 207–214.
- Mueller MJ** (2004) Archetype signals in plants: the phytoprostanenes. *Current Opinion in Plant Biology* **7**: 441–448.
- Mueller MJ and Berger S** (2009) Reactive electrophilic oxylipins: pattern recognition and signalling. *Phytochemistry* **70**: 1511–1521.
- Mueller S, Hilbert B, Dueckershoff K, Roitsch T, Krischke M, Mueller MJ et al.** (2008) General detoxification and stress responses are mediated by oxidized lipids through TGA transcription factors in *Arabidopsis*. *The Plant Cell* **20**: 768–785.
- Nakashima K, Shinwari ZK, Sakuma Y, Seki M, Miura S, Shinozaki K et al.** (2000) Organization and expression of two *Arabidopsis* DREB2 genes encoding DRE-binding proteins involved in dehydration- and high-salinity-responsive gene expression. *Plant Molecular Biology* **42**: 657–665.
- Niedernhofer LJ, Daniels JS, Rouzer CA, Greene RE and Marnett LJ** (2003) Malondialdehyde, a product of lipid peroxidation, is mutagenic in human cells. *The Journal of Biological Chemistry* **278**: 31426–31433.
- Ohlogge J, Browse J and Ohloggeav J** (1995) Lipid biosynthesis. *The Plant Cell* **7**: 957–970.
- Okuley J, Lightner J, Feldmann K, Yadav N, Lark E and Browse J** (1994) *Arabidopsis*

REFERENCES

- FAD2 gene encodes the enzyme that is essential for polyunsaturated lipid synthesis. *The Plant Cell* **6**: 147–158.
- Oppenheimer C and Stern K** (1939) Biological Oxidation. The Hague.
- Pan X, Welti R and Wang X** (2008) Simultaneous quantification of major phytohormones and related compounds in crude plant extracts by liquid chromatography-electrospray tandem mass spectrometry. *Phytochemistry* **69**: 1773–1781.
- Placer Z, Veselkova A and Rath R** (1965) Kinetik des Malondialdehydes im Organismus. *Cellular and Molecular Life Sciences* **1**: 19–20.
- Porra RJ** (2002) The chequered history of the development and use of simultaneous equations for the accurate determination of chlorophylls a and b. *Photosynthesis Research* **73**: 149–156.
- Reed TT** (2011) Lipid peroxidation and neurodegenerative disease. *Free Radical Biology & Medicine* **51**: 1302–1319.
- Refsgaard HH, Tsai L and Stadtman ER** (2000) Modifications of proteins by polyunsaturated fatty acid peroxidation products. *Proceedings of the National Academy of Sciences of the United States of America* **97**: 611–616.
- Reymond P, Bodenhausen N, Van Poecke RMP, Krishnamurthy V, Dicke M and Farmer EE** (2004) A conserved transcript pattern in response to a specialist and a generalist herbivore. *The Plant Cell* **16**: 3132–3147.
- Robinson T** (1963) Water-soluble organic acids. In: *The Organic Constituents of Higher Plants: Their Chemistry and Interrelationships*, vol. 40, chap. 3, pp. 36–44, American Chemical Society.
- Robinson WG and Coon MJ** (1963) Synthesis of malonic semialdehyde, β -hydroxypropionate, and β -hydroxyisobutyrate. *Methods in Enzymology* **6**: 549–553.
- Rodríguez VM, Chételat A, Majcherczyk P, Farmer EE and Che A** (2010) Chloroplastic phosphoadenosine phosphosulfate metabolism regulates basal levels of the prohormone jasmonic acid in Arabidopsis leaves. *Plant Physiology* **152**: 1335–1345.
- Sattler SE, Mène-Saffrané L, Farmer EE, Krischke M, Mueller MJ, Dellapenna D et al.** (2006) Nonenzymatic lipid peroxidation reprograms gene expression and activates defense markers in Arabidopsis tocopherol-deficient mutants. *The Plant Cell* **18**: 3706–3720.
- Schalk M, Cabello-Hurtado F, Pierrel M, Atanossova R, Saindrenan P and Werck-Reichhart D** (1998) Piperonylic acid, a selective, mechanism-based inactivator of the trans-cinnamate 4-hydroxylase: A new tool to control the flux of metabolites in the phenylpropanoid pathway. *Plant Physiology* **118**: 209–218.
- Schmid-Siegert E, Loscos J and Farmer EE** (2012) Inducible malondialdehyde pools in zones of cell proliferation and developing tissues in Arabidopsis. *The Journal of Biological Chemistry* **287**: 8954–8962.
- Scholem RD and Brown GK** (1983) Metabolism of malonic semialdehyde in man. *The Biochemical Journal* **216**: 81–85.
- Shaikh S and Edidin M** (2006) Polyunsaturated fatty acids, membrane organization, T cells, and antigen presentation. *The American Journal of Clinical Nutrition* **84**: 1277–1289.
- Shara MA and Dickson PH** (1992) Excretion of formaldehyde, malondialdehyde, acetaldehyde and acetone in the urine of rats in response and carbon tetrachloride. *Journal of Chromatography* **576**: 221–233.
- Sharma P, Jha AB, Dubey RS and Pessarakli M** (2012) Reactive Oxygen Species, Oxidative Damage, and Antioxidative Defense Mechanism in Plants under Stressful Conditions. *Journal of Botany* **2012**: 1–26.
- Simpson PJ, Tantitadapitak C, Reed AM, Mather OC, Bunce CM, White Sa et al.** (2009) Characterization of two novel aldo-keto reductases from Arabidopsis: expression patterns, broad substrate specificity, and an open active-site structure suggest a role in toxicant metabolism following stress. *Journal of Molecular Biology* **392**: 465–80.
- Sinnhuber RO, Yu TC and Yu TC** (1958) Characterization of the red pigment formed in the 2-thiobarbituric acid determination of oxidative rancidity. *Journal of Food Science* **23**: 626–634.
- Siu GM and Draper HH** (1982) Metabolism of malonaldehyde in vivo and in vitro. *Lipids* **17**: 349–355.

- Smith W** (1992) Prostanoid biosynthesis and mechanisms of action. *American Journal of Physiology-Renal Physiology* **263**: F181–F191.
- Smoot ME, Ono K, Ruscheinski J, Wang PL and Ideker T** (2011) Cytoscape 2.8: new features for data integration and network visualization. *Bioinformatics* **27**: 431–432.
- Somerville C and Browse J** (1991) Plant lipids: metabolism, mutants, and membranes. *Science* **252**: 80–87.
- Staswick PE, Su W and Howell SH** (1992) Methyl jasmonate inhibition of root growth and induction of a leaf protein are decreased in an Arabidopsis thaliana mutant. *Proceedings of the National Academy of Sciences of the United States of America* **89**: 6837–6840.
- Stoffel W, Holz B, Jenke B, Binczek E, Günter RH, Kiss C et al.** (2008) Delta6-desaturase (FADS2) deficiency unveils the role of omega3- and omega6-polyunsaturated fatty acids. *The EMBO journal* **27**: 2281–2292.
- Stroud CK, Nara TY, Roqueta-Rivera M, Radlowski EC, Lawrence P, Zhang Y et al.** (2009) Disruption of FADS2 gene in mice impairs male reproduction and causes dermal and intestinal ulceration. *Journal of Lipid Research* **50**: 1870–1880.
- Stumpf DK and Burris RH** (1979) A micromethod for the purification and quantification of organic acids of the tricarboxylic acid cycle in plant tissue. *Analytical Biochemistry* **315**: 311–315.
- Summerfield FW and Tappel AL** (1978) Enzymatic synthesis of malonaldehyde. *Biochemical and Biophysical Research Communications* **82**: 547–552.
- Sun Q, Faustman C, Senecal A, Wilkinson aL and Furr H** (2001) Aldehyde reactivity with 2-thiobarbituric acid and TBARS in freeze-dried beef during accelerated storage. *Meat Science* **57**: 55–60.
- Sunkar R, Bartels D and Kirch HH** (2003) Over-expression of a stress-inducible aldehyde dehydrogenase gene from Arabidopsis thaliana in transgenic plants improves stress tolerance. *The Plant Journal* **35**: 452–464.
- Talarico TL and Dobrogosz WJ** (1989) Chemical characterization of an antimicrobial substance produced by Lactobacillus reuteri. *Antimicrobial Agents and Chemotherapy* **33**: 674–679.
- Tatum VL, Changchit C and Chow CK** (1990) Measurement of malondialdehyde by high performance liquid chromatography with fluorescence detection. *Lipids* **25**: 226–229.
- Taylor P, Khan MF, Wu X, Ansari GAS and Boor P** (2011) Malondialdehyde-protein adducts in the spleens of aniline-treated rats : immunochemical detection and localization. *Journal of Toxicology and Environmental Health* **66**: 37–41.
- Theorell H and Yonetani T** (1963) Liver alcohol dehydrogenase-DPN-pyrazole complex: a model of a ternary intermediate in the enzyme reaction. *Biochemische Zeitschrift* **338**: 537–553.
- Triantaphylidès C, Krischke M, Hoerberichs FA, Ksas B, Gresser G, Havaux M et al.** (2008) Singlet oxygen is the major reactive oxygen species involved in photooxidative damage to plants. *Plant Physiology* **148**: 960–968.
- Veronese P, Nakagami H, Dietrich RA, Hirt H and Mengiste T** (2006) The membrane-anchored BOTRYTIS-INDUCED KINASE1 plays distinct roles in Arabidopsis resistance to necrotrophic and biotrophic pathogens. *The Plant Cell* **18**: 257–273.
- Vijayan P** (2002) Photoinhibition in mutants of Arabidopsis deficient in thylakoid unsaturation. *Plant Physiology* **129**: 876–885.
- Voisenet M** (1910) Formation d'acroléine dans la maladie de l'amertume des vins. *C. R. Acad. Sci.* **150**: 1614–1616.
- Voitkun V and Zhitkovich A** (1999) Analysis of DNA-protein crosslinking activity of malondialdehyde in vitro. *Mutation Research* **424**: 97–106.
- Vollenweider S, Grassi G, König I and Puhani Z** (2003) Purification and structural characterization of 3-hydroxypropionaldehyde and its derivatives. *Journal of Agricultural and Food Chemistry* **51**: 3287–3293.
- Vollenweider S, Weber H, Stolz S, Chételat A and Farmer EE** (2000) Fatty acid ketodienes and fatty acid ketotrienes: Michael addition acceptors that accumulate in wounded and diseased Arabidopsis leaves. *The Plant Journal* **24**: 467–476.
- Wallis JG and Browse J** (2002) Mutants of Arabidopsis reveal many roles for membrane lipids. *Progress in Lipid Research* **41**: 254–278.

REFERENCES

- Weber H, Chételat A, Reymond P, Farmer EE and Chételat A (2004) Selective and powerful stress gene expression in Arabidopsis in response to malondialdehyde. *The Plant Journal* **37**: 877–888.
- Wu J, Seregard S and Algvere PV (2006) Photochemical damage of the retina. *Survey of Ophthalmology* **51**: 461–481.
- Yamauchi Y, Furutera A, Seki K, Toyoda Y, Tanaka K and Sugimoto Y (2008) Malondialdehyde generated from peroxidized linolenic acid causes protein modification in heat-stressed plants. *Plant Physiology and Biochemistry* **46**: 786–793.
- Yamauchi Y, Hasegawa A, Taninaka A, Mizutani M and Sugimoto Y (2011) NADPH-dependent reductases involved in the detoxification of reactive carbonyls in plants. *The Journal of Biological Chemistry* **286**: 6999–7009.
- Yamauchi Y and Sugimoto Y (2010) Effect of protein modification by malondialdehyde on the interaction between the oxygen-evolving complex 33 kDa protein and photosystem II core proteins. *Planta* **231**: 1077–1088.
- Yamazaki S, Ozawa N, Hiratsuka A and Watabe T (1999) Photogeneration of 3-beta-hydroxy-5-alpha-cholest-6-ene-5-hydroperoxide in rat skin: evidence for occurrence of singlet oxygen in vivo. *Free Radical Biology & Medicine* **27**: 301–308.
- Yehuda S, Rabinovitz S, Carasso RL and Mostofsky DI (2002) The role of polyunsaturated fatty acids in restoring the aging neuronal membrane. *Neurobiology of Aging* **23**: 843–853.
- Yeo HC, Helbock HJ, Chyu DW and Ames BN (1994) Assay of malondialdehyde in biological fluids by gas chromatography-mass spectrometry. *Analytical Biochemistry* **220**: 391–396.
- Yoval-Sánchez B and Rodríguez-Zavala JS (2012) Differences in susceptibility to inactivation of human aldehyde dehydrogenases by lipid peroxidation byproducts. *Chemical Research in Toxicology* **25**: 722–729.
- Zhang J, Liu H, Sun J, Li B, Zhu Q, Chen S et al. (2012) Arabidopsis fatty acid desaturase FAD2 is required for salt tolerance during seed germination and early seedling growth. *PLoS One* **7**: 1–12.
- Zhang JT, Zhu JQ, Zhu Q, Liu H, Gao XS and Zhang HX (2009) Fatty acid desaturase-6 (Fad6) is required for salt tolerance in Arabidopsis thaliana. *Biochemical and Biophysical Research Communications* **390**: 469–474.
- Zoeller M, Stingl N and Krischke M (2012) Lipid profiling of the Arabidopsis hypersensitive response reveals specific lipid peroxidation and fragmentation processes: biogenesis of pimelic and azelaic acid. *Plant Physiology* **160**: 365–378.

8

Supplementary material ¹

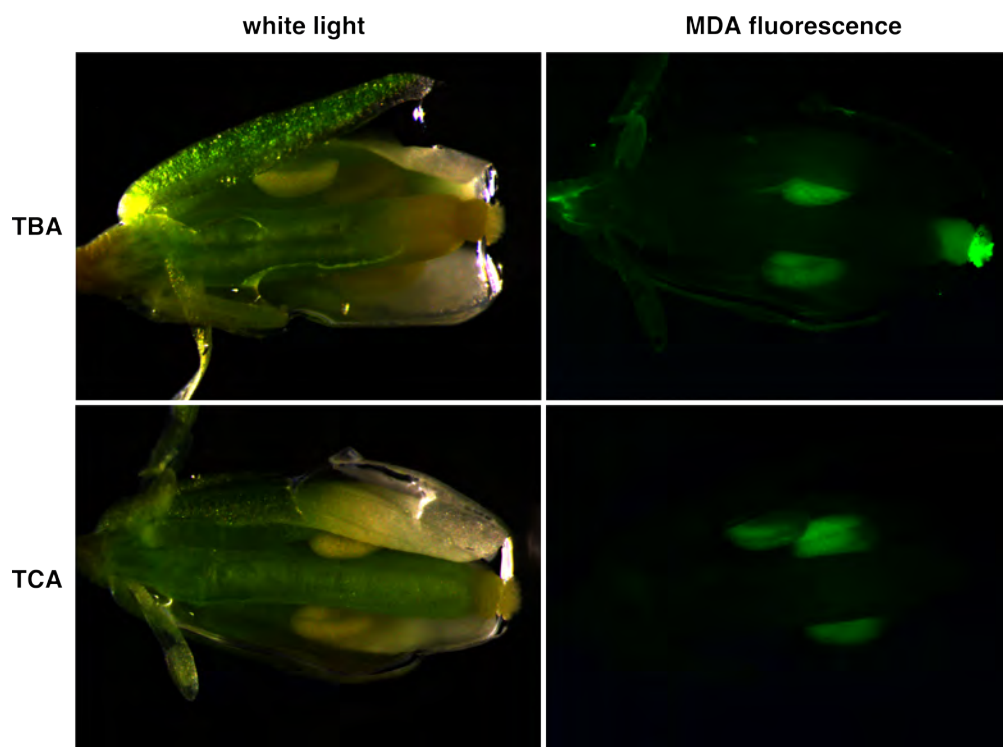


Figure 8.1: MDA fluorescence in *Arabidopsis* flowers - TBA-assay of flowers from adult *Arabidopsis* plants stained with 35 mM TBA or TCA for 1.5 h at 28°C. MDA specific fluorescence in the stigma and style, unspecific artificial fluorescence in anthers.

¹Staining of *C. elegans* (Figure 8.2) was done in collaboration with J. Loscos, experimental part of the MDA-microarray analysis (Figure 8.1) was conducted by S. Stolz

8. SUPPLEMENTARY MATERIAL

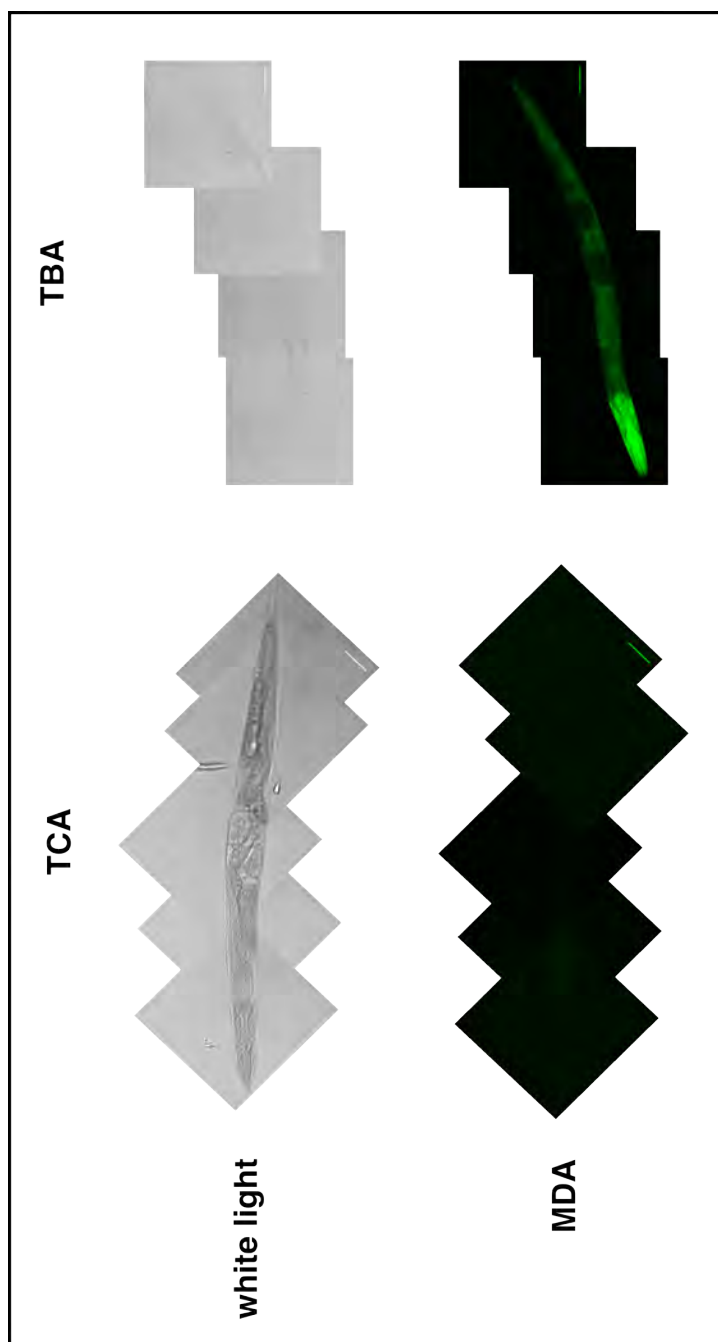


Figure 8.2: MDA staining in *C. elegans* - TBA-assay of adult *Caenorhabditis elegans* for 2h at 25°C with 35 mM TBA and TCA as control. For microscopy worms were immobilized with 1 μ M levamisole hydrochloride (Scale = 50 μ m)

Table 8.1: Microarray of MDA-treated *Arabidopsis* plants. Microarray analysis of differential expressed genes from MDA treated plants. Adult *Arabidopsis* plants were exposed for 2 h to 10 μ m MDA or pyruvaldehyde as control in Plexiglass boxes (6 replicates). Significance of gene expression was evaluated against mock control plants (5 replicates, $p \geq 0.05$ excluded). Two fold induction/repression was used as cut-off. ¹

Locus	Gene	Description	ratio (log ₂)	T-test
At3g09350	FES1A (Fes1A)	Suggested to be involved in acquired thermotolerance.	4.30	1.61E-04
At1g07400		HSP20-like chaperones superfamily protein	4.24	1.17E-03
At5g59820	RESPONSIVE TO HIGH LIGHT 41 (RHL41)	Encodes a zinc finger protein involved in high light and cold acclimation.	3.74	1.04E-04
At3g28730	HIGH MOBILITY GROUP (HMG)	encodes a component of the Facilitates Chromatin Transcription (FACT) complex, SSRP1	3.58	1.94E-04
At5g05410	DRE-BINDING PROTEIN 2A (DREB2A)	Encodes a transcription factor that specifically binds to DRE/CRT cis elements (responsive to drought and low-temperature stress).	3.52	5.65E-04
At1g76600		unknown protein	3.47	1.35E-05
At4g01870		tolB protein-related	3.45	7.44E-05
At2g29500		HSP20-like chaperones superfamily protein	3.37	6.45E-04
At5g14730		unknown protein	3.34	3.50E-03
At5g49480	CA ²⁺ -BINDING PROTEIN 1 (CP1)	shares sequence similarities with calmodulins. The expression of AtCP1 is induced by NaCl.	3.34	4.38E-05
At1g79410		organic cation/carnitine transporter5	3.29	1.23E-04
At5g52640	HEAT SHOCK PROTEIN 90.1 (HSP90.1)	AtHSP90.1 interacts with disease resistance signaling components SGT1b and RAR1 and is required for RPS2-mediated resistance.	3.24	5.22E-03
At2g15490	UDP-glycosyltransferase 73B4 (UGT73B4)		3.22	1.80E-03
At2g20560		DNAJ heat shock family protein	3.14	6.41E-04
At5g61820		unknown protein	3.10	8.34E-05
At1g75270	dehydroascorbate reductase 2 (DHAR2)		3.09	1.41E-06
At3g12580	heat shock protein 70 (HSP70)		3.06	2.66E-04
At5g48570	(ROF2)	Encodes one of the 36 carboxylate clamp (CC)-tetratricopeptide repeat (TPR) proteins	2.97	2.88E-03
At3g44190		FAD/NAD(P)-binding oxidoreductase family protein	2.96	8.77E-05
At1g74310	HEAT SHOCK PROTEIN 101 (HSP101)	Encodes ClpB1, which belongs to the Casein lytic proteinase/heat shock protein 100 (Clp/Hsp100) family. AtHsp101 is a cytosolic heat shock protein required for acclimation to high temperature.	2.94	1.71E-02

8. SUPPLEMENTARY MATERIAL

Locus	Gene	Description	ratio (log ₂)	T-test
At2g29420	GLUTATHIONE S-TRANSFERASE TAU 7 (GSTU7)	Encodes glutathione transferase belonging to the tau class of GSTs.	2.93	2.22E-03
At5g39050	PHENOLIC GLUCOSIDE MALONYL-TRANSFERASE 1 (PMAT1)	Encodes a malonyltransferase that may play a role in phenolic xenobiotic detoxification.	2.86	4.05E-05
At2g36750	UDP-glucosyl transferase 73C1 (UGT73C1)		2.83	1.56E-03
At4g24160		Encodes a soluble lysophosphatidic acid acyltransferase	2.82	3.72E-04
At4g34131	UDP-glucosyl transferase 73B3 (UGT73B3)		2.80	3.73E-03
At5g04340	ZINC FINGER OF ARABIDOPSIS THALIANA 6 (ZAT6)	putative c2h2 zinc finger transcription factor mRNA,	2.80	5.04E-04
At3g14200		Chaperone DnaJ-domain superfamily protein	2.78	1.77E-04
At3g28210	(PMZ)	Encodes a putative zinc finger protein (PMZ).	2.77	6.11E-03
At5g64310	ARABINOGLACTAN PROTEIN 1 (AGP1)	Encodes arabinogalactan-protein (AGP1).	2.73	2.16E-03
At1g55920	SERINE ACETYL-TRANSFERASE 2	involved in sulfur assimilation and cysteine biosynthesis	2.72	1.63E-04
At4g13180		NAD(P)-binding Rossmann-fold superfamily protein	2.69	2.58E-05
At1g28480	(GRX480)	Encodes GRX480, a member of the glutaredoxin family that regulates protein redox state.	2.69	1.62E-03
At4g35180		LYS/HIS transporter 7 (LHT7)	2.66	3.03E-04
At3g22600		Bifunctional inhibitor/lipid-transfer protein/seed storage 2S albumin superfamily protein	2.61	4.41E-06
At5g13750	zinc induced facilitator-like 1 (ZIFL1)		2.60	1.66E-06
At5g64250		Aldolase-type TIM barrel family protein	2.58	3.46E-04
At4g22530		S-adenosyl-L-methionine-dependent methyltransferases superfamily protein	2.56	5.85E-06
At5g24660	RESPONSE TO LOW SULFUR 2 (LSU2)		2.51	4.48E-04
At1g59860		HSP20-like chaperones superfamily protein	2.51	3.41E-02
At3g09440		Heat shock protein 70 (Hsp 70) family protein	2.46	4.73E-03
At2g47730	GLUTATHIONE S-TRANSFERASE PHI 8 (GSTF8)	Encodes glutathione transferase belonging to the phi class of GSTs.	2.46	3.81E-05
At4g27652		unknown protein	2.43	3.46E-03
At2g36950		Heavy metal transport/detoxification superfamily protein	2.42	2.00E-04

Locus	Gene	Description	ratio (log ₂)	T-test
At1g36370	SERINE HYDROXYMETHYLTRANSFERASE 7 (SHM7)	Encodes a putative serine hydroxymethyltransferase.	2.41	2.29E-06
At2g26150	HEAT SHOCK TRANSCRIPTION FACTOR A2 (HSFA2)	member of Heat Stress Transcription Factor (Hsf) family. Involved in response to misfolded protein accumulation in the cytosol.	2.39	2.16E-02
At3g24500	MULTIPROTEIN BRIDGING FACTOR 1C (MBF1C)	transcriptional coactivator. Constitutive expression enhances the tolerance of transgenic plants to various biotic and abiotic stresses.	2.37	5.52E-03
At4g01070	(GT72B1)	the glycosyl-transferase (UGT72B1) is involved in metabolizing xenobiotica (chloroaniline and chlorophenole).	2.37	2.33E-07
At1g14200		RING/U-box superfamily protein	2.36	1.71E-03
At4g04610	APS REDUCTASE 1 (APR1)	Encodes a protein disulfide isomerase-like (PDIL) protein, a member of a multigene family within the thioredoxin (TRX) superfamily.	2.36	9.68E-04
At5g12030	HEAT SHOCK PROTEIN 17.6A (HSP17.6A)	Encodes a cytosolic small heat shock protein with chaperone activity that is induced by heat and osmotic stress	2.33	3.27E-02
At5g63790	NAC DOMAIN CONTAINING PROTEIN 102 (NAC102)	ANAC102 appears to have a role in mediating response to low oxygen stress (hypoxia) in germinating seedlings.	2.33	1.44E-04
At2g43820	UDP-GLUCOSYLTRANSFERASE 74F2 (UGT74F2)	Induced by Salicylic acid, virus, fungus and bacteria. Involved in the tryptophan synthesis pathway.	2.32	2.82E-04
At1g07350	SERINE/ARGININE RICH-LIKE PROTEIN 45A (SR45a)	Involved in the regulation of stress-responsive alternative splicing.	2.29	7.77E-04
At5g24030	SLAC1 HOMOLOGUE 3 (SLAH3)	Encodes a protein with ten predicted transmembrane helices. The SLAH3 protein has similarity to the SLAC1 protein involved in ion homeostasis in guard cells.	2.28	9.76E-03
At4g03460		Ankyrin repeat family protein	2.26	5.03E-04
At4g30490		AFG1-like ATPase family protein	2.26	9.30E-04
At1g55850	CELLULOSE SYNTHASE LIKE E1 (CSLE1)	encodes a protein similar to cellulose synthase	2.24	1.29E-03
At4g02940		oxidoreductase, 2OG-Fe(II) oxygenase family protein	2.24	5.99E-07
At5g51830		pfkB-like carbohydrate kinase family protein	2.23	6.11E-03
At1g72680	cinnamyl-alcohol dehydrogenase (CAD1)		2.23	4.90E-05
At1g33110		MATE efflux family protein	2.20	3.38E-04
At5g25930		Protein kinase family protein with leucine-rich repeat domain	2.19	5.86E-03

8. SUPPLEMENTARY MATERIAL

Locus	Gene	Description	ratio (log ₂)	T-test
At1g66580	senescence associated gene 24 (SAG24)		2.19	5.66E-07
At5g35320		unknown protein	2.19	1.18E-02
At3g16050	PYRIDOXINE BIOSYNTHESIS 1.2 (PDX1.2)	detected mostly in roots and accumulate during senescence.	2.18	1.62E-02
At5g54700		Ankyrin repeat family protein	2.18	2.42E-04
At4g15760	MONOOXYGENASE 1 (MO1)	Encodes a protein with similarity to monooxygenases that are known to degrade salicylic acid (SA).	2.17	1.22E-03
At5g56030	HEAT SHOCK PROTEIN 81-2 (HSP81-2)	Interacts with HsfA1d in the cytosol and the nucleus and negatively regulates HsfA1d.	2.16	3.09E-04
At4g18010	INOSITOL(1,4,5)P3 5-PHOSPHATASE II (IP5PII)	Encodes an inositol polyphosphate 5-phosphatase that appears to have Type I activity.	2.10	1.40E-02
At1g62180	5'ADENYLYL-PHOSPHOSULFATE REDUCTASE 2 (APR2)	involved in sulfate assimilation.	2.09	4.59E-03
At1g75280		isoflavone reductase, putative, identical to SP:P52577 Isoflavone reductase homolog P3	2.09	1.67E-06
At5g64230		unknown protein	2.07	4.50E-04
At5g67350		unknown protein	2.07	7.42E-04
At3g25230	ROTAMASE FKBP 1 (ROF1)	Encodes a a high molecular weight member of the FK506 binding protein (FKBP) family.	2.06	1.51E-03
At1g32920		unknown protein	2.05	1.73E-03
At4g21990	APS REDUCTASE 3 (APR3)	Encodes a protein disulfide isomerase-like (PDIL) protein	2.04	1.19E-03
At4g24380		INVOLVED IN: 10-formyltetrahydrofolate biosynthetic process, folic acid and derivative biosynthetic process	2.03	8.10E-03
At5g56010	HEAT SHOCK PROTEIN 81-3 (HSP81-3)	Overexpression reduced tolerance to heat and conferred higher tolerance to calcium.	2.01	3.25E-02
At5g17380		Thiamine pyrophosphate dependent pyruvate decarboxylase family protein	2.01	3.41E-05
At1g17860		Kunitz family trypsin and protease inhibitor protein	2.00	2.97E-04
At2g34355		Major facilitator superfamily protein	2.00	6.59E-04
At3g23605		Ubiquitin-like superfamily protein	1.99	1.60E-03
At1g15430		Protein of unknown function (DUF1644)	1.99	3.66E-04
At3g56710		Sig1 binding protein	1.98	2.04E-02
At5g14470		GHMP kinase family protein	1.98	3.01E-03
At5g51440		HSP20-like chaperones superfamily protein	1.97	3.26E-02
At3g13310		Chaperone DnaJ-domain superfamily protein	1.97	2.06E-03

Locus	Gene	Description	ratio (log ₂)	T-test
At4g12400	HOP3 (Hop3)	Encodes one of the 36 carboxylate clamp (CC)-tetratricopeptide repeat (TPR) proteins (Prasad 2010, Pubmed ID: 20856808) with potential to interact with Hsp90/Hsp70 as co-chaperones.	1.95	4.85E-02
At3g24420		alpha/beta-Hydrolases superfamily protein	1.94	7.43E-05
At2g47890		B-box type zinc finger protein with CCT domain	1.94	4.87E-03
At1g67810	SULFUR E2 (SUFE2)	Encodes a protein capable of stimulating the cysteine desulfurase activity of CpNifS (AT1G08490) in vitro..	1.92	1.93E-03
At1g19020		unknown protein	1.92	5.58E-04
At3g55430		O-Glycosyl hydrolases family 17 protein	1.91	1.05E-02
At4g05020	NAD(P)H dehydrogenase B2 (NDB2)		1.91	2.02E-04
At4g17500	ETHYLENE RESPONSIVE ELEMENT BINDING FACTOR 1 (ERF1)	Encodes a member of the ERF (ethylene response factor) subfamily B-3 of ERF/AP2 transcription factor family (ATERF-1).	1.90	2.64E-03
At5g64750	ABA REPRESSOR1 (ABR1)	Expressed in response to ABA, osmotic stress, sugar stress and drought.	1.90	8.76E-04
At3g14620	CYTOCHROME P450, FAMILY 72, SUBFAMILY A, POLYPEPTIDE 8	putative cytochrome P450	1.90	1.31E-04
At1g17420	LIPOXYGENASE 3 (LOX3)	LOX3 encode a Lipoxygenase. Lipoxygenases (LOXs) catalyze the oxygenation of fatty acids (FAs).	1.90	4.91E-03
At2g29450	GLUTATHIONE S-TRANSFERASE TAU 5 (GSTU5)	Encodes a member of the TAU glutathione S-transferase gene family. Gene expression is induced by exposure to auxin, pathogen and herbicides.	1.90	1.99E-04
At4g24110		unknown protein	1.89	3.66E-03
At5g27760		Hypoxia-responsive family protein	1.88	4.32E-05
At2g34500		Encodes a protein with C22-sterol desaturase activity.	1.87	2.12E-02
At1g05670		Pentatricopeptide repeat (PPR-like) superfamily protein	1.86	7.87E-03
At2g24500	(FZF)	Encodes a C2H2 zinc finger protein FZF.	1.83	1.89E-05
At3g02800	PFA-DSP3	Encodes an atypical dual-specificity phosphatase.	1.82	3.45E-02
At1g78380	GLUTATHIONE S-TRANSFERASE TAU 19 (GSTU19)	Encodes a glutathione transferase that is a member of Tau GST gene family. Expression is induced by drought stress, oxidative stress, and high doses of auxin and cytokinin.	1.82	7.13E-07
At5g52810		NAD(P)-binding Rossmann-fold superfamily protein	1.81	3.25E-04

8. SUPPLEMENTARY MATERIAL

Locus	Gene	Description	ratio (log ₂)	T-test
At1g03850	GLUTAREDOXIN 13 (GRXS13)	Encodes glutaredoxin ATGRXS13, required to facilitate Botrytis cinerea infection	1.81	1.09E-04
At4g15550	INDOLE-3-ACETATE BETA-D-GLUCOSYL- TRANSFERASE (IAGLU)	UDP-glucose:indole-3-acetate beta-D-glucosyltransferase	1.78	2.45E-02
At3g03440		ARM repeat superfamily protein	1.77	1.26E-02
At2g46240	BCL-2-ASSOCIATED ATHANOGENE 6 (BAG6)	A member of Arabidopsis BAG (Bcl-2-associated athanogene) proteins, plant homologs of mammalian regulators of apoptosis.	1.75	3.52E-02
At4g23570	(SGT1A)	Closely related to SGT1B, may function in SCF(TIR1) mediated protein degradation. AtSGT1a and AtSGT1b are functionally redundant in the resistance to pathogens.	1.75	1.56E-04
At2g17500		Auxin efflux carrier family protein	1.74	6.69E-04
At1g35140	PHOSPHATE- INDUCED 1 (PHI-1)	EXL1 is involved in the C-starvation response.	1.74	3.24E-02
At3g50260	COOPERATIVELY REGULATED BY ETHYLENE AND JASMONATE 1 (CEJ1)	Encodes a member of the DREB subfamily A-5 of ERF/AP2 transcription factor family.	1.73	2.40E-03
At1g80840	WRKY DNA- BINDING PROTEIN 40 (WRKY40)	Pathogen-induced transcription factor	1.70	2.28E-02
At2g02710	PAS/LOV PROTEIN B (PLPB)	Encodes a putative blue light receptor protein.	1.70	1.23E-03
At1g27730	SALT TOLERANCE ZINC FINGER (STZ)	involved in response to photooxidative stress.	1.69	4.32E-02
At4g11280	1-AMINO- CYCLOPROPANE- 1-CARBOXYLIC ACID (ACC) SYNTHASE 6 (ACS6)	encodes a a member of the 1-aminocyclopropane-1-carboxylate (ACC) synthase (S-adenosyl-L-methionine methylthioadenosine-lyase, EC 4.4.1.14) gene family	1.68	1.95E-02
At5g65230	MYB DOMAIN PRO- TEIN 53 (MYB53)	Member of the R2R3 factor gene family.	1.68	5.64E-03
At2g29020		Rab5-interacting family protein	1.68	2.30E-04
At5g62020	HEAT SHOCK TRAN- SCRIPTION FACTOR B2A (HSFB2A)	member of Heat Stress Transcription Factor (Hsf) family	1.68	7.07E-03
At5g48180	NITRILE SPECIFIER PROTEIN 5 (NSP5)	Encodes a nitrile-specifier protein NSP5.	1.68	1.96E-03
At5g26340	(MSS1)	Encodes a protein with high affinity, hexose-specific/H ⁺ symporter activity.	1.68	4.14E-04

Locus	Gene	Description	ratio (log ₂)	T-test
At4g32210	SUCCINATE DEHYDROGENASE 3-2 (SDH3-2)	Encodes one of the membrane anchor subunits of the mitochondrial respiratory complex II.	1.67	1.74E-03
At1g30070		SGS domain-containing protein	1.67	1.61E-02
At5g35735		Auxin-responsive family protein	1.66	2.32E-04
At4g39670		Glycolipid transfer protein (GLTP) family protein	1.66	9.06E-02
At2g15380		transposable element gene	1.65	2.12E-04
At3g17611	RHOMBOID-like protein 14 (RBL14)		1.64	5.60E-03
At3g63380		ATPase E1-E2 type family protein / haloacid dehalogenase-like hydrolase family protein	1.63	3.30E-02
At2g34660	ATP-BINDING CASSETTE C2 (ABCC2)	encodes a multidrug resistance-associated protein that is MgATP-energized glutathione S-conjugate pump.	1.63	3.79E-04
At4g02380	SENESCENCE-ASSOCIATED GENE 21 (SAG21)	Encodes AtLEA5 (late embryogenesis abundant like protein). Also known as SENESCENCE-ASSOCIATED GENE 21 (SAG21). Has a role on oxidative stress tolerance	1.61	3.53E-03
At1g68410		Protein phosphatase 2C family protein	1.61	1.08E-02
At5g38530	TRYPTOPHAN SYNTHASE BETA TYPE 2 (TSBtype2)	catalyzes a condensation reaction between serine and indole to generate tryptophan.	1.61	7.10E-03
At4g34138		UDP-glucosyl transferase 73B1 (UGT73B1)	1.60	2.35E-02
At5g64300	GTP CYCLOHYDROLASE II (GCH)	encodes GTP cyclohydrolase II	1.60	9.17E-05
At1g64780	AMMONIUM TRANSPORTER 1	encodes an ammonium transporter protein believed to act as a high affinity transporter.	1.58	9.38E-04
At2g41380		S-adenosyl-L-methionine-dependent methyltransferases superfamily protein	1.58	8.23E-03
At3g51910	HEAT SHOCK TRANSCRIPTION FACTOR A7A (HSFA7A)	member of Heat Stress Transcription Factor (Hsf) family	1.58	1.28E-02
At3g09010		Protein kinase superfamily protein	1.56	4.29E-04
At2g24100		unknown protein	1.55	1.44E-05
At3g12050		Aha1 domain-containing protein	1.54	1.04E-02
At2g43840	UDP-GLYCOSYLTRANSFERASE 74 F1 (UGT74F1)	UGT74F1 transfers UDP:glucose to salicylic acid (forming a glucoside), benzoic acid, quercetin, and athranilate in vitro	1.54	9.47E-02
At2g03760	SULPHO-TRANSFERASE 12 (SOT12)	Encodes a brassinosteroid sulfotransferase.	1.54	1.23E-03
At5g62970		Protein with RNI-like/FBD-like domains	1.53	7.61E-03
At1g02850	beta glucosidase 11 (BGLU11)		1.53	2.07E-03

8. SUPPLEMENTARY MATERIAL

Locus	Gene	Description	ratio (log ₂)	T-test
At5g19440		similar to Eucalyptus gunnii alcohol dehydrogenase	1.51	1.93E-05
At5g02500	HEAT SHOCK COGNATE PROTEIN 70-1 (HSC70-1)	encodes a member of heat shock protein 70 family.	1.51	3.28E-03
At1g30320		Remorin family protein	1.51	1.00E-04
At1g22340	UDP-glucosyl transferase 85A7 (UGT85A7)		1.50	5.03E-05
At4g34710	ARGININE DECARBOXYLASE 2 (ADC2)	rate-limiting enzyme that catalyzes the first step of polyamine (PA) biosynthesis via ADC pathway	1.50	4.87E-04
At3g07720		Galactose oxidase/kelch repeat superfamily protein	1.49	5.84E-05
At3g46670	UDP-glucosyl transferase 76E11 (UGT76E11)		1.49	4.94E-05
At1g66080		unknown protein	1.48	5.40E-02
At4g11600	GLUTATHIONE PEROXIDASE 6 (GPX6)	Encodes glutathione peroxidase.	1.48	1.55E-04
At3g07090		PPPDE putative thiol peptidase family protein	1.47	1.04E-02
At5g54170		Polyketide cyclase/dehydrase and lipid transport superfamily protein	1.47	8.27E-03
At3g04010		O-Glycosyl hydrolases family 17 protein	1.46	7.30E-03
At3g10500	NAC DOMAIN CONTAINING PROTEIN 53 (NAC053)	Encodes a transcriptional activator- thought to promote ROS production by binding directly to the promoters of genes encoding ROS biosynthetic enzymes during drought-induced leaf senescence.	1.46	3.61E-05
At1g26800		RING/U-box superfamily protein	1.45	6.05E-04
At1g54050		HSP20-like chaperones superfamily protein	1.44	5.50E-02
At4g21510		F-box family protein	1.43	1.92E-03
At2g29440	GLUTATHIONE S-TRANSFERASE TAU 6 (GSTU6)	Encodes glutathione transferase belonging to the tau class of GSTs.	1.43	4.99E-03
At3g11250		Ribosomal protein L10 family protein	1.42	2.26E-02
At3g44110	(J3)	homologous to the co-chaperon DNAJ protein from E coli	1.42	7.69E-06
At1g52200		PLAC8 family protein	1.42	2.40E-04
At5g35690		unknown protein	1.42	7.46E-04
At5g14180	Myzus persicae-induced lipase 1 (MPL1)		1.42	2.95E-03
At4g18950		Integrin-linked protein kinase family	1.41	1.69E-04
At5g13490	ADP/ATP CARRIER 2 (AAC2)	Encodes mitochondrial ADP/ATP carrier	1.40	7.91E-04
At4g16680		P-loop containing nucleoside triphosphate hydrolases superfamily protein	1.40	7.54E-02

Locus	Gene	Description	ratio (log ₂)	T-test
At5g07440	GLUTAMATE DE-HYDROGENASE 2 (GDH2)	Encodes the beta-subunit of the glutamate dehydrogenase. The enzyme is almost exclusively found in the mitochondria of stem and leaf companion cells.	1.40	1.87E-03
At2g28510		Dof-type zinc finger DNA-binding family protein	1.40	3.85E-04
At1g66090		Disease resistance protein (TIR-NBS class)	1.38	7.06E-02
At5g22300	NITRILASE 4 (NIT4)	encodes a nitrilase isomer	1.38	1.63E-02
At5g48500		unknown protein	1.38	2.66E-02
At1g70530	CYSTEINE-RICH RLK (RECEPTOR-LIKE PROTEIN KINASE) 3 (CRK3)	Encodes a cysteine-rich receptor-like protein kinase.	1.38	1.01E-03
At5g11520	ASPARTATE AMINO-TRANSFERASE 3 (ASP3)	Encodes the chloroplastic isozyme of aspartate aminotransferase	1.38	4.63E-04
At1g73730	ETHYLENE-INSENSITIVE3-LIKE 3 (EIL3)	Encodes a putative transcription factor involved in ethylene signalling. Isolated DNA binding domain has been shown to bind DNA in vitro.	1.38	6.60E-03
At3g25250	(AGC2-1)	Arabidopsis protein kinase	1.37	4.83E-02
At1g79920		Heat shock protein 70 (Hsp 70) family protein	1.36	9.28E-03
At4g27657		unknown protein	1.35	1.28E-02
At3g13520	ARABINOGLACTAN PROTEIN 12 (AGP12)	Encodes a GPI-anchored arabinogalactan (AG) peptide with a short 'classical' backbone of 10 amino acids, seven of which are conserved among the 4 other Arabidopsis AG peptides.	1.35	8.07E-04
At4g05390	ROOT FNR 1 (RFNR1)	Encodes a root-type ferredoxin:NADP(H) oxidoreductase.	1.34	3.95E-03
At3g14990	DJ-1 HOMOLOG A (DJ1A)	Encodes a homolog of animal DJ-1 superfamily protein. Among the homologs, DJ1C is essential for chloroplast development and viability.	1.34	5.26E-04
At1g04770		Tetratricopeptide repeat (TPR)-like superfamily protein	1.33	2.29E-05
At2g20550		HSP40/DnaJ peptide-binding protein	1.33	7.05E-02
At4g29670	ATYPICAL CYS HIS RICH THIOREDOXIN 2 (ACHT2)	Encodes a member of the thioredoxin family protein.	1.33	1.52E-03
At1g63840		RING/U-box superfamily protein	1.32	5.49E-03
At5g66070		RING/U-box superfamily protein	1.32	1.97E-02
At5g59550	RING AND DOMAIN OF UNKNOWN FUNCTION 1117 2 (RDUF2)	Encodes an ABA- and drought-induced RING-DUF1117 gene	1.31	6.05E-02
At5g02490		Heat shock protein 70 (Hsp 70) family protein	1.30	2.48E-04
At5g20010	RAS-RELATED NUCLEAR PROTEIN-1 (RAN-1)	A member of RAN GTPase gene family. Encodes a small soluble GTP-binding protein.	1.30	4.95E-06

8. SUPPLEMENTARY MATERIAL

Locus	Gene	Description	ratio (log ₂)	T-test
At2g46560		transducin family protein / WD-40 repeat family protein	1.30	5.66E-03
At4g33540		metallo-beta-lactamase family protein	1.30	5.58E-05
At4g20860		FAD-binding Berberine family protein	1.30	1.16E-02
At3g01640	GLUCURONOKINASE G (GLCAK)	AtGlcAK is a sugar kinase able to phosphorylate D-GlcA to D-GlcA-1-phosphate in the presence of ATP.	1.30	4.48E-04
At2g06050	OXO-PHYTODIENOATE-REDUCTASE 3 (OPR3)	Encodes a 12-oxophytodienoate reductase that is required for jasmonate biosynthesis.	1.30	1.22E-02
At2g25030		pseudogene, HSP100/ClpB, putative, similar to HSP100/ClpB GI:9651530 (<i>Phaseolus lunatus</i>)	1.30	4.58E-02
At1g55500	evolutionarily conserved C-terminal region 4 (ECT4)		1.29	1.57E-05
At1g33600		Leucine-rich repeat (LRR) family protein	1.29	9.54E-04
At3g06420		autophagy 8h (ATG8H)	1.29	1.64E-04
At3g06500		Plant neutral invertase family protein	1.28	6.75E-03
At5g03210	DBP-INTERACTING PROTEIN 2 (DIP2)	Encodes a small polypeptide contributing to resistance to potyvirus.	1.28	7.53E-02
At3g13080	ATP-BINDING CASSETTE C3 (ABCC3)	encodes an ATP-dependent MRP-like ABC transporter able to transport glutathione-conjugates as well as chlorophyll catabolites.	1.26	6.84E-03
At1g32170	XYLOGLUCAN ENDOTRANSGLUCOSYLASE/HYDROLASE 30 (XTH30)	xyloglucan endotransglycosylase-related protein (XTR4)	1.26	4.43E-03
At3g05420	ACYL-COA BINDING PROTEIN 4 (ACBP4)	Acyl-CoA binding protein with high affinity for oleoyl-CoA. Expressed in all plant organs. Involved in fatty acid transport.	1.26	5.37E-03
At5g43180		Protein of unknown function, DUF599	1.26	5.74E-03
At1g15670		Galactose oxidase/kelch repeat superfamily protein	1.26	1.42E-02
At1g66760		MATE efflux family protein	1.26	8.57E-03
At4g24420		RNA-binding (RRM/RBD/RNP motifs) family protein	1.26	1.83E-01
At4g01950	GLYCEROL-3-PHOSPHATE ACYLTRANSFERASE 3 (GPAT3)	Encodes a member of a family of proteins with glycerol-3-phosphate acyltransferase activity.	1.25	2.37E-02
At1g54100	ALDEHYDE DEHYDROGENASE 7B4 (ALDH7B4)	Aldehyde dehydrogenase	1.25	4.16E-03

Locus	Gene	Description	ratio (log ₂)	T-test
At3g28340	GALACTURONOSYL- TRANSFERASE-LIKE 10 (GATL10)	Encodes a protein with putative galacturonosyl- transferase activity.	1.25	7.71E-03
At3g62150	P-glycoprotein 21 (PGP21)		1.25	8.64E-04
At3g08970	(ATERDJ3A)	J domain protein localized in ER lumen	1.25	1.72E-03
At5g45110	NPR1-LIKE PROTEIN 3 (NPR3)	Involved in negative regulation of defense responses against bacterial and oomycete pathogens.	1.25	1.34E-02
At2g23810	TETRASPANIN8 (TET8)	Member of TETRASPANIN family	1.24	1.82E-02
At2g40340	(DREB2C)	Encodes a member of the DREB subfamily A-2 of ERF/AP2 transcription factor family. The pro- tein contains one AP2 domain. T	1.24	4.26E-03
At4g31860		Protein phosphatase 2C family protein	1.24	1.05E-05
At1g76650		calmodulin-like 38 (CML38)	1.24	2.84E-02
At1g68440		unknown protein	1.24	5.02E-05
At1g67360		Rubber elongation factor protein (REF)	1.23	1.88E-02
At1g07030		Mitochondrial substrate carrier family protein	1.23	2.16E-02
At5g58760	DAMAGED DNA BINDING 2 (DDB2)	required for UV-B tolerance and genomic in- tegrity.	1.22	2.28E-02
At5g60790	ATP-BINDING CAS- SETTE F1 (ABCF1)	member of GCN subfamily	1.22	2.32E-04
At1g28190		unknown protein	1.22	1.54E-02
At3g57760		Protein kinase superfamily protein	1.22	1.55E-02
At5g48850	SULPHUR DEFICIENCY- INDUCED 1 (ATSDI1)	homologous to the wheat sulphate deficiency- induced gene sdi1.	1.21	2.16E-02
At2g47520	ETHYLENE RE- SPONSE FACTOR 71 (ERF71)	encodes a member of the ERF (ethylene response factor) subfamily B-2 of ERF/AP2 transcription factor family.	1.21	5.64E-02
At2g21620		Encodes gene that is induced in response to dessi- cation	1.21	4.35E-04
At5g22350		ELONGATED MITOCHONDRIA 1 (ELM1)	1.20	1.45E-04
At4g25530	FLOWERING WA- GENINGEN (FWA)	Encodes a homeodomain-containing transcription factor that controls flowering.	1.20	1.23E-01
At1g06870		Peptidase S24/S26A/S26B/S26C family protein	1.20	2.97E-03
At5g57050	ABA INSENSITIVE 2 (ABI2)	Encodes a protein phosphatase 2C and is involved in ABA signal transduction.	1.20	2.79E-02
At3g19240		Vacuolar import/degradation, Vid27-related pro- tein	1.19	1.06E-02
At3g04000		aldehyde reductase that catalyzes the reduction of the aldehyde carbonyl groups on saturated and alpha,beta-unsaturated aldehydes	1.19	1.65E-02

8. SUPPLEMENTARY MATERIAL

Locus	Gene	Description	ratio (log ₂)	T-test
At5g06905	CYTOCHROME P450, FAMILY 712, SUBFAMILY A, POLYPEPTIDE 2	member of CYP712A	1.19	3.59E-02
At4g29780		unknown protein	1.18	2.37E-01
At1g79720		Eukaryotic aspartyl protease family protein	1.18	2.05E-02
At5g54206		12-oxophytodienoate reductase-related, similar to 12-oxophytodienoate reductase OPR1	1.18	4.45E-02
At3g11340	UDP-DEPENDENT GLYCOSYLTRANSFERASE 76B1 (UGT76B1)	Encodes a glucosyltransferase that conjugates isoleucic acid and modulates plant defense and senescence.	1.18	4.31E-03
At5g01100		O-fucosyltransferase family protein	1.17	4.62E-04
At3g46640	PHYTOCLOCK 1 (PCL1)	Encodes a myb family transcription factor with a single Myb DNA-binding domain (type SHAQKYF) that is unique to plants and is essential for circadian rhythms	1.17	2.27E-02
At1g76070		unknown protein	1.17	5.82E-03
At1g54090	EXOCYST SUBUNIT EXO70 FAMILY PROTEIN D2 (EXO70D2)	A member of EXO70 gene family, putative exocyst subunits, conserved in land plants.	1.17	4.85E-03
At2g40000		ortholog of sugar beet HS1 PRO-1 2 (HSPRO2)	1.16	8.31E-03
At3g59350		Protein kinase superfamily protein	1.16	4.42E-03
At3g04120	GLYCERALDEHYDE-3-PHOSPHATE DEHYDROGENASE C SUBUNIT 1 (GAPC1)	encodes cytosolic GADPH (C subunit) involved in the glycolytic pathway but also interacts with H2O2 potentially placing it in a signalling cascade induced by ROS.	1.16	6.12E-04
At5g18400		Cytokine-induced anti-apoptosis inhibitor 1, Fe-S biogenesis	1.16	4.44E-04
At3g16330		unknown protein	1.16	3.11E-03
At3g26390		unknown protein	1.16	6.10E-02
At3g28910	MYB DOMAIN PROTEIN 30 (MYB30)	transcription factor myb homologue	1.16	1.89E-02
At1g36840		transposable element gene	1.16	1.39E-02
At5g46450		Disease resistance protein (TIR-NBS-LRR class) family	1.15	7.80E-02
At3g46620	RING AND DOMAIN OF UNKNOWN FUNCTION 1117 1 (RDUF1)	Encodes an ABA- and drought-induced RING-DUF1117 gene	1.15	3.30E-02
At1g51760	IAA-ALANINE RESISTANT 3 (IAR3)	conjugates IAA-Ala in vitro.	1.15	5.76E-03
At3g60680		Plant protein of unknown function (DUF641)	1.15	1.20E-03
At3g59140	ATP-BINDING CASSETTE C10 (ABCC10)	member of MRP subfamily	1.15	9.37E-04

Locus	Gene	Description	ratio (log ₂)	T-test
At5g14570	HIGH AFFINITY NITRATE TRANS- PORTER 2.7 (NRT2.7)	Encodes ATNRT2.7, a nitrate transporter that controls nitrate content in seeds.	1.14	6.16E-04
At1g55530		RING/U-box superfamily protein	1.14	9.45E-05
At2g18193		P-loop containing nucleoside triphosphate hydro- lases superfamily protein	1.14	3.66E-04
At5g43450		encodes a protein whose sequence is similar to ACC oxidase	1.13	1.74E-02
At1g21680		DPP6 N-terminal domain-like protein	1.13	3.07E-02
At2g15430		Non-catalytic subunit of nuclear DNA-dependent RNA polymerases II, IV and V	1.13	5.69E-03
At4g09030	ARABINOGALACTAN PROTEIN 10 (AGP10)	Encodes arabinogalactan protein (AGP10).	1.12	4.09E-02
At4g15420		Ubiquitin fusion degradation UFD1 family pro- tein	1.12	3.01E-03
At1g23440		Peptidase C15, pyroglutamyl peptidase I-like	1.12	9.83E-03
At5g43540		C2H2 and C2HC zinc fingers superfamily protein	1.12	3.16E-01
At1g27760	SALT-TOLERANCE 32 (SAT32)	Encodes a protein with similarity to hu- man interferon-related developmental regulator (IFRD)that is involved in salt tolerance	1.12	3.78E-03
At3g09000		proline-rich family protein	1.12	2.01E-04
At5g04410	NAC DOMAIN CON- TAINING PROTEIN 2 (NAC2)	NAC family member, functions as a transcrip- tional activator, regulates flavonoid biosynthesis under high light.	1.12	1.25E-03
At3g23990	HEAT SHOCK PRO- TEIN 60 (HSP60)	mitochondrial chaperonin HSP. assist in rapid as- sembly of the oligomeric protein structures in the mitochondria.	1.11	1.77E-03
At2g19450	TRIACYLGLYCEROL BIOSYNTHESIS DE- FECT 1 (TAG1)	catalyzes the final step of the triacylglycerol syn- thesis pathway.	1.11	1.36E-02
At4g35940		unknown protein	1.11	2.17E-02
At5g51980		Transducin/WD40 repeat-like superfamily pro- tein	1.11	1.99E-02
At3g50970	LOW TEMPERATURE- INDUCED 30 (LTI30)	Belongs to the dehydrin protein family. LTI29 and LTI30 double overexpressors confer freeze tol- erance.	1.10	2.29E-03
At5g53400	BOBBER1 (BOB1)	non-canonical small heat shock protein required for both development and thermotolerance.	1.10	1.36E-02
At3g08690		ubiquitin-conjugating enzyme 11 (UBC11)	1.10	2.46E-02
At2g31945		unknown protein	1.10	2.74E-02
At2g23420		nicotinate phosphoribosyltransferase 2 (NAPRT2)	1.09	2.56E-04
At1g75860		unknown protein	1.09	1.03E-02
At5g44050		MATE efflux family protein	1.09	2.17E-01
At2g29060		GRAS family transcription factor	1.09	2.26E-04

8. SUPPLEMENTARY MATERIAL

Locus	Gene	Description	ratio (log ₂)	T-test
At5g49920		Octicosapeptide/Phox/Bem1p family protein	1.09	3.10E-02
At5g15850	CONSTANS-LIKE 1 (COL1)	Homologous to the flowering-time gene CONSTANS.	1.08	1.73E-02
At4g22980		unknown protein	1.08	6.54E-03
At3g21780	UDP-GLUCOSYL TRANSFERASE 71B6 (UGT71B6)	was shown to preferentially glucosylates abscisic acid (ABA), and not its catabolite	1.08	2.09E-03
At1g04990		Zinc finger C-x8-C-x5-C-x3-H type family protein	1.08	7.77E-03
At5g54860		Major facilitator superfamily protein	1.08	4.00E-04
At2g38470	WRKY DNA- BINDING PROTEIN 33 (WRKY33)	Member of the plant WRKY transcription factor family	1.08	2.21E-01
At1g35660		unknown protein	1.08	1.73E-03
At4g28480		DNAJ heat shock family protein	1.07	1.08E-03
At1g76340	GOLGI NUCLEOTIDE SUGAR TRANS- PORTER 3 (GONST3)	Encodes a nucleotide-sugar transporter.	1.06	4.03E-03
At2g02220	PHYTOSULFOKIN RECEPTOR 1 (PSKR1)	Encodes a protein interacting with phytosulfokine, a five amino acid sulfated peptide (YIYTQ).	1.06	6.50E-03
At5g33290	XYLO- GALACTURONAN DEFICIENT 1 (XGD1)	Acts as a xylogalacturonan xylosyltransferase within the XGA biosynthesis pathway. Involved in pectin biosynthesis.	1.06	1.05E-04
At3g22370	ALTERNATIVE OXI- DASE 1A (AOX1A)	alternative oxidase of plant mitochondria transfers electrons from the ubiquinone pool to oxygen without energy conservations.	1.06	1.13E-02
At1g15520	ATP-BINDING CAS- SETTE G40 (ABCG40)	ABC transporter family involved in ABA transport and resistance to lead.	1.06	1.11E-01
At1g76980		BEST Arabidopsis thaliana protein match is: embryo defective 2170 (TAIR:AT1G21390.1)	1.06	2.66E-02
At1g01120	3-KETOACYL-COA SYNTHASE 1 (KCS1)	involved in the critical fatty acid elongation process in wax biosynthesis.	1.05	3.83E-03
At1g61690		phosphoinositide binding	1.05	4.77E-02
At3g13470	CHAPERONIN- 60BETA2 (CPN60BETA2)	Encodes a subunit of chloroplasts chaperonins	1.05	7.23E-02
At5g07180	ERECTA-LIKE 2 (ERL2)	Encodes a receptor-like kinase important for maintaining stomatal stem cell activity	1.05	2.66E-02
At4g27350		Protein of unknown function (DUF1223)	1.04	8.47E-03
At2g30140	UDP-GLUCOSYL TRANSFERASE 87A2 (UGT87A2)	Encodes a putative glycosyltransferase. Regulates flowering time via FLOWERING LOCUS C.	1.04	2.64E-03
At2g41160		Ubiquitin-associated (UBA) protein	1.04	3.67E-03
At3g22980		Ribosomal protein S5/Elongation factor G/III/V family protein	1.04	2.43E-04

Locus	Gene	Description	ratio (log ₂)	T-test
At2g38290	AMMONIUM TRANS- PORTER 2 (AMT2)	encodes a high-affinity ammonium transporter, which is expressed in shoot and root. Expression in root and shoot is under nitrogen and carbon dioxide regulation, respectively.	1.04	1.05E-03
At3g53830		Regulator of chromosome condensation (RCC1) family protein	1.04	2.93E-03
At2g37150		RING/U-box superfamily protein	1.03	1.30E-04
At5g07280	EXCESS MI- CROSPOROCYTES1 (EMS1)	putative leucine-rich repeat receptor protein kinase that controls somatic and reproductive cell fates in Arabidopsis anther.	1.03	1.44E-02
At4g17840		unknown protein	1.03	8.63E-03
At1g02820		Late embryogenesis abundant 3 (LEA3) family protein	1.03	1.23E-02
At4g25230	RPM1 INTERACTING PROTEIN 2 (RIN2)	RPM1 interacting protein 2, has a CUE domain which is sufficient for the interaction with RPM1.	1.03	1.11E-04
At5g57910		unknown protein	1.03	1.61E-04
At2g39660	BOTRYTIS-INDUCED KINASE1 (BIK1)	Encodes a plasma membrane-localized ser/thr protein kinase that is a crucial component of host response signaling required to activate the resistance responses to Botrytis and A. Brassicicola infection. I	1.03	8.81E-04
At2g36220		unknown protein	1.03	2.74E-02
At1g03457		RNA-binding (RRM/RBD/RNP motifs) family protein	1.03	1.15E-03
At1g17745	3-PHOSPHO- GLYCERATE DE- HYDROGENASE (PGDH)	encodes a 3-Phosphoglycerate dehydrogenase	1.03	3.51E-02
At3g16480		mitochondrial processing peptidase alpha subunit (MPPalpha)	1.02	4.70E-02
At1g71000		Chaperone DnaJ-domain superfamily protein	1.02	9.44E-02
At5g58770		Undecaprenyl pyrophosphate synthetase family protein	1.02	5.32E-03
At2g40140		CZF1	1.02	4.43E-01
At1g26270		Phosphatidylinositol 3- and 4-kinase family protein	1.01	1.02E-04
At3g01290		SPFH/Band 7/PHB domain-containing membrane-associated protein family	1.01	3.02E-03
At4g22820		A20/AN1-like zinc finger family protein	1.01	1.65E-03
At3g21250	ATP-BINDING CAS- SETTE C8 (ABCC8)	member of MRP subfamily	1.01	9.85E-01
At5g63370		Protein kinase superfamily protein	1.01	3.44E-03
At1g65390		phloem protein 2 A5 (PP2-A5)	1.01	3.78E-02
At3g56880		VQ motif-containing protein	1.01	1.94E-02

8. SUPPLEMENTARY MATERIAL

Locus	Gene	Description	ratio (log ₂)	T-test
At5g59480		Haloacid dehalogenase-like hydrolase (HAD) superfamily protein	1.01	3.30E-02
At1g05520		Sec23/Sec24 protein transport family protein	1.01	1.06E-01
At5g57710		Double Clp-N motif-containing P-loop nucleoside triphosphate hydrolases superfamily protein	1.01	7.95E-04
At5g03630		ATMDAR2	1.00	4.15E-03
At1g07890	ASCORBATE PEROXIDASE 1 (APX1)	Ascorbate peroxidases are enzymes that scavenge hydrogen peroxide in plant cells.	1.00	1.93E-02
At4g17650		Polyketide cyclase / dehydrase and lipid transport protein	1.00	1.10E-02
At3g28040		Leucine-rich receptor-like protein kinase family protein	-1.00	6.40E-04
At5g20150	SPX DOMAIN GENE 1 (SPX1)	Expression is upregulated in the shoot of cax1/cax3 mutant.	-1.00	4.16E-03
At1g49010		Duplicated homeodomain-like superfamily protein	-1.00	2.10E-02
At4g15440	HYDROPEROXIDE LYASE 1 (HPL1)	Encodes a hydroperoxide lyase. Also a member of the CYP74B cytochrome p450 family.	-1.01	4.63E-02
At2g40670	RESPONSE REGULATOR 16 (RR16)	response regulator 16	-1.01	1.20E-01
At5g41400		RING/U-box superfamily protein	-1.01	9.87E-03
At5g52100	CHLORO-RESPIRATION REDUCTION 1 (crr1)	Is essential for chloroplast NAD(P)H dehydrogenase activity, which is involved in electron transfer between PSII and PSI.	-1.01	3.99E-02
At1g25440		B-box type zinc finger protein with CCT domain	-1.02	1.87E-01
At3g50340		unknown protein	-1.02	1.36E-02
At3g63440	CYTOKININ OXIDASE /DEHYDROGENASE 6 (CKX6)	This gene used to be called AtCKX7. It encodes a protein whose sequence is similar to cytokinin oxidase/dehydrogenase, which catalyzes the degradation of cytokinins.	-1.02	8.19E-03
At5g07690	MYB DOMAIN PROTEIN 29 (MYB29)	Encodes a putative transcription factor (MYB29).	-1.02	3.65E-03
At1g72430		SAUR-like auxin-responsive protein family	-1.02	2.09E-01
At5g39530		Protein of unknown function (DUF1997)	-1.02	3.92E-03
At4g35750		SEC14 cytosolic factor family protein / phosphoglyceride transfer family protein	-1.03	1.07E-01
At1g01430	TRICHOME BIREFRINGENCE-LIKE 25 (TBL25)	containing a plant-specific DUF231 (domain of unknown function) domain.	-1.03	1.44E-02
At1g69040	ACT DOMAIN REPEAT 4 (ACR4)	ACT-domain containing protein involved in feedback regulation of amino acid metabolism	-1.03	2.84E-03
At2g42870	PHY RAPIDLY REGULATED 1 (PAR1)	Encodes PHYTOCHROME RAPIDLY REGULATED1 (PAR1), an atypical basic helix-loop-helix (bHLP) protein.	-1.04	2.36E-01

Locus	Gene	Description	ratio (log ₂)	T-test
At5g66590		CAP (Cysteine-rich secretory proteins, Antigen 5, and Pathogenesis-related 1 protein) superfamily protein	-1.04	1.62E-03
At1g23080	PIN-FORMED 7 (PIN7)	component of auxin efflux	-1.04	3.49E-03
At4g22190		unknown protein	-1.04	7.53E-02
At4g23810		member of WRKY Transcription Factor	-1.05	1.59E-03
At5g56870		beta-galactosidase 4 (BGAL4)	-1.05	3.02E-02
At3g23880		F-box and associated interaction domains-containing protein	-1.06	1.15E-04
At2g46710		Rho GTPase activating protein with PAK-box/P21-Rho-binding domain	-1.06	8.69E-04
At1g13700		6-phosphogluconolactonase 1 (PGL1)	-1.06	2.27E-02
At1g68400		leucine-rich repeat transmembrane protein kinase family protein	-1.06	1.63E-02
At4g28220		NAD(P)H dehydrogenase B1 (NDB1)	-1.06	1.50E-02
At2g15890		maternal effect embryo arrest 14 (MEE14)	-1.06	7.88E-02
At1g23400	(CAF2)	Promotes the splicing of chloroplast group II introns.	-1.06	2.88E-04
At4g23820		Pectin lyase-like superfamily protein	-1.07	6.06E-03
At3g56360		unknown protein	-1.08	1.10E-02
At1g69530	EXPANSIN A1 (EXPA1)	Member of Alpha-Expansin Gene Family. Involved in the formation of nematode-induced syncytia in roots of <i>Arabidopsis thaliana</i> .	-1.08	8.86E-03
At5g21100		Plant L-ascorbate oxidase	-1.09	1.16E-03
At1g01240		unknown protein	-1.09	7.81E-03
At5g04190	PHYTOCHROME KINASE SUBSTRATE 4 (PKS4)	Encodes phytochrome kinase substrate 4, a phytochrome signaling component involved in phototropism.	-1.09	7.34E-02
At5g63180		Pectin lyase-like superfamily protein	-1.09	1.04E-03
At2g28630	3-KETOACYL-COA SYNTHASE 12 (KCS12)	Encodes KCS12, a member of the 3-ketoacyl-CoA synthase family involved in the biosynthesis of VLCFA (very long chain fatty acids).	-1.09	5.75E-03
At1g60010		unknown protein	-1.09	3.35E-02
At2g15050	LIPID TRANSFER PROTEIN (LTP)	Predicted to encode a PR (pathogenesis-related) protein. Belongs to the lipid transfer protein (PR-14) family	-1.10	6.63E-03
At2g28720		Histone superfamily protein	-1.10	3.45E-03
At2g28950	EXPANSIN A6 (EXPA6)	Encodes an expansin. Involved in the formation of nematode-induced syncytia in roots of <i>Arabidopsis thaliana</i> .	-1.10	3.21E-03
At1g48300		unknown protein	-1.11	1.05E-03
At2g25900	(ATCTH)	putative Cys3His zinc finger protein (ATCTH) mRNA, complete	-1.11	2.87E-02
At4g33666		unknown protein	-1.11	1.92E-01

8. SUPPLEMENTARY MATERIAL

Locus	Gene	Description	ratio (log ₂)	T-test
At1g70940	PIN-FORMED 3 (PIN3)	A regulator of auxin efflux and involved in differential growth.	-1.11	3.20E-03
At1g19330		unknown protein	-1.11	1.10E-04
At1g71970		unknown protein	-1.12	1.26E-02
At4g34980	SUBTILISIN-LIKE SERINE PROTEASE 2 (SLP2)	Serine protease similar to subtilisin.	-1.12	5.52E-05
At3g10525	LOSS OF GIANT CELLS FROM OR- GANS (LGO)	required for endoreduplication in sepal giant cell formation. LGO is a member of a plant specific cell cycle inhibitor family SIAMESE and was originally named as SMR1(SIAMESE RELATED 1).	-1.12	4.04E-03
At3g52840		beta-galactosidase 2 (BGAL2)	-1.13	1.55E-02
At4g34220		Leucine-rich repeat protein kinase family protein	-1.13	4.50E-03
At4g11000		Ankyrin repeat family protein	-1.13	6.59E-04
At1g75470	PURINE PERMEASE 15 (PUP15)	Member of a family of proteins related to PUP1, a purine transporter.	-1.15	1.29E-03
At3g11090		LOB domain-containing protein 21 (LBD21)	-1.15	9.46E-06
At1g68560	ALPHA-XYLOSIDASE 1 (XYL1)	Encodes a bifunctional alpha-l-arabinofuranosidase/beta-d-xylosidase that belongs to family 3 of glycoside hydrolases.	-1.15	1.26E-04
At5g57760		unknown protein	-1.16	1.44E-02
At1g78100		F-box family protein	-1.16	5.10E-03
At4g37300		maternal effect embryo arrest 59 (MEE59)	-1.17	1.48E-03
At1g19000		Homeodomain-like superfamily protein	-1.17	4.29E-02
At2g45340		Leucine-rich repeat protein kinase family protein	-1.17	1.20E-03
At3g61820		Eukaryotic aspartyl protease family protein	-1.17	9.20E-03
At2g32100		ovate family protein 16 (OFP16)	-1.17	1.29E-02
At4g10120	(ATSPS4F)	Encodes a protein with putative sucrose-phosphate synthase activity.	-1.18	1.65E-02
At1g76110		HMG (high mobility group) box protein with ARID/BRIGHT DNA-binding domain	-1.18	2.96E-03
At5g10150		unknown protein	-1.19	1.49E-03
At2g18300		basic helix-loop-helix (bHLH) DNA-binding superfamily protein	-1.19	2.77E-02
At2g42380	(BZIP34)	Encodes a member of the BZIP family of transcription factors.	-1.19	3.98E-02
At1g19050	RESPONSE REGULA- TOR 7 (ARR7)	Encodes a member of the Arabidopsis response regulator (ARR) family	-1.20	2.09E-02
At2g04790		unknown protein	-1.20	9.40E-03
At1g14700		purple acid phosphatase 3 (PAP3)	-1.21	3.83E-03
At1g49500		unknown protein	-1.21	1.81E-01
At2g39250	SCHNARCHZAPFEN (SNZ)	Encodes a AP2 domain transcription factor that can repress flowering	-1.22	1.59E-03

Locus	Gene	Description	ratio (log ₂)	T-test
At5g39210	CHLORO- RESPIRATORY RE- DUCTION 7 (CRR7)	Encodes a protein of the chloroplastic NAD(P)H dehydrogenase complex (NDH Complex) involved in respiration, photosystem I (PSI) cyclic electron transport and CO ₂ uptake.	-1.22	5.46E-03
At3g13750	BETA GALACTOSI- DASE 1 (BGAL1)	beta-galactosidase, glycosyl hydrolase family 35	-1.24	5.10E-01
At5g57780	P1R1 (P1R1)	Encodes a atypical member of the bHLH (basic helix-loop-helix) family transcriptional factors.	-1.24	4.23E-04
At5g01520		RING/U-box superfamily protein	-1.25	5.92E-03
At5g47370	(HAT2)	homeobox-leucine zipper genes induced by auxin, but not by other phytohormones.	-1.25	4.68E-03
At5g50160	FERRIC REDUCTION OXIDASE 8 (FRO8)	Encodes a ferric chelate reductase that is expressed in shoots and flowers.	-1.26	4.93E-03
At5g11420		unknown protein	-1.26	6.98E-04
At4g24810		similar to ABC1 family protein, contains InterPro domain ABC1 protein (InterPro:IPR004147)	-1.26	8.62E-04
At3g63200		PATATIN-like protein 9 (PLP9)	-1.27	1.85E-03
At4g28270	RING MEMBRANE- ANCHOR 2 (RMA2)	Encodes a RING finger E3 ubiquitin ligase. Binds and ubiquitinates ABP1 in vivo and in vitro.	-1.27	1.32E-02
At1g68190		B-box zinc finger family protein	-1.28	3.32E-03
At4g38840		SAUR-like auxin-responsive protein family	-1.29	3.09E-02
At1g06760		winged-helix DNA-binding transcription factor family protein	-1.30	9.56E-03
At1g68520		B-box type zinc finger protein with CCT domain	-1.30	5.45E-04
At5g16030		unknown protein	-1.32	3.78E-03
At1g09760		U2 small nuclear ribonucleoprotein A (U2A')	-1.33	1.94E-03
At5g52780		Protein of unknown function (DUF3464)	-1.33	1.12E-03
At2g01420	PIN-FORMED 4 (PIN4)	Encodes a putative auxin efflux carrier that is localized in developing and mature root meristems.	-1.37	9.50E-06
At3g18050		unknown protein	-1.38	8.15E-04
At2g41560	AUTOINHIBITED CA(2+)-ATPASE, ISOFORM 4	Encodes a calmodulin-regulated Ca(2+)-ATPase that improves salt tolerance in yeast.	-1.38	1.23E-04
At5g43700	AUXIN INDUCIBLE 2- 11 (ATAUX2-11)	Auxin inducible protein similar to transcription factors.	-1.40	1.92E-04
At4g34760		SAUR-like auxin-responsive protein family	-1.40	9.68E-02
At4g38860		SAUR-like auxin-responsive protein family	-1.40	3.47E-02
At3g20820		Leucine-rich repeat (LRR) family protein	-1.41	6.66E-04
At3g62550		Adenine nucleotide alpha hydrolases-like superfamily protein	-1.42	1.79E-02
At5g49730	FERRIC REDUCTION OXIDASE 6 (FRO6)	Encodes a plasma membrane-located ferric chelate reductase.	-1.42	1.04E-02
At1g19510		RAD-like 5 (RL5)	-1.44	1.14E-02
At3g58120	(BZIP61)	Encodes a member of the BZIP family of transcription factors.	-1.45	9.55E-03

8. SUPPLEMENTARY MATERIAL

Locus	Gene	Description	ratio (log ₂)	T-test
At3g12610	DNA-DAMAGE RE-PAIR/TOLERATION 100 (DRT100)	Plays role in DNA-damage repair/toleration. Partially complements RecA- phenotypes.	-1.46	1.64E-03
At4g24780		Pectin lyase-like superfamily protein	-1.47	2.37E-04
At3g60290		2-oxoglutarate (2OG) and Fe(II)-dependent oxygenase superfamily protein	-1.49	1.46E-04
At1g54820		Protein kinase superfamily protein	-1.53	2.19E-04
At5g65310	HOMEBOX PROTEIN 5 (HB5)	positive regulator of ABA-responsiveness	-1.54	3.39E-04
At1g56150		SAUR-like auxin-responsive protein family	-1.55	7.64E-04
At4g03060	ALKENYL HYDROX-ALKYL PRODUCING 2 (AOP2)	Encodes a truncated and null function protein, due to a 5-bp deletion in cDNA. The functional allele in ecotype Cvi, AOP2, encodes a 2-oxoglutarate-dependent dioxygenase which is involved in glucosinolate biosynthesis.	-1.60	7.93E-03
At5g44680		DNA glycosylase superfamily protein	-1.62	7.45E-03
At3g15570		Phototropic-responsive NPH3 family protein	-1.64	1.92E-03
At4g26530		Aldolase superfamily protein	-1.70	7.70E-04
At4g19170	NINE-CIS-EPOXYCAROTENOID DIOXYGENASE 4 (NCED4)	chloroplast-targeted member of a family of enzymes similar to nine-cis-epoxycarotenoid dioxygenase	-1.71	1.51E-04
At2g40610	EXPANSIN A8 (EXPA8)	member of Alpha-Expansin Gene Family. Involved in the formation of nematode-induced syncytia in roots of <i>Arabidopsis thaliana</i> .	-1.75	1.15E-03
At4g36540		BR enhanced expression 2 (BEE2)	-1.77	3.39E-04
At5g62280		Protein of unknown function (DUF1442)	-1.78	3.37E-03
At5g02760		Protein phosphatase 2C family protein	-1.93	4.41E-03
At5g52900	MEMBRANE-ASSOCIATED KINASE REGULATOR 6 (MAKR6)	Encodes a member of the MAKR (MEMBRANE-ASSOCIATED KINASE REGULATOR) gene family.	-2.13	4.83E-03

8.0.9.1 List of upregulated genes from MDA microarray, organized in GO-terms by GOrilla

response to stress

AT1G70530 AT4G31860 AT5G12030 AT4G17500 AT4G24380 AT3G28210 AT5G48180
AT5G11520 AT5G57910 AT1G28480 AT3G02800 AT5G52640 AT1G76650 AT1G27730
AT5G54860 AT3G63380 AT1G51760 AT2G02220 AT5G48850 AT3G50970 AT1G73730
AT1G72680 AT5G46450 AT1G03850 AT1G80840 AT3G07720 AT1G66760 AT3G56710
AT3G28910 AT1G02820 AT1G71000 AT5G20010 AT1G52200 AT4G23570 AT4G30490
AT1G15430 AT2G20560 AT1G76600 AT3G51910 AT1G32920 AT2G19450 AT4G01070
AT4G18950 AT3G25230 AT3G16330 AT1G75280 AT2G47730 AT5G62020 AT3G28730
AT5G03210 AT3G10500 AT1G59860 AT2G06050 AT3G11340 AT3G09000 AT1G17420
AT2G40000 AT1G54050 AT2G47520 AT1G35140 AT3G16050 AT5G49480 AT3G28340
AT4G29780 AT5G15850 AT2G21620 AT4G20860 AT3G23990 AT1G76070 AT1G74310
AT4G22980 AT2G29450 AT2G36220 AT5G52810 AT2G23810 AT3G25250 AT3G24500
AT1G15520 AT3G09440 AT5G27760 AT1G17860 AT5G64750 AT1G01120 AT3G09350
AT2G47890 AT2G34500 AT3G16480 AT4G35180 AT1G79410 AT3G46620 AT3G08970
AT4G02380 AT1G71100 AT1G54100 AT5G51440 AT5G02490 AT5G54170 AT5G35735
AT1G14200 AT3G22370 AT5G56030 AT5G25930 AT5G07440 AT3G21780 AT5G35320
AT5G57050 AT5G58760 AT5G14180 AT1G27760 AT2G30140 AT5G05410 AT1G19020
AT4G24160 AT5G59820 AT3G01290 AT3G44110 AT5G66070 AT5G45110 AT3G08690
AT4G11280 AT1G07400 AT1G17745 AT1G66080 AT1G55920 AT5G63790 AT2G29500
AT4G12400 AT2G26150 AT5G59550 AT3G04010 AT4G11600 AT3G12050 AT3G44190
AT2G46240 AT2G38470 AT3G50260 AT1G30070 AT4G39670 AT5G02500 AT2G39660
AT5G56010 AT2G40140 AT1G65390 AT2G03760 AT4G18010 AT1G66090 AT4G34710
AT2G38290 AT1G63840 AT1G07890 AT3G11250 AT4G22530 AT5G53400 AT5G03630
AT5G22300 AT1G33600 AT2G40340 AT3G04120 AT1G78380 AT5G48570 AT3G12580

response to abiotic stimulus

AT4G31860 AT5G12030 AT4G17500 AT3G28210 AT5G57710 AT5G57910 AT1G28480
AT3G02800 AT5G52640 AT1G27730 AT3G50970 AT1G73730 AT1G80840 AT3G56710
AT1G71000 AT5G20010 AT4G30490 AT4G25530 AT1G15430 AT2G20560 AT3G51910
AT2G19450 AT4G01070 AT3G25230 AT4G18950 AT2G47730 AT3G05420 AT1G59860
AT3G10500 AT2G06050 AT3G09000 AT4G24110 AT2G40000 AT1G17420 AT1G54050
AT3G16050 AT1G35140 AT2G47520 AT5G49480 AT4G29780 AT2G21620 AT3G23990
AT1G74310 AT2G36220 AT2G23810 AT1G15520 AT3G24500 AT3G09440 AT5G27760
AT1G17860 AT5G64750 AT1G01120 AT3G09350 AT2G34500 AT5G13750 AT1G79410
AT5G04410 AT3G46620 AT3G08970 AT4G02380 AT1G71100 AT1G54100 AT5G51440
AT5G02490 AT1G14200 AT3G22370 AT5G07440 AT5G56030 AT3G21780 AT5G35320

8. SUPPLEMENTARY MATERIAL

AT5G57050 AT5G58760 AT1G27760 AT5G05410 AT5G59820 AT3G44110 AT5G48500
AT3G08690 AT4G11280 AT1G07400 AT1G66080 AT1G55920 AT5G63790 AT2G29500
AT4G12400 AT5G59550 AT2G26150 AT3G04010 AT4G11600 AT3G12050 AT2G46240
AT3G50260 AT2G38470 AT1G30070 AT4G39670 AT5G02500 AT5G56010 AT1G66580
AT2G40140 AT2G03760 AT4G18010 AT1G07350 AT4G34710 AT2G38290 AT1G63840
AT1G07890 AT3G11250 AT5G53400 AT5G03630 AT4G02940 AT2G40340 AT2G36750
AT3G04120 AT1G78380 AT5G48570 AT3G12580

response to biotic stimulus

AT1G15520 AT3G09440 AT1G70530 AT4G31860 AT4G24380 AT1G33110 AT5G64750
AT1G28480 AT5G52640 AT1G76650 AT5G07180 AT5G07280 AT1G27730 AT5G54860
AT3G63380 AT3G50970 AT2G15490 AT1G73730 AT4G02380 AT1G72680 AT1G71100
AT5G02490 AT1G03850 AT1G80840 AT5G54170 AT5G35735 AT5G56030 AT3G07720
AT1G66760 AT3G56710 AT3G28910 AT5G14180 AT5G61820 AT2G30140 AT1G19020
AT1G15430 AT3G09010 AT5G59820 AT3G01290 AT5G45110 AT1G32920 AT1G17745
AT2G47730 AT4G15760 AT3G28730 AT5G03210 AT2G46240 AT2G38470 AT3G50260
AT2G06050 AT4G39670 AT3G11340 AT5G02500 AT2G39660 AT1G17420 AT2G40000
AT2G40140 AT2G03760 AT1G66090 AT4G34710 AT2G38290 AT2G21620 AT1G64780
AT1G76070 AT5G64250 AT4G34131 AT4G22980 AT1G33600 AT5G52810 AT2G23810
AT3G12580

metabolic process

AT2G41380 AT1G70530 AT4G17500 AT5G12030 AT1G33110 AT5G11520 AT5G57910
AT5G14730 AT5G52640 AT5G07180 AT5G07280 AT1G27730 AT1G51760 AT2G02220
AT1G22340 AT1G55850 AT1G36370 AT1G72680 AT5G46450 AT1G80840 AT3G07720
AT5G33290 AT3G06420 AT3G14620 AT1G71000 AT4G28480 AT5G06905 AT4G23570
AT1G15430 AT2G20560 AT1G76600 AT3G51910 AT1G06870 AT3G14200 AT3G17611
AT2G47730 AT5G62020 AT2G06050 AT2G20550 AT3G16050 AT4G05390 AT5G15850
AT2G21620 AT3G13520 AT3G23990 AT4G20860 AT1G68440 AT5G38530 AT4G22980
AT5G52810 AT3G24500 AT1G15520 AT3G22980 AT4G21990 AT1G17860 AT1G01120
AT1G68410 AT2G34500 AT5G64300 AT2G43840 AT3G46620 AT3G08970 AT1G02850
AT2G36950 AT4G05020 AT5G02490 AT4G33540 AT5G54170 AT4G01870 AT3G22370
AT5G07440 AT5G25930 AT5G56030 AT5G35320 AT5G57050 AT2G24500 AT1G75270
AT2G30140 AT5G59820 AT3G24420 AT5G66070 AT3G44110 AT5G45110 AT4G11280
AT5G01100 AT1G66080 AT1G17745 AT4G01950 AT2G29500 AT3G46220 AT4G12400
AT5G59550 AT2G26150 AT4G15760 AT2G46240 AT2G38470 AT3G50260 AT1G30070
AT5G24030 AT5G56010 AT1G66580 AT2G40140 AT1G21680 AT4G25230 AT1G07350
AT1G66090 AT4G34710 AT3G59140 AT1G64780 AT1G07890 AT5G53400 AT1G79720
AT5G03630 AT5G22300 AT4G02940 AT2G36750 AT1G78380 AT3G12580 AT4G31860

AT4G24380 AT3G28210 AT5G48180 AT1G28480 AT3G02800 AT2G18193 AT1G76650
AT1G05670 AT5G54860 AT2G29420 AT3G63380 AT3G62150 AT2G15490 AT2G17500
AT1G03850 AT1G66760 AT3G56710 AT3G28910 AT5G63370 AT5G20010 AT1G52200
AT4G30490 AT4G25530 AT5G51830 AT3G09010 AT2G31945 AT3G46670 AT5G19440
AT1G32920 AT2G19450 AT2G43820 AT4G01070 AT2G23420 AT3G25230 AT4G18950
AT3G28730 AT1G59860 AT3G10500 AT3G13470 AT3G11340 AT2G29440 AT1G17420
AT1G54050 AT1G61690 AT3G28340 AT5G39050 AT1G74310 AT4G34131 AT4G15420
AT5G60790 AT2G29450 AT2G36220 AT3G14990 AT2G23810 AT4G34138 AT3G25250
AT3G06500 AT5G43450 AT3G09440 AT5G14470 AT4G16680 AT3G55430 AT4G15550
AT2G47890 AT3G09350 AT3G57760 AT4G29670 AT3G16480 AT1G79410 AT3G01640
AT3G21250 AT4G02380 AT1G62180 AT1G71100 AT1G54100 AT1G26270 AT5G51440
AT1G14200 AT4G32210 AT3G21780 AT4G04610 AT5G58760 AT3G04000 AT5G14180
AT1G32170 AT5G61820 AT5G05410 AT2G02710 AT4G24160 AT3G08690 AT1G55920
AT5G59480 AT5G17380 AT3G04010 AT5G58770 AT4G11600 AT3G12050 AT3G44190
AT4G39670 AT3G13080 AT5G02500 AT2G39660 AT1G23440 AT2G03760 AT4G18010
AT2G34660 AT2G38290 AT2G15430 AT5G13490 AT3G11250 AT4G22530 AT3G13310
AT3G59350 AT5G64250 AT4G13180 AT3G04120 AT5G48570

response to endogenous stimulus

AT3G24500 AT1G15520 AT4G17500 AT4G24380 AT3G28210 AT5G27760 AT5G11520
AT5G64750 AT1G28480 AT3G02800 AT1G76650 AT3G46620 AT5G07180 AT1G27730
AT3G50970 AT2G15490 AT1G73730 AT4G02380 AT1G71100 AT1G54100 AT1G03850
AT1G80840 AT5G54170 AT4G01870 AT5G25930 AT1G66760 AT3G21780 AT5G57050
AT3G28910 AT4G23570 AT5G61820 AT1G15430 AT5G59820 AT1G76600 AT5G45110
AT4G11280 AT1G32920 AT2G19450 AT4G18950 AT1G28190 AT5G59550 AT3G05420
AT2G38470 AT3G50260 AT2G06050 AT4G39670 AT1G17420 AT2G03760 AT4G18010
AT3G28340 AT1G66090 AT4G29780 AT4G34710 AT2G38290 AT1G63840 AT5G03630
AT4G22980 AT1G33600 AT2G40340 AT2G29450

cell communication

AT3G24500 AT1G15520 AT4G31860 AT4G17500 AT3G28210 AT5G57910 AT1G28480
AT2G34500 AT4G35180 AT3G02800 AT1G79410 AT1G76650 AT3G46620 AT5G07180
AT5G07280 AT1G27730 AT3G63380 AT2G02220 AT5G48850 AT1G73730 AT4G02380
AT1G54100 AT5G02490 AT5G46450 AT1G80840 AT5G35735 AT4G01870 AT3G22370
AT5G56030 AT5G25930 AT3G56710 AT3G21780 AT5G20010 AT5G61820 AT4G30490
AT1G15430 AT1G19020 AT2G02710 AT5G59820 AT3G01290 AT1G76600 AT5G66070
AT5G45110 AT1G32920 AT1G55920 AT4G18950 AT5G63790 AT5G62020 AT1G28190
AT5G59550 AT3G28730 AT2G38470 AT3G50260 AT2G06050 AT4G39670 AT2G39660
AT2G40140 AT1G65390 AT2G03760 AT1G61690 AT4G18010 AT3G28340 AT1G66090

8. SUPPLEMENTARY MATERIAL

AT4G29780 AT4G34710 AT2G38290 AT2G21620 AT1G63840 AT4G22530 AT4G22980
AT1G33600 AT1G78380

cellular process

AT2G41380 AT1G70530 AT4G17500 AT5G12030 AT1G33110 AT5G11520 AT5G57910
AT5G14730 AT5G22350 AT5G52640 AT5G07180 AT1G27730 AT5G07280 AT2G02220
AT1G55850 AT1G36370 AT1G72680 AT5G46450 AT1G80840 AT3G07720 AT3G06420
AT4G28480 AT1G71000 AT4G23570 AT1G15430 AT2G20560 AT1G76600 AT3G51910
AT3G14200 AT2G47730 AT5G62020 AT2G06050 AT2G20550 AT3G16050 AT5G15850
AT2G21620 AT3G13520 AT3G23990 AT4G20860 AT1G68440 AT5G38530 AT4G22980
AT5G52810 AT1G15520 AT3G24500 AT1G04770 AT2G46560 AT3G22980 AT4G21990
AT1G17860 AT1G01120 AT1G68410 AT2G34500 AT4G35180 AT5G64300 AT2G43840
AT3G46620 AT3G08970 AT2G36950 AT5G02490 AT5G54170 AT5G35735 AT4G01870
AT3G22370 AT5G07440 AT5G25930 AT5G56030 AT5G35320 AT5G57050 AT1G75270
AT2G30140 AT1G19020 AT5G59820 AT5G66070 AT3G44110 AT5G45110 AT4G11280
AT1G66080 AT1G17745 AT4G01950 AT2G29500 AT3G46220 AT4G12400 AT1G28190
AT5G59550 AT2G26150 AT2G46240 AT3G50260 AT2G38470 AT1G30070 AT5G24030
AT1G66580 AT5G56010 AT2G40140 AT1G21680 AT4G25230 AT1G07350 AT1G66090
AT4G34710 AT3G59140 AT1G64780 AT1G07890 AT5G53400 AT5G03630 AT5G22300
AT1G33600 AT1G78380 AT3G12580 AT4G31860 AT4G24380 AT3G28210 AT5G48180
AT1G28480 AT5G26340 AT3G02800 AT2G18193 AT1G76650 AT5G54860 AT2G29420
AT3G63380 AT5G48850 AT3G62150 AT1G67810 AT2G15490 AT1G73730 AT2G17500
AT1G03850 AT1G66760 AT3G56710 AT3G28910 AT5G63370 AT5G20010 AT1G52200
AT4G30490 AT1G05520 AT4G25530 AT5G51830 AT3G09010 AT2G31945 AT5G19440
AT1G32920 AT2G19450 AT2G43820 AT4G01070 AT2G23420 AT3G25230 AT4G18950
AT3G28730 AT1G59860 AT3G10500 AT3G13470 AT2G29440 AT1G54090 AT1G17420
AT1G54050 AT1G61690 AT5G24660 AT3G28340 AT4G29780 AT2G34355 AT1G74310
AT4G15420 AT5G60790 AT2G29450 AT2G36220 AT3G14990 AT2G23810 AT3G25250
AT3G06500 AT3G09440 AT5G14470 AT5G14570 AT4G16680 AT5G44050 AT4G15550
AT2G47890 AT3G09350 AT3G57760 AT4G29670 AT3G16480 AT5G13750 AT1G79410
AT3G01640 AT3G21250 AT4G02380 AT1G62180 AT1G71100 AT1G54100 AT5G51440
AT1G14200 AT4G32210 AT3G21780 AT4G04610 AT5G58760 AT3G04000 AT5G14180
AT1G32170 AT5G61820 AT5G05410 AT2G02710 AT4G24160 AT3G01290 AT3G08690
AT1G55920 AT5G63790 AT5G17380 AT5G58770 AT1G07030 AT4G11600 AT3G12050
AT3G44190 AT4G39670 AT3G13080 AT5G02500 AT2G39660 AT1G65390 AT1G23440
AT2G03760 AT4G18010 AT2G34660 AT2G38290 AT1G63840 AT2G15430 AT5G13490
AT3G11250 AT4G22530 AT3G13310 AT3G59350 AT5G64250 AT3G04120 AT5G48570

cytosol

AT3G09440 AT5G12030 AT3G22980 AT5G48180 AT1G79920 AT1G01120 AT5G52640
AT3G01640 AT2G29420 AT2G15490 AT1G72680 AT1G71100 AT1G54100 AT5G02490
AT3G07720 AT5G56030 AT5G20010 AT1G75270 AT2G30140 AT1G05520 AT5G51830
AT3G44110 AT5G19440 AT1G66080 AT1G17745 AT1G55920 AT3G25230 AT4G18950
AT1G55500 AT3G05420 AT5G17380 AT4G11600 AT3G12050 AT3G13470 AT2G29440
AT5G02500 AT1G54090 AT1G66580 AT5G56010 AT3G16050 AT5G49480 AT3G23990
AT4G20860 AT1G07890 AT3G11250 AT4G22530 AT5G53400 AT5G39050 AT5G64250
AT5G03630 AT3G04120 AT1G78380 AT2G29450 AT3G14990 AT3G12580

signal transduction

AT3G24500 AT1G15520 AT4G17500 AT3G28210 AT1G28480 AT4G35180 AT3G02800
AT1G76650 AT3G46620 AT5G07180 AT5G07280 AT1G27730 AT3G63380 AT2G02220
AT1G73730 AT4G02380 AT1G54100 AT5G02490 AT5G46450 AT1G80840 AT5G35735
AT4G01870 AT3G22370 AT5G25930 AT5G56030 AT3G56710 AT3G21780 AT5G20010
AT5G61820 AT1G19020 AT1G15430 AT2G02710 AT5G59820 AT3G01290 AT1G76600
AT5G66070 AT5G45110 AT1G32920 AT4G18950 AT5G63790 AT5G62020 AT1G28190
AT5G59550 AT2G38470 AT3G50260 AT2G06050 AT4G39670 AT2G39660 AT2G40140
AT1G65390 AT2G03760 AT1G61690 AT4G18010 AT3G28340 AT1G66090 AT4G29780
AT4G34710 AT2G38290 AT1G63840 AT4G22530 AT4G22980 AT1G33600

catabolic process

AT2G41380 AT1G15520 AT3G09440 AT3G28210 AT4G16680 AT3G22980 AT5G48180
AT5G11520 AT5G57910 AT5G14730 AT3G57760 AT2G34500 AT3G16480 AT2G18193
AT1G79410 AT3G21250 AT2G29420 AT3G63380 AT3G62150 AT2G15490 AT2G36950
AT1G72680 AT1G71100 AT1G54100 AT4G01870 AT5G07440 AT5G56030 AT3G21780
AT3G06420 AT3G04000 AT5G14180 AT5G20010 AT1G75270 AT4G23570 AT1G52200
AT4G30490 AT2G30140 AT1G15430 AT4G24160 AT2G31945 AT3G08690 AT1G17745
AT4G01070 AT2G47730 AT2G26150 AT5G17380 AT3G10500 AT4G11600 AT3G44190
AT2G06050 AT5G24030 AT3G13080 AT2G29440 AT5G02500 AT1G23440 AT1G21680
AT4G18010 AT2G34660 AT4G34710 AT3G13520 AT3G59140 AT4G20860 AT1G68440
AT1G07890 AT5G13490 AT1G74310 AT5G03630 AT4G15420 AT3G04120 AT1G78380
AT2G29450 AT5G60790

protein binding

AT3G25250 AT3G53830 AT3G09440 AT5G12030 AT1G28480 AT3G09350 AT5G52640
AT5G07280 AT3G63380 AT3G08970 AT5G18400 AT1G26270 AT5G02490 AT1G80840
AT5G56030 AT3G56710 AT3G06420 AT5G57050 AT3G28910 AT3G04000 AT1G71000
AT4G28480 AT5G63370 AT5G20010 AT4G23570 AT4G30490 AT5G05410 AT4G25530
AT2G20560 AT3G44110 AT5G45110 AT4G11280 AT3G14200 AT1G17745 AT3G25230
AT5G63790 AT2G26150 AT3G05420 AT3G12050 AT2G46240 AT2G38470 AT5G02500

8. SUPPLEMENTARY MATERIAL

AT5G56010 AT2G40000 AT2G20550 AT3G16050 AT4G25230 AT5G15850 AT2G15430
AT5G13490 AT3G13310 AT3G59350 AT5G38530 AT4G13180 AT1G74310 AT2G40340
AT5G48570 AT3G12580

response to external stimulus

AT3G09010 AT4G31860 AT1G80840 AT1G35140 AT4G11280 AT1G55920 AT3G56710
AT5G56030 AT4G29780 AT2G38290 AT5G57910 AT2G21620 AT1G28480 AT2G34500
AT1G79410 AT3G46620 AT1G27730 AT5G48850 AT4G30490 AT1G73730 AT1G78380
AT4G02380 AT1G15430 AT2G23810 AT3G09000

plasma membrane

AT1G15520 AT1G30320 AT3G09440 AT1G70530 AT4G31860 AT5G14570 AT1G33110
AT1G79920 AT5G44050 AT5G26340 AT5G13750 AT4G35180 AT5G52640 AT1G79410
AT1G76650 AT3G21250 AT2G02220 AT1G51760 AT3G62150 AT1G55850 AT5G02490
AT4G09030 AT5G35735 AT5G25930 AT1G66760 AT4G32210 AT1G35660 AT5G20010
AT1G75270 AT1G52200 AT3G22600 AT2G02710 AT3G01290 AT3G44110 AT5G19440
AT3G17611 AT4G18950 AT1G75280 AT3G10500 AT4G11600 AT1G30070 AT5G24030
AT3G13080 AT5G02500 AT2G39660 AT5G56010 AT4G25230 AT1G76340 AT2G38290
AT2G21620 AT3G13520 AT3G59140 AT1G64780 AT1G07890 AT1G76070 AT3G59350
AT5G64310 AT5G22300 AT1G33600 AT3G04120 AT1G78380 AT5G60790 AT2G29450
AT3G14990 AT2G23810 AT3G12580

vacuole

AT1G66580 AT3G01290 AT3G09440 AT1G21680 AT5G14570 AT2G34660 AT5G07440
AT1G67360 AT2G47730 AT3G59140 AT3G23990 AT3G16480 AT5G13490 AT1G79410
AT3G21250 AT3G62150 AT5G61820 AT3G04120 AT1G78380 AT5G48570 AT3G13080
AT3G14990 AT5G02500 AT3G12580

protein metabolic process

AT3G25250 AT3G24500 AT3G09440 AT1G70530 AT4G31860 AT5G12030 AT3G22980
AT5G48180 AT1G17860 AT5G11520 AT3G09350 AT3G57760 AT3G16480 AT3G02800
AT5G52640 AT3G46620 AT5G07180 AT5G07280 AT3G08970 AT2G02220 AT1G51760
AT5G51440 AT5G02490 AT1G14200 AT4G01870 AT5G56030 AT5G25930 AT5G35320
AT5G57050 AT1G71000 AT4G28480 AT5G63370 AT1G75270 AT2G24500 AT4G23570
AT5G05410 AT2G02710 AT2G20560 AT3G09010 AT3G44110 AT3G51910 AT1G06870
AT3G08690 AT3G14200 AT1G66080 AT4G18950 AT3G25230 AT2G29500 AT4G12400
AT2G26150 AT5G59550 AT1G59860 AT3G12050 AT2G46240 AT1G30070 AT3G13470
AT5G02500 AT2G39660 AT5G56010 AT1G66580 AT2G20550 AT1G54050 AT1G23440
AT3G16050 AT1G61690 AT4G25230 AT3G23990 AT1G07890 AT5G13490 AT3G11250
AT3G13310 AT3G59350 AT5G53400 AT1G74310 AT1G79720 AT4G15420 AT3G04120

AT1G78380 AT5G48570 AT3G12580

transport

AT1G15520 AT4G24380 AT3G28210 AT5G14570 AT4G16680 AT1G33110 AT5G44050
AT1G17860 AT1G28480 AT5G26340 AT5G13750 AT4G35180 AT1G79410 AT3G21250
AT5G54860 AT3G63380 AT3G62150 AT1G73730 AT4G02380 AT2G36950 AT2G17500
AT1G03850 AT1G80840 AT5G35735 AT5G07440 AT5G25930 AT1G66760 AT5G20010
AT1G52200 AT3G22600 AT1G05520 AT1G15430 AT3G01290 AT5G45110 AT1G17745
AT1G55920 AT2G43820 AT4G01070 AT4G18950 AT5G59480 AT1G28190 AT3G05420
AT3G04010 AT1G07030 AT2G38470 AT4G39670 AT5G24030 AT3G13080 AT2G39660
AT1G54090 AT2G40140 AT2G03760 AT1G76340 AT2G34660 AT1G66090 AT4G34710
AT2G38290 AT3G59140 AT1G64780 AT3G23990 AT4G20860 AT1G07890 AT2G34355
AT5G13490 AT4G22980 AT1G33600 AT3G04120 AT5G60790

catalytic activity

AT2G41380 AT1G70530 AT4G31860 AT5G11520 AT1G28480 AT3G02800 AT2G18193
AT5G07180 AT1G05670 AT5G07280 AT2G29420 AT3G63380 AT1G51760 AT2G02220
AT3G62150 AT1G22340 AT1G55850 AT2G15490 AT1G36370 AT1G72680 AT5G46450
AT1G03850 AT5G33290 AT3G14620 AT5G63370 AT5G20010 AT5G06905 AT4G30490
AT5G51830 AT3G09010 AT3G46670 AT5G19440 AT1G06870 AT3G17611 AT2G19450
AT2G43820 AT4G01070 AT2G23420 AT3G25230 AT4G18950 AT2G47730 AT2G06050
AT3G11340 AT2G29440 AT1G17420 AT3G16050 AT4G05390 AT3G28340 AT4G20860
AT5G38530 AT5G39050 AT1G74310 AT4G34131 AT5G60790 AT2G29450 AT5G52810
AT3G14990 AT4G34138 AT3G25250 AT3G06500 AT1G15520 AT5G43450 AT5G14470
AT4G16680 AT3G22980 AT4G21990 AT4G15550 AT3G55430 AT1G01120 AT4G29670
AT3G57760 AT1G68410 AT2G34500 AT3G16480 AT5G64300 AT3G01640 AT2G43840
AT3G46620 AT3G21250 AT3G08970 AT1G02850 AT1G62180 AT1G71100 AT1G54100
AT1G26270 AT4G05020 AT4G33540 AT3G22370 AT5G07440 AT5G25930 AT5G56030
AT4G32210 AT3G21780 AT5G57050 AT4G04610 AT3G04000 AT5G14180 AT1G75270
AT1G32170 AT2G30140 AT2G02710 AT4G24160 AT3G24420 AT3G08690 AT4G11280
AT5G01100 AT1G17745 AT1G55920 AT5G59480 AT4G01950 AT5G59550 AT4G15760
AT5G17380 AT3G04010 AT5G58770 AT4G11600 AT3G44190 AT3G13080 AT2G39660
AT1G23440 AT2G03760 AT4G25230 AT4G18010 AT2G34660 AT1G66090 AT4G34710
AT2G15430 AT3G59140 AT1G07890 AT4G22530 AT3G59350 AT5G64250 AT4G13180
AT1G79720 AT5G03630 AT5G22300 AT4G02940 AT2G36750 AT3G04120 AT1G78380
AT5G48570

response to extracellular stimulus

AT2G34500 AT4G31860 AT1G79410 AT5G48850 AT1G55920 AT3G56710 AT4G30490
AT1G78380 AT4G02380 AT2G38290 AT2G21620 AT5G57910

8. SUPPLEMENTARY MATERIAL

cell wall

AT3G44110 AT5G02490 AT3G09440 AT1G35140 AT1G21680 AT5G56030 AT1G79920
AT1G17860 AT3G55430 AT5G52640 AT1G07890 AT5G20010 AT1G32170 AT1G33600
AT5G02500 AT3G12580

membrane

AT1G30320 AT1G70530 AT4G31860 AT4G17500 AT1G33110 AT5G11520 AT5G22350
AT5G26340 AT5G52640 AT1G76650 AT5G07280 AT5G54860 AT3G63380 AT1G51760
AT2G02220 AT3G62150 AT1G55850 AT3G50970 AT2G17500 AT5G33290 AT1G66760
AT1G35660 AT5G20010 AT1G52200 AT3G22600 AT1G05520 AT5G19440 AT1G06870
AT3G17611 AT2G19450 AT3G25230 AT4G18950 AT1G75280 AT2G47730 AT3G10500
AT4G05390 AT1G76340 AT2G21620 AT3G13520 AT3G23990 AT1G76070 AT2G34355
AT5G64310 AT5G60790 AT2G29450 AT3G14990 AT2G23810 AT1G15520 AT3G09440
AT5G14570 AT5G44050 AT1G79920 AT1G01120 AT4G35180 AT3G16480 AT5G13750
AT1G79410 AT5G64300 AT4G17840 AT3G21250 AT4G05020 AT5G02490 AT4G09030
AT5G35735 AT5G07440 AT5G25930 AT4G32210 AT3G21780 AT1G75270 AT2G02710
AT3G44110 AT3G01290 AT3G04010 AT1G07030 AT4G11600 AT1G30070 AT5G24030
AT3G13080 AT2G39660 AT5G02500 AT1G66580 AT5G56010 AT1G21680 AT4G25230
AT2G34660 AT2G38290 AT3G59140 AT1G64780 AT1G07890 AT3G59350 AT3G11250
AT5G13490 AT5G22300 AT1G33600 AT3G04120 AT1G78380 AT5G48570 AT3G12580

transferase activity

AT2G41380 AT3G25250 AT1G70530 AT5G14470 AT5G11520 AT4G15550 AT1G01120
AT3G57760 AT1G05670 AT2G43840 AT5G07180 AT3G01640 AT2G29420 AT5G07280
AT2G02220 AT2G15490 AT1G55850 AT1G22340 AT1G36370 AT1G26270 AT5G25930
AT5G33290 AT3G21780 AT5G63370 AT1G32170 AT2G30140 AT2G02710 AT5G51830
AT4G24160 AT3G09010 AT3G46670 AT4G11280 AT5G01100 AT2G19450 AT1G55920
AT2G43820 AT4G01070 AT2G23420 AT4G18950 AT4G01950 AT2G47730 AT5G17380
AT5G58770 AT3G11340 AT2G29440 AT2G39660 AT2G03760 AT3G28340 AT2G15430
AT4G22530 AT3G59350 AT5G39050 AT4G34131 AT2G36750 AT1G78380 AT2G29450
AT4G34138

Declaration

I herewith declare that I have produced this thesis without the prohibited assistance of third parties and without making use of aids other than those specified; notions taken over directly or indirectly from other sources have been identified as such. This thesis has not previously been presented in identical or similar form to any other Swiss or foreign examination board.

Lausanne,